

Antitubercular Benzothiazinones: Synthesis, Activity, Properties and SAR



Dissertation

zur Erlangung des
Doktorgrades der Naturwissenschaften (Dr. rer. nat.)

der

Naturwissenschaftlichen Fakultät I – Biowissenschaften

der

Martin-Luther-Universität Halle-Wittenberg

vorgelegt von

Andrea Ines Rudolph

geboren am 27.01.1983 in Karl-Marx-Stadt

Datum der Verteidigung: 04.06.2014, Halle (Saale)

Gutachter: Prof. Dr. Peter Imming
Prof. Dr. Martin Schlitzer
Dr. Ute Möllmann
Prof. Dr. Andrea Sinz

CONTENT

Content	I
Abbreviations.....	VII
List of figures	XI
List of tables.....	XV
Abstract	XVII
1 Tuberculosis and antitubercular drug development	1
1.1 Tuberculosis.....	1
1.2 Mycobacterium tuberculosis.....	1
1.3 Mycobacterial cell envelope	3
1.4 Antibiotic treatment of tuberculosis.....	4
1.5 The drug pipeline.....	5
1.5.1 Benzothiazinones	7
1.5.2 Fluoroquinolones.....	11
1.6 Objective of thesis	13
2 Syntheses.....	15
2.1 Synthetic pathways to benzothiazinones.....	15
2.1.1 Method A – the classic pathway	16
2.1.2 Method B – dithiocarbamate pathway	17
2.1.3 Method C – alkylxanthogenate pathway	17
2.1.4 Method D – alkylsulfanyl BTZ pathway	17
2.1.5 Method E – a new pathway: thiourea pathway.....	17
2.1.6 Evaluation of the synthetic routes	19
2.1.7 Unfamiliar NMR spectra	22
2.2 Novel BTZ derivatives	24
2.2.1 Unsubstituted arene moiety	25
2.2.2 Shifting the nitro group	26
2.2.3 Varying substituents at the arene	27
2.2.4 Substituents at position 2 of the heterocycle	33
2.2.5 2,3-Dihydro-5 <i>H</i> -imidazo[2,1- <i>b</i>][1,3]benzothiazin-5-one derivatives.....	45
2.3 Syntheses of benzoxazinones.....	47
2.3.1 Adaption of method E	47
2.3.2 Adaption of the classic pathway method A	48
2.4 Dual action molecules - thiochromenones	50
2.4.1 Essential pharmacophores of fluoroquinolones and benzothiazinones.....	50
2.4.2 Synthetic approaches to 3-carboxyl-thiochromen-4-ones	51
3 Biological Evaluation	55
3.1 Agar diffusion test	55
3.2 Minimal inhibitory concentration	59

3.3	In vivo activity: ultra-fast murine model	62
3.4	Cytotoxic and antiproliferative effects	66
4	Pharmacokinetic Evaluation	69
4.1	Calculated Lipinski rule-of-five parameters.....	69
4.2	Solubility.....	72
4.2.1	Methods of solubility determination.....	72
4.2.2	Calculated solubility of selected BTZs and BOZs.....	73
4.2.3	Solubility determination via the shake-flask method.....	74
4.3	Microsomal stability.....	79
5	Co-Crystallization with DprE1	83
5.1	Crystal structure of BOZ IR 95 with DprE1.....	85
6	Conclusion and suggestions for further BTZ development	87
7	Experimental Section	95
7.1	Chemicals and materials	95
7.2	Instrumental settings and analyses	95
7.3	Pharmacokinetic evaluation methods	97
7.3.1	Solubility determination	97
7.3.2	Calculated Lipinski rule-of-five.....	98
7.3.3	Microsomal stability.....	98
7.4	Biological evaluation methods.....	99
7.4.1	Agar diffusion assay	99
7.4.2	MIC determination.....	100
7.4.3	Antiproliferative and cytotoxicity assays.....	101
7.4.4	Co-Crystallization experimental methods	102
7.5	Syntheses	105
7.5.1	2-chloro-3-nitro-5-(trifluoromethyl)benzoic acid (IR 05)	106
7.5.2	N-[(2-chlorophenyl)carbonyl]piperidine-1-carboimidothioic acid (IR 12).....	106
7.5.3	1-([2-chloro-3-nitro-5-(trifluoromethyl)phenyl]carbonyl)piperidine (IR 13).....	107
7.5.4	2-(piperidin-1-yl)-4 <i>H</i> -1,3-benzothiazin-4-one (IR 16)	108
7.5.5	sodium (piperidin-1-yl)carbothioylsulfanide (IR 17).....	109
7.5.6	2-chloro-3-nitro-5-(trifluoromethyl)benzamide (IR 18)	110
7.5.7	8-nitro-2-(piperidin-1-yl)-6-(trifluoromethyl)-4 <i>H</i> -1,3-benzothiazin-4-one (IR 20) ^{np}	110
7.5.8	2-chloro-4,5-difluoro-3-nitrobenzoic acid (IR 29).....	112
7.5.9	2-chloro-4,5-difluoro-3-nitrobenzamide (IR 32) ⁿ	112
7.5.10	2,4-dichloro-5-fluoro-3-nitrobenzamide (IR 39) ⁿ	113
7.5.11	1-(cyclohexylmethyl)piperazine (IR 40)	114
7.5.12	sodium (ethoxymethanethioyl)sulfanide (IR 42).....	114
7.5.13	imidazolidine-2-thione (IR 45)	115
7.5.14	pyridine-2-carboxamide (IR 46)	115
7.5.15	8-chloro-7-fluoro-9-nitro-2,3-dihydro-5 <i>H</i> -imidazo[2,1- <i>b</i>][1,3]benzothiazin-5- one (IR 47) ^{np}	116

7.5.16	pyridine-2-carbothioamide (IR 48).....	117
7.5.17	morpholine-4-carbothioamide (IR 49)	118
7.5.18	piperidine-1-carbothioamide (IR 50).....	118
7.5.19	8-nitro-2-(pyridin-2-yl)-6-(trifluoromethyl)-4 <i>H</i> -1,3-benzothiazin-4-one (IR 51) ^{np}	119
7.5.20	6,7-difluoro-8-nitro-2-(pyridin-2-yl)-4 <i>H</i> -1,3-benzothiazin-4-one (IR 52) ^{np}	120
7.5.21	6,7-difluoro-2-(morpholin-4-yl)-8-nitro-4 <i>H</i> -1,3-benzothiazin-4-one (IR 53) ^{np}	121
7.5.22	2,5-difluoro-3-nitrobenzoic acid (IR 54)	121
7.5.23	6,7-difluoro-8-nitro-2-(piperidin-1-yl)-4 <i>H</i> -1,3-benzothiazin-4-one (IR 56) ^{np}	122
7.5.24	6-fluoro-2,7-bis(morpholin-4-yl)-8-nitro-4 <i>H</i> -1,3-benzothiazin-4-one (IR 57) ^{np}	123
7.5.25	2-(morpholin-4-yl)-8-nitro-6-(trifluoromethyl)-4 <i>H</i> -1,3-benzothiazin-4-one (IR 58) ^{np}	124
7.5.26	7-fluoro-8-(morpholin-4-yl)-9-nitro-2,3-dihydro-5 <i>H</i> -imidazo[2,1- <i>b</i>][1,3]benzothiazin-5-one (IR 59) ^{np}	125
7.5.27	N-[(2-chloro-4-nitrophenyl)carbonyl]morpholine-4-carboimidothioic acid (IR 60) ⁿ	126
7.5.28	6-fluoro-8-nitro-2-(pyridin-2-yl)-4 <i>H</i> -1,3-benzothiazin-4-one (IR 61) ^{np}	127
7.5.29	7-chloro-6-fluoro-8-nitro-2-(piperidin-1-yl)-4 <i>H</i> -1,3-benzothiazin-4-one (IR 62) ^{np}	128
7.5.30	6-fluoro-7-(morpholin-4-yl)-8-nitro-2-(piperidin-1-yl)-4 <i>H</i> -1,3-benzothiazin-4- one (IR 64) ^{np}	129
7.5.31	2-(morpholin-4-yl)-7-nitro-4 <i>H</i> -1,3-benzothiazin-4-one (IR 67) ^{np}	129
7.5.32	2,4-dichloro-5-iodobenzoic acid (IR 68)	130
7.5.33	7-chloro-6-fluoro-2-(morpholin-4-yl)-8-nitro-4 <i>H</i> -1,3-benzothiazin-4-one (IR 69) ^{np}	131
7.5.34	ethyl 2,4-dichloro-5-iodobenzoate (IR 70) ⁿ	131
7.5.35	ethyl 2,4-dichloro-5-(trifluoromethyl)benzoate (IR 71) ⁿ	132
7.5.36	2,4-dichloro-3-nitro-5-(trifluoromethyl)benzoic acid (IR 73) ⁿ	133
7.5.37	7-chloro-8-nitro-2-(piperidin-1-yl)-6-(trifluoromethyl)-4 <i>H</i> -1,3-benzothiazin- 4-one (IR 74) ^{np}	133
7.5.38	7-(morpholin-4-yl)-8-nitro-2-(piperidin-1-yl)-6-(trifluoromethyl)-4 <i>H</i> -1,3- benzothiazin-4-one (IR 75) ^{np}	134
7.5.39	7-chloro-2-(morpholin-4-yl)-8-nitro-6-(trifluoromethyl)-4 <i>H</i> -1,3- benzothiazin-4-one (IR 76) ^{np}	135
7.5.40	2,7-bis(morpholin-4-yl)-8-nitro-6-(trifluoromethyl)-4 <i>H</i> -1,3-benzothiazin-4- one (IR 77) ^{np}	136
7.5.41	8-chloro-9-nitro-7-(trifluoromethyl)-2,3-dihydro-5 <i>H</i> -imidazo[2,1- <i>b</i>][1,3]benzothiazin-5-one (IR 78) ^{np}	137
7.5.42	8-(morpholin-4-yl)-9-nitro-7-(trifluoromethyl)-2,3-dihydro-5 <i>H</i> -imidazo[2,1- <i>b</i>][1,3]benzothiazin-5-one (IR 79) ^{np}	138
7.5.43	9-nitro-7-(trifluoromethyl)-2,3-dihydro-5 <i>H</i> -imidazo[2,1- <i>b</i>][1,3]benzo- thiazin-5-one (IR 80) ^{np}	138

7.5.44	ethyl 3-[2-chloro-3-nitro-5-(trifluoromethyl)phenyl]-3-oxopropanoate (IR 81).....	140
7.5.45	8-nitro-2-phenyl-6-(trifluoromethyl)-4 <i>H</i> -1,3-benzothiazin-4-one (IR 82) ^{np}	141
7.5.46	2,6-dimethylpiperidin-4-one (IR 83)	142
7.5.47	N-[(2-chlorophenyl)carbonyl]morpholine-4-carboimidothioic acid (IR 84)	143
7.5.48	2-(2,6-dimethylpiperidin-1-yl)-8-nitro-6-(trifluoromethyl)-4 <i>H</i> -1,3-benzothiazin-4-one (IR 85) ^{np}	144
7.5.49	2-(morpholin-4-yl)-4 <i>H</i> -1,3-benzothiazin-4-one (IR 86).....	146
7.5.50	2-(4-methoxyphenyl)-8-nitro-6-(trifluoromethyl)-4 <i>H</i> -1,3-benzothiazin-4-one (IR 87) ^{np}	147
7.5.51	2-(4-chlorophenyl)-8-nitro-6-(trifluoromethyl)-4 <i>H</i> -1,3-benzothiazin-4-one (IR 88) ^{np}	148
7.5.52	2-(2,6-dimethylpiperidin-1-yl)-8-nitro-6-(trifluoromethyl)-4 <i>H</i> -1,3-benzoxazin-4-one (IR 95) ^{np}	149
7.5.53	6-fluoro-2-(morpholin-4-yl)-8-nitro-7-(pyrrolidin-1-yl)-4 <i>H</i> -1,3-benzothiazin-4-one (IR 96) ^{np}	150
7.5.54	6-fluoro-8-nitro-2-(piperidin-1-yl)-7-(pyrrolidin-1-yl)-4 <i>H</i> -1,3-benzothiazin-4-one (IR 97) ^{np}	151
7.5.55	9-nitro-8-(pyrrolidin-1-yl)-7-(trifluoromethyl)-2,3-dihydro-5 <i>H</i> -imidazo[2,1- <i>b</i>][1,3]benzothiazin-5-one (IR 98) ^{np}	151
7.5.56	8-nitro-2-(piperidin-1-yl)-7-(pyrrolidin-1-yl)-6-(trifluoromethyl)-4 <i>H</i> -1,3-benzothiazin-4-one (IR 100) ^{np}	152
7.5.57	2-(morpholin-4-yl)-8-nitro-7-(pyrrolidin-1-yl)-6-(trifluoromethyl)-4 <i>H</i> -1,3-benzothiazin-4-one (IR 101) ^{np}	153
7.5.58	7-fluoro-2-(morpholin-4-yl)-8-nitro-6-(trifluoromethyl)-4 <i>H</i> -1,3-benzothiazin-4-one (IR 102) ^{np}	154
7.5.59	7-(dimethylamino)-2-(morpholin-4-yl)-8-nitro-6-(trifluoromethyl)-4 <i>H</i> -1,3-benzothiazin-4-one (IR 103) ^{np}	154
7.5.60	7-(dimethylamino)-8-nitro-2-(piperidin-1-yl)-6-(trifluoromethyl)-4 <i>H</i> -1,3-benzothiazin-4-one (IR 104) ^{np}	155
7.5.61	8-(dimethylamino)-9-nitro-7-(trifluoromethyl)-2,3-dihydro-5 <i>H</i> -imidazo[2,1- <i>b</i>][1,3]benzothiazin-5-one (IR 105) ^{np}	156
7.5.62	7-(dimethylamino)-6-fluoro-8-nitro-2-(piperidin-1-yl)-4 <i>H</i> -1,3-benzothiazin-4-one (IR 106) ^{np}	156
7.5.63	7-(dimethylamino)-6-fluoro-2-(morpholin-4-yl)-8-nitro-4 <i>H</i> -1,3-benzothiazin-4-one (IR 107) ^{np}	157
7.5.64	7-fluoro-8-nitro-2-(piperidin-1-yl)-6-(trifluoromethyl)-4 <i>H</i> -1,3-benzothiazin-4-one (IR 108) ^{np}	158
7.5.65	piperidine-1-carboxamide (IR 110)	158
7.5.66	morpholine-4-carboxamide (IR 111).....	159
7.5.67	8-nitro-2-(piperidin-1-yl)-6-(trifluoromethyl)-4 <i>H</i> -1,3-benzoxazin-4-one (IR 112) ^{np}	160

7.5.68	2-(morpholin-4-yl)-8-nitro-6-(trifluoromethyl)-4 <i>H</i> -1,3-benzoxazin-4-one (IR 113) ^{np}	161
7.5.69	8-nitro-2-(2,2,6,6-tetramethylpiperidin-1-yl)-6-(trifluoromethyl)-4 <i>H</i> -1,3-benzoxazin-4-one (IR 114) ^{np}	162
7.5.70	8-nitro-2-(2,2,6,6-tetramethylpiperidin-1-yl)-6-(trifluoromethyl)-4 <i>H</i> -1,3-benzothiazin-4-one (IR 115) ^{np}	163
7.5.71	3,5-dimethylpiperidine-1-carbothioamide (IR 116).....	164
7.5.72	2,6-dimethylpiperidine-1-carbothioamide (IR 118).....	164
7.5.73	4-(cyclohexylmethyl)piperazine-1-carbothioamide (IR 119) ⁿ	165
7.5.74	4-(cyclohexylmethyl)piperazine-1-carboxamide (IR 120) ⁿ	166
7.5.75	2-[4-(cyclohexylmethyl)piperazin-1-yl]-8-nitro-6-(trifluoromethyl)-4 <i>H</i> -1,3-benzothiazin-4-one (IR 124 = PBTZ169).....	166
7.5.76	2-[4-(cyclohexylmethyl)piperazin-1-yl]-8-nitro-6-(trifluoromethyl)-4 <i>H</i> -1,3-benzoxazin-4-one (IR 125) ^{np}	168
7.5.77	2-(3,5-dimethylpiperidin-1-yl)-8-nitro-6-(trifluoromethyl)-4 <i>H</i> -1,3-benzothiazin-4-one (IR 127) ⁿ	169
7.5.78	Mixture: 2-[(4 <i>aS</i> ,7 <i>aS</i>)-octahydro-1 <i>H</i> -pyrrolo[3,4- <i>b</i>]pyridin-6-yl]-8-nitro-6-(trifluoromethyl)-4 <i>H</i> -1,3-benzothiazin-4-one and 2-[(4 <i>aS</i> ,7 <i>aS</i>)-octahydro-1 <i>H</i> -pyrrolo[3,4- <i>b</i>]pyridin-1-yl]-8-nitro-6-(trifluoromethyl)-4 <i>H</i> -1,3-benzothiazin-4-one (IR 128) ⁿ	171
7.5.79	2-ethoxy-8-nitro-6-(trifluoromethyl)-4 <i>H</i> -1,3-benzothiazin-4-one (IR 129).....	172
7.5.80	2,2,7,7-tetramethyl-3,6-dioxa-2,7-disilaoctane (IR 131).....	172
7.5.81	2,2,4,7,7-pentamethyl-3,6-dioxa-2,7-disilaoctane (IR 132).....	173
7.5.82	benzyl 2,6-dimethyl-4-oxopiperidine-1-carboxylate (IR 133).....	174
7.5.83	2-[(2 <i>R</i> ,6 <i>S</i>)-2,6-dimethyl-4-oxopiperidin-1-yl]-8-nitro-6-(trifluoromethyl)-4 <i>H</i> -1,3-benzothiazin-4-one (IR 140) ⁿ	174
7.5.84	8-nitro-2-(2,2,6,6-tetramethyl-4-oxopiperidin-1-yl)-6-(trifluoromethyl)-4 <i>H</i> -1,3-benzothiazin-4-one (IR 141) ⁿ	175
7.5.85	4-[[2-chloro-3-nitro-5-(trifluoromethyl)phenyl]carbonyl]-morpholine (IR 150).....	176
7.5.86	ethyl 5-nitro-8-oxo-3-(trifluoromethyl)bicyclo[4.2.0]octa-1,3,5-triene-7-carboxylate (IR 154) ⁿ	177
	References.....	179
	Acknowledgments.....	XIX
	Curriculum Vitae.....	XXI
	List of publications.....	XXIII
	Declaration of academic integrity.....	XXV

ABBREVIATIONS

ACN	acetonitrile
ADME	absorption, distribution, metabolism, excretion
AG	arabinogalactan
aq.	aqueous
Araf	D-arabinofuranosyl
AUC	area under the curve
BCG	Bacillus Calmette-Guérin
BOZ	benzoxazinone
BTZ	benzothiazinone
calc.	calculated
CC ₅₀	50 % cytotoxicity concentration
CFU	colony forming units
CL _{int}	intrinsic clearance
DCM	dichloromethane
Ddn	deazaflavin dependent nitroreductase
DIPEA	diisopropylethylamine (Hunig base)
DMEM	Dulbecco's modified media
DMF	dimethyl formamide
DMSO	dimethyl sulfoxide
DNB	dinitrobenzamide
DOTS	directly observed therapy short course
DPA	decaprenylphosphoryl arabinose
DPR	decaprenylphosphoryl ribose
DprE1	decaprenylphosphoryl- β -D-ribose-2'-oxidase
DprE2	decaprenylphosphoryl-2-keto- β -D-erythro pentose reductase
DPX	decaprenylphosphoryl-2-keto- β -D-erythro pentofuranose
EA	ethyl acetate
EDTA	ethylenediamine tetraacetic acid
EE	diethyl ether
EI	electron impact ionization
EMA	European Medicines Agency
ESI	electrospray ionization
EMB	ethambutol
FAD	flavin adenine dinucleotide
FPR	farnesylphosphoryl- β -D-ribofuranose
GC	gas chromatography
GI ₅₀	50 % inhibition of proliferation
GMP	Good Manufacturing Practice

VIII Abbreviations

GSK	GlaxoSmithKline
HSAB	hard and soft (Lewis) acids and bases
HeLa	human cervical cancer cells (immortal cell line derived from cervical cancer cells taken from Henrietta Lacks)
HepG2	human liver carcinoma cells (perpetual cell line derived from liver tissue of a 15-year-old Caucasian American male with hepatocellular carcinoma)
HIV	human immunodeficiency virus
HPLC	high performance liquid chromatography
HTS	high throughput screening
HUVEC	human umbilical vein endothelial cells (derived from the endothelium of veins from the umbilical cord)
INH	isoniazid
K-562	human chronic myeloid leukemia cells (immortalized myelogenous leukemia cell line of the erythroleukemia type, derived from 53 year old female CML patient in blast crisis)
LAM	lipoarabinomannan
LM	lipomannan
log	logarithm
MDR	multidrug resistant
MFSDA	methylfluorosulfonyldifluoroacetate
MIC	minimal inhibitory concentration
MM4TB	More Medicines for Tuberculosis Consortium
m.p.	melting point
MPLC	medium pressure liquid chromatography
MS	mass spectrometry
<i>Mtb</i>	<i>Mycobacterium tuberculosis</i>
NAD	nicotinamide adenine dinucleotide
NCCLS	National Committee for Clinical Laboratory Standards
nd	not determined
NfnB	nitroreductase from <i>M. smegmatis</i>
NMR	nuclear magnetic resonance
PBS	phosphate buffered saline
PBTZ	2-piperazinyl-benzothiazinone
PE	petrol ether
PG	peptidoglycan
PIM	phosphatidylinositol mannosides
PPP	public-private partnership
PYR	pyrazinamide
REMA	resazurin reduction microtiter assay
RIF	rifampicin
ROS	reactive oxygen species
rt	ambient temperature

SAR	structure activity relationship
sat.	saturated
SI	selectivity index
SS18b	streptomycin-starved <i>Mtb</i> 18b (<i>Mtb</i> strain with streptomycin-dependent growth, functions as in vitro model of non-replicating <i>Mtb</i>)
STR	streptomycin
TB	tuberculosis
TBAB	tetrabutylammonium bromide
TBME	<i>tert</i> -butyl methylether
TDM	trehalose dimycolate
TEA	triethylamine
THF	tetrahydrofuran
TLC	thin layer chromatography
TFA	trifluoroacetic acid
TMM	trehalose monomycolate
TMSOTf	trimethylsilyl trifluoromethanesulfonate
UV	ultraviolet
WHO	World Health Organization
XDR	extensively drug resistant

LIST OF FIGURES

Figure 1:	Scanning electron micrograph of <i>Mycobacterium tuberculosis</i> (http://phil.cdc.gov)	2
Figure 2:	Structure of the cell envelope of <i>Mycobacterium tuberculosis</i> ²⁴	3
Figure 3:	Targets of antitubercular drugs in use (purple) and in the pipeline (red), modified after Rudolph et al. ⁵¹	7
Figure 4:	Structure of BTZ043, its amino (BTZ045) and hydroxylamino (BTZ046) derivative	8
Figure 5:	Biosynthesis of DPA from DPR via DprE1 and DprE2 and its inhibition by BTZ043, modified after Neres et al. ⁵⁷	8
Figure 6:	Proposed mechanism of action of BTZ043: reduction to nitroso-BTZ043 via FADH ₂ or von Richter reaction, subsequent formation of stable „semimercaptal“ with Cys387 of DprE1, modified after Trefzer et al. ⁵⁵ and Tiwari et al. ⁶²	9
Figure 7:	Structure of second generation piperazinyl-benzothiazinones PBTZ169 and PBTZ A	11
Figure 8:	Chemical structure of fluoroquinolones moxifloxacin and gatifloxacin	11
Figure 9:	Chemical scaffolds of substances described in this thesis	15
Figure 10:	Synthetic pathways to 2-amino-4H-1,3-benzothiazin-4-ones.....	16
Figure 11:	Synthesis of 2-amino-4H-1,3-benzothiazin-4-one derivatives via thiourea reagents	18
Figure 12:	Possible formation of 1,3-BTZ/BOZ and 3,1-BTZ/BOZ via the synthetic method E	18
Figure 13:	Comparison of synthetic pathways for IR 20 and IR 58	19
Figure 14:	Nucleophilic attack at carboxyl or thiocarbonyl carbon in the classic pathway method A	20
Figure 15:	Proton and carbon NMR spectra of IR 20 (top) and IR 58 (bottom) in CDCl ₃	23
Figure 16:	¹³ C NMR spectra of IR 12 at 27 °C (top) and 60 °C (bottom), in DMSO-d ₆	23
Figure 17:	Compounds 6a, 6h and 8a of Nosova et al. ⁸⁵ with MICs against Mtb H37Rv	24
Figure 18:	Synthesis of unsubstituted BTZs IR 16 and IR 86	25
Figure 19:	Synthesis of IR 67 and IR 28	26
Figure 20:	Formation of N-benzylbenzamide 5 and 1-benzoyl-3-benzyl urea 6, modified after Caubere et al. ⁸⁸	27
Figure 21:	Synthesis of 2-chloro-4,5-difluoro-3-nitrobenzoic acid IR 29 and side product 2-chloro-4,5-difluoro-1,3-dinitrobenzene IR 152	28
Figure 22:	Proposed reaction mechanism of trifluoromethylation of aryl halides with MFSDA ^{93,94}	29
Figure 23:	Synthesis of 2,4-dichloro-3-nitro-5-(trifluoromethyl)benzoic acid IR 73	30
Figure 24:	Part from ¹³ C NMR (116-140 ppm) of IR 71	30

Figure 25: Synthesis of BTZs with different halide and trifluoromethyl substituents at the arene moiety	31
Figure 26: Synthesis of 7-amino-substituted 8-nitro-benzothiazinones	32
Figure 27: Synthesis of 8-nitro-2-(pyridin-2-yl)-4H-1,3-benzothiazin-4-ones IR 51 , IR 52 and IR 61	33
Figure 28: Synthesis of 2-aryl-8-nitro-4H-1,3-benzothiazin-4-ones IR 82 , IR 87 , and IR 88 ..	34
Figure 29: Synthesis of IR 85 and IR 115	35
Figure 30: ¹ H NMR spectra of diastereomers of 3,5-dimethylpiperidine (top) and IR 116 (bottom)	35
Figure 31: Synthesis of IR 127	36
Figure 32: ¹ H NMR spectra of IR 127 cis (top) and IR 127 trans (bottom)	36
Figure 33: Synthesis of 2,6-dimethylpiperidin-4-one IR 83 via double Mannich reaction	37
Figure 34: ¹ H NMR spectrum of IR 83	38
Figure 35: Synthetic plan of methyl substituted spiroketal piperidine derivatives.....	39
Figure 36: Synthetic plan of branched 1,4-dioxo-8-azaspiro[4.5]decane substituted BTZs ..	41
Figure 37: Synthesis of IR 128 with formation of both structural isomers.....	43
Figure 38: Synthesis of PBTZ IR 124 (= PBTZ169) and the hydrochloride IR 124xHCl	44
Figure 39: Synthesis of 8-chloro-9-nitro-2,3-dihydro-5H-imidazo[2,1-b][1,3]benzothiazin-5-ones IR 47 , IR 80 , and IR 78 , and 8-amino-9-nitro-2,3-dihydro-5H-imidazo[2,1-b][1,3]benzothiazin-5-ones IR 59 , IR 79 , IR 98 , and IR 105	45
Figure 40: Possible mechanism of benzoylchloride activation by POCl ₃	46
Figure 41: Synthesis of asymmetrically substituted urea derivatives IR 110 , IR 111 , and IR 120	47
Figure 42: Synthesis of BOZs IR 112 , IR 113 , and IR 125	48
Figure 43: Synthesis of BOZs IR 95 and IR 114	49
Figure 44: Scaffold of fluoroquinolones with essential pharmacophores indicated by arrows.....	50
Figure 45: Debated scaffolds for dual action compounds	51
Figure 46: Part from reaction scheme of Hashimoto et al.: synthesis of thiochromenone 10 as side product ¹²⁶	52
Figure 47: Synthetic attempts to IR 81 according to (adapted) Grohe-Heitzer conditions... 53	
Figure 48: Synthetic attempts to thiochromenone IR 126 with isolation of by-product IR 154	53
Figure 49: log ₁₀ CFU reduction in the ultra-fast murine model of acute TB for IR 85 , IR 124 , IR 124xHCl , and moxifloxacin (one dot accounts for one test animal)	62
Figure 50: HPLC chromatograms of BTZs IR 20 , IR 124xHCl , IR 124 , IR 85 , IR 74 , and IR 76 after 48 h, PBS buffer 7.4. Red arrows indicate the common degradation peak at 4.2 min or 4.5 min.....	77
Figure 51: HPLC chromatogram of BOZ IR 95 after 48 h shaking in PBS buffer pH 7.4	78
Figure 52: Chemical structures of DNB1 and CT325	83
Figure 53: CT325 and its mode of binding at Mtb DprE1 ⁶³	83
Figure 54: Mode of binding of nitroso-BTZ043 at DprE1 from <i>M. smegmatis</i> ⁵⁷	84

Figure 55: Surface diagram (A) and close-up view (B) of Mtb DprE1 with inhibitor IR 95 bound in the active site	85
Figure 56: Mode of binding of nitroso- IR 95 in the active site of Mtb DprE1.....	86
Figure 57: Structure activity relationships of BTZs and BOZs.....	91

LIST OF TABLES

Table 1:	Treatment schemes for drug-susceptible TB and MDR/XDR-TB according to WHO ²⁶	4
Table 2:	Comparison of synthetic pathways to build the BTZ scaffold	22
Table 3:	Synthesis of IR 29 with different reaction conditions	29
Table 4:	Results of agar diffusion experiments for BTZ and BOZ derivatives, n=1	55
Table 5:	MIC of selected compounds against <i>M. vaccae</i> , <i>Mtb H37Rv</i> , <i>M. bovis</i> BCG, and <i>M. bovis</i> BCG over-expressing DprE1	59
Table 6:	log ₁₀ CFU reduction in the ultra-fast murine model.....	62
Table 7:	Comparison of the different mouse models of acute TB	64
Table 8:	Cytotoxic and antiproliferative effects of selected BTZ and BOZ compounds.....	66
Table 9:	Calculated Lipinski rule-of-five values	70
Table 10:	Calculated solubility of selected BTZ and BOZ compounds	73
Table 11:	Experimental solubility of selected BTZ and BOZ compounds.....	74
Table 12:	Solubility classification of the European Pharmacopoeia	75
Table 13:	Microsomal stability in human and mouse liver microsomes for selected BTZ and BOZ compounds (n=2)	79
Table 14:	Statistics of X-ray diffraction data and of model refinement.....	104

ABSTRACT

Tuberculosis is one of the most widespread infectious diseases worldwide, accounting for approximately 1.3 million deaths each year. Despite the omnipresent prevalence of tuberculosis, the disease has drifted out of focus in industrialized countries and drug research proceeded slowly, resulting in no market authorization of novel antitubercular drugs for almost 40 years. However, the emergence of multidrug and extremely drug-resistant *Mycobacterium tuberculosis* strains led to a rethinking and accelerated drug development. In 2009, 8-nitro-1,3-benzothiazinones (BTZ) were discovered as novel and highly active antitubercular agents, covalently inhibiting the newly discovered cell wall enzyme DprE1. In the scope of this work, novel antimycobacterial compounds belonging to 1,3-benzothiazinones and to 1,3-benzoxazinones were investigated.

The synthesis of the BTZ scaffold can be carried out via different synthetic pathways. The feasibility and yield of each of the synthetic pathways was found to depend on the nature of the substituent at position 2 and the respective substitution pattern of the arene moiety. Additionally, the simplification of the multi-step BTZ synthesis has been a matter of interest in several reports. We found an original pathway to form the BTZ scaffold in a straightforward and easily adaptable two-step synthesis, viz. from benzoic acid and thiourea derivatives (thiourea pathway). A variety of new BTZ derivatives were synthesized and tested against *M. vaccae* and *M. tuberculosis*. Some of the new compounds comprise very good activity against both mycobacteria species. Toxicity profile, solubility data and microsomal stability data were determined for the most active compounds, showing that the novel BTZs exhibit a favorable toxicity profile and microsomal stability but still display insufficient solubility.

A second novel antimycobacterial scaffold was developed by replacing the sulfur of BTZs with its isoster oxygen – 8-nitro-1,3-benzoxazinones (BOZ). They are accessible via a modified two-step procedure analogous to the thiourea pathway, viz. from benzoic acid and urea derivatives. BOZs are slightly less active against mycobacteria in vitro than their BTZ counterparts, but more stable towards liver microsomes. Additionally, one BOZ derivative was co-crystallized with DprE1 to reveal the crystal structure of the active enzyme-compound adduct, clearly proving covalent bonding. Hence, BOZs share the same mechanism of action with previously reported BTZs and are established as novel antitubercular scaffold.

Structure activity relationships are discussed for the novel BTZ and BOZ derivatives, underlining the essentiality of the nitro group and showing that medicinal chemistry variations to improve BTZ's/BOZ's pharmacologic and pharmacokinetic properties only tolerate complex cyclic amino substituents at position 2 but not many substituents at the arene moiety.

Chapter One

1 TUBERCULOSIS AND ANTITUBERCULAR DRUG DEVELOPMENT

1.1 TUBERCULOSIS

In 2012, one human life was extinguished every 24 seconds by tuberculosis (TB). With these numbers, TB ties with HIV (one life every 18 seconds) and diabetes (one life every 24 seconds). Despite declining rates for incidence and mortality for the first time within 15 years of data collection and ongoing surveillance by the World Health Organization (WHO) during the last two years, the numbers of the WHO report on tuberculosis still show the distressing statistic of the “white plague”. In 2012, 8.6 million new cases occurred and leading countries with the highest number of incident cases were India, China, South Africa, Indonesia, and Pakistan. 1.1 million newly infected TB patients were HIV positive. Besides a global prevalence of 12 million cases of active TB in 2012, WHO estimates the number of patients infected with the TB bacillus but not yet having developed the active disease at 2 billion – almost one third of the world’s population – which renders TB the most widespread infectious disease worldwide.¹⁻³

Tuberculosis is a bacterial infection, which affects the respiratory system in about 90 % of all cases. It can also affect other organs, such as skeleton, soft tissue, lymph nodes, or it can disseminate through the blood vessels and affect multiple organs (“Miliary TB”). Common symptoms of active lung TB are cough with sputum and blood, general weakness, weight loss, fever, chest pain, and night sweats. Bacilli are transmitted from one person to another via droplet infection, whereupon infectious droplets only carry a small number of bacilli. One actively ill patient will so infect 10-15 new patients within one year. Depending on the host’s immune status, infected patients have a 10 % lifetime risk to develop the disease. Since immune competence correlates with general health and nutrition status, coinfections and comorbidities, it is not surprising that high TB incident rates are found in countries with poorly developed hygiene and low living and health standards.^{2,4} Coinfection with HIV forms a lethal combination, each infection speeding the other’s progress and hampering the other’s treatment.⁴⁻⁸

However, TB is not a sole problem of the developing world, the emergence of multidrug resistant (MDR) and/or extensively drug resistant (XDR) TB has been reported in all countries with TB surveillance programs. Rates of MDR TB within new TB cases range from 0-30 %, with highest MDR rates worldwide occurring in some regions of the Russian Federation.^{2,9,10}

1.2 MYCOBACTERIUM TUBERCULOSIS

Most mycobacteria species are saprophytic soil inhabitants, but a few are important pathogens, including the *Mycobacterium tuberculosis complex*, which can cause TB in humans (*M. tuberculosis*, *M. africanum*, *M. caprae*, *M. bovis*, *M. canetti*, *M. microti*, *M.*

pinnipedii) and *M. leprae* which causes leprosy. Atypical mycobacteria, which include the *M. avium complex*, *M. kansasii*, *M. fortuitum*, and *M. chelonae*, can cause opportunistic infections in immunologically compromised patients.¹¹

The main causative agent of tuberculosis – *Mycobacterium tuberculosis* (*Mtb*) – was discovered and isolated by Robert Koch in 1882.¹² It is a rod-shaped bacillus of 1-4 μm length and 0.3-0.6 μm width (Figure 1). Cell division of *Mtb* occurs every 12-24 h, which represents a very slow growth rate compared to other microorganisms (15-60 min) and hampers antibiotic treatment since most antibiotics interfere with cell division processes.^{4,13}

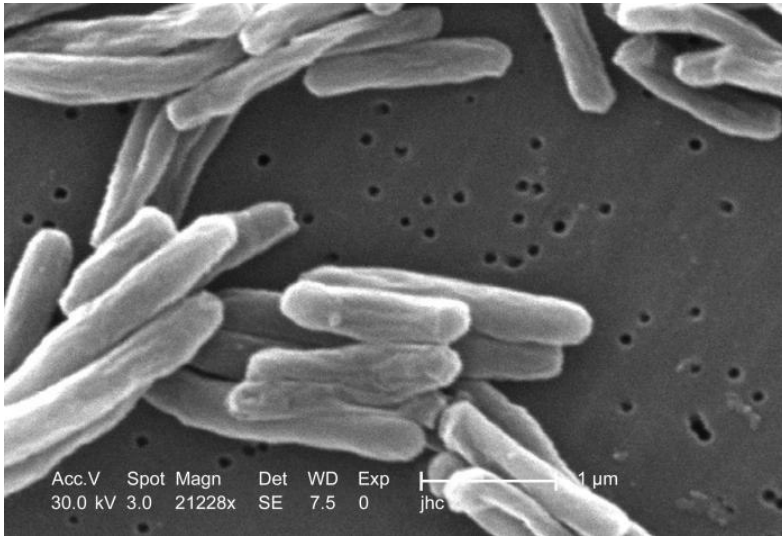


Figure 1: Scanning electron micrograph of *Mycobacterium tuberculosis* (<http://phil.cdc.gov>)

The infection with the microorganism mainly occurs through droplet infection. Once *Mtb* has entered the host, the immune system will fight the infection by phagocytosis of *Mtb* into macrophages. Generally, bacteria are assimilated within macrophages by uptake into phagosomes, an intracellular compartment with low pH, several enzymes, and reactive oxygen species (ROS). However, *Mtb* possesses mechanisms to interfere with the host signaling cascade, which prevents the maturation of phagosomes and therefore maintains the intracellular survival of *Mtb*.¹⁴⁻¹⁸ Thus, *Mtb* is a facultative intracellular pathogen.

Furthermore, *Mtb* is capable of down-regulation of its entire metabolism when stressed with exogenous factors such as acidic pH, oxidative stress, and nutrition starvation. This metabolic state is also referred to as dormancy. Dormant bacilli can survive for years in the host organism and initiate a new outbreak of the disease upon major changes in the host's immune status. Distinct from dormancy, which describes a physiological state of *Mtb*, are persisters – a phenomenon of bacteria in general, which are a subpopulation of bacteria that survive the cidal action of antibiotics. Persisters are genetically identical to susceptible bacteria and appear to be non-replicating or slowly growing. They possess non-inheritable phenotypic resistance or tolerance to antibiotics, however, the mechanisms leading to persistence are not yet fully understood.¹⁹ Persisters are a second reason why *Mtb* can outlast several years in the host and lead to a new outbreak of the disease upon triggers not yet fully understood.

1.3 MYCOBACTERIAL CELL ENVELOPE

The uniqueness of all mycobacteria species is their cell envelope, which is particularly rich in lipids and forms an efficient and strong defense shield to different environmental influences, e.g. antibiotics and chemical disinfectants.

The cell wall is composed of two segments. The inner part contains a peptidoglycan (PG) layer, which is attached to the plasma membrane via the cell wall glycolipid phosphatidylinositol mannosides (PIM). Covalently attached to the PG is a hydrophobic polysaccharide, the arabinogalactan (AG) with branched arabinose side chains, which in turn are esterified at the distal ends to the mycolic acids.^{20,21} Mycolic acids are long-chained (70-90 carbons) α -alkyl, β -hydroxy fatty acids, which represent 40-60 % of the cell's dry weight.²² The outer segment contains extractable lipids, e.g. trehalose monomycolate (TMM), trehalose dimycolate (TDM), sulfolipids, phenolic glycolipids, phthiocerol dimycocerosates, and complex polysaccharides as well as small amounts of proteins. Together with the mycolic acid chains, the free lipids form an asymmetrical bilayer, which is also called the mycobacterial outer membrane.²³ The cell envelope is interspersed with complex free cell wall lipids, namely lipomannans (LM) and lipoarabinomannans (LAM, Figure 2).^{20,21} The integrity of the mycobacterial cell envelope is important for virulence and intracellular survival of *Mtb*.²³

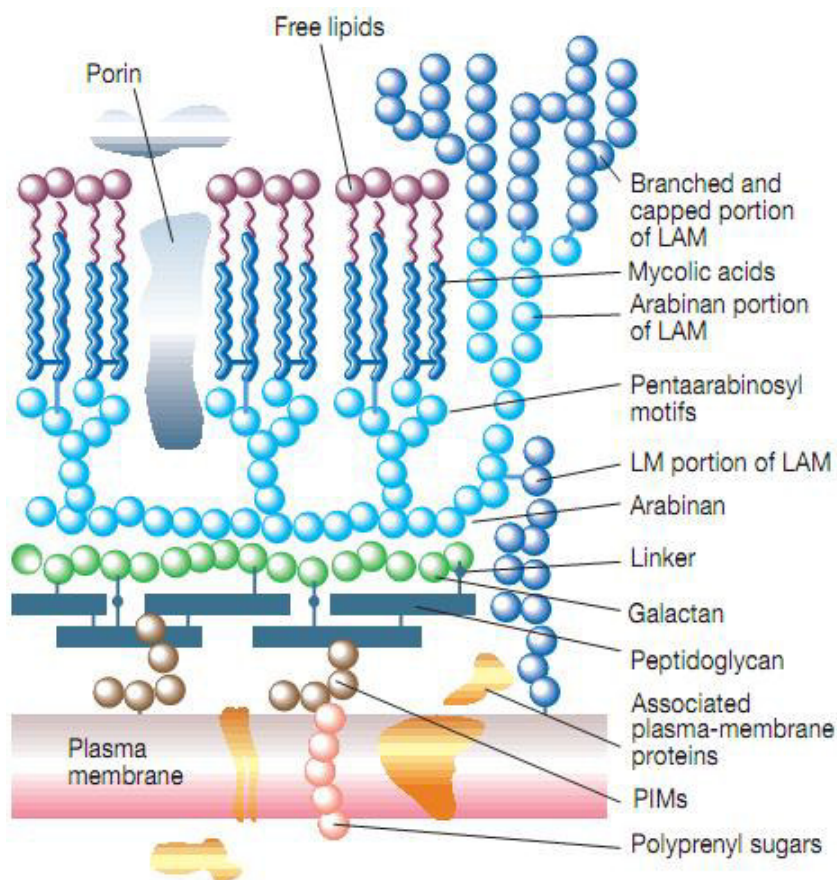


Figure 2: Structure of the cell envelope of *Mycobacterium tuberculosis*²⁴

This excellent barrier exacerbates the antibiotic treatment of tuberculosis due to its low permeability to drugs. However, this unique cell wall also comprises several unique biosynthetic pathways, which include several enzymes that are specific to mycobacteria and serve as targets for the antimycobacterial chemotherapy. Thus, not surprisingly, many antitubercular drugs inhibit biosynthetic pathways of cell wall components.

1.4 ANTIBIOTIC TREATMENT OF TUBERCULOSIS

Mycobacteria are resistant to common antibiotics except aminoglycosides, rifamycins, and fluoroquinolones. Mycobacteria are also relatively resistant to drying, alkali and many chemical disinfectants, which complicates prevention of transmission. This general resistance to therapeutic agents is related to the unique structure of the mycobacterial cell envelope resulting in low permeability to exogenous factors.¹¹ Therefore several chemotherapeutic agents specifically active against *Mtb* were developed. After streptomycin – the first antitubercular agent – and 4-aminosalicylic acid in the 1940s, isoniazid was introduced in 1952 and still is the major element of the antibiotic treatment of TB. Pyrazinamide, an important agent to eradicate persisters, was introduced in 1954 and became a basic constituent of the standard drug regimen in the 1980s. Ethambutol and rifampicin followed in 1961 and 1963.²⁵

The WHO classifies first-line and second-line antitubercular agents depending upon their efficacy and tolerance. First-line drugs are isoniazid (INH), rifampicin (RIF), pyrazinamide (PYR), ethambutol (EMB), and streptomycin (STR).

Table 1: Treatment schemes for drug-susceptible TB and MDR/XDR-TB according to WHO²⁶

drug-susceptible TB	first-line	6 months	2 months INH+RIF+PYR+EMB 4 months INH+RIF	
new outbreak of drug-susceptible TB	intensi-fied first-line	8 months	2 months INH+RIF+PYR+EMB+STR 1 month INH+RIF+PYR+EMB 5 months INH+RIF+EMB	
MDR-TB/ XDR-TB	indivi-dualized second-line	18-24 months or longer	group 1: first-line, oral	PYR, EMB, rifabutin (for HIV patients only)
			group 2: second-line, injectable	kanamycin, amikacin, capreomycin, streptomycin
			group 3: second-line, fluoroquinolones	levofloxacin, moxifloxacin, ofloxacin
			group 4: second-line, bacteriostatic, oral	4-aminosalicylic acid, cycloserine, terizidone, ethionamide, protionamide
			group 5: not preliminary approved by WHO, additional therapy if no sufficient treatment is achieved with group 1-4	clofazimine, linezolid, amoxicillin/clavulanic acid, thioacetazone, imipenem/cilastatine, high-dose INH, clarithromycin

A drug susceptible *Mtb* infection is usually treated with a combination of INH+RIF+PYR+EMB for two months, followed by a four month treatment of INH+RIF (Table 1). The combination of drugs with different mode of actions and the long duration of treatment are necessary due to the slow cell division rate of *Mtb* and particularly ineluctable in order to kill all bacilli, including the dormant bacilli and persisters. The application of a drug combination is crucial to avoid the emergence of resistant strains.

Second-line therapeutics are implemented if the infection is caused by MDR/XDR strains or if treatment with first-line drugs fails. Second-line drugs are less effective and accompanied by more severe side effects. The treatment of MDR/XDR TB lasts at least 18-24 months (Table 1) and consists of individualized combinations of drugs of group 1-5.²⁶

One major obstacle of the long-term antibiotic treatment is the occurrence of side effects and the low patient compliance. Monotherapy or early abandonment of the antibiotic therapy leads to insufficient eradication of the infection and the emergence of resistant bacilli. In 1995, the WHO implemented the “directly observed therapy short course” (DOTS) strategy, which includes five major points for a country’s TB control: a) political commitment, b) early case detection through quality-assured diagnosis, c) standardized treatment with supervision and patient support, d) drug supply and management system, and e) monitoring and evaluation. With the implementation of a strict surveillance program by the local health organizations, patients are supported and motivated to retain the antibiotic treatment throughout the recommended time with no need for hospital admission.²⁷

1.5 THE DRUG PIPELINE

For about 40 years, it was alarmingly quiet in the field of antitubercular drug development. The last first-line drug was introduced in the 1960s, followed by new combinations and adaptations of the treatment regimens. But increasing mortality rates in the subpopulation of HIV-coinfected patients and the emergence of MDR/XDR TB has led to a rethinking: WHO started surveillance and control programs, companies initiated TB drug development programs, and public private partnerships (PPPs) were initiated to spark the drug development pipeline and connect researchers from academia and industry (e.g. TB Alliance, Stop TB Partnership). The European Commission supported anti TB research with approx. 120 million € within its FP6 and FP7 programs. Apart from the re-evaluation and repurposing of existing antibiotics for the treatment of TB, a small number of new drug entities have since entered the pipeline. Despite in-depth research and funding efforts, the TB drug pipeline still is disturbingly empty. Reasons for the difficult development of antibiotics and antitubercular agents in particular have been discussed and reviewed elsewhere.²⁸⁻³²

Which qualities does a new antitubercular drug require? It should be selective and efficient against *Mtb*, including dormant bacilli, persisters as well as intra- and extracellular bacilli. It should show a rapid antibiotic action and act through new targets in order to avoid cross-resistance with existing drugs. It should be well tolerated with minimal side effects and be compatible with HIV drug treatment and combinable with other antitubercular drugs.³²

To the group of re-purposed drugs belong the fluoroquinolones moxifloxacin and gatifloxacin. The DNA gyrase inhibitors have been used off-label to treat MDR TB and could replace INH or EMB in first-line regimens by 2015, which is currently evaluated in phase III clinical trials.^{33,34}

Ansamycins rifapentine and rifabutin, which inhibit the DNA-dependent RNA polymerase, are investigated to replace rifampicin for better pharmacokinetic properties (e.g. reduced half life, decreased CYP3A4 induction) and are also evaluated in phase III.^{32,35}

A new drug entity is the diarylquinoline TMC207 (bedaquiline). Bedaquiline inhibits the proton transfer chain of the mycobacterial ATP synthase and is very efficient and selective against *Mtb* and *M. avium complex*. It is the first drug targeting the ATP synthase, exhibiting a novel mode of action by destructing the bacilli's energy production and at the same time reveals no cross-resistance with existing drugs. Bedaquiline is currently in clinical trials phase II but has already been approved by the FDA in 2012 for the treatment of MDR TB. Approval in Europe was submitted based on phase II data.^{34,36,37}

Nitroimidazoles OPC-67683 (delamanid) and PA-824 are prodrugs that require reduction by the deazaflavin dependent nitroreductase (Ddn) to the corresponding active des-nitro metabolites. PA-824, currently in phase II, was shown to be active against replicating and non-replicating bacilli via intracellular NO release. Inhibition of mycolic acid biosynthesis is also discussed.^{34,38} Delamanid inhibits biosynthesis of methoxy mycolic and keto mycolic acids,³⁹ but the complete mechanism of action is still under investigation. Delamanid has recently entered phase III clinical trials, and a after a negative opinion earlier in 2013 a conditional marketing authorization based on phase II data was recommended by the European Medicines Agency (EMA).⁴⁰⁻⁴³

Originally developed as an ethambutol analog, the ethylenediamine derivative SQ109 shows activity against EMB-resistant strains and targets a recently discovered membrane transporter (MmpL3) and hence, disables the correct assembly of the mycobacterial cell wall.^{21,44} SQ109 is currently in phase II clinical trials. Oxazolidinones linezolid, its thiomorpholine analog PNU-100480 (sutezolid), and AZD5847, which inhibit protein biosynthesis via binding to the 23S rRNA of the 50S ribosome subunit, are in phase II as well.^{28,41,45-47} ITB-01 (unknown structure) was recently published as a cell wall inhibitor in clinical trial phase II.⁴⁸

Many drug development projects are in preclinical development, such as fluoroquinolone DC-159a, caprazamycine derivative CPZEN-45, diamine derivative SQ609, DprE1 inhibitors benzothiazinones (BTZ043, PBTZ169) and dinitrobenzamides (DNB1), imidazopyridine Q203, back-up nitroimidazole TBA-345, riminophenazine derivative TBI-166, and capuramycine derivative SQ641. Capuramycines inhibit translocase-1 (TL-1), a new target in the peptidoglycan biosynthesis.^{34,41,47} Further details on current TB pipeline drugs are collated in comprehensive reviews.^{34,49,50}

Figure 3 summarizes targets of current antitubercular agents (purple) as well as those of current pipeline drugs (red).

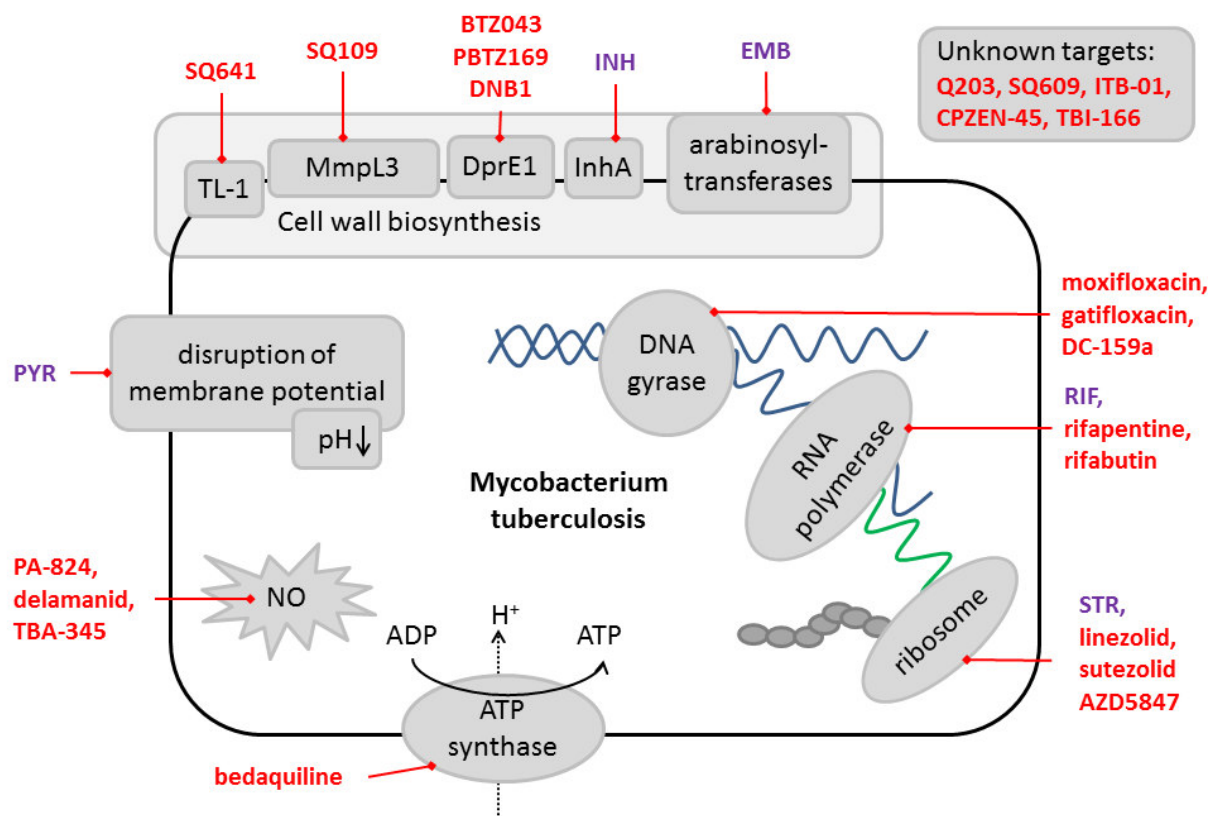


Figure 3: Targets of antitubercular drugs in use (purple) and in the pipeline (red), modified after Rudolph et al.⁵¹

1.5.1 Benzothiazinones

Benzothiazinones (BTZ) are a novel class of antitubercular agents with very high activity against *Mtb* H37Rv in vitro (MIC 1 ng/ml) as well as MDR and XDR strains of *Mtb*, including clinical isolates (MIC 0.75-30 ng/ml). The lead compound BTZ043 (Figure 4) protects infected macrophages at concentrations as low as 10 ng/ml and also satisfies in vivo in acute and chronic TB mouse models (acute model: log CFU (colony forming units) reduction in lungs and spleen > 0.54 compared to untreated control, reference compound INH log CFU reduction > 0.48; chronic model: reduction of CFU in lungs and spleen after four weeks of treatment by one and two logs, respectively).

They were discovered at the Hans-Knöll-Institut Jena (Germany) and have quickly elated TB researchers owing to their exceptionally high activity against *Mtb*, as well as favorable toxicity data in vitro and in vivo so far (namely low plasma protein binding, no mutagenicity, high metabolic stability in human liver microsomes, low cytochrome P450 inhibition, no hERG channel inhibition, and LD₅₀ (mice) > 2 g/kg body weight).⁵²⁻⁵⁴

The nitro group of BTZ043 was shown to be essential for its activity, since the amino derivative BTZ045 and the hydroxylamino derivative BTZ046 (Figure 4) have an increased MIC by 500-5000 fold.⁵⁴

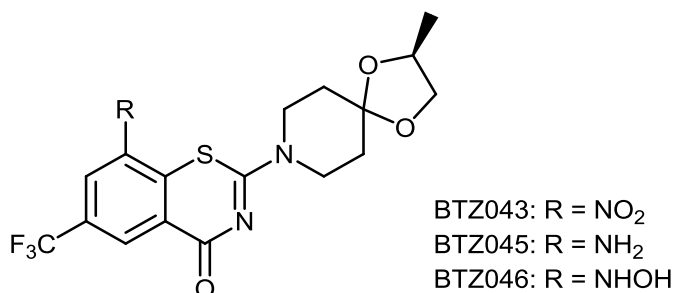


Figure 4: Structure of BTZ043, its amino (BTZ045) and hydroxylamino (BTZ046) derivative

The target of BTZ was identified to be the decaprenylphosphoryl- β -D-ribose-2'-oxidase DprE1, a membrane-associated enzyme involved in the cell wall biosynthesis. DprE1 catalyzes the first step in the FAD-dependent epimerization of decaprenylphosphoryl ribose (DPR) via the intermediate decaprenylphosphoryl-2-keto- β -D-erythro-pentofuranose (DPX) to decaprenylphosphoryl arabinose (DPA), which is the only precursor of arabinan moieties in the mycobacterial cell wall (Figure 5).⁵⁴⁻⁵⁶ The second step is catalyzed by decaprenylphosphoryl-2-keto- β -D-erythro-pentose-reductase (DprE2) with NADH as a cofactor. The conversion of DPR to DPA only takes place if both enzymes and the cofactors are present.

DPA is utilized by arabinosyltransferases as the sole donor of D-arabinofuranosyl residues (Araf), which are subsequently incorporated into the arabinogalactan and lipoarabino-

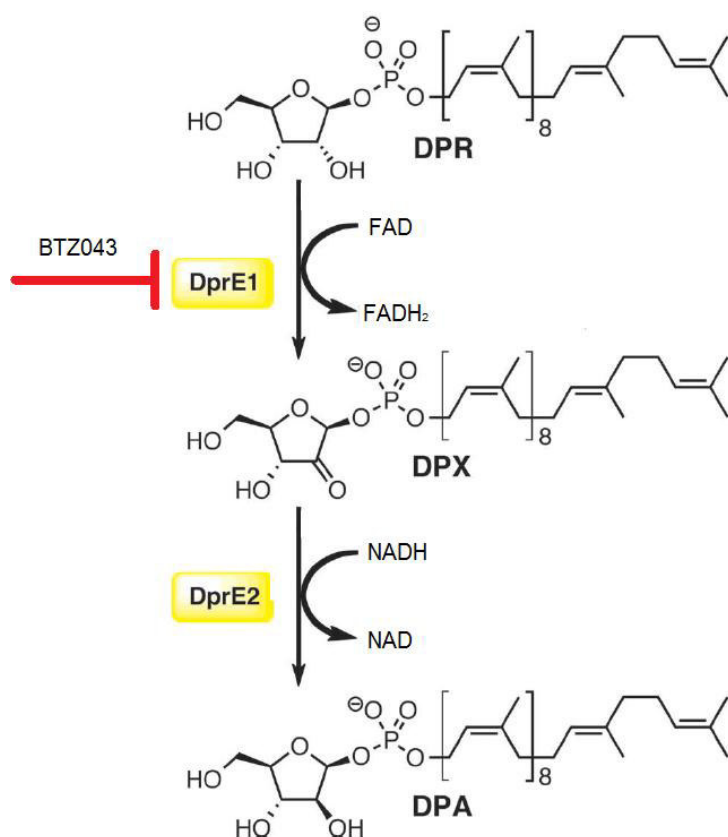


Figure 5: Biosynthesis of DPA from DPR via DprE1 and DprE2 and its inhibition by BTZ043, modified after Neres et al.⁵⁷

mannan of the mycobacterial cell envelope.^{56,58,59} DprE1 has been validated as a selective and highly vulnerable target for the development of novel antitubercular agents, since it has no human orthologue and is essential for extra- and intracellular growth of *Mtb* and *M. smegmatis*.^{56,60,61} The high conservation of DprE1 throughout several mycobacteria species and the fact that no mutations in the DprE1 encoding gene *rv3790* were found in clinical isolates of *Mtb* (all of them were susceptible to BTZ043) further suggest that DprE1 is a very attractive target for MDR- and XDR TB strains.^{52,54,56} Manina et al. therefore describe DprE1 as a novel and “magic” drug target.⁵⁶

BTZ043 is a prodrug, which undergoes reduction of the nitro to a nitroso group and then covalently binds to a cysteine residue of DprE1 (Cys387) to form a stable N-hydroxy-sulfenamide (“semimercaptal”, Figure 6), which renders the enzyme inactive and, hence, blocks the biosynthesis of arabinan moieties.⁵⁵

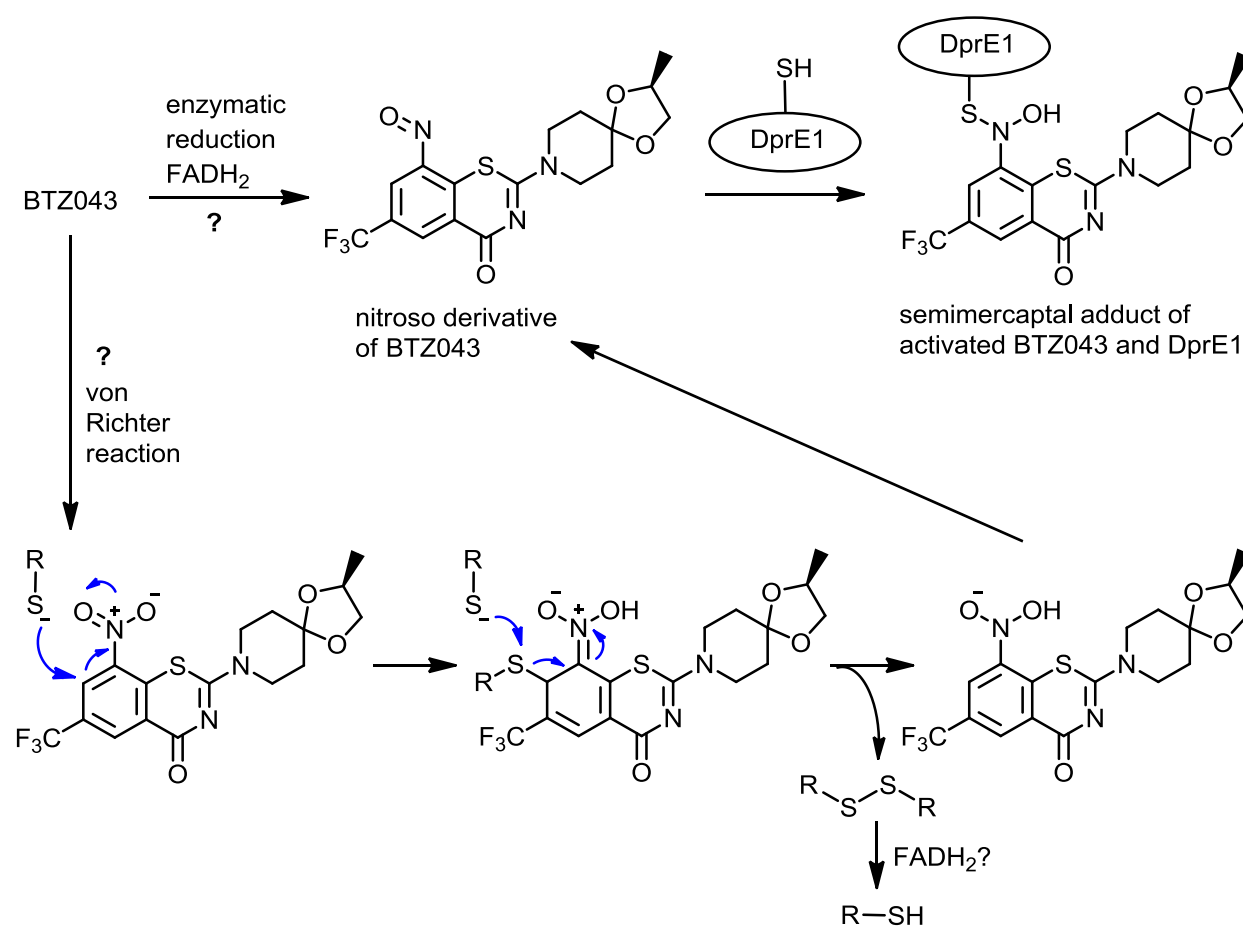


Figure 6: Proposed mechanism of action of BTZ043: reduction to nitroso-BTZ043 via FADH₂ or von Richter reaction, subsequent formation of stable „semimercaptal“ with Cys387 of DprE1, modified after Trefzer et al.⁵⁵ and Tiwari et al.⁶²

The covalent bond between BTZ043 and DprE1 was confirmed by the crystal structure of BTZ-related compound CT325 with *Mtb* DprE1⁶³ and BTZ043 with *M. smegmatis* DprE1.⁵⁷ Benzothiazinones appear to be suicide inhibitors of DprE1, because their bioactivation (reduction of nitro to nitroso) most likely occurs through DprE1 itself after BTZ043 is non-

covalently bound inside the DprE1 binding pocket, utilizing FADH₂ that results from the reduction of FAD cofactor via oxidation of DPR to DPX.^{57,58} The mode of bioactivation of BTZ043 is not yet fully understood, and another possible reduction mechanism was reported recently by Tiwari et al.⁶² The authors' experiments provided evidence that thiolates, such as the SH group of Cys387, are capable of reducing nitro groups to nitroso intermediates via the von Richter reaction (Figure 6).⁶⁴

Whatever the mechanism of the formation of the active nitroso metabolite is, once it is formed, it reacts with the Cys387 (Cys394 in *M. smegmatis*) to form the covalent BTZ-DprE1 adduct. This type of inhibition is very efficient and could explain the extremely low MICs of BTZ043.^{58,63}

A mechanism of resistance against BTZs has been demonstrated by genome sequencing of spontaneously resistant mutants. All resistant mutants carried a missense mutation in *rv3790*, which resulted in the exchange of the amino acid Cys387 in the active center for serine or glycine. This single amino acid exchange also explained the innate resistance of *M. aurum* and *M. avium* to BTZs, which carry alanine or serine at the corresponding positions.⁵⁴ Strangely, this missense mutation was not found in any of the clinical isolates of *Mtb* tested for BTZ043 sensitivity.⁵² Another mechanism of resistance was found in *M. smegmatis*, in which over-expression of the mycobacterial nitroreductase NfnB led to increased resistance against BTZ043 (reduction of nitro to amino group). While no NfnB homologue is present in *Mtb*, Manina et al. demur that 13 putative nitroreductases have been identified in the genome of *Mtb*. However, none of them led to BTZ043-resistance when over-expressed. But since the amino metabolite of BTZ043 (BTZ045) was found in blood and urine of mice, this strongly suggests that either host or mycobacterial nitroreductases are capable of inactivating BTZs by reducing their nitro group.^{60,65} However, clinical resistance to BTZ043 is very unlikely, since mutations in the target DprE1 are accompanied by a strong negative effect on bacterial fitness and therefore are very rare, arising at a frequency of 10⁻⁸.^{54,60}

The elucidation of BTZ043's mechanism of action as inhibition of the biosynthesis of essential cell wall building blocks explains its poor activity both in vitro and in vivo against non-replicating *Mtb* (SS18b, streptomycin-starved *Mtb* 18b, in vitro: reduction of CFU < 1 log after seven days of treatment; in vivo mouse model: reduction of CFU 0.5 log after eight weeks), since cell wall synthesis is only important for actively growing bacilli.⁶⁶

A drawback of these first generation benzothiazinones is their poor solubility in aqueous media. Several research groups have developed 2-piperazinyl-substituted second generation benzothiazinones (PBTZ) to overcome solubility problems by forming salts with the basic nitrogen atom of the piperazinyl ring system.⁶⁷⁻⁶⁹ The novel compounds PBTZ169 and PBTZ A (Figure 7) comprise even better or equal MICs than their ancestor BTZ043 (MIC PBTZ169: *Mtb* H37Rv ≤ 0.19 ng/ml; MIC PBTZ A: *Mtb* 2745/09 MDR 30 ng/ml; MIC BTZ043: *Mtb* H37Rv 1 ng/ml, *Mtb* 2745/09 MDR ≤ 15 ng/ml)^{67,69} and therefore might serve as highly active back-up compounds.

Both fluoroquinolones were well tolerated in long-term administrations. To date, the promising results from these studies raise hope that fluoroquinolones could shorten the treatment duration from 6-8 to 4 months and become a permanent component of the first-line DOTS regimen by 2015.^{33,34}

Fluoroquinolones target the topoisomerase II and subsequently lead to DNA double strand breaks which are fatal for bacteria.⁷¹ Since DNA replication is only essential in actively growing bacilli, fluoroquinolones are not active against dormant mycobacteria and persisters. However, their good in vivo activity and favorable safety profile render them essential novel drugs in the treatment of TB.³⁴

The structural similarity of small drug molecules of fluoroquinolones and benzothiazinones and the antimycobacterial activity of both compound classes motivated us to design novel molecules which comprise structural elements of fluoroquinolones and benzothiazinones to obtain dual action antibiotics.

Dual action antitubercular drugs could lead to simplified treatment regimens of TB. Recently, Wang et al. identified the novel DprE1 inhibitor TCA1, which also targets MoeW, an enzyme in molybdenum cofactor synthesis. Molybdenum cofactors are essential for nitrate assimilation and thus indispensable for *Mtb* survival in media that contain nitrate as nitrogen source. Nitrate environments are associated with subpopulations of persistent bacilli, thus TCA1 showed activity against replicating and non-replicating bacteria and is the first compound with this unique dual mode of action in TB drug development.⁷²

1.6 OBJECTIVE OF THESIS

Benzothiazinones are very potent and promising antitubercular agents in preclinical development. To date, three members of this structural scaffold have been reported for its excellent in vitro and in vivo activity, but studies on extensive structure activity relationships are rare. The present work will address the synthesis of novel structural analogs of BTZ043. In particular, the chemical space at the arene moiety, introducing different substituents at positions 6 and 7 will be investigated. Furthermore, the influence of the position 2 substituent on BTZ activity will be investigated by introducing different cyclic amines as well as aryl and heteroaryl substituents.

The introduction of branched amino substituents at position 2 will also address a possible sterical effect on the stability of the sulfur atom of the BTZ scaffold, for example enhancing metabolic stability by sterical shielding towards oxidation processes to sulfoxides and sulfones.

In a second approach, the sulfur will be exchanged by its bioisoster oxygen, in order to avoid possible oxidation reactions at the sulfur during metabolic turnover. The in vitro activity of this novel compound class – the benzoxazinones – will be investigated in order to evaluate the influence of the sulfur exchange on activity and in order to introduce a novel chemical scaffold to the antitubercular drug development.

Lead BTZ043 was synthesized in a 7-step synthesis. Alternative published synthetic pathways to BTZs consist of 4-7 steps. In most cases, the introduction of the heterocyclic sulfur necessitates the use of toxic carbon disulfide. Considering a possible clinical development for BTZ043 or PBTZ169, the synthesis of the compound must follow GMP regulations and therefore should avoid toxic reagents and solvents. Therefore, a main part of this thesis will evaluate the applicability of the different synthetic pathways to BTZs and aim on the development of an easier and faster synthetic approach. The novel synthetic pathway should be robust, GMP compliant and easily adaptable to give a variety of different congeners.

This thesis will also address the design and synthesis of dual action compounds, which unite essential pharmacophores of two different antimycobacterial scaffolds: benzothiazinones and fluoroquinolones. Combining benefits of the fluoroquinolone compound class (antimycobacterial activity in vitro and in vivo, well tolerated) with the highly active benzothiazinones could introduce a novel antitubercular compound class with a dual mode of action, viz. the thiochromenones.

Antimycobacterial activity will be determined for all novel benzothiazinone and benzoxazinone compounds to evaluate the impact of modifications of the scaffold and derive structure activity relationships.

Chapter Two

2 SYNTHESSES

This chapter will give an overview of all compound classes (Figure 9) that were synthesized for this thesis. The main attention is drawn to the benzothiazinone (BTZ) scaffold (chapter 2.1 - 2.2). In a second approach, derivatives of the most active BTZs with replacement of the sulfur by oxygen, the benzoxazinones (BOZ) will be discussed (chapter 2.3). The last chemical scaffold described in this thesis belongs to the class of thiochromenones (chapter 2.4).

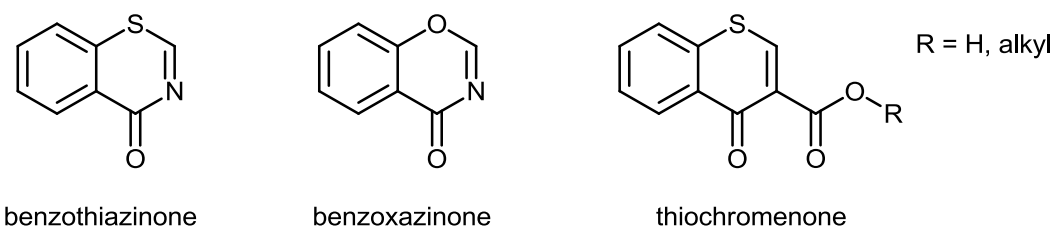


Figure 9: Chemical scaffolds of substances described in this thesis

2.1 SYNTHETIC PATHWAYS TO BENZOTHIAZINONES

Benzothiazinones are a class of sulfur and nitrogen containing heterocyclic compounds that has attracted little attention in the past. So far, no approved drug compound belongs to the 4*H*-1,3-benzothiazin-4-ones. (SciFinder and www.drugbank.ca research, accessed on 06.08.2013).

Several synthetic pathways have been described in the past for the synthesis of the substructure of 2-amino-4*H*-1,3-benzothiazin-4-one. The common starting point of all pathways are substituted 2-chlorobenzoic acid derivatives. The different synthetic strategies to build the heterocyclic ring system are depicted in Figure 10 and described in detail in the following paragraphs.

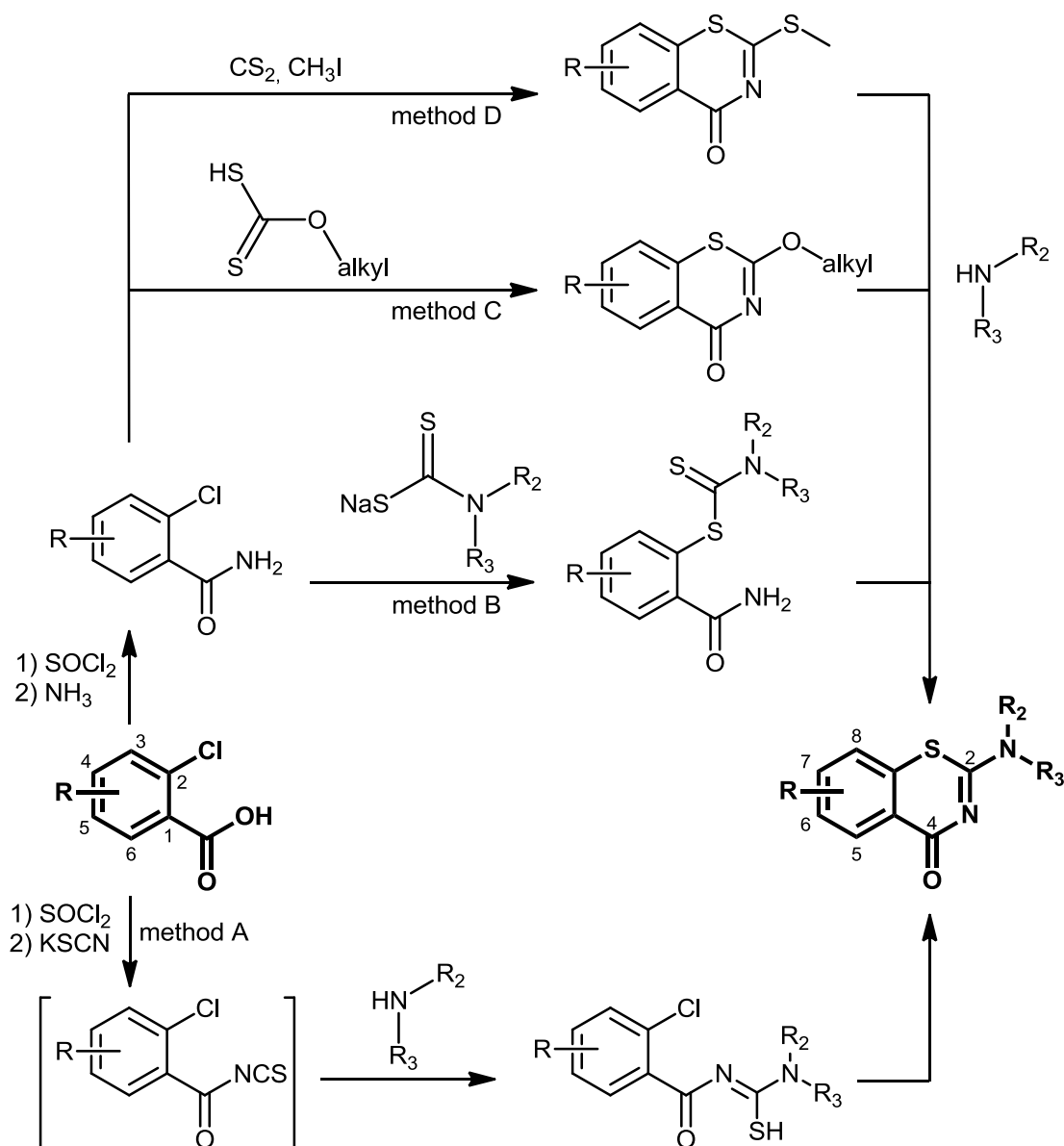


Figure 10: Synthetic pathways to 2-amino-4H-1,3-benzothiazin-4-ones

Paragraphs 2.1.1-2.1.5 will give an overview of all approaches to BTZs used in the literature to synthesize antitubercular BTZs. Paragraph 2.1.5 will shortly summarize a novel synthetic route developed by us. The practical evaluation of some of the methods will be described later (2.1.6 and 2.2).

2.1.1 Method A – the classic pathway

Method A is also referred to as classic benzothiazinone synthesis.^{53,73} In dependence upon previous reports,⁷⁴⁻⁷⁶ 2-chlorobenzoylchloride derivatives are treated with potassium-, sodium- or ammonium thiocyanate to form the intermediate acylisothiocyanates by the halogenide-pseudohalogenide replacement. Acylisothiocyanates are highly reactive intermediates,⁷⁵ which are instantly treated with the corresponding secondary amines to form a thiourea derivative, which subsequently undergoes ring closure by nucleophilic substitution of the aryl halide. This last step is particularly favored if nitroarenes are used

since the $-I$ effect of the neighboring nitro group increases the electrophilicity of the carbon atom and accelerates the nucleophilic attack of the sulfur.

2.1.2 Method B – dithiocarbamate pathway

Method B was developed by Makarov et al., the inventors of BTZ043, as an alternative to the classic BTZ synthesis.⁵³ The treatment of 2-chlorobenzcarboxamides with alkali salts of dithiocarbamates yields the intermediate 2-dithiocarbamoylbenzcarboxamides, which are subsequently treated with weak bases to complete the ring closure. Optimization of this procedure was reported by the same authors two years later by circumventing the last step of ring closure when the starting 2-chlorobenzcarboxamides are treated with excess of dithiocarbamate salts at higher temperatures.⁷³ A drawback of this procedure is the required derivatization of the amino moiety to dithiocarbamate reagents.

2.1.3 Method C – alkylxanthogenate pathway

Method C was described and patented by the BTZ043 inventors as a second alternative to the classic pathway.⁷³ The starting material 2-chlorobenzcarboxamide is treated with alkylxanthogenates to build the benzothiazinone scaffold. The amine substituent at position 2 is introduced in the last step, leaving a higher potential for quick variations at position 2. However, compared to method B, method C does not save any steps in the synthesis of BTZ043 when summing all synthetic steps.

2.1.4 Method D – alkylsulfanyl BTZ pathway

In 2011, Makarov developed another synthetic pathway for the synthesis of antitubercular benzothiazinone derivatives (method D)⁷⁷ with the advantage of adding the amine moiety to a stable 2-(alkylsulfanyl)-4*H*-1,3-benzothiazin-4-one intermediate. This procedure circumvents the derivatization of the amine substituent (e.g. dithiocarbamates in method B) and can easily be adapted for automatic combinatorial chemistry purposes with quick variations of the amine moiety at position 2. Compared with the previously reported method B, method D saves one step of the formation of dithiocarbamates in the synthesis of BTZ043. Compared to method C, the formation of alkylxanthogenates is economized in Makarov's new procedure. A severe drawback of method D is the use of toxic methyl iodide as well as toxic and very flammable carbon disulfide.

2.1.5 Method E – a new pathway: thiourea pathway

To facilitate the synthesis of benzothiazinones we created a new synthesis, in which the sulfur and nitrogen of the benzothiazinone scaffold are incorporated during one step (Figure 11). This is realized by the use of asymmetrically substituted thiourea reagents. The 2-amino-4*H*-1,3-benzothiazin-4-one scaffold is divided into two parts – the arene moiety and the heterocyclic 2-amino-substituted moiety. This approach is also suitable for combinatorial chemistry purposes and, in the case of BTZ043, would require only five synthetic steps: one step for the formation of the arene, two steps for the formation of the thiourea moiety, and finally two steps for the formation of the BTZ system.

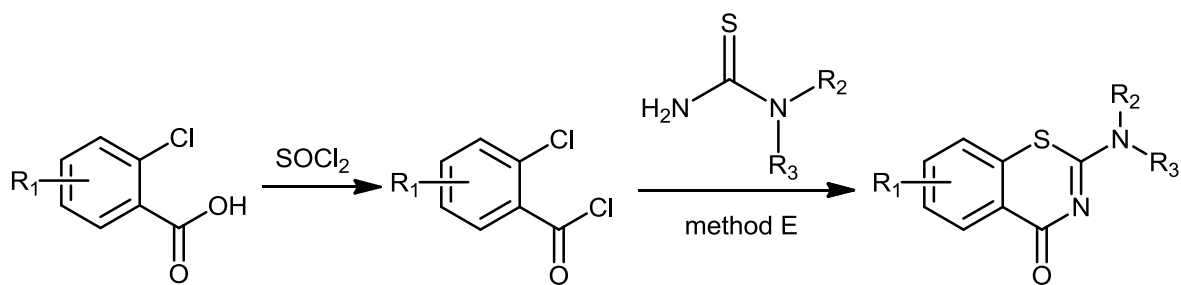


Figure 11: Synthesis of 2-amino-4H-1,3-benzothiazin-4-one derivatives via thiourea reagents

A second advantage of this procedure is the avoidance of toxic reagents, such as methyl iodide and carbon disulfide. The procedure has been included in a patent application to the German Patent Office as a new process for the formation of 2-amino-4H-1,3-benzothiazin-4-ones (AZ DE102012012117.2; 20.06.2012).

The synthesis of BTZs via thiourea reagents theoretically could lead to two different products, 1,3-BTZs and 3,1-BTZs (Figure 12). In the latter case, the nitrogen atom (rather than the sulfur) would undergo a $S_{\text{N}}\text{AR}$ reaction to replace the aryl chloride. Subsequently, the sulfur would attack the carboxyl carbon to form a thioester. Although this is a possible reaction, it is unlikely. According to the “hard and soft acids and bases” (HSAB) theory, nitrogen is the harder nucleophile and would preferentially attack the carboxyl carbon, which is the harder electrophile. Sulfur as the soft nucleophile preferentially replaces the aryl chloride in the $S_{\text{N}}\text{AR}$ reaction, since the aryl carbon is the softer electrophile compared to the carboxyl carbon. Accordingly, any side products referring to the 3,1-BTZs (or 3,1-BOZs, compare chapter 2.3.1) were never identified when analyzing products and side products of the respective reaction steps. The existence of 1,3-BTZs and 1,3-BOZs was extensively investigated and confirmed by ^{13}C NMR and IR analyses of the reaction products of the corresponding trials.

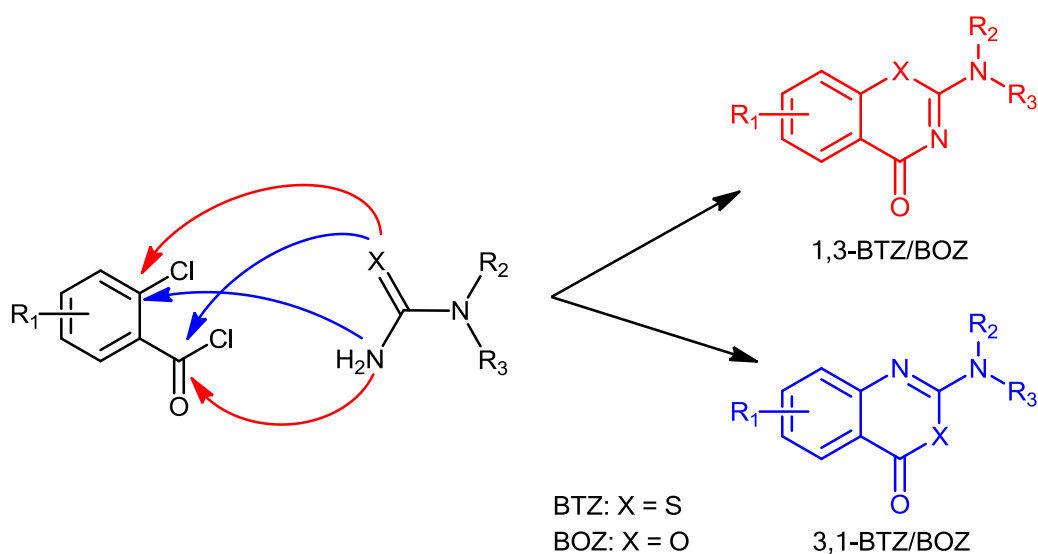


Figure 12: Possible formation of 1,3-BTZ/BOZ and 3,1-BTZ/BOZ via the synthetic method E

2.1.6 Evaluation of the synthetic routes

The applicability of different synthetic pathways was evaluated with a set of model compounds with simple amines (piperidine, **IR 20**, and morpholine, **IR 58**) at position 2 and fixed substituents at the arene moiety (Figure 13).

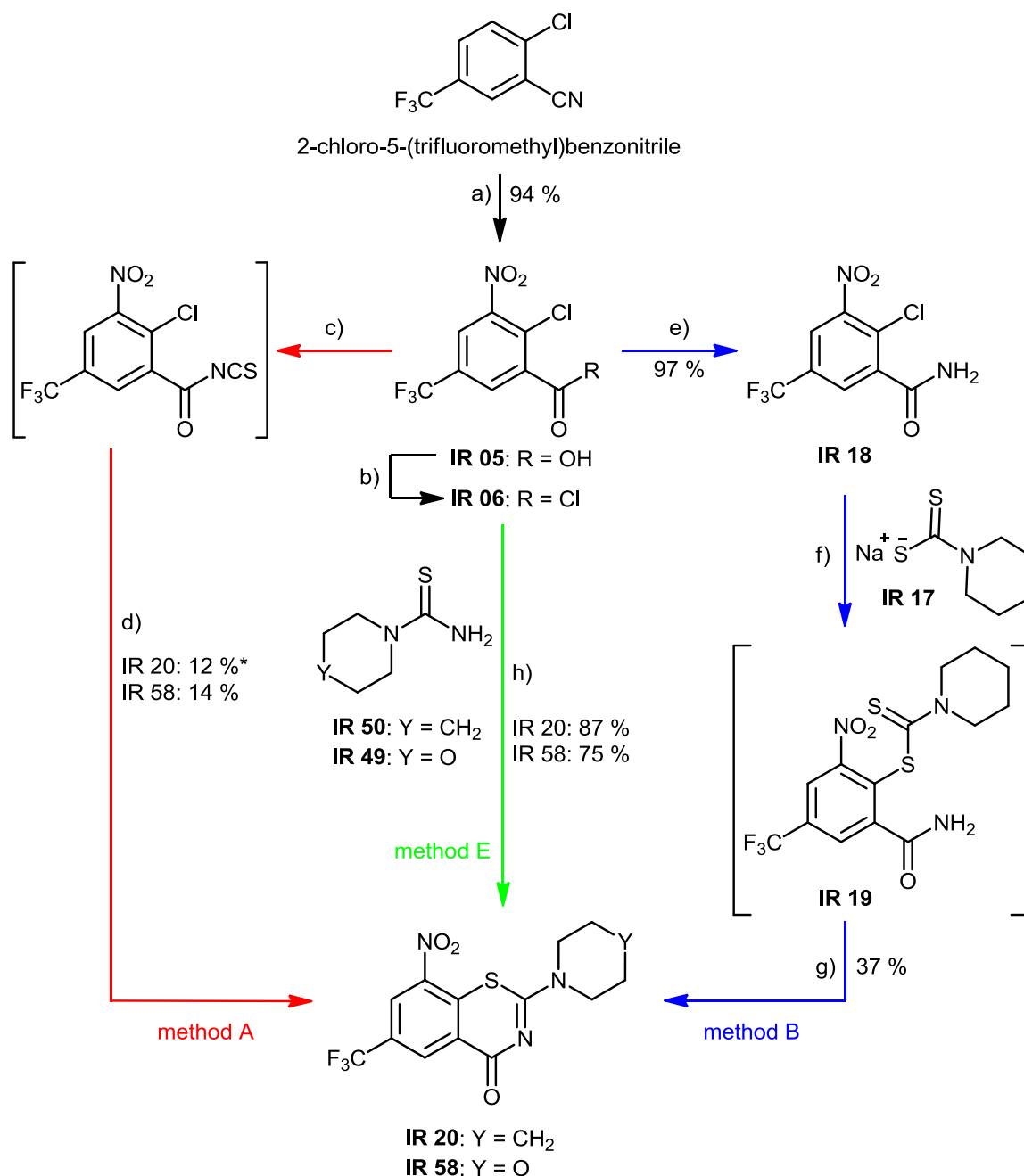


Figure 13: Comparison of synthetic pathways for **IR 20** and **IR 58**

Reaction conditions: a) H_2SO_4 100 %, HNO_3 100 %, 10 °C → 120 °C, 45 min; b) $SOCl_2$, toluene, reflux, 2 h; c) **IR 58**: argon atmosphere, **IR 06**, $KSCN$, acetone, rt → 40 °C, 5 min; **IR 20**: argon atmosphere, **IR 06**, $NaSCN$, acetone, 5 °C, 2h; d) **IR 58**: argon atmosphere, morpholine, acetone, rt, 30 min → reflux, 2 min; *adapted temperature: **IR 20**: argon atmosphere, piperidine, acetone, 12 °C → 22 °C, 2 h; e) **IR 06**, aq. NH_3 25 %, -20 °C, 10 min; f) **IR 17**, ethanol, rt, 20 h; g) Na_2HPO_4 , ethanol, reflux, 6 h; h) **IR 06**, toluene, 70 °C → 90 °C, 2 h

The classic benzothiazinone pathway ‘method A’ was tested first (Figure 13, red arrows).⁷⁴⁻⁷⁶ Commercially available 2-chloro-5-(trifluoromethyl)benzonitrile was nitrated with nitrosulfuric acid, including acid saponification of the nitrile group, according to Welch et al.⁷⁸ to yield the arene core **IR 05**. Subsequently, KSCN was treated with the benzoylchloride **IR 06** to yield the intermediate acylisothiocyanate, which was immediately treated with either morpholine or piperidine to obtain the benzothiazinones **IR 58** and **IR 20**. It is noteworthy that in both cases a variety of by-products were visible on TLC. The isolated main product of the trial with piperidine was the benzamide derivative **IR 13** (Figure 14), instead of the desired BTZ **IR 20**, which was only detected in the reaction mixture via GC-MS. The formation of the benzamide derivative **IR 13** implicates that the nucleophilic attack of the piperidine nitrogen atom occurs at the carboxyl carbon rather than the thiocarbonyl carbon of the acylisothiocyanate intermediate (Figure 14). Although BTZ **IR 58** was isolated in sufficient yield (14 %) for structure determination and assays, the corresponding benzamide by-product **IR 150** was formed in about equal amount (yield 13 %, Figure 14).

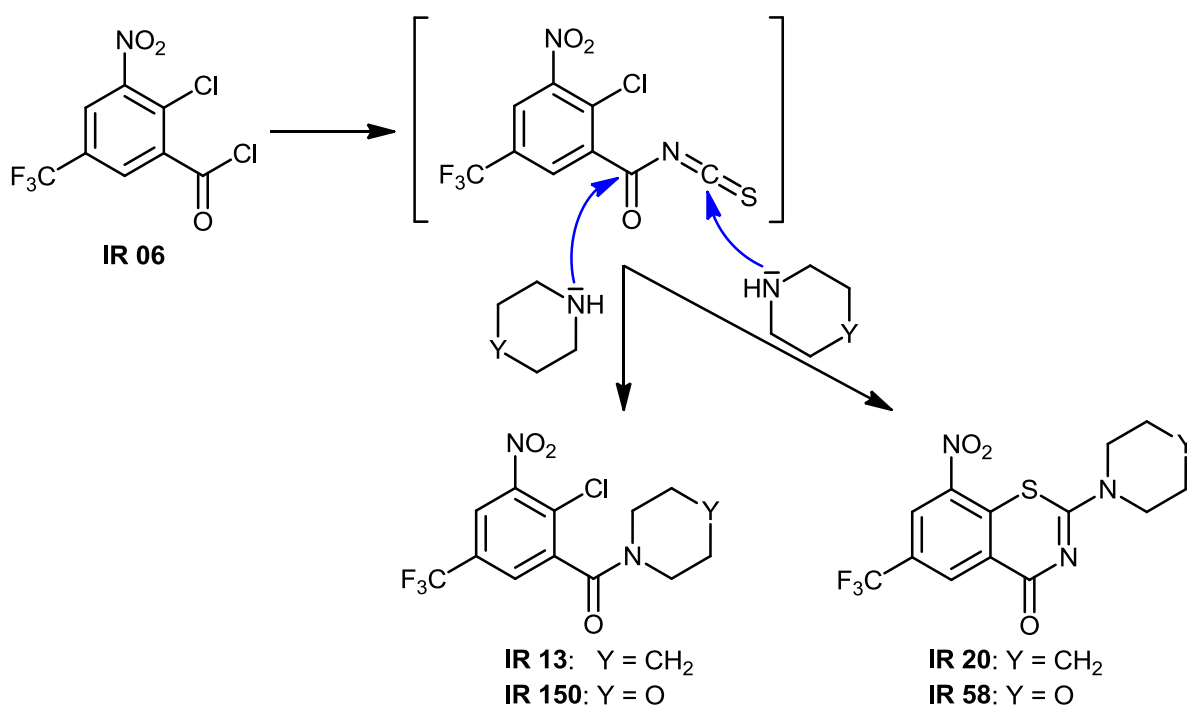


Figure 14: Nucleophilic attack at carboxyl or thiocarbonyl carbon in the classic pathway method A

Investigating the reasons for the different formation of the benzamide by-products of morpholine and piperidine in the classic BTZ synthetic pathway drew the attention to the basicity of both amines. The pK_B values of piperidine and morpholine are 2.78 and 5.64.⁷⁹ The stronger basicity of piperidine correlates with higher nucleophilicity. This strong nucleophilicity may cause piperidine to not distinguish between the two electrophilic centers in the acylisothiocyanate intermediate – the carboxyl and the thiocarbonyl carbon. The HSAB theory suggests that piperidine is a ‘harder’ nucleophile than morpholine due to a higher electron density at the nitrogen. Within the acylisothiocyanate intermediate, the carboxyl carbon is the ‘harder’ electrophile, since it is influenced by the strong electron-withdrawing

effect of the neighboring arene with strong $-I$ substituents (NO_2 and CF_3). In comparison, the thiocarbonyl carbon has a higher electron density because of better polarizability influenced by the neighboring sulfur and therefore serves as a 'softer' electrophile. This could explain why the thiocarbonyl carbon is more prone to the attack of the morpholine, whereas piperidine as a 'hard' nucleophile prefers the carboxyl carbon as a 'hard' electrophile (Figure 14).

To avoid the undesired attack at the carboxyl carbon, a trial with lower temperatures according to Seybold and Hartmann^{80,81} was undertaken, and for **IR 20**, the desired BTZ product was obtained in sufficient amount (yield 12 %). Notwithstanding, the benzamide **IR 13** was visible as side product on TLC in this trial as well. In conclusion, decreasing the temperature was a benefit for the route to BTZs via method A.

The unsatisfactory implementation of method A to synthesize **IR 20** led to the application of patented 'method B' (Figure 13, blue arrows).⁵³ The core arene **IR 06** was treated with aqueous ammonia, yielding the corresponding 2-chloro-3-nitro-5-(trifluoromethyl) benzamide **IR 18** in almost quantitative yield. In the next step the sulfur of the benzothiazinone scaffold was introduced utilizing dithiocarbamate salt **IR 17** (synthesized from carbon disulfide, piperidine, and NaOH according to Lieber et al.⁸²). In contrast to the reported method B,⁵³ the isolation of the intermediate 2-carbamoyl-6-nitro-4-(trifluoromethyl)phenyl piperidine-1-carbodithioate (**IR 19**) was cumbersome. TLC and mass spectra, however, showed that some BTZ **IR 20** had already formed. Therefore, the crude reaction mixture of the intermediate was subsequently treated with Na_2HPO_4 in refluxing ethanol to complete ring closure to yield **IR 20**.

Since the number of steps to build the BTZ scaffold in 'method B' was even larger than in method A (five versus four steps, not counting the synthesis of the dithiocarbamate reagent) we developed our own original pathway – 'method E' – in order to decrease the number of steps and facilitate the synthesis by introducing the sulfur and nitrogen of the BTZ ring in one step. The core arene **IR 06** was treated with thiourea derivatives **IR 49** and **IR 50** (synthesis according to Seybold and Hartmann;^{80,81} the synthesis via aminolysis reaction according to Barry et al.⁸³ failed) in toluene for 2 h to yield the BTZs **IR 58** and **IR 20** in very high yields of 75 % and 87 %. The formation of side products was considerably decreased compared to both other methods tested (TLC), which simplified work-up procedure (flash chromatography with TBME on normal phase silica gel).

The comparison of the three methods clearly shows the superiority of the novel method E (Table 2): decreased number of steps, increased overall yield, avoidance of toxic reagents (e.g. CS_2) as well as toxic and problematic cleavage reagents (e.g. H_2S).

Makarov et al. described the synthesis of BTZ043 in 7 steps with 36 % overall yield.⁵⁴ Compared with related BTZ derivatives **IR 20** and **IR 58**, overall yields of the novel method E are considerably higher (82 % and 71 %). The avoidance of H_2S as cleavage reagent is particularly beneficial, since H_2S could lead to lower yield due to side reactions. Thus,

Makarov also designed a pathway without evolving H₂S during the synthesis of BTZs, but his alkylsulfanyl BTZ pathway still comprises methyl iodide as a toxic and alkylating reagent (method D, Figure 10).⁷⁷ The feasibility of methods C and D was not evaluated for BTZs **IR 20** and **IR 58**.

Table 2: Comparison of synthetic pathways to build the BTZ scaffold

	method A	method B	method C	method D	method E
number of steps	4	5	5	5	3
introduction of heterocyclic nitrogen & sulfur	KSCN	dithio-carbamate salt, benzamide	alkylxanthogenate salt, benzamide	CS ₂ , benzamide	thiourea derivative
toxic reagents	–	CS ₂	CS ₂	CS ₂ , CH ₃ I	–
cleavage reagents	HCl	H ₂ S, HCl	HCl, H ₂ S, ethanol	HCl, HI, CH ₃ SH	HCl
by-products	benzamide				
overall yield	11 % (IR 20)* 13 % (IR 58)	34 % (IR 20)	not tested	not tested	82 % (IR 20) 71 % (IR 58)

*adapted temperature

2.1.7 Unfamiliar NMR spectra

Proton NMR spectra of **IR 20** and **IR 58** revealed poorly resolved signals for the methylene groups next to the nitrogen atom attached to the benzothiazinone heterocycle (10/14-H). Instead of multiplets, the four protons give one broad wavy signal. The same phenomenon was observed in the carbon NMR spectra. Instead of two sharp singlets for C-10/14 and C-11/13, these atoms give broad singlets of low intensity (Figure 15).

This NMR behavior was investigated with N-[(2-chlorophenyl)-carbonyl]piperidine-1-carboimidothioic acid (**IR 12**, compare chapter 2.2.1) as model compound and found to be temperature-dependent. At 27 °C, carbon signals for the methylene groups C-2 and C-6 as well as C-3 and C-5 are slightly separated and poorly resolved. Increasing the temperature to 60 °C led to a merging of the carbon signals for the nitrogen-neighboring methylene groups C-2/C-6 to give a sharp singlet. This effect is visible for the methylene groups C-3/C-5 as well (Figure 16). It indicates a slow rotation of the single bond connecting piperidine and BTZ scaffold, which is enhanced by temperature. Forsyth et al.⁸⁴ studied specific rotations of N-alkyl substituted 4-*tert*-butylpiperidines and also found a temperature-dependent separation of C-2 and C-6 signals in the ¹³C NMR spectra. The distinction of those two carbons is a result of a *gauche-gauche'* equilibrium shift of the alignment of the alkyl substituent and the lone electron pair of the piperidine nitrogen. Whereas in some cases, the shift separation of C-2 and C-6 was very small, it became more pronounced with bulky substituents at the nitrogen.⁸⁴

We believe that in the case of the benzothiazinone scaffold the rotation of the C-N single bond is hampered. The poor resolution of the nitrogen-neighboring methylene groups in ¹H and ¹³C NMR spectra was observed for all BTZ derivatives investigated in this thesis.

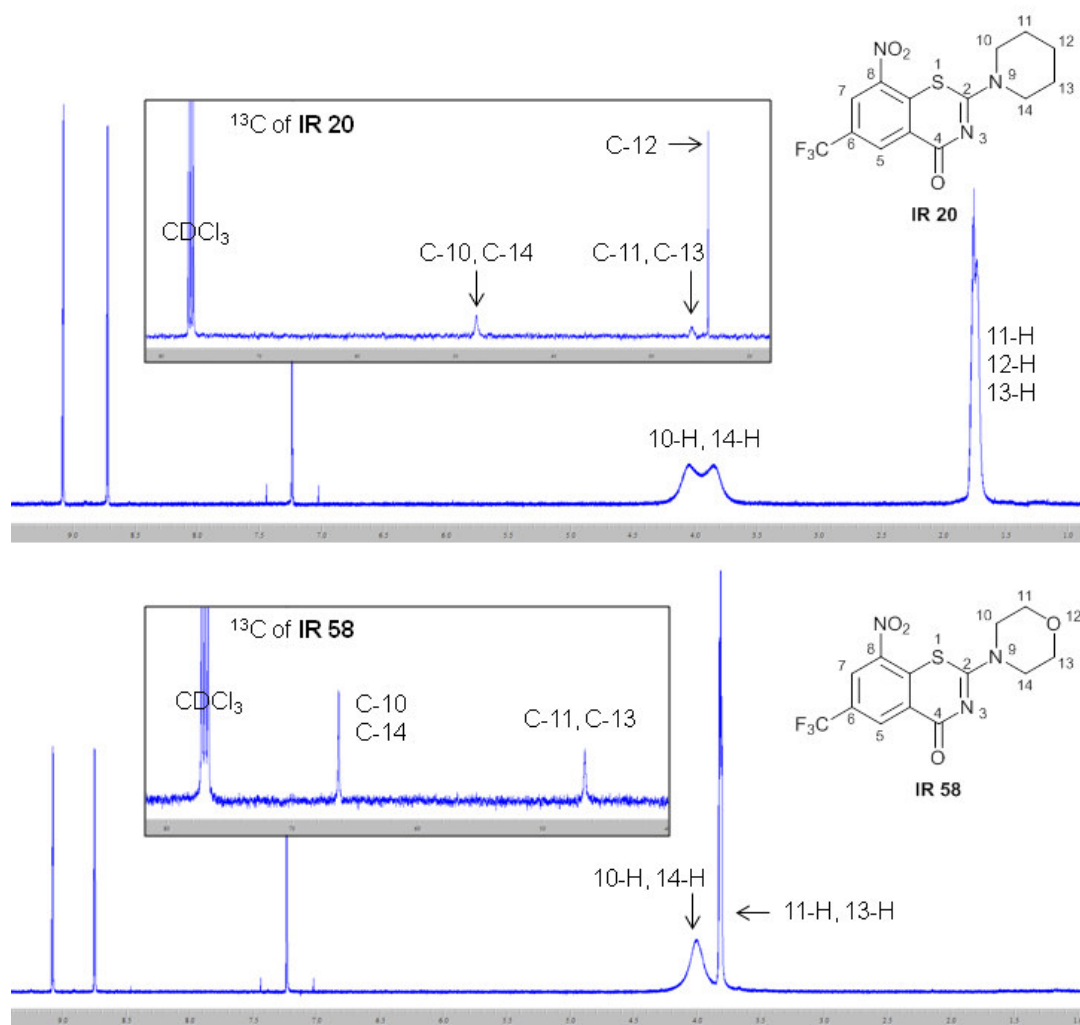


Figure 15: Proton and carbon NMR spectra of IR 20 (top) and IR 58 (bottom) in CDCl_3

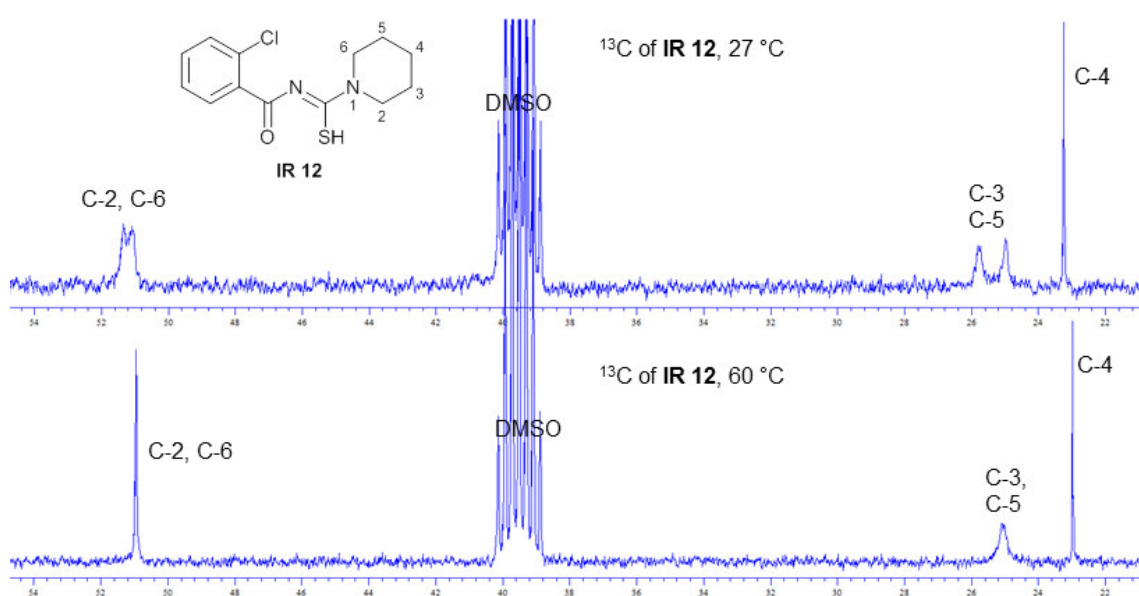


Figure 16: ^{13}C NMR spectra of IR 12 at 27 °C (top) and 60 °C (bottom), in DMSO-d_6

2.2 NOVEL BTZ DERIVATIVES

About 300 antimycobacterial BTZ derivatives are covered by the patents of Möllmann, Makarov, Cole, and Cooper et al.^{53,68,69,73} They all comprise the nitro group at position 8 as the essential pharmacophore.

In a first set of compounds, unsubstituted BTZs and BTZs with the nitro group at position 7 were synthesized by us to confirm the essentiality of the 8-nitro group for antimycobacterial activity (chapter 2.2.1 - 2.2.2).

The second set of novel BTZ derivatives addressed the effect of miscellaneous substituents at the arene moiety of the BTZ scaffold (chapter 2.2.3). Most BTZs for which MICs against different mycobacteria species are available possess the 8-nitro group and a second electron-withdrawing group at position 6 (e.g. NO₂, CF₃, CN). In 2008, Nosova et al. published a set of fluorine and morpholine containing BTZ derivatives with antimycobacterial activity (Figure 17).⁸⁵ Based on compounds 6a and 6h of Nosova et al., novel BTZs containing the 8-nitro group and fluorine, chlorine or amino substituents at position 7 were developed.

Chapter 2.2.4 will examine different substituents at position 2 of the BTZ scaffold, based on compound 6h of Nosova et al.⁸⁵ (Figure 17). The benefit of pyridyl- and phenyl substituents for antimycobacterial activity was investigated.

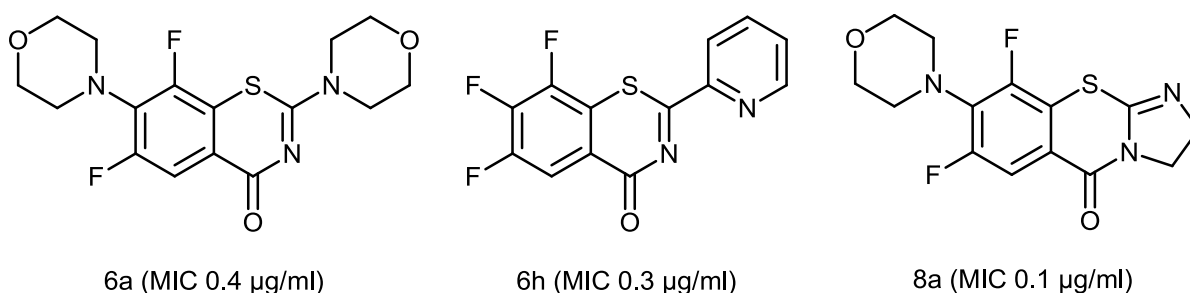


Figure 17: Compounds 6a, 6h and 8a of Nosova et al.⁸⁵ with MICs against *Mtb H37Rv*

In 2012, second generation BTZs with piperazinyl substituents at position 2 were reported by Makarov et al. and Cooper et al.^{68,69} Both research groups claimed that varying the substituents at position 2 could lead to a pharmacological “tuning” of the BTZs whereas the substituents at the arene moiety are more or less fixed. A set of BTZs with more complex amino substituents (compared to BTZ043) at position 2 was synthesized by us to examine the chemical space for variations at this position while maintaining or enhancing the antimycobacterial activity.

The last set of novel BTZ derivatives belongs to the class of imidazobenzothiazinones, which are also based on fluorine-containing imidazobenzothiazinones for which antimycobacterial activity was reported by Nosova et al. (compound 8a, Figure 17).⁸⁵ The influence on mycobacterial activity by merging the imidazobenzothiazinone scaffold with the essential nitro group was investigated (chapter 2.2.5).

2.2.1 Unsubstituted arene moiety

Benzothiazinone derivatives with an unsubstituted arene moiety were synthesized for proof of concept purposes to evaluate the essentiality of the nitro group for the antimycobacterial BTZs.

Starting from 2-chlorobenzoic acid, ring open intermediates **IR 12** and **IR 84** were synthesized via the classic pathway (method A).^{74,76} Ring closure did not occur easily since nucleophilic substitutions are difficult at the electron-rich unsubstituted arene π -system. To achieve ring closure, nucleophilicity of the thiol group had to be increased by deprotonation with sodium hydride in DMF, according to a previously described procedure.⁸⁶ Eventually, the BTZs **IR 16** and **IR 86** were obtained after two weeks of reaction time and purification via flash chromatography (Figure 18).

Implementation of the synthetic pathway method B⁵³ (Figure 18) failed, due to the aforementioned impeded nucleophilic attack of the sulfur of dithiocarbamate **IR 17** at the electron-rich arene **IR 24** and the fairly poor chloride leaving group (compare Liu et al.⁸⁷: appreciable product formation only occurred if aryl iodides were treated with different dithiocarbamate sodium salts). These trials as well as trials with thiourea derivatives according to method E were not pursued further. For unsubstituted BTZ derivatives **IR 16** and **IR 84**, the classic pathway method A seemed to be the pathway of choice.

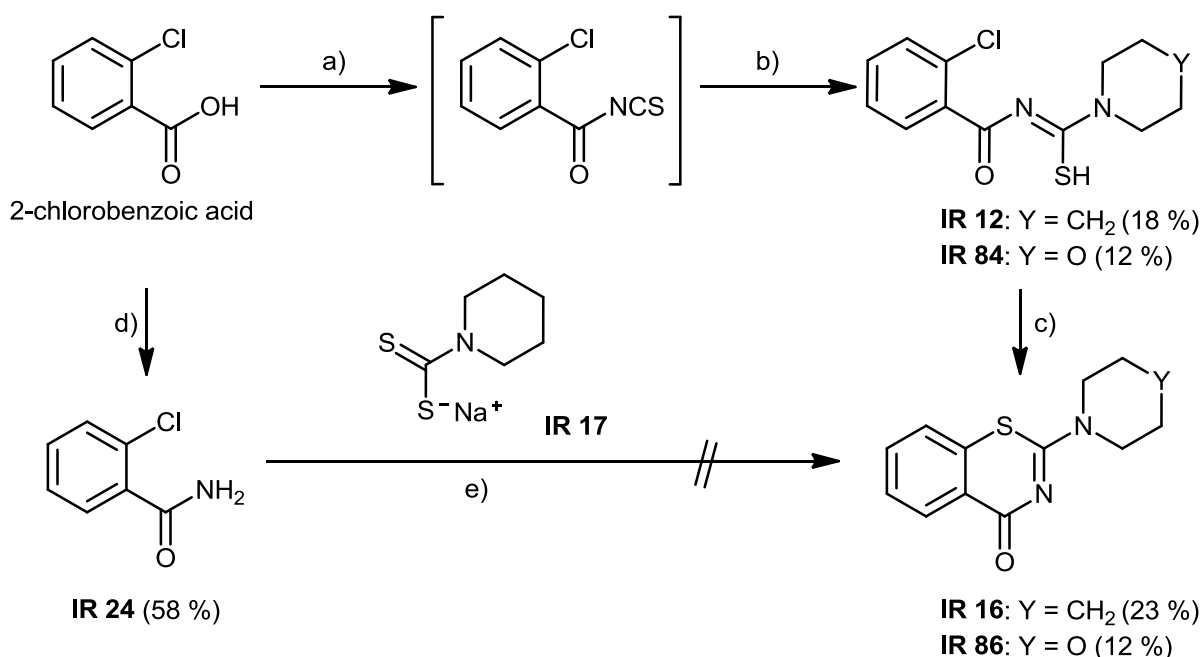


Figure 18: Synthesis of unsubstituted BTZs **IR 16** and **IR 86**

Reaction conditions: a) 1. SOCl₂, toluene, reflux, 2 h, 2. argon atmosphere, KSCN, acetone, rt → 40 °C, 5 min; b) argon atmosphere, piperidine (**IR 12**) or morpholine (**IR 84**), acetone, rt, 30 min → reflux, 2 min; c) argon atmosphere, NaH, DMF, 0 °C → 80 °C, 14 d; d) 1. SOCl₂, toluene, reflux, 2 h, 2. aq. NH₃ 25 %, -20 °C, 10 min; e) ethanol, rt → reflux, 20 h

2.2.2 Shifting the nitro group

Another approach to evaluate the essentiality of the nitro group at position 8 in the BTZ scaffold was shifting the nitro group to position 7, in meta position to the sulfur atom. The reaction conditions of the classic pathway (method A) were not applicable for the BTZ **IR 28** (Figure 19, blue arrows). Instead, only two different benzamide derivatives were isolated (Figure 19, green arrow). The formation of the piperidyl benzamide **IR 151** was due to the nucleophilic attack of piperidine at the carboxyl carbon, as described above in chapter 2.1.6. The formation of 2-chloro-4-nitrobenzamide was first thought to be due to the usage of ammonium thiocyanate, but the benzamide side product was also found in experiments with potassium thiocyanate, which indicates a hydrolysis of the intermediate acylisothiocyanate instead of the nucleophilic attack of the ammonium reagent at the 2-chloro-4-nitrobenzoylchloride.

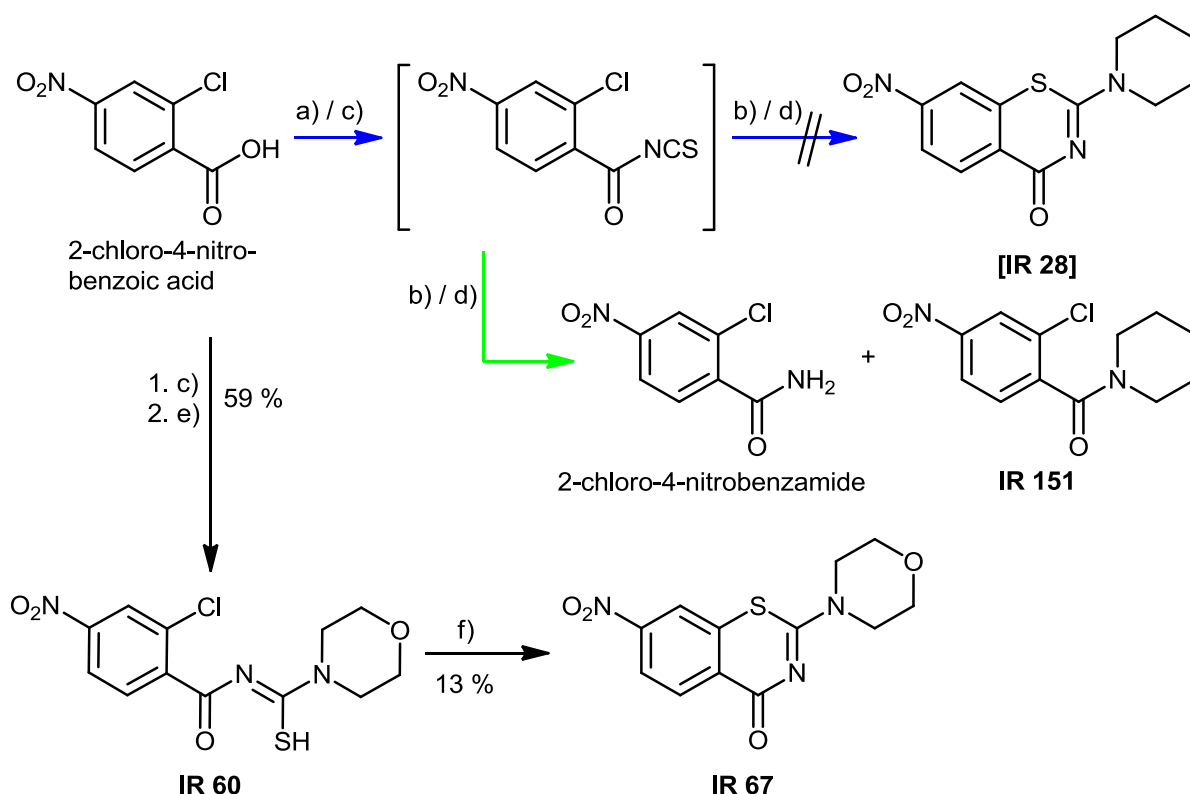


Figure 19: Synthesis of **IR 67** and **IR 28**

Reaction conditions: a) 1. SOCl_2 , toluene, reflux, 2 h, 2. argon atmosphere, $\text{KSCN}/\text{NH}_4\text{SCN}$, acetone, $\text{rt} \rightarrow 40^\circ\text{C}$, 5 min; b) argon atmosphere, piperidine, acetone, rt , 30 min \rightarrow reflux, 2 min; c) 1. SOCl_2 , toluene, reflux, 2 h, 2. argon atmosphere, NaSCN , 1,2-dichlorobenzene, SnCl_4 , 180°C , 2 h; d) piperidine, 1,2-dichlorobenzene, rt , 30 min; e) morpholine, 1,2-dichlorobenzene, rt , 30 min; f) acetone, rt , 28 d

Investigating reaction conditions for the preparation of acylisocyanates, Caubere et al.⁸⁸ described the formation of two different products when benzoylisocyanate **3** was treated with benzylamine **4**: N-benzylbenzamide **5**, indicating a nucleophilic attack of the amino group at the benzoyl-carbonyl carbon, and 1-benzoyl-3-benzyl urea **6**, where nucleophilic attack of the amino group occurred at the isocyanate-carbonyl carbon (Figure 20).

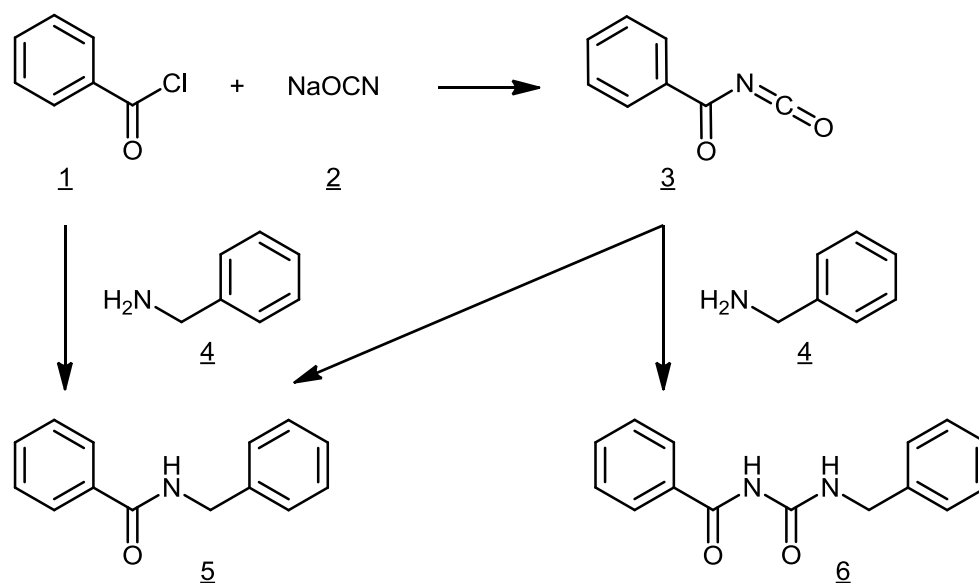


Figure 20: Formation of *N*-benzylbenzamide **5** and 1-benzoyl-3-benzyl urea **6**, modified after Caubere et al.⁸⁸

Caubere et al. found the formation of both products to depend on solvent and catalyst used, and after several studies, 1,2-dichlorobenzene as solvent and SnCl₄ as catalyst seemed to favor the formation of the 1-benzoyl-3-benzyl-urea **6**.⁸⁸

The transfer of Caubere's procedure to the preparation of BTZ **IR 28** failed (piperidinyl benzamide **IR 151** was formed again, see Figure 19, green arrow), however, ring-open morpholinyl acylthiourea **IR 60** precipitated from the reaction mixture and was isolated in good yield (Figure 19, black arrows). TLC investigations showed that ring closure to BTZ **IR 67** slowly occurred when **IR 60** was kept in acetone for several days, indicating that the polar aprotic solvent acetone and the electron withdrawing effect of the neighboring nitro group mediated the ring closure without the influence of an auxiliary base (Figure 19, black arrows).

2.2.3 Varying substituents at the arene

In 2008, Nosova et al.⁸⁵ published a set of fluorine containing derivatives of quinolones, quinazolinones, and benzothiazinones. Some of the benzothiazinones showed remarkable MICs against *Mtb* H37Rv (0.1 – 0.36 µg/ml). But the authors did not hypothesize about a mechanism of action of these fluorine containing BTZs. The similarity of these fluorine containing BTZs with the recently reported antimycobacterial 8-nitro-BTZs⁵⁴ led to the idea of merging structural properties of both BTZ subclasses, viz. introduction of fluorine, chlorine and amino substituents at positions 6 and 7 of the BTZ scaffold.

2.2.3.1 Arene starting materials

The application of the thiourea pathway (method E) requires two building blocks: appropriately substituted arene starting materials and thiourea derivatives. Only one nitro arene with particular substituents was commercially available, 2,4-dichloro-5-fluoro-3-nitrobenzoic acid. The synthesis of other nitro arenes will be described in the following

paragraphs, systematically elaborating the optimized synthetic protocols and implementing newer synthetic methods.

2-Chloro-4,5-difluoro-3-nitrobenzoic acid

2-Chloro-4,5-difluoro-3-nitrobenzoic acid **IR 29** was synthesized from 2-chloro-4,5-difluorobenzoic acid via nitration following previously described procedures.^{89,90} A side product of this nitration was 2-chloro-4,5-difluoro-1,3-dinitrobenzene (**IR 152**, Figure 21), which was isolated as a yellow oil in 10-16 % yield, implicating partial decarboxylation of the carboxyl group, presumably caused by heating the reaction mixture and a second electrophilic attack of nitronium ions.

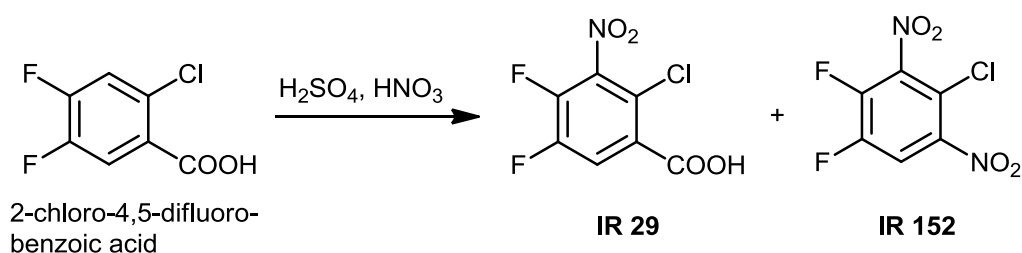


Figure 21: Synthesis of 2-chloro-4,5-difluoro-3-nitrobenzoic acid **IR 29** and side product 2-chloro-4,5-difluoro-1,3-dinitrobenzene **IR 152**

Reaction conditions: H₂SO₄ 100 %, HNO₃ 100 %, 110 °C, 2 h

According to the literature,^{91,92} nitration of various fluorine substituted benzoic acids was carried out at ambient temperature (rt) or at 0 °C, suggesting an investigation of the role of temperature (0 °C, rt, 60 °C, 110 °C). The resulting optimized reaction conditions for the formation of **IR 29** are the following: dropwise addition of 100 % nitric acid to a solution of 2-chloro-4,5-difluorobenzoic acid in 100 % sulfuric acid, stirring of the mixture at rt for 2 h, pouring onto crushed ice, filtration of the crude product and purification by flash chromatography. Higher temperatures promoted the formation of the dinitro derivative **IR 152** (compare trials no. III and IV, Table 3), lower temperatures (0 °C) resulted in insufficient conversion of the starting material (compare trial no. I, ≈ 20 % of crude product were starting material, detected via ¹H NMR spectra of crude product, Table 3).

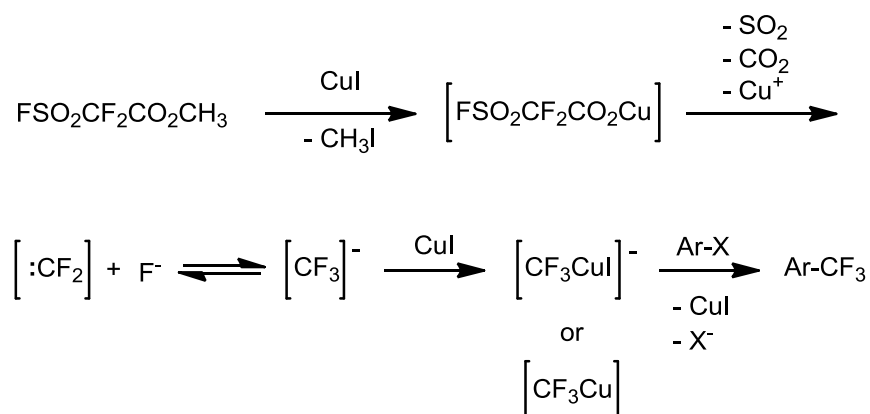
Table 3: Synthesis of **IR 29** with different reaction conditions

trial no.	I	II	III	IV
reaction temperature	0 °C	rt	60 °C	110 °C
reaction time	2 h	2 h	15 min	2 h
isolated IR 152	0 %	0.2 %	0.9 %	16.3 %
isolated IR 29	19 % (+ 5 % starting material in ¹ H NMR)	28 %	29 %	13.4 %

2,4-Dichloro-3-nitro-5-(trifluoromethyl)benzoic acid

For BTZ derivatives with the 6-trifluoromethyl group and a halide substituent at position 7, no suitable starting material was commercially available, hence, the trifluoromethyl substituted arene had to be synthesized from 2,4-dichlorobenzoic acid.

In 2011, Roy et al.⁹³ published a valuable and comprehensive review on trifluoromethylation agents. Methylfluorosulfonyldifluoroacetate (FSO₂CF₂CO₂Me, MFSDA) is the reagent of choice. It tolerates a number of substituents at the arene moiety, is air- and moisture stable and commercially available. Trifluoromethylation with MFSDA occurs easily at aryl halides, preferably iodine or bromine, utilizing CuI as catalyst. The proposed reaction mechanism is the formation of an active trifluoromethyl copper species [FSO₂CF₂CO₂Cu], which forms difluorocarbene [:CF₂] upon release of sulfur dioxide, carbon dioxide, and Cu⁺. The difluorocarbene is in equilibrium with trifluoromethide anion [CF₃]⁻, forming a complex with CuI [CF₃CuI]⁻, which is the actual nucleophilic reagent for the trifluoromethylation reaction (Figure 22).^{93,94} Iodine seems to be the best leaving group for these S_NAR reactions. The trifluoromethylation reaction does not tolerate acidic protons or water, hence, reactions have to be performed under dry conditions and acidic protons as in carboxylic acids have to be esterified.

Figure 22: Proposed reaction mechanism of trifluoromethylation of aryl halides with MFSDA^{93,94}

The complete reaction scheme of the synthesis of 2,4-dichloro-3-nitro-5-(trifluoromethyl)benzoic acid is depicted in Figure 23. 2,4-Dichlorobenzoic acid was iodized in a S_E reaction with iodine in H₂SO₄ as reported earlier.^{95,96} 2,4-Dichloro-5-iodobenzoic acid **IR 68** was subsequently esterified with ethanol in toluene in a Dean Stark apparatus according to the literature^{97,98} to yield ethyl 2,4-dichloro-5-iodobenzoate **IR 70** as a colorless oil with fruity smell. Trifluoromethylation of **IR 70** was carried out under argon atmosphere

in oven-dried glass ware in dry DMF with 1.6 equivalents MFSDA and 0.1 equivalents CuI. The procedure was robust and afforded similar yields when repeated with 3 or 1.5 equivalents MFSDA.

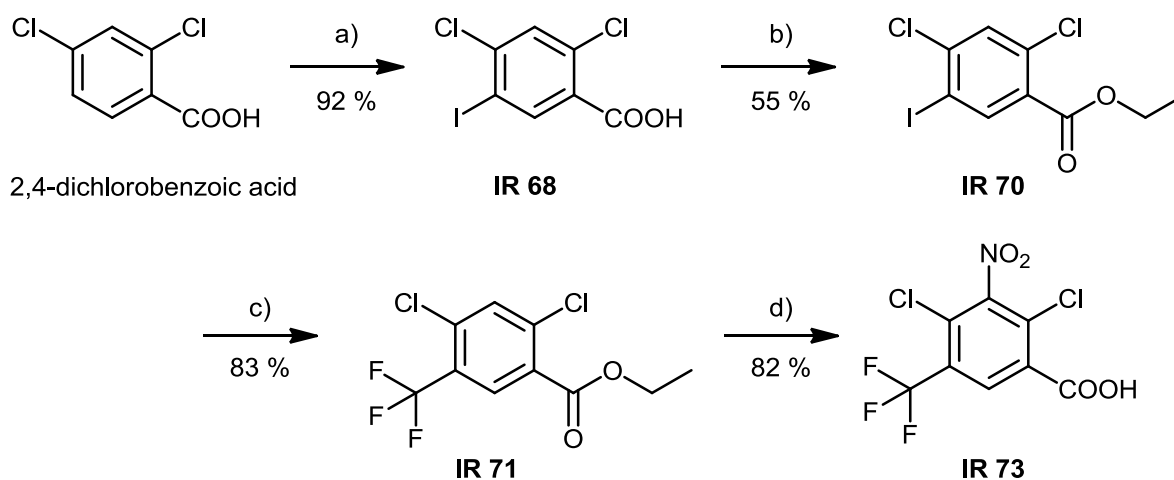


Figure 23: Synthesis of 2,4-dichloro-3-nitro-5-(trifluoromethyl)benzoic acid **IR 73**

Reaction conditions: a) NaIO_3 , I_2 , H_2SO_4 (95-97 %), rt, 12 h & 24 h; b) Dean Stark apparatus, ethanol, H_2SO_4 (95-97 %), toluene, reflux, 16 h & 24 h; c) argon atmosphere, CuI, MFSDA, DMF, 85 °C, 12 h; d) H_2SO_4 100 %, HNO_3 100 %, 10 °C \rightarrow 110 °C, 2 h

Mass spectra and the characteristic quartet signals in ^{13}C NMR (Figure 24) clearly confirmed formation of ethyl 2,4-dichloro-5-(trifluoromethyl)-benzoate **IR 71**. Nitration was carried out according to Welch et al.⁷⁸ and afforded 2,4-dichloro-3-nitro-5-(trifluoromethyl)benzoic acid **IR 73** in 34 % over-all yield. This is the first procedure reported for the preparation of compounds **IR 70**, **IR 71** and **IR 73**.

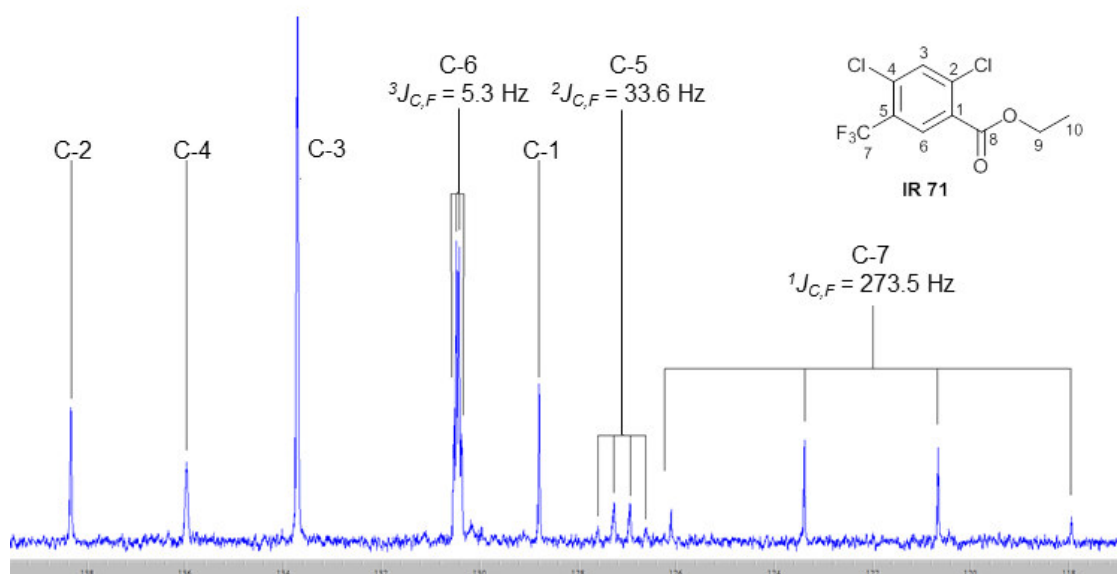


Figure 24: Part from ^{13}C NMR (116-140 ppm) of **IR 71**

2.2.3.2 Halide substituents

Inspired by the fluorine-containing BTZs of Nosova et al.,⁸⁵ a set of novel BTZs was developed, which conjoin the essential nitro group of antimycobacterial BTZs⁵³ with fluoride, chloride or trifluoromethyl substituents at position 7 and 6. Chloride next to the nitro group was chosen as almost “neutral” –I/+M substituent, fluoride as strong –I but weak +M substituent and trifluoromethyl at position 6 as strong –I substituent.

Two synthetic routes were evaluated: The previously described method B⁵³ and the novel pathway, method E. The dithiocarbamate pathway (method B) proved to be unsuitable. Starting from **IR 29** or commercially available 2,4-dichloro-5-fluoro-3-nitrobenzoic acid, the corresponding benzamides **IR 32** and **IR 39** were obtained after treatment with SOCl₂ and aq. NH₃. **IR 32** was treated with sodium (piperidin-1-yl)carbothioylsulfanide (**IR 17**) in ethanol at rt and subsequently refluxed with NaH₂PO₄. Unfortunately, no product formation was detectable with TLC (Figure 25).

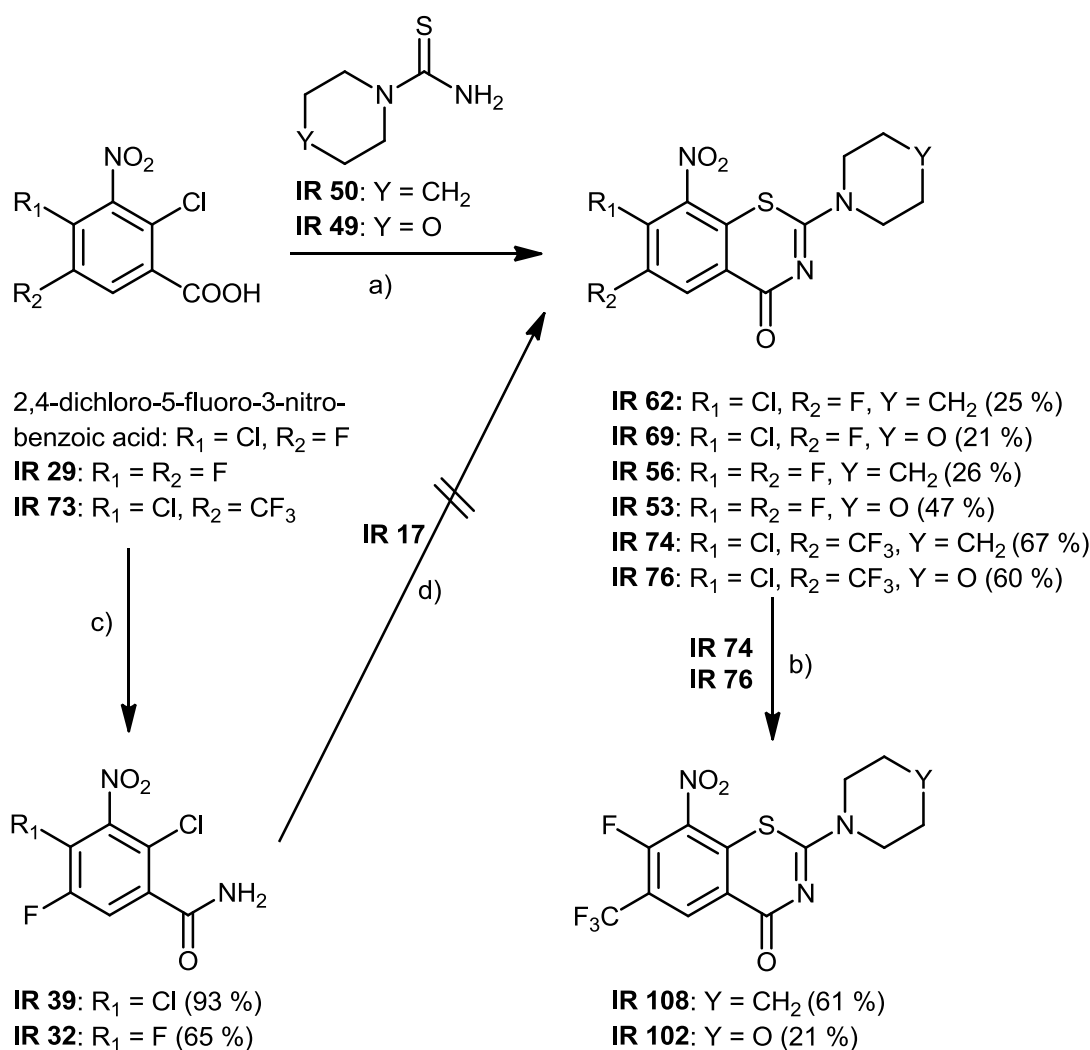


Figure 25: Synthesis of BTZs with different halide and trifluoromethyl substituents at the arene moiety

Reaction conditions: a) 1. SOCl₂, toluene, reflux, 2 h, 2. **IR 49** or **IR 50**, toluene, 50-90 °C → 80°-reflux, 1-18 h; b) argon atmosphere, **IR 74** and **IR 76**, freeze dried KF, DMF, reflux, 5 h; c) 1. SOCl₂, toluene, reflux, 2 h, 2. aq. NH₃ 10-25 %, -20 °C, 10 min; d) 1. **IR 17**, ethanol, rt, 18 h, 2. NaH₂PO₄, ethanol, reflux, 6 h

Instead, BTZs **IR 53**, **IR 56**, **IR 62**, **IR 69**, **IR 74**, and **IR 76** were easily accessible via the thiourea pathway (method E), where the corresponding benzoylchlorides were treated with thiourea derivatives **IR 49** or **IR 50** in toluene at temperatures between 55-111 °C for 1-18 h (Figure 25). Product work-up was performed via flash chromatography on normal phase silica gel. The 7-fluoro-8-nitro-6-(trifluoromethyl)benzothiazinones **IR 102** and **IR 108** were obtained from **IR 76** and **IR 74** by chloride-fluoride-substitution with freeze-dried KF in DMF.⁹⁹

2.2.3.3 Amino substituents

In order to develop a set with -I/+M substituents next to the nitro group, different amines were introduced at position 7 of the BTZ scaffold. Amines investigated were morpholine, dimethylamine, and pyrrolidine with pK_B values of 5.64, 3.36, and 2.73,⁷⁹ indicating increasing nucleophilicity of the nitrogen. Hence, pyrrolidine should have the highest +M effect and contribute most electrons to the arene π -system compared to dimethylamine and morpholine. Dimethylamine and pyrrolidine were chosen instead of piperidine, since they are less bulky and should sterically less influence the bioactivation of the nitro group (enzymatic reduction to nitroso).

Applying standard S_{NAR} conditions, 7-chlorobenzothiazinone derivatives **IR 62**, **IR 69**, **IR 74**, and **IR 76** were treated with an excess of the corresponding amine and equimolar amounts of diisopropylethylamine (DIPEA) in DMF. Work-up was performed via flash chromatography on normal phase silica gel to yield the 7-amino-BTZs **IR 57**, **IR 64**, **IR 75**, **IR 77**, **IR 96**, **IR 97**, **IR 100**, **IR 101**, **IR 103**, **IR 104**, **IR 106**, and **IR 107** (Figure 26).

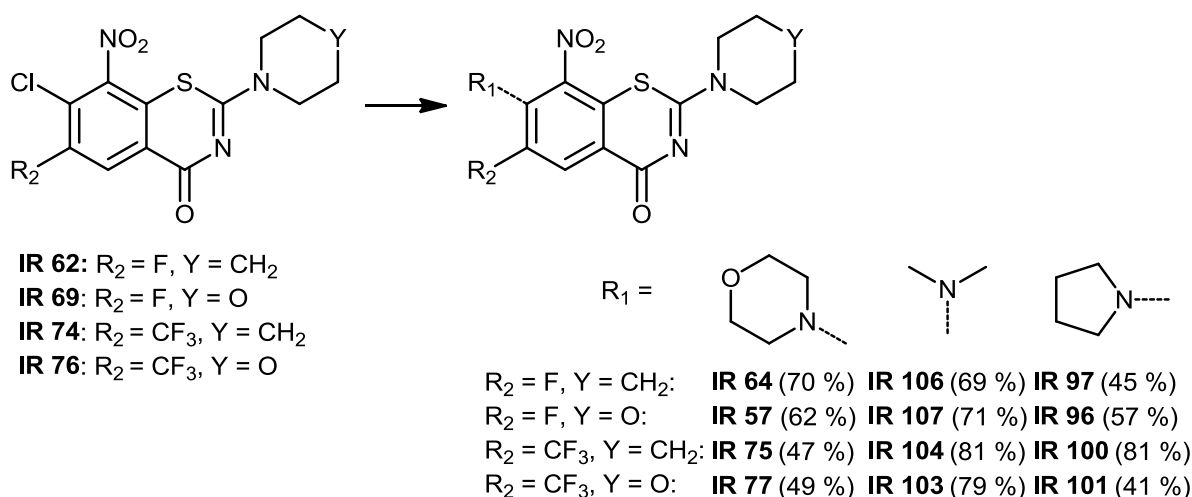


Figure 26: Synthesis of 7-amino-substituted 8-nitro-benzothiazinones

Reaction conditions: morpholine, dimethylamine (25 % in H_2O), or pyrrolidine, DIPEA, DMF, rt-60 °C, 1-12 h

2.2.4 Substituents at position 2 of the heterocycle

2.2.4.1 Arenes and heteroarenes

To investigate the role of aryl substituents at position 2 for the antitubercular activity of BTZs, two different sets of BTZs with aryl or heteroaryl substituents at position 2 were synthesized (compare chapter 2.2).

8-Nitro-2-(pyridin-2-yl)-4*H*-1,3-benzothiazin-4-ones

The first set, 8-nitro-2-(pyridin-2-yl)-4*H*-1,3-benzothiazin-4-ones, feature an electron-withdrawing pyridyl substituent at position 2, which influences the electron density at the sulfur-nitro-pharmacophore, probably increasing the redox potential of the nitro group.

The BTZ system again was constructed via our 'method E'. The thiourea derivative **IR 48** was synthesized from pyridine-2-carboxamide (**IR 46**).¹⁰⁰ 2-Chloro-3-nitro-5-(trifluoromethyl)benzoic acid **IR 05**, 2-chloro-4,5-difluoro-3-nitrobenzoic acid **IR 29**, and 2,5-difluoro-3-nitrobenzoic acid **IR 54** (synthesized according to Chupak et al.⁹¹) were treated with thionyl chloride in toluene to yield the corresponding benzoylchlorides, then added to a solution of **IR 48** in toluene and refluxed for 3-4 h. Subsequently, 8-nitro-2-(pyridin-2-yl)-4*H*-1,3-benzothiazin-4-ones **IR 51**, **IR 52**, and **IR 61** were obtained after work-up via flash chromatography on normal phase silica gel (Figure 27).

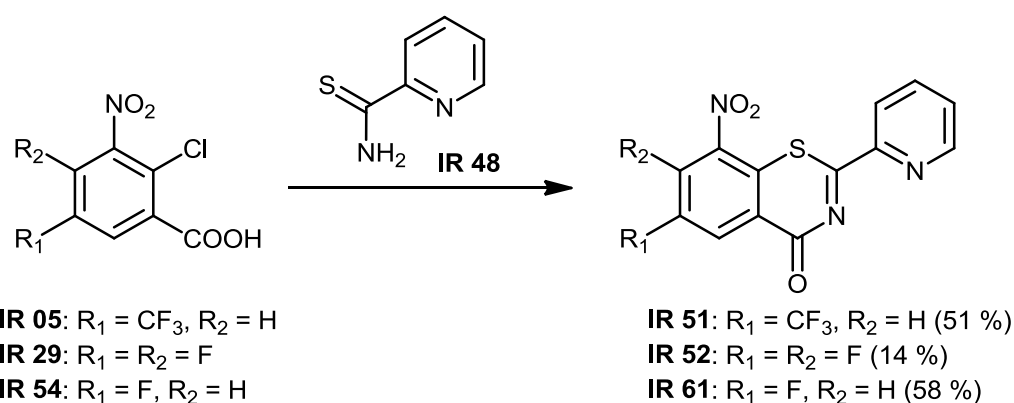


Figure 27: Synthesis of 8-nitro-2-(pyridin-2-yl)-4*H*-1,3-benzothiazin-4-ones **IR 51**, **IR 52** and **IR 61**

Reaction conditions: 1. SOCl₂, toluene, reflux, 2 h, 2. **IR 48**, toluene, reflux, 3-4 h

2-Aryl-8-nitro-4*H*-1,3-benzothiazin-4-ones

In a second set of compounds, unsubstituted and substituted phenyl moieties were incorporated at position 2, whereas the nitro and trifluoromethyl arene substituents were kept at their usual positions. Reaction conditions for BTZ formation followed the lines of 'method E' and were adapted from the previous chapter (see chapter 2.2.4.1). **IR 05** was treated with commercially available thiobenzamide, 4-methoxy-thiobenzamide, and 4-chloro-benzamide in refluxing toluene to yield the 2-aryl-8-nitro-4*H*-1,3-benzothiazin-4-ones **IR 82**, **IR 87**, and **IR 88** (Figure 28). Further variations with +M substituents in para position of the C-2 aryl moiety were discontinued due to the inactivity of **IR 82**, **IR 87**, and **IR 88** in the antimycobacterial in vitro assays (see chapter 3.1).

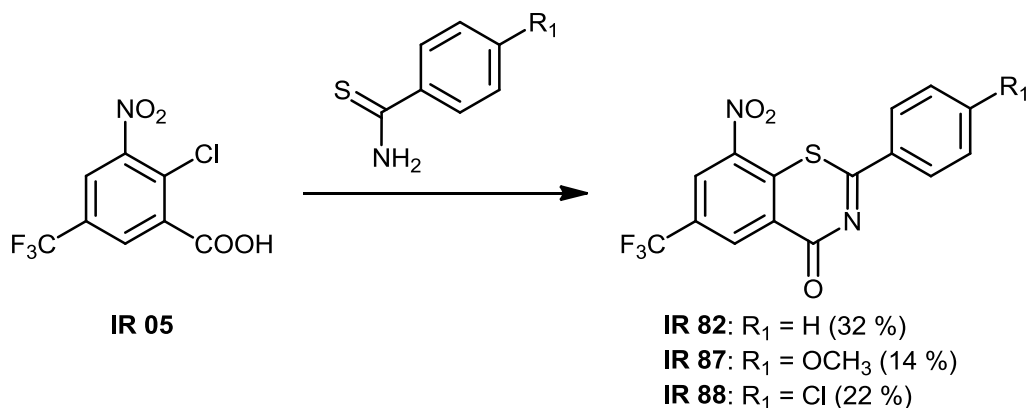


Figure 28: Synthesis of 2-aryl-8-nitro-4H-1,3-benzothiazin-4-ones **IR 82**, **IR 87**, and **IR 88**

Reaction conditions: 1. $SOCl_2$, toluene, reflux, 2 h, 2. thiobenzoic acid amide ($R_1 = H$), 4-methoxy-thiobenzoic acid amide ($R_1 = OCH_3$) or 4-chloro-thiobenzoic acid amide ($R_1 = Cl$), toluene, reflux, 1-5 h

2.2.4.2 Branched piperidinyl substituents

Novel BTZs with branched piperidinyl substituents at position 2 were synthesized. Alkyl side chains in ortho position to the binding nitrogen atom were introduced in order to shield the sulfur atom of the thioether and therefore achieve greater stability of the thioether group. Besides, the more voluminous branched amino substituents at position 2 could influence the binding of the BTZ substrate at its target's binding pocket and consequently influence the activity. They will also restrict rotation at the bond between the BTZ scaffold and piperidine rings and conformational possibilities, which apart from 3D shape will affect electron delocalization and thus redox properties of the essential BTZ nitro group.

Commercially available 2,6-dimethylpiperidine (predominantly *cis*), 2,2,6,6-tetramethylpiperidine, and 3,5-dimethylpiperidine (mixture of *cis* and *trans* diastereomers) were chosen as model substituents. BTZ synthetic methods A (classic) and E (thiourea pathway) were evaluated. In all cases, amines had to be distilled prior to use, otherwise syntheses failed, even if NMR spectra of the amine reagents showed no considerable impurities.

The BTZ **IR 85** was obtained following both alternatives of the classic method A: high temperatures according to Kosczik et al.⁷⁶ and low temperatures according to Hartmann and Seybold et al.^{80,81} Not surprisingly, yields could be significantly increased if the synthesis was conducted at low temperatures (34 % versus 15 %). Following the synthetic method E, **IR 85** was afforded in 24 % yield (Figure 29), utilizing thiourea derivative **IR 118**, which was synthesized as described in the literature.^{80,81} It is noteworthy that despite the lower yields via the method E, work-up of the BTZ-product was more facile than in the method A due to the lower number of by-products. A drawback of the method E was the marginal yield in production of the thiourea reagent **IR 118** (2 %), which is presumably due to the sterical hindrance of the nitrogen by the neighboring methyl groups.

BTZ **IR 115** was obtained in 11 % yield following the classic method A (Figure 29) and no further trials were conducted.

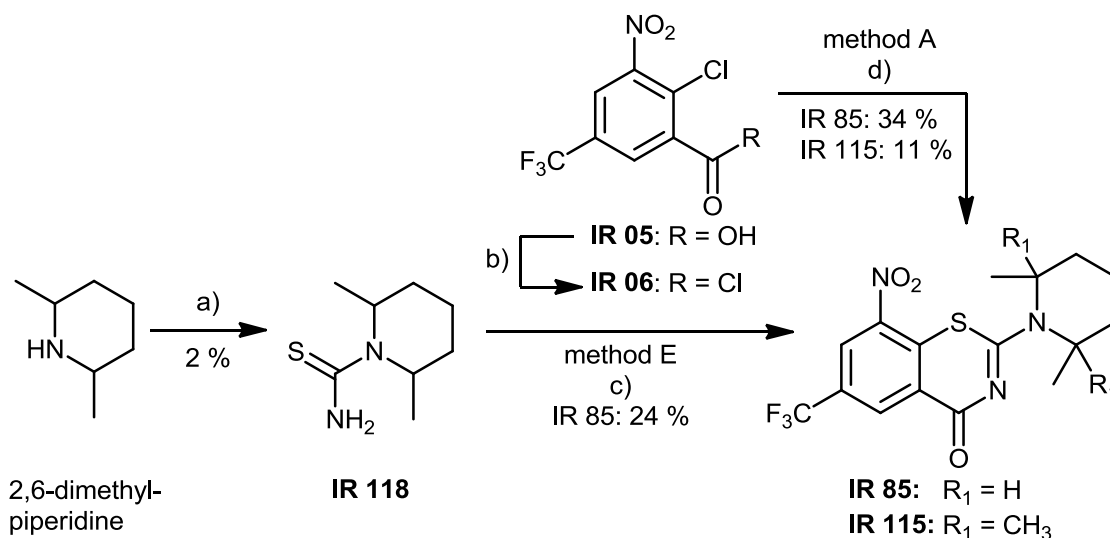


Figure 29: Synthesis of **IR 85** and **IR 115**

Reaction conditions: a) 1. benzoylchloride, NaSCN, acetone, 5 °C, 2 h, 2. 2,6-dimethylpiperidine, acetone, 12 °C → 22 °C, 2 h, 3. HCl, 90 °C, 1.5 h; b) SOCl₂, toluene, reflux, 2 h; c) **IR 118**, **IR 06**, toluene, 70 °C, 2 h; d) **IR 85**: 1. argon atmosphere, **IR 06**, KSCN, acetone, 5 °C, 2 h, 2. argon atmosphere, 2,6-dimethylpiperidine, acetone, 5 °C, 1 h; **IR 115**: 1. argon atmosphere, **IR 06**, KSCN, acetone, rt → 40 °C, 5 min, 2. argon atmosphere, 2,2,6,6-tetramethylpiperidine, acetone, rt, 30 min → reflux, 2 min

Shifting the methyl groups one position further away from the nitrogen, the synthesis of the thiourea reagent **IR 116** according to the literature^{80,81} yielded a satisfactory 34 % of product (Figure 31). ¹H NMR spectra of the starting material 3,5-dimethylpiperidine were recorded (Figure 30, top) to determine the ratio of cis/trans diastereomers, which was calculated by the height of integrals of proton signals of both diastereomers. NMR data were consistent with the literature.¹⁰¹

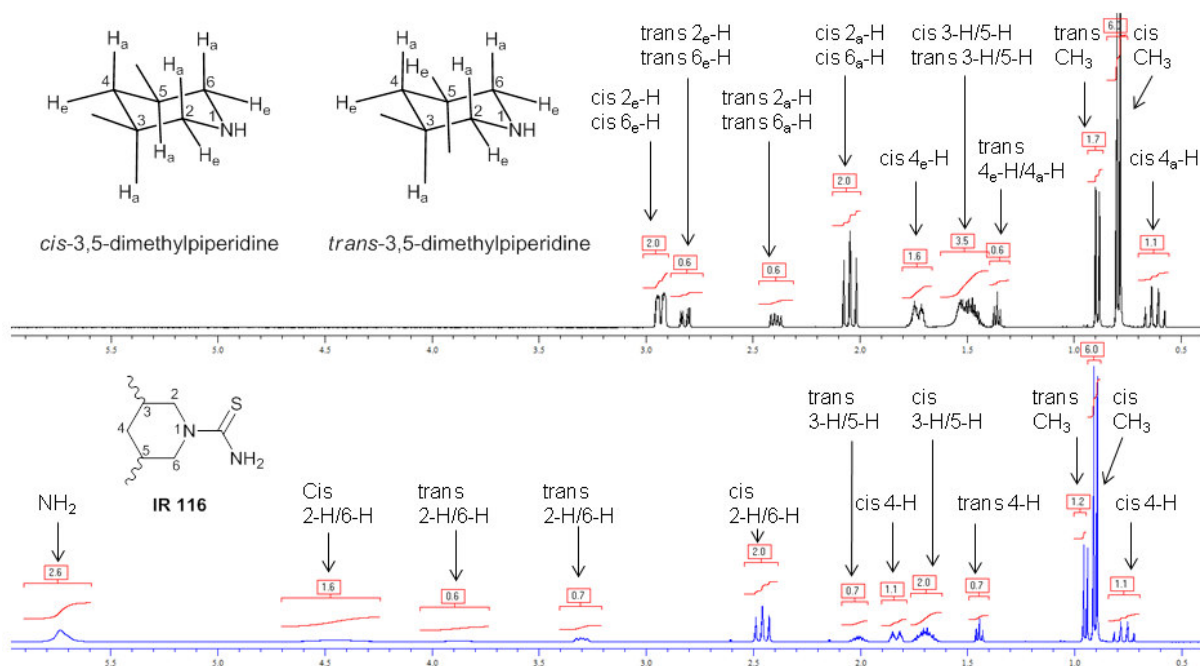


Figure 30: ¹H NMR spectra of diastereomers of 3,5-dimethylpiperidine (top) and **IR 116** (bottom)

For thiourea **IR 116** both diastereomers were obtained as a mixture whereas for the end product of this synthetic sequence, BTZ **IR 127** via the method E, the diastereomers were separated during work-up via flash chromatography (Figure 31).

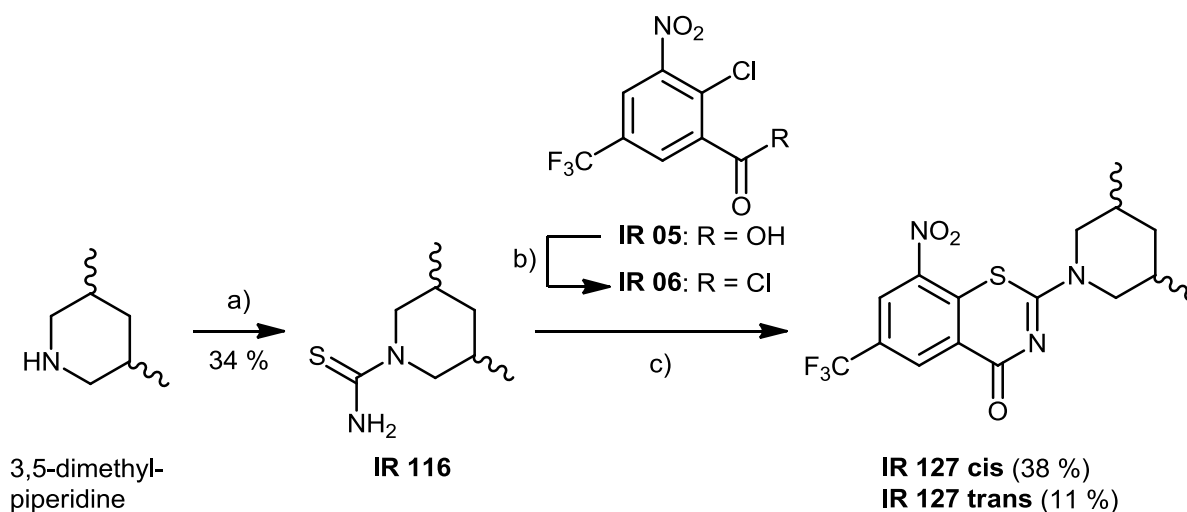


Figure 31: Synthesis of **IR 127**

Reaction conditions: a) 1. benzoylchloride, NaSCN, acetone, 5 °C, 2 h, 2. 3,5-dimethylpiperidine, acetone, 12 °C \rightarrow 22 °C, 2 h, 3. HCl, 90 °C, 1.5 h; b) SOCl₂, toluene, reflux, 2 h; c) **IR 116**, **IR 06**, toluene, 70 °C \rightarrow reflux, 1 h

The ratio of cis/trans diastereomers remained constant throughout the synthesis – about two thirds of the cis and one third of the trans diastereomer were obtained (comparison of proportion of cis and trans diastereomers in ¹H NMR spectra: 3,5-dimethylpiperidine cis:trans = 3:1, **IR 116** cis:trans = 2.3:1, **IR 127** (isolated yield) cis:trans = 3.5:1, Figure 30, bottom and Figure 32).

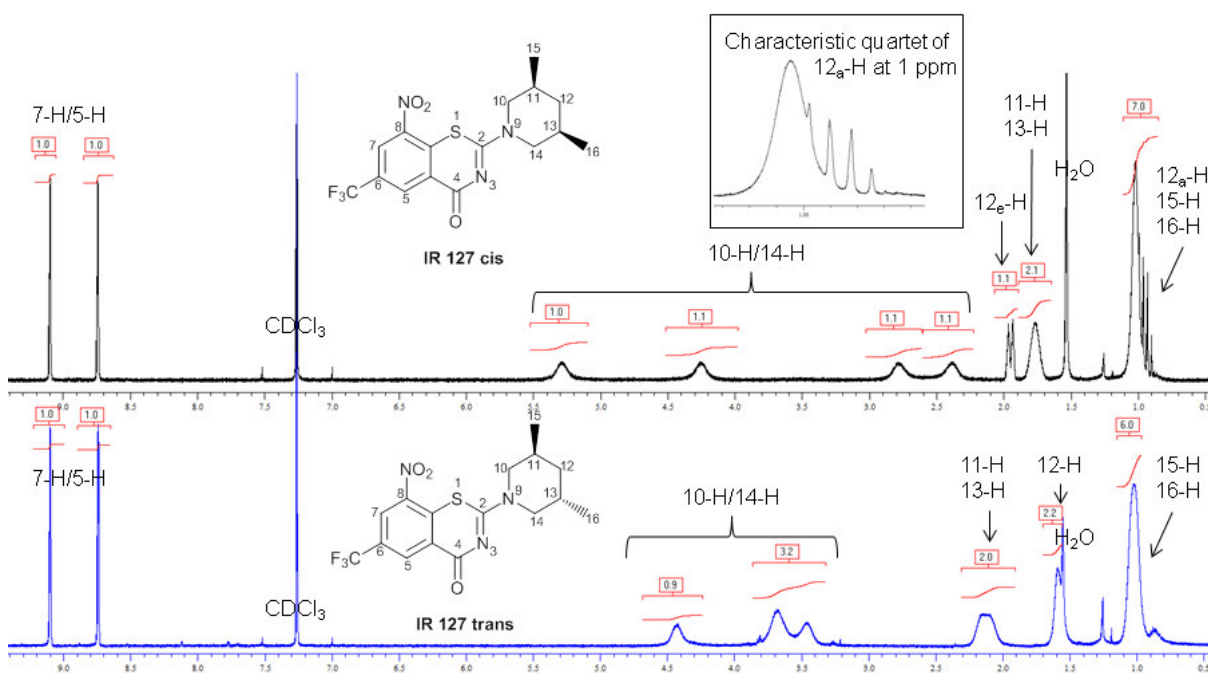


Figure 32: ¹H NMR spectra of **IR 127 cis** (top) and **IR 127 trans** (bottom)

2.2.4.3 Branched 1,4-dioxo-8-azaspiro[4.5]decane substituents

The promising MIC values (see chapter 3.1) of the 2-dimethyl-/tetramethylpiperidinyl substituted BTZs **IR 85** and **IR 115** suggested the idea of merging structural elements of these BTZ derivatives with the spiro moiety as the structural element of BTZ043. Therefore, a set of 7,9-dimethyl-/7,7,9,9-tetramethyl-1,4-dioxo-8-azaspiro[4.5]decane substituted BTZs was synthesized.

The incorporation of the spiro moiety is generally achieved by ketalisation of piperidin-4-one derivatives with the corresponding diols. Two different approaches were investigated: Ketalisation of the amine reagent before and after the formation of the BTZ scaffold.

2,2,6,6-tetramethylpiperidin-4-one (commercially available) and 2,6-dimethylpiperidin-4-one (**IR 83**) were used as the corresponding piperidin-4-one starting materials. **IR 83** was synthesized via double Mannich reaction from acetone-1,3-dicarboxylic acid methyl ester, ammonium bromide and two equivalents of formaldehyde in accordance with previously described procedures (Figure 33).¹⁰²⁻¹⁰⁵

It is noteworthy that a tricky and very crucial step of the double Mannich reaction was the crystallization of the 3,5-bis(methoxycarbonyl)-2,6-dimethyl-4-oxopiperidin-1-ium bromide (**IR 130**), which required some practice and is therefore described in some detail. After three days of stirring, the precipitation of **IR 130** was achieved quite nicely if the solvent was almost completely removed under reduced pressure and then the mixture was kept in a small flask with a small amount of EA at rt over night instead of setting it aside at 5 °C for 6 h. The next step of the ester hydrolysis and decarboxylation also required some practice in the work-up, since the crystallization procedure described by Goebel¹⁰⁴ was unsuccessful. Hence, the procedure of Ulmer¹⁰³ was implied: **IR 130** was heated with a few ml conc. HCl to 70 °C for 18 h to achieve ester hydrolysis and decarboxylation and after cooling the excess HCl was removed under reduced pressure to yield the hydrochloride salt of **IR 83**. In some cases, no crystals precipitated. The residue was then adjusted to a basic pH with aq. NH₃, extracted with chloroform, subsequently the organic solvent was evaporated and the free base **IR 83** purified by flash chromatography. The free base **IR 83** was isolated in considerably lower yields than its hydrochloride salt, presumably due to its instability against alkali,¹⁰⁶ which resulted in notable loss of **IR 83** during the extraction process.

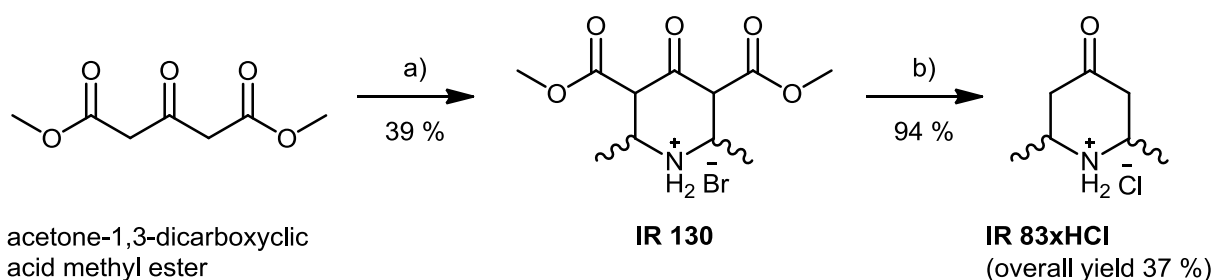


Figure 33: Synthesis of 2,6-dimethylpiperidin-4-one **IR 83** via double Mannich reaction

reaction conditions: a) 1. NH₄Br, formaldehyde, H₂O:methanol 1:1, rt, 3 d, 2. EA, rt, 12 h; b) conc. HCl, 70 °C, 18 h

Since Mannich reactions are not stereoselective, the two stereoisomers of **IR 83** were obtained during the synthesis. ^1H NMR spectrum clearly showed an excess formation of the cis isomer (cis:trans ratio approx. 4:1 according to ^1H NMR integrals, Figure 34), which is on the one hand consistent with findings by Goebel et al.¹⁰⁵ but on the other hand in contrast to observations by Ulmer¹⁰³ who described that only the cis isomer was formed.

Nevertheless, the ratio of cis/trans stereoisomers varied throughout different synthetic trials. In some cases only the cis isomer was obtained. **IR 83** was used as a mixture of both stereoisomers for the following steps.

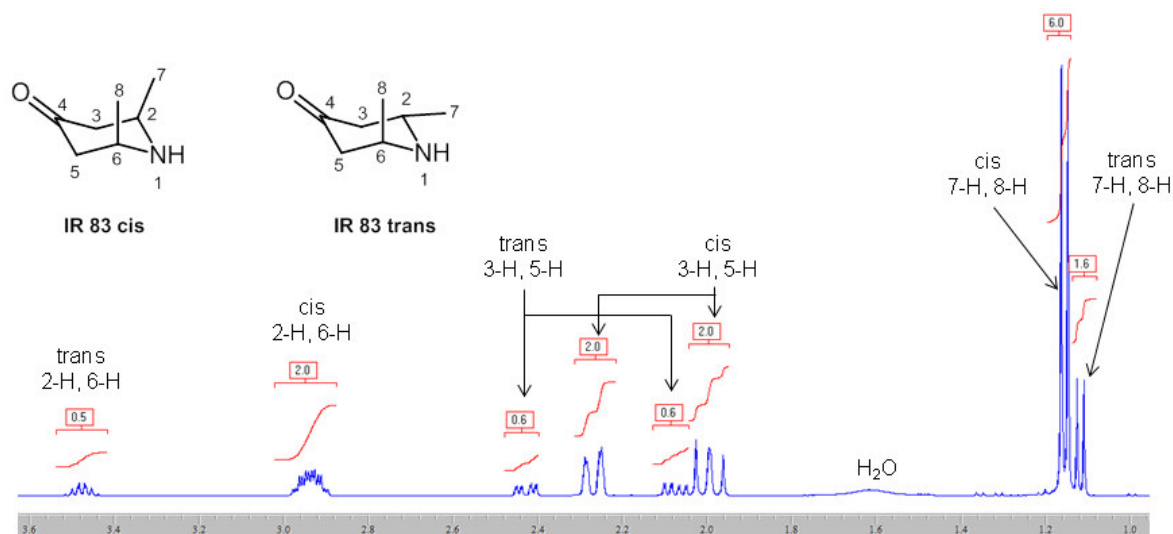


Figure 34: ^1H NMR spectrum of **IR 83**

According to standard ketalisation conditions,^{106,107} **IR 83** or 2,2,6,6-tetramethylpiperidinone and ethylene glycol were dissolved in toluene and heated with a Dean Stark apparatus with catalytic amounts of tosylic acid or sulfuric acid (Figure 35, black arrow).

Unfortunately, the corresponding ketals **IR 93** and **IR 121** could not be obtained, which is consistent with findings by Karoli et al.⁶⁷ who claimed that Dean Stark conditions are tedious or do not work in small scale ketalisations. Instead, Karoli and coworkers successfully conducted ketalisations with trimethylsilyl ether activated diols according to Tsunoda et al.¹⁰⁸

The trimethylsilyl ethers of ethylene glycol and propylene glycol, **IR 131** and **IR 132**, were synthesized according to Mash et al.¹⁰⁹ (Figure 35, blue arrow). Subsequently, **IR 83** was treated with silyl ether **IR 131** and catalytic amounts of trimethylsilyl trifluoromethanesulfonate (TMSOTf) in DCM according to Tsunoda et al.¹⁰⁸ but the corresponding ketal **IR 93** was not obtained either (Figure 35, blue arrow). Reasons for the failure remain unclear. The electrophilic reactivity of the carbonyl carbon could be impeded, a competing reaction to hemiaminal with another molecule di-/or tetramethylpiperidin-4-one could take place or sterical obstruction by the methyl groups could hamper the ketalisation.

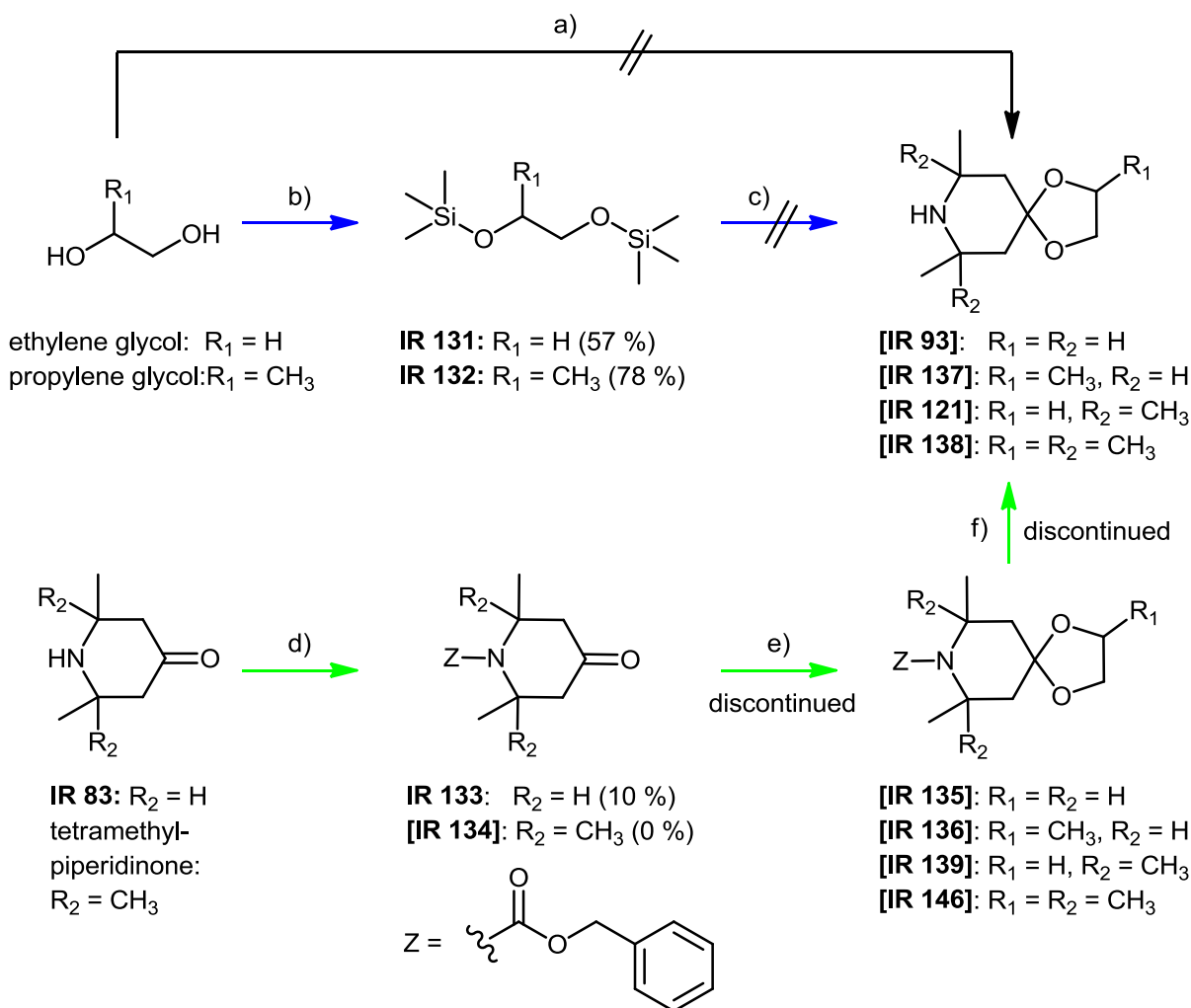


Figure 35: Synthetic plan of methyl substituted spiroketal piperidine derivatives

Reaction conditions: a) 2,2,6,6-tetramethylpiperidin-4-one or **IR 83**, ethylene glycol, tosylic acid or H_2SO_4 (95 – 97 %), Dean Stark, reflux, 12-24 h; b) argon atmosphere, TEA, chlorotrimethylsilane, DCM, $0\text{ }^\circ\text{C} \rightarrow \text{rt}$; c) argon atmosphere, **IR 83**, DIPEA, TMSOTf, DCM, $-78\text{ }^\circ\text{C}$, 3 h; d) argon atmosphere, benzyl chloroformate (Z), DIPEA, toluene, $0\text{ }^\circ\text{C} \rightarrow \text{rt}$, 30 min

We resorted to a detour via protection of the amino group of the piperidin-4-one derivatives with benzyl carbamate (Z), a common protective group for amino groups,¹¹⁰ and subsequent ketalisation according to Karoli et al.⁶⁷ (Figure 35, green arrows). The benzyl formate of **IR 83**, **IR 133**, was obtained in low yield following the procedure of Makings et al.¹¹¹ It is noteworthy that the synthesis failed if the hydrochloride salt of **IR 83** was used although three equivalents of DIPEA were added to bind the HCl. However, 2,2,6,6-tetramethylpiperidin-4-one could not be converted into its N-protected derivative **IR 134**, presumably due to the sterical hindrance of the four methyl groups.

During the search for alternative pathways for the incorporation of the benzyl carbamate protection group into **IR 83**, our attention was drawn to the synthesis of 2,6-alkylsubstituted N-protected piperidinones, synthesized from 4-methoxypyridine. The reaction of 4-methoxypyridine with benzyl chloroformate followed by Grignard addition of

alkylmagnesium bromide yielded the corresponding 2-alkylsubstituted N-protected 2,3-dihydropyridinone, which in turn can undergo a second Grignard addition to yield 2,6-alkylsubstituted N-protected piperidin-4-one.¹¹²⁻¹¹⁴ This alternative pathway to 2,6-alkylsubstituted N-protected piperidin-4-ones leaves space for a variety of different alkyl substituents at positions 2 and 6, depending on the Grignard reagent used. However, the feasibility of this procedure also supports the idea of the decreased reactivity of the carbonyl group of the piperidinone since it easily survives the nucleophilic attack of Grignard reagents. Regarding the consecutive ketalisation step, this reduced electrophilic reactivity of the carbonyl group presumably fails ketalisation, which was also observed in ketalisation trials of **IR 83** with diols or activated diol **IR 131**.

Further trials to convert **IR 133** to ketals **IR 135** and **IR 136** as well as alternative synthetic pathways via Grignard reagents were also postponed and will be investigated in future work.⁷⁰

In conclusion, no spiroketal piperidine building block was available for the formation of the BTZ scaffold (compare Figure 36, green arrow). Hence, this chemical pathway was aborted. Instead, the BTZ scaffold was built with the piperidin-4-one derivatives, to be followed by ketalisation as the final step (see Figure 36, blue and black arrows).

For the synthesis of BTZs **IR 142**, **IR 143**, **IR 144**, and **IR 145**, the intermediate BTZs **IR 140** and **IR 141** were initially synthesized according to the classic method A under optimized temperature conditions (Figure 36, blue arrow).^{76,80,81} The thiourea method E was not investigated, since the formation of the thiourea reagent had yielded unsatisfying results with dimethyl- and tetramethylpiperidine (compare chapter 2.2.4.2).

According to the optimized synthetic method A, BTZs **IR 140** and **IR 141** were easily accessible in acceptable yields by treating the benzoylchloride **IR 06** with KSCN and 2,6-dimethylpiperidin-4-one **IR 83** or commercially available 2,2,6,6-tetramethylpiperidin-4-one (Figure 36, blue arrow). It is noteworthy that standard work-up procedures via flash chromatography with hexane:EA gradients were cumbersome due to increased retention of the BTZ products at the silica gel flash column. In the case of **IR 140**, work-up was optimized by washing the crude product with an aq. NH₃/chloroform mixture followed by only one flash chromatography (eluent chloroform). For **IR 141**, avoiding EA during the flash chromatography was also beneficial, mixtures of hexane:chloroform were used instead.

For the formation of BTZ **IR 140**, the hydrochloride salt of **IR 83** was used as amine moiety and an additional 2.5 equivalents DIPEA added to the reaction mixture to capture evolving HCl. Despite the fact that in the case of **IR 140**, the 2,6-dimethylpiperidin-4-one starting material **IR 83** was used as mixture of both stereoisomers, NMR spectra of the isolated BTZ **IR 140** showed only signals of the cis isomer, indicating a presumably sterically driven attack of only the cis isomer of **IR 83** at the intermediate acylisothiocyanate.

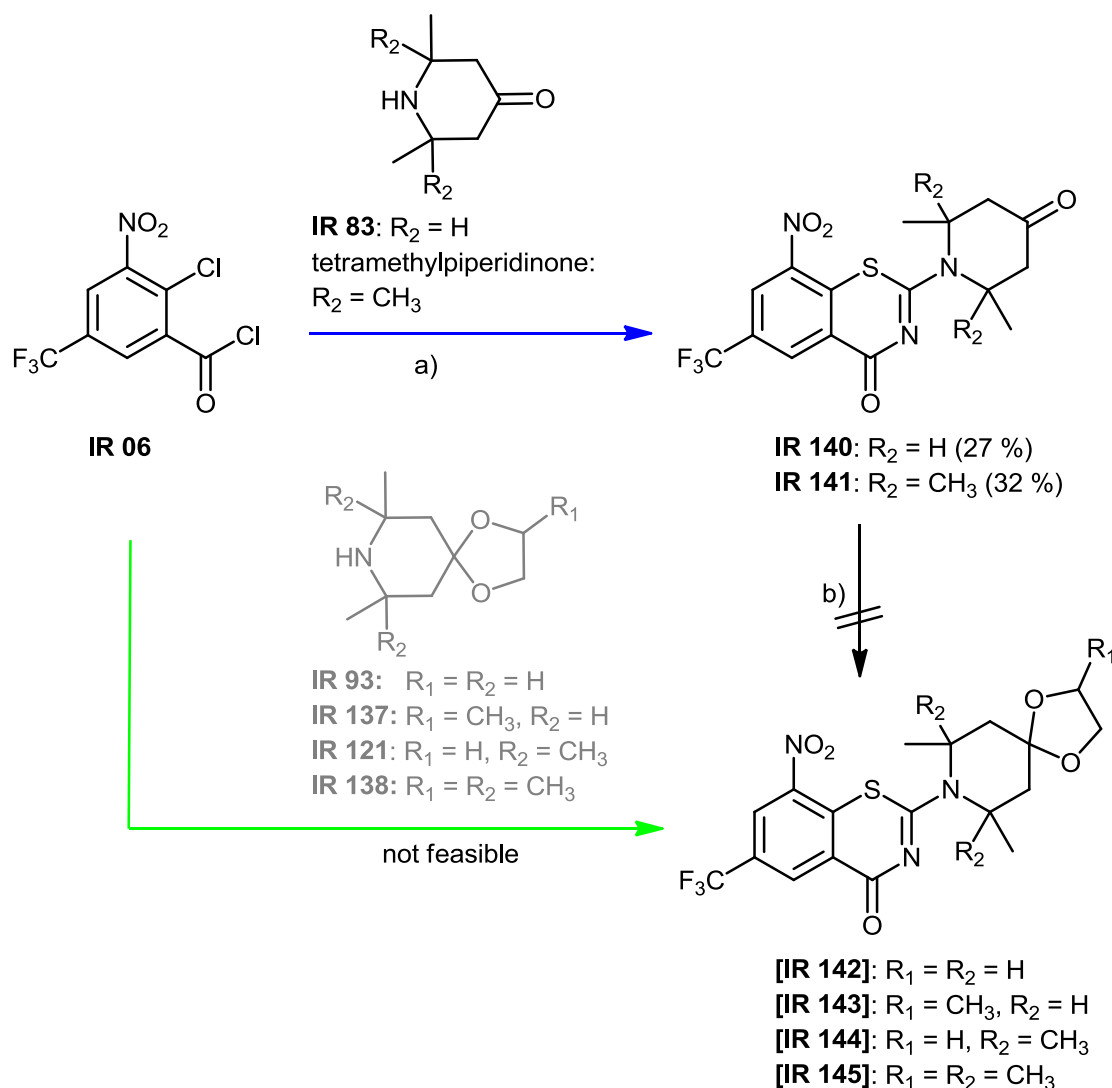


Figure 36: Synthetic plan of branched 1,4-dioxo-8-azaspiro[4.5]decane substituted BTZs

Reaction conditions: a) 1. argon atmosphere, **IR 06**, KSCN, acetone, 5 °C, 2 h, 2. argon atmosphere, 2,2,6,6-tetramethylpiperidin-4-one or **IR 83**·HCl, DIPEA, acetone, 5 °C, 2 h; b) argon atmosphere, TMSOTf, **IR 131**, DCM, -78 °C, 3 h

Thereafter, the ketalisation of **IR 140** and **IR 141** was conducted with activated ethylene glycol **IR 131** according to Tsunoda et al.¹⁰⁸ and Karoli et al.⁶⁷ (Figure 36, black arrow). Unfortunately, several attempts of ketalisation failed, presumably due to the aforementioned decreased electrophilic activity of the carbonyl group or due to the sterical influence of the methyl groups at the piperidin-4-one substituent. The troublesome synthesis of 1,4-dioxo-8-azaspiro[4.5]decane-substituted BTZs **IR 142**, **IR 143**, **IR 144**, and **IR 145** was eventually discontinued and only intermediates **IR 140** and **IR 141** were considered for biological evaluation.

2.2.4.4 2-(2,8-Diazabicyclononane)-benzothiazinones

In order to incorporate a more bulky substituent with a second basic amino group at position 2 of the BTZ scaffold, the synthesis of BTZ **IR 128** with a diazabicyclononane moiety was investigated. (1*S*,6*S*)-2,8-Diazabicyclo[4.3.0]nonane was chosen since it is also incorporated in the fluoroquinolone moxifloxacin, and is commercially available.

The synthesis of **IR 128** was initially investigated via the thiourea pathway method E (Figure 37, d). Unfortunately, no thiourea derivative **IR 41** was obtained from various experiments using known procedures.^{80,81}

The classic pathway method A (Figure 37, e) was also rejected since work-up was generally cumbersome due to the formation of a variety of side products (TLC) and no product was detectable via mass spectrometry of the crude reaction mixture.

Therefore, a synthetic pathway was chosen in which the amine moiety did not need any derivatization (e.g. thiourea, dithiocarbamate) and a trial according to method C (compare chapter 2.1.3 and Figure 37, a-c) was employed, which was described as the alkylxanthogenate pathway by Möllmann et al.⁷³

The core arene **IR 05** was treated with thionyl chloride and aq. NH₃ to obtain the corresponding 2-chloro-3-nitro-5-(trifluoromethyl)benzamide **IR 18** in almost quantitative yields. In the next step the sulfur of the benzothiazinone scaffold was introduced utilizing sodium (ethoxymethanethiyl)sulfanide **IR 42** (synthesized from carbon disulfide, ethanol and NaOH according to Abad et al.¹¹⁵). The intermediate 2-ethoxy-8-nitro-6-(trifluoromethyl)-4*H*-1,3-benzothiazin-4-one (**IR 129**) and the (1*S*,6*S*)-2,8-diazabicyclo[4.3.0]nonane were subsequently refluxed in acetic acid for a full exchange of the alkoxy group according to Möllmann et al.⁷³ Unfortunately, this procedure was unsuccessful. However, a slight change in the reaction conditions led to the isolation of **IR 128**: **IR 129** was dissolved in toluene and only catalytic amounts of glacial acetic acid (0.2 equivalents) were added. The (1*S*,6*S*)-2,8-diazabicyclo[4.3.0]nonane was added in a 1.5 fold excess so as to simultaneously serve as base catalyst and reactant, and the mixture was stirred at 40 °C for 2 h until no further conversion of starting materials was detectable via TLC. A brown residue was obtained after purification with a mass peak of 401.3 *m/z* (ESI, [M+H]⁺), which complies with the molecular mass of **IR 128** (400.38 g/mol).

Although TLC showed only one spot in various eluents, NMR spectra revealed a mixture of two compounds. Both compounds bear two aromatic protons with a chemical shift around 9 ppm, which is typical for the 8-nitro-6-(trifluoromethyl)-BTZ scaffold. Alkyl protons resonate between 1.5 and 4.1 ppm, corresponding to the protons at the diazabicyclononane substituent. Since (1*S*,6*S*)-2,8-diazabicyclo[4.3.0]nonane has two nucleophilic nitrogens which could undergo S_N reactions, we assume that both structural isomers were formed during the synthesis. The existence of a product with a molecular formula of C₁₆H₁₅F₃N₄O₃S (= **IR 128**) was later confirmed by high resolution mass spectrometry (HR MS *m/z* 401.0892 [M+H]⁺, calc. for [C₁₆H₁₆F₃N₄O₃S]⁺ 401.0890). Any attempts to isolate these isomers failed and the mixture of **IR 128** was used for biological evaluation (compare chapter 3.1).

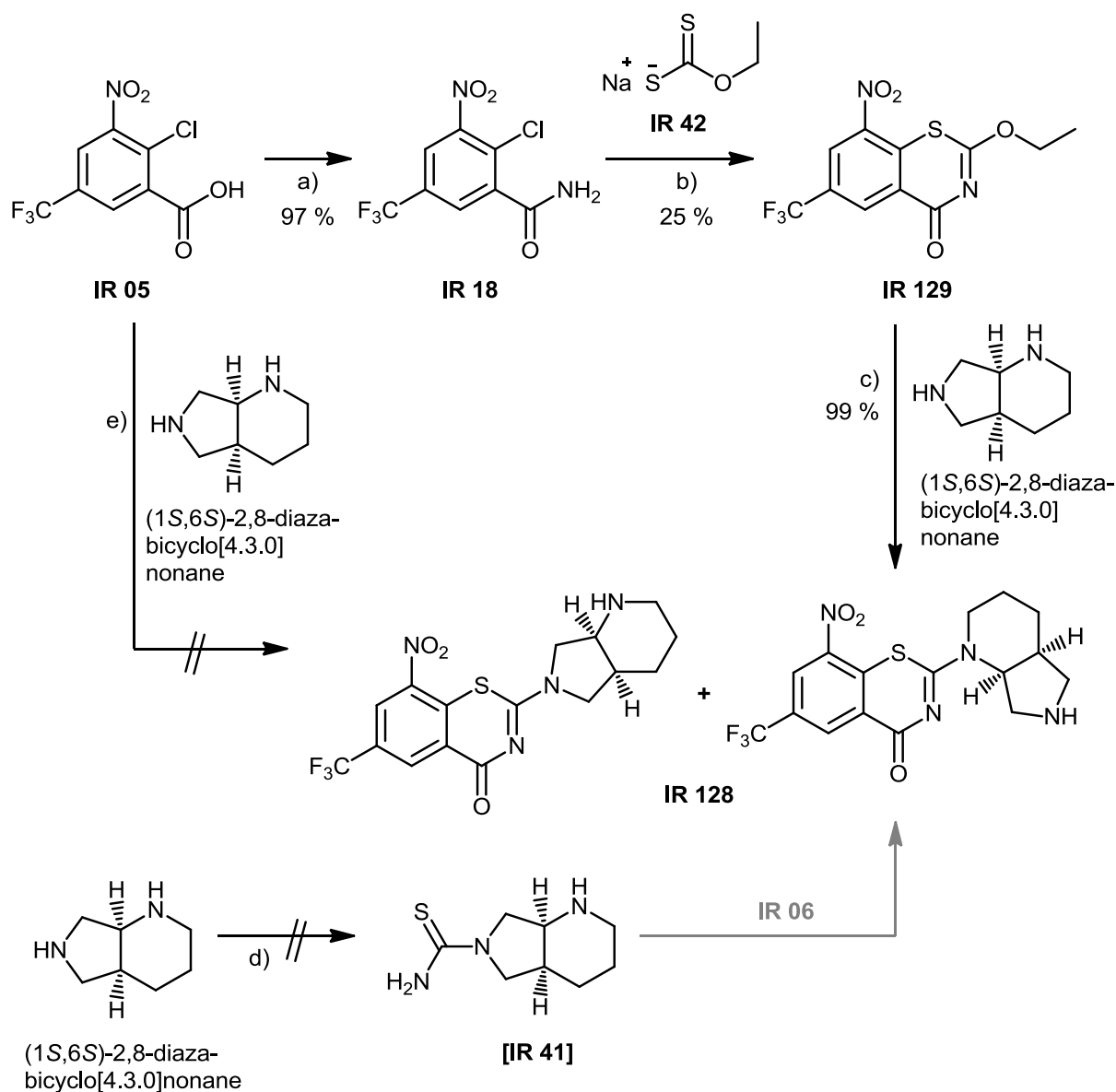


Figure 37: Synthesis of **IR 128** with formation of both structural isomers

Reaction conditions: a) 1. SOCl_2 , toluene, reflux, 2 h, 2. aq. NH_3 25 %, -20°C , 10 min; b) **IR 42**, ethanol, rt, 20 h; c) argon atmosphere, glacial acetic acid, (1S,6S)-2,8-diazabicyclo[4.3.0]nonane, toluene, 40°C , 2 h; d) 1. benzoylchloride, NaSCN , acetone, 5°C , 2 h, 2. (1S,6S)-2,8-diazabicyclo[4.3.0]nonane, acetone, $12^\circ\text{C} \rightarrow 16^\circ\text{C}$, 2 h, 3. HCl , 90°C , 1.5 h; e) 1. SOCl_2 , toluene, reflux, 2 h, 2. argon atmosphere, KSCN , acetone, 5°C , 1.5 h, 3. argon atmosphere, (1S,6S)-2,8-diazabicyclo[4.3.0]nonane, acetone, $5-10^\circ\text{C}$, 2 h

2.2.4.5 2-Piperazinyl-benzothiazinones

The recently reported second generation benzothiazinone PBTZ169 (Figure 7) was selected to investigate whether the novel synthetic pathway E is applicable to the synthesis of PBTZs. Starting from commercially available cyclohexylmethylbromide and formylpiperazine, cyclohexylmethylpiperazine **IR 40** was synthesized according to Meanwell et al.¹¹⁶ Formation of the corresponding thiourea derivative **IR 119** was performed according to Hartmann and Seybold et al. (Figure 38).^{80,81}

With the thiourea reagent in hand, the PBTZ **IR 124** (=PBTZ169) was synthesized by treating **IR 119** with 2-chloro-3-nitro-5-(trifluoromethyl)benzoylchloride (**IR 06**) in refluxing toluene

according to synthetic pathway method E. Shortly after the addition of **IR 06** to the solution of **IR 119**, a white precipitate formed. TLC showed complete turnover of starting materials after one hour. The white precipitate was filtered off and dried (recrystallization from acetone was necessary in some cases). Spectral analysis of the precipitate showed it was the hydrochloride of the PBTZ **IR 124** (yield 61 %, Figure 38). This implicates that the second amino group in the piperazine ring easily forms a hydrochloride salt with the HCl released by the reaction itself and leads to precipitation of the product, which drives the chemical equilibrium towards the product and renders work-up of the product very comfortable. The free base **IR 124** was easily accessible when **IR 124xHCl** was treated with NaOH, extracted with chloroform and the organic solvent evaporated.

Nonetheless, the temperature-modified classic pathway method A is also applicable for the synthesis of **IR 124** (Figure 38), the free base **IR 124** was obtained in about 35 % yield.

Compared to the synthetic procedure of Makarov et al.,⁶⁹ who obtained the PBTZ169 in 71 % yield, the synthesis via our thiourea pathway method E leads to comparable yield (68 %) in fewer steps, with easier isolation of the final product and without the use of toxic reagents such as CH_3I and CS_2 .

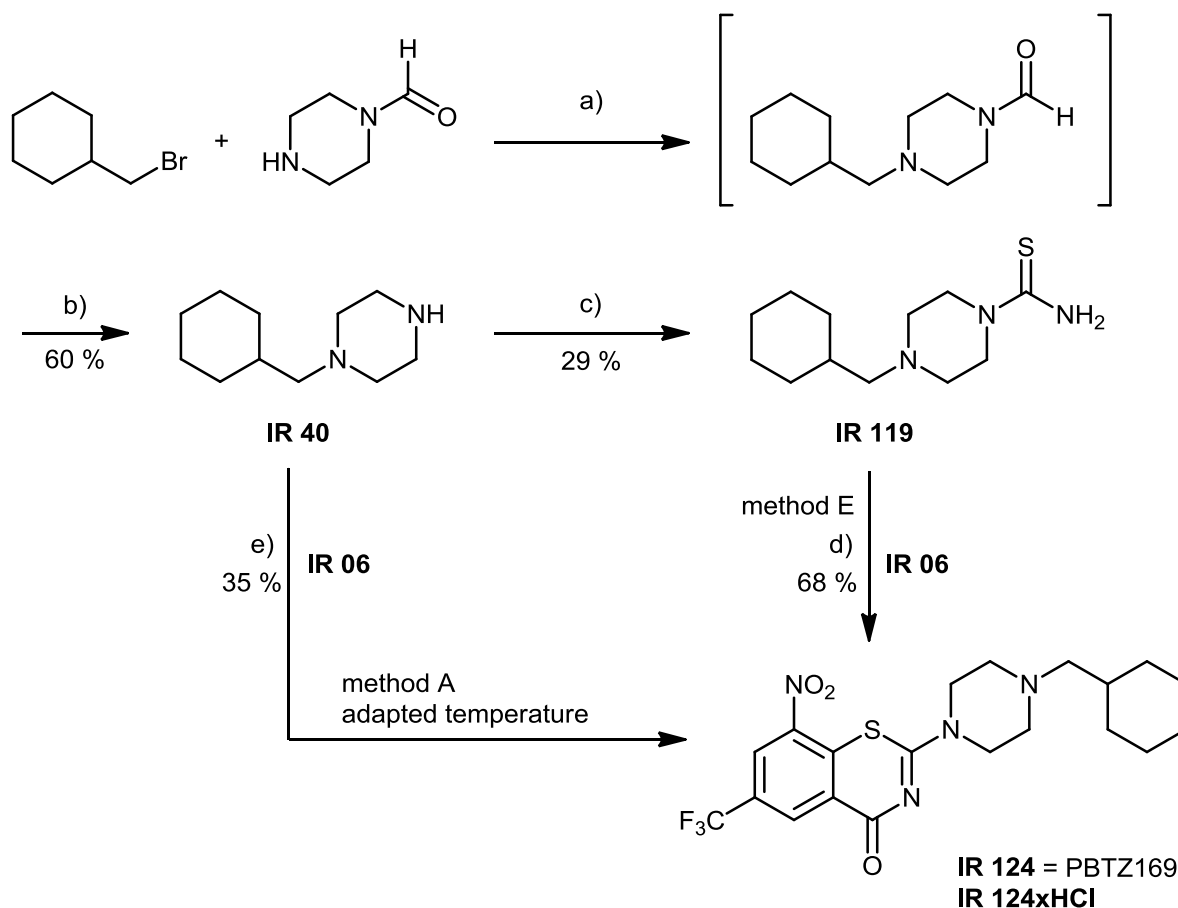


Figure 38: Synthesis of PBTZ **IR 124** (= PBTZ169) and the hydrochloride **IR 124xHCl**

Reaction conditions: a) argon atmosphere, K_2CO_3 , KI, ACN, reflux, 23 h; b) NaOH, EtOH, reflux, 4 h; c) 1. argon atmosphere, benzoylchloride, NaSCN, acetone, 5 °C, 2 h, 2. argon atmosphere, **IR 40**, acetone, 10 °C → 22 °C, 2 h, 3. HCl, 90 °C, 1.5 h; d) **IR 119**, **IR 06**, toluene, 70 °C → reflux, 1 h; e) 1. argon atmosphere, **IR 06**, KSCN, acetone, 5 °C, 1.5 h, 2. argon atmosphere, **IR 40**, acetone, 5-10 °C, 2 h

2.2.5 2,3-Dihydro-5H-imidazo[2,1-b][1,3]benzothiazin-5-one derivatives

Nosova et al.⁸⁵ reported a set of antimycobacterial fluorine-containing 2,3-dihydro-5H-imidazo[2,1-b][1,3]benzothiazin-5-ones, derived from the corresponding polyfluorobenzoylchlorides and imidazolidine-2-thione. To investigate the influence of the dihydroimidazolidine moiety on antimycobacterial activity, these fluorine-containing 2,3-dihydro-5H-imidazo[2,1-b][1,3]benzothiazin-5-ones were modified at the arene moiety with the essential nitro group of BTZ043 at position 9 and different substituents at positions 7 and 8.

Lipunova et al.¹¹⁷ performed the synthesis of 7,8,9-trifluoro-2,3-dihydro-5H-imidazo[2,1-b][1,3]benzothiazin-5-ones with imidazolidine-2-thione and tetrafluorobenzoylchloride in anhydrous pyridine (which serves as solvent and weak base) at 0 °C. These conditions were found to be unelible for our imidazobenzothiazinones. Starting from **IR 73**, treatment with imidazolidine-2-thione (**IR 45**, synthesized from ethylenediamine and carbon disulfide in pyridine according to Zhivotova et al.¹¹⁸) in pyridine at 0 °C, rt or 50 °C yielded no product, TLC showed recovery of starting materials.

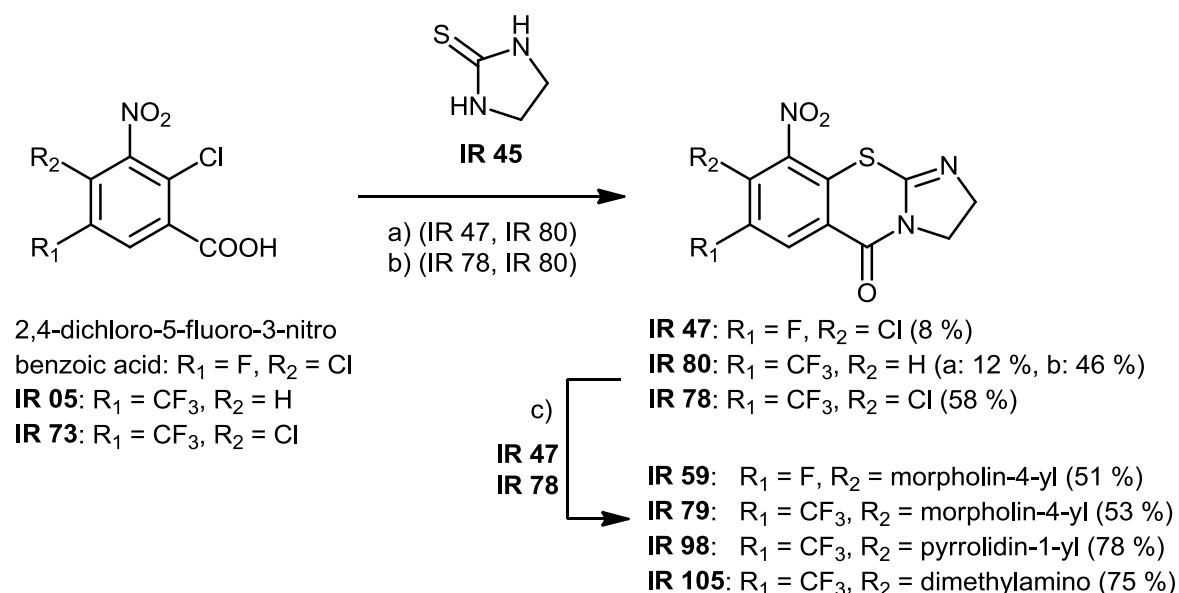


Figure 39: Synthesis of 8-chloro-9-nitro-2,3-dihydro-5H-imidazo[2,1-b][1,3]benzothiazin-5-ones **IR 47**, **IR 80**, and **IR 78**, and 8-amino-9-nitro-2,3-dihydro-5H-imidazo[2,1-b][1,3]benzothiazin-5-ones **IR 59**, **IR 79**, **IR 98**, and **IR 105**

Reaction conditions: a) 1. $SOCl_2$, toluene, reflux, 2 h, 2. argon atmosphere, **IR 45**, pyridine, 0 °C \rightarrow 50 °C, 40 min; b) 1. $SOCl_2$, toluene, reflux, 2 h, 2. argon atmosphere, $POCl_3$, **IR 45**, toluene, 40 °C \rightarrow 90 °C, 2-12 h; c) morpholine, pyrrolidine or dimethylamine (25 % in H_2O), DIPEA, **IR 47** or **IR 78**, DMF, rt, 2.5-4.5 h

Dolbier et al.¹¹⁹ described the failure of the related reaction of pentafluorobenzoic acid with imidazolidine-2-thione, but instead suggested triethylamine (TEA) as the base for deprotonation the imidazolidine-2-thione and acetonitrile as solvent. Experiments with different solvents (acetonitrile, toluene, DMF) and TEA as base again only showed recovery of starting materials, indicating a failure of the base catalysis for this reaction.

Hence, a trial with Lewis acid phosphorous oxychloride (POCl_3) as catalyst was conducted. POCl_3 was added to the intermediate benzoylchloride of **IR 73**, and **IR 45**, dissolved in toluene, treated with this mixture for 2 h at 90 °C. Indeed, imidazobenzothiazinone **IR 78** was obtained in acceptable yield after flash chromatography (Figure 39).

The success of the addition of POCl_3 indicates the necessity of the additional activation of the benzoylchloride moiety by Lewis acids. The possible formation of an intermediate trichlorophosphate of phosphorous oxychloride and benzoylchloride explains the increased electrophilicity of the carboxyl carbon, which facilitates the nucleophilic attack of the imidazolidine-2-thione **IR 45** (Figure 40).

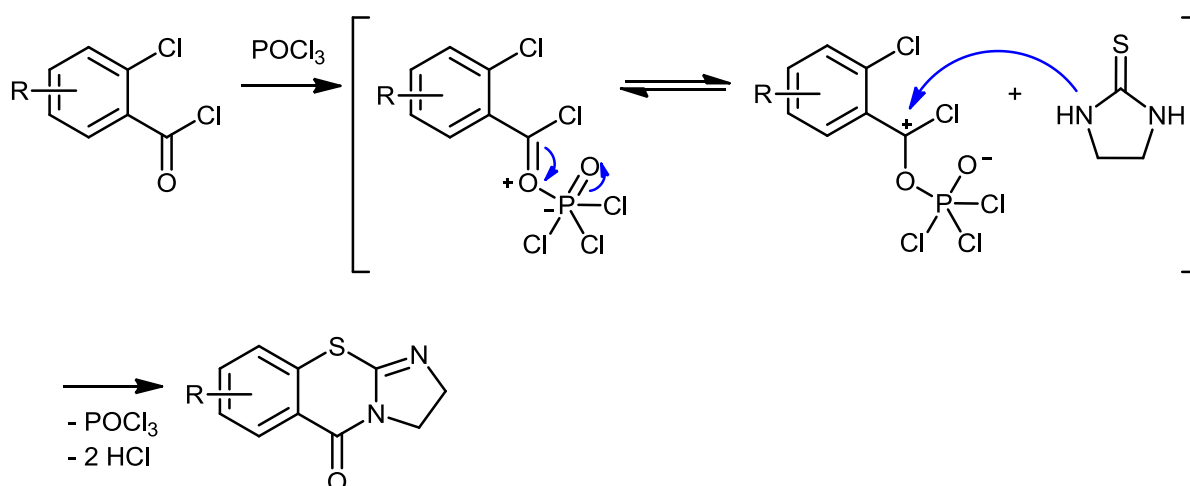


Figure 40: Possible mechanism of benzoylchloride activation by POCl_3

In contrast, the imidazobenzothiazinone **IR 80** was obtained in a yield of approx. 12 % following the procedure described by Lipunova et al.¹¹⁷ with pyridine as solvent (slight change of procedure regarding temperature: start at 0 °C, slowly heat to 50-60 °C for about 1 h). Work-up was cumbersome due to residual pyridine, which hampered precipitation of the crude product. Changing solvent (DMF) and base (NaH) led to even lower yields of about 9 %. Since base catalysis of this reaction remained unsatisfying, a trial with acid catalysis POCl_3 was performed as aforementioned: **IR 45** was dissolved in toluene and treated with a mixture of benzoylchloride **IR 06** and POCl_3 at 90 °C for 12 h. TLC showed product formation after 2 h, **IR 80** was obtained in 46 % yield after flash chromatography (Figure 39).

Notwithstanding, imidazobenzothiazinone **IR 47** was not obtained utilizing POCl_3 as an acid catalyst. **IR 47** was only obtained following the procedure described by Lipunova et al.¹¹⁷ with a slight change in reaction temperature and time (0 °C \rightarrow 50 °C, 40 min). Work-up was cumbersome due to a variety of side products (TLC). It required several flash chromatographies and crystallization procedures, which resulted in a low yield of **IR 47** (8 %, Figure 39).

Finally, the 8-amino-9-nitro-2,3-dihydro-5H-imidazo[2,1-b][1,3]benzothiazin-5-ones **IR 59**, **IR 79**, **IR 98**, and **IR 105** were obtained in good yields (51-78 %) from treating **IR 47** and **IR 78** under standard S_{NAR} conditions with excess of the corresponding amine and DIPEA as auxiliary base in DMF (Figure 39).

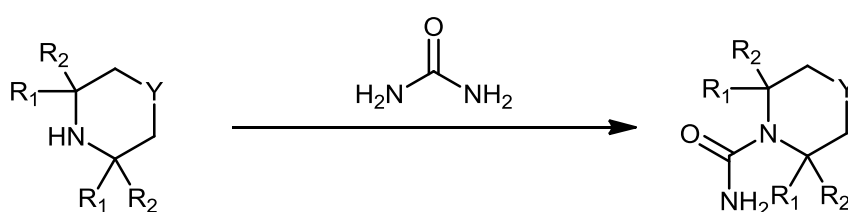
2.3 SYNTHESIS OF BENZOXAZINONES

In contrast to earlier reports, in which the nitro group and the sulfur atom have been claimed to be essential pharmacophores of BTZ043,⁵⁴ it was recently shown that only the nitro group is essential for BTZ043's activity.^{55,58} Besides, other nitro group containing compounds without sulfur – the dinitrobenzamides (DNBs) – have been reported with antimycobacterial activity and inhibition of DprE1 via the same mechanism of action as BTZ043.^{55,57,63,120}

Sulfur in sulfidic bindings is only found in about 5 % of drugs listed in the Merck index.¹²¹ Sulfides are prone to oxidation to sulfoxides or sulfones that influences their metabolic stability as well as electron density around the sulfidic sulfur, which will influence the redox potential of neighboring groups, such as reduction of the nitro group in antimycobacterial BTZs. To create a compound class, structurally and topologically similar to BTZs, but without the oxidizable sulfur atom, sulfur was replaced by its bioisoster oxygen. The resulting 2-amino-8-nitro-4*H*-1,3-benzoxazin-4-ones (BOZs) represent a novel class of antimycobacterial compounds.

2.3.1 Adaption of method E

The aforementioned synthetic pathway via thiourea derivatives was adapted to the synthesis of BOZs, utilizing the corresponding asymmetrically substituted urea derivatives. Ureas **IR 110**, **IR 111**, and **IR 120** were much easier accessible than their thiourea counterparts utilizing the synthesis via aminolysis of urea⁸³ in excess of the corresponding amine (Figure 41). Notwithstanding, synthesis of urea derivatives **IR 122** and **IR 123** was unsuccessful, the aminolysis trials only revealed starting materials, assuming that the methyl groups next to the nitrogen sterically shield the reaction site and hamper the nucleophilic attack of the nitrogen at the carbonyl carbon of urea.



piperidine: $R_1 = R_2 = H$, $Y = CH_2$

morpholine: $R_1 = R_2 = H$, $Y = O$

IR 40: $R_1 = R_2 = H$,
 $Y = N$ -cyclohexylmethyl

2,2,6,6-tetramethyl-piperidine:
 $R_1 = R_2 = CH_3$, $Y = CH_2$

2,6-dimethyl-piperidine:
 $R_1 = CH_3$, $R_2 = H$, $Y = CH_2$

IR 110: $R_1 = R_2 = H$, $Y = CH_2$ (75 %)

IR 111: $R_1 = R_2 = H$, $Y = O$ (76 %)

IR 120: $R_1 = R_2 = H$,
 $Y = N$ -cyclohexylmethyl (75 %)

[IR 122]: $R_1 = R_2 = CH_3$, $Y = CH_2$ (0 %)

[IR 123]: $R_1 = CH_3$, $R_2 = H$, $Y = CH_2$ (0 %)

Figure 41: Synthesis of asymmetrically substituted urea derivatives **IR 110**, **IR 111**, and **IR 120**

Reaction conditions: urea, piperidine, morpholine, **IR 40**, 2,2,6,6-tetramethylpiperidine or 2,6-dimethylpiperidine, 100-130 °C, 40-48 h

With urea derivatives **IR 110**, **IR 111**, and **IR 120**, the corresponding BOZs **IR 112**, **IR 113**, and **IR 125** were synthesized via treating a solution of the urea compounds with the benzoylchloride **IR 06** in refluxing toluene (Figure 42). In all cases, DIPEA was added to promote the $S_{\text{N}}\text{AR}$ reaction and capture the evolving HCl, otherwise yields of BOZs were vanishingly small and work-up cumbersome due to the formation of side products, implicating a much slower and less effective nucleophilic attack of the oxygen compared to the sulfur of thiourea derivatives. Work-up of products was performed via flash chromatography. Interestingly, contrary to its BTZ analog **IR 124**, BOZ **IR 125** did not precipitate from the reaction mixture, and whereas no auxiliary base was necessary in the trial of **IR 124**, three equivalents DIPEA had to be added for acceptable yields of BOZ **IR 125**.

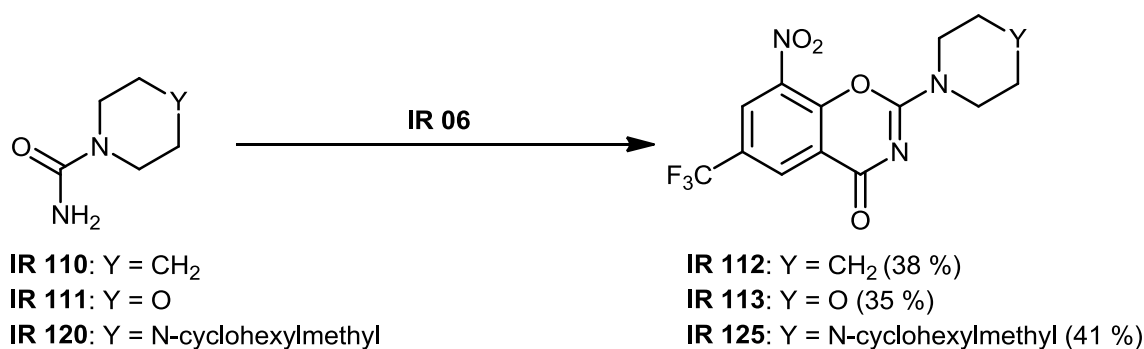


Figure 42: Synthesis of BOZs **IR 112**, **IR 113**, and **IR 125**

Reaction conditions: **IR 06**, DIPEA, toluene, 70 °C → reflux, 3 h

2.3.2 Adaption of the classic pathway method A

BOZs with branched amino substituents at position 2 were not accessible via the novel urea pathway since urea reagents **IR 122** and **IR 123** were not synthesized (compare chapter 2.3.1). Therefore, the classic synthetic pathway (method A) was investigated for its applicability for BOZ synthesis.

Following the procedure described by Kosciak et al.⁷⁶ but using potassium cyanate instead of potassium thiocyanate, BOZs **IR 95** and **IR 114** were obtained in very low yields (6 % and 1 %). For **IR 95**, changing the temperature from 40 °C to 5 °C in the step of the halogenide-pseudohalogenide exchange, increasing reaction time of the last step to 9 d, additionally adding DIPEA as auxiliary base to capture evolving HCl increased the yield to 15 % (Figure 43).

The difficulty in the synthesis of the BOZ **IR 114** was the sterical obstruction of the nitrogen nucleophile by four methyl groups of the 2,2,6,6-tetramethylpiperidine reagent. Temperature of the step of the halogenide-pseudohalogenide exchange was decreased to 5 °C, DIPEA was added during the addition of the 2,2,6,6-tetramethylpiperidine and, subsequently, the mixture was refluxed for 12 h. Notwithstanding, yields leveled out at 2-3 %, implicating that the additional methyl groups in ortho position to the nitrogen sterically hamper the reaction (Figure 43).

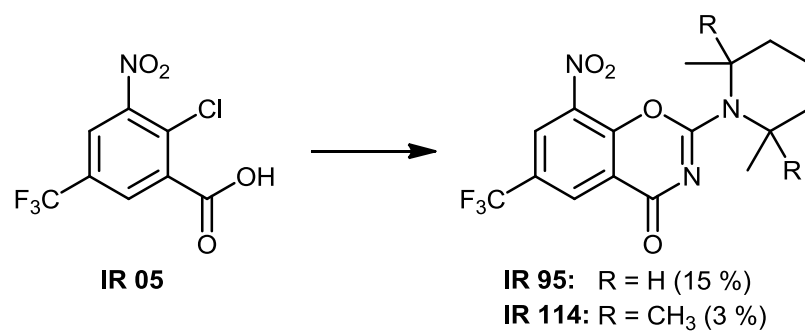


Figure 43: Synthesis of BOZs **IR 95** and **IR 114**

Reaction conditions: 1. SOCl₂, toluene, reflux, 2 h, 2. argon atmosphere, KOCN, acetone, 5 °C, 2 h, 3. **IR 95**: argon atmosphere, 2,6-dimethylpiperidine, DIPEA, 5-10 °C, 2 h → rt, 9 d; **IR 114**: argon atmosphere, 2,2,6,6-tetramethylpiperidine, DIPEA, 5-10 °C, 2 h → reflux, 12 h

2.4 DUAL ACTION MOLECULES - THIOCHROMENONES

2.4.1 Essential pharmacophores of fluoroquinolones and benzothiazinones

All fluoroquinolones share a common mechanism of action: They bind to bacterial topoisomerases of type II, mainly to topoisomerase IV and DNA gyrase, essential enzymes in DNA replication, transcription and repair. Fluoroquinolones stabilize the complex of the topoisomerases with DNA, which finally results in fatal double strand breaks and cell death. The exact mode of binding of fluoroquinolones to the DNA-enzyme-complex is still being investigated. Presently, a ternary complex of two molecules of fluoroquinolones, DNA and enzyme, stabilized by Mg^{2+} ions, has been elucidated.⁷¹

However, extensive structure activity relationship studies were undertaken with first and second generation fluoroquinolones and the following pharmacophores were found to be essential: C-3-carboxyl and C-4-oxo for activity, N-alkyl in order to stabilize the C-4-oxo group and prevent the formation of an enol tautomer. The fluoro substituent at position 6 and the amino substituent at position 7 improve pharmacokinetics and expand the antibacterial spectra to Gram-positive bacteria (Figure 44).⁷¹

Presumptively, the same pharmacophores are responsible for the inhibition of mycobacterial topoisomerase II.

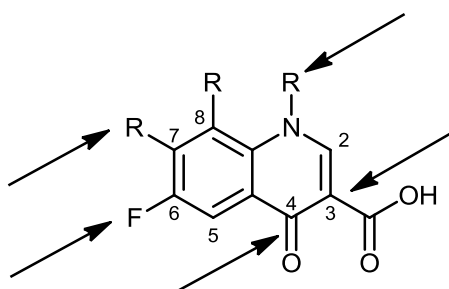


Figure 44: Scaffold of fluoroquinolones with essential pharmacophores indicated by arrows

Our intention was to design novel compounds, which combine essential elements of the fluoroquinolone and benzothiazinone class: C-3-carboxyl, C-4-oxo and C-8-nitro. Nitro groups at position 8 in the class of fluoroquinolones could be unfavorable according to Boteva et al.¹²² but the authors also stated this substituent needs to be investigated further. The aim with these novel compounds was to get a set of molecules with a dual mode of action: activity on mycobacterial gyrase through C-3-carboxyl and C-4-oxo as well as DprE1 inhibition through the C-8-nitro group. Besides, two different substituents at position 6 were to be compared, viz. the C-6 trifluoromethyl group of the BTZ scaffold to enhance activity against DprE1 and the C-6 fluoro substituent for enhanced topoisomerase inhibition.

Two different scaffolds were envisaged: Sulfur-containing thiochromenones and N-alkyl substituted dihydroquinolones (Figure 45). Replacing the N-alkyl group of fluoroquinolones by a sulfur atom as in the thiochromenones could negatively influence the efficacy of these compounds on the topoisomerases, due to the loss of the vinylogous amide group (U. Holzgrabe, personal communication, Boteva et al.¹²²) but we decided to give it a try.

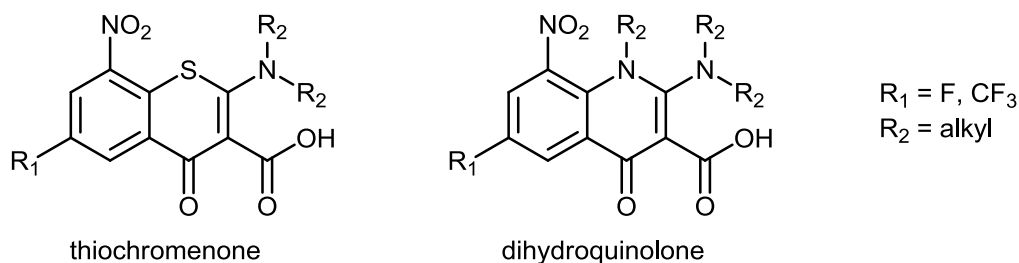


Figure 45: Debated scaffolds for dual action compounds

2.4.2 Synthetic approaches to 3-carboxyl-thiochromen-4-ones

From the various synthetic pathways to fluoroquinolones,¹²³ the Grohe-Heitzer reaction was selected to build the thiochromenone scaffold. The incorporation of the sulfur into the thiochromenone scaffold should take place at a late step during the synthesis. Most reports on thiochromenone synthesis show that the sulfur is already included in the starting material (e.g. thiosalicylic acid derivatives^{124,125}), which highly limits variations in the substitution pattern of the arene moiety and renders nitration impossible without concomitant oxidation of the thiol function.

The Grohe-Heitzer reaction utilizes benzoic acid derivatives with an ortho halide substituent, which are elaborated into benzoylmalonate esters.¹²³ In order to build the thiochromenone scaffold, the activated methylene group of these benzoylmalonate esters is then treated with isothiocyanate according to Hashimoto et al.,¹²⁶ affording a thiolate intermediate (compound 8, Figure 46) in which either the nitrogen or the sulfur atom act as nucleophiles to undergo ring closure in a S_{NAR} reaction with the ortho halide. Hashimoto et al. isolated the thiochromenone 10 as a side product during the synthesis of compound 9 (Figure 46).

Since we intended to turn this thiochromenone side product into a main product, the alkylation of the intermediate thiolate anion was omitted in order to maintain the nucleophilicity of the thiolate. Cyclopropyl isothiocyanate was replaced with the more economical isopropyl isothiocyanate.

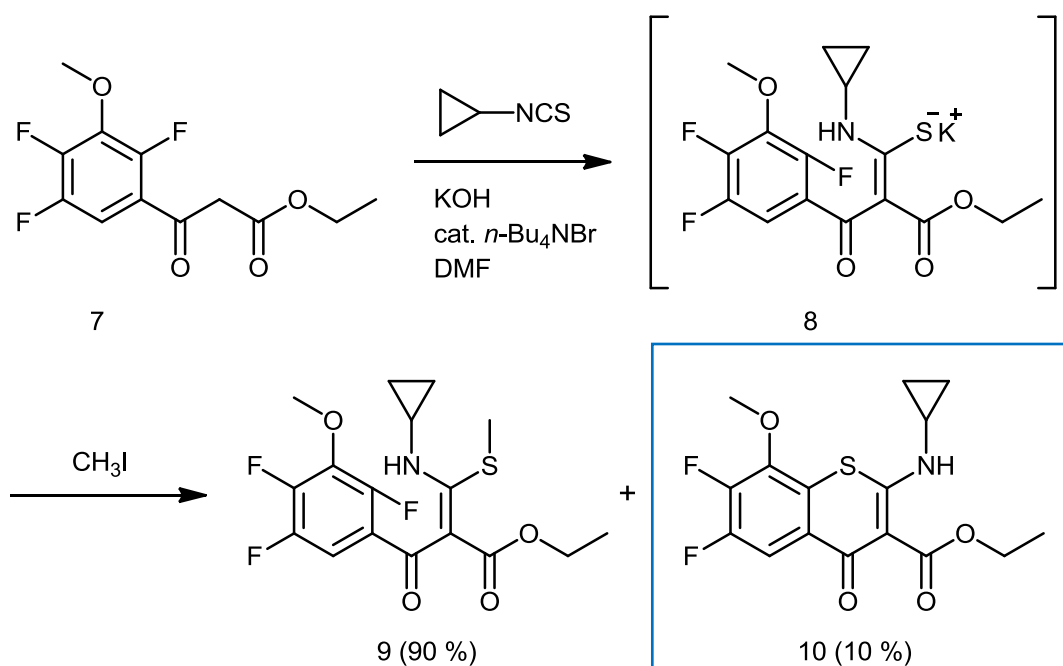


Figure 46: Part from reaction scheme of Hashimoto et al.: synthesis of thiochromenone 10 as side product¹²⁶

The first step of the synthesis was the formation of the corresponding 2-chloro-3-nitro-5-(trifluoromethyl)- β -oxobenzenepropanoic acid ethyl ester **IR 81** from the core arene **IR 05**. Experimental conditions were chosen according to classic Grohe-Heitzer conditions¹²⁷⁻¹²⁹ as well as slightly adapted Grohe-Heitzer conditions,^{126,130} but none of these trials led to isolation of the product **IR 81**. This synthetic step was not assumed to be critical, since it has been reported for different arene moieties including nitro arenes,¹²⁷⁻¹²⁹ but never for arenes with trifluoromethyl substituents. In some cases, we isolated the intermediate 1,3-diethylpropanedioate derivative **IR 153**, but various attempts at selective hydrolysis and decarboxylation of one ethyl ester function failed (Figure 47).

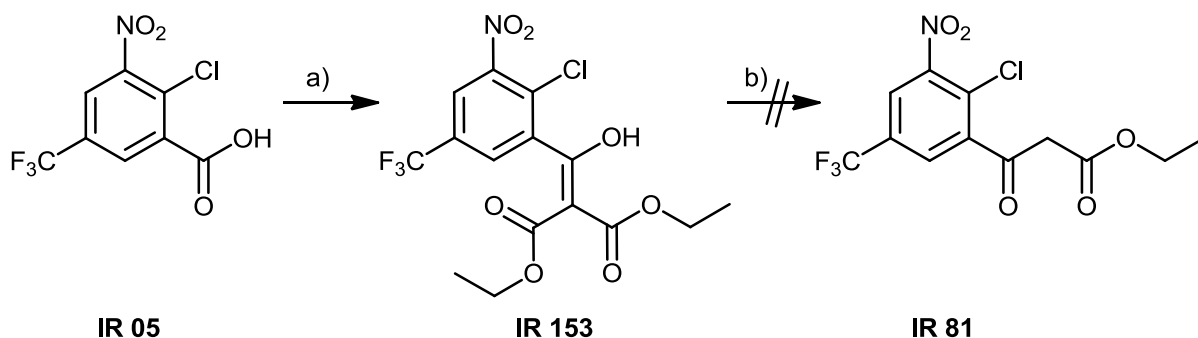


Figure 47: Synthetic attempts to **IR 81** according to (adapted) Grohe-Heitzer conditions

Reaction conditions:

literature	a)	b)
Grohe et al. ¹²⁹ , Schriewer ¹²⁸ , adapted via B. Dobner (personal communication)	1. SOCl_2 , toluene, reflux, 2 h, 2. argon atmosphere, Mg, CH_3OH or $\text{C}_2\text{H}_5\text{OH}$, CCl_4 , evaporation of solvent to yield dry $\text{Mg}(\text{OCH}_3)_2$ or $\text{Mg}(\text{C}_2\text{H}_5\text{O})_2$, addition of diethylmalonate dissolved in toluene, 50-60 °C \rightarrow 65 °C, 1 h \rightarrow -10 °C, addition of IR 06 , 0 °C, 2 h \rightarrow rt, 12 h	<i>p</i> -toluene-sulfonic acid, H_2O , reflux 3-5 h
Belliotti et al. ¹³⁰	carbonyldiimidazole, THF, rt, 4 h, addition of potassium monoethylmalonate, reflux, 18 h, quenching: addition of $\text{H}_2\text{O}/\text{HCl}$	
Hashimoto et al. ¹²⁶	1. SOCl_2 , toluene, reflux, 2 h, 2. argon atmosphere, MgCl_2 , potassium monoethylmalonate, EA, rt, 30 min, addition of TEA, rt, 30 min, addition of IR 06 dissolved in EA, reflux, 2 h, quenching: addition of $\text{H}_2\text{O}/\text{HCl}$	

Finally, **IR 81** was obtained in low yield from the synthesis according to Chu et al.¹³¹ (Figure 48).

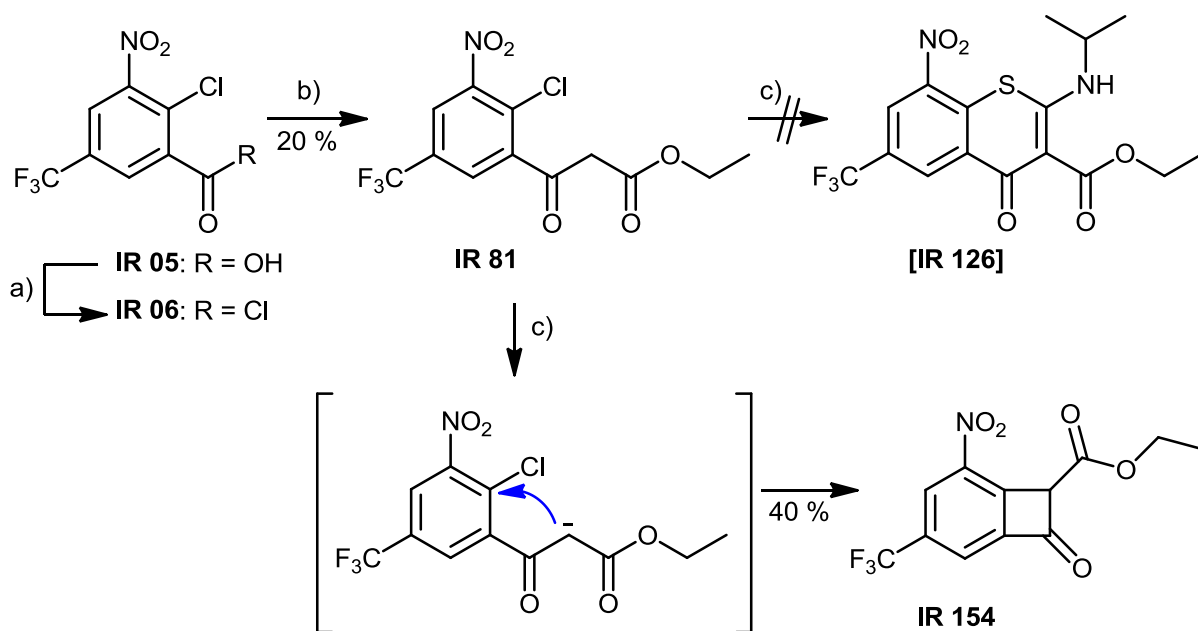


Figure 48: Synthetic attempts to thiochromenone **IR 126** with isolation of by-product **IR 154**

Reaction conditions: a) SOCl_2 , toluene, reflux, 2 h; b) argon atmosphere, monoethylmalonate, 2,2'-biquinoline, THF, -50 °C, addition of *n*-BuLi (2.5 M in hexane) \rightarrow -78 °C, addition of **IR 06**, -78 °C \rightarrow rt; c) **IR 81**, KOH (85%), TBAB, DMF, rt, 30 min \rightarrow 0 °C, addition of isopropyl isothiocyanate, rt, 16 h

Subsequent treatment of **IR 81** with KOH and isopropyl isothiocyanate in the presence of tetrabutylammonium bromide (TBAB) in DMF according to Hashimoto et al.¹²⁶ afforded a new product with molecular mass of 303 g/mol. NMR and IR spectra revealed the structure of this compound to be ethyl 5-nitro-8-oxo-3-(trifluoromethyl)bicyclo[4.2.0]octa-1,3,5-triene-7-carboxylate (**IR 154**), indicating the formation of the carbanion of the malonester moiety upon addition of the base (KOH) and a nucleophilic attack of the intermediate carbanion at the C-2 carbon (Figure 48).

This $S_{\text{N}}\text{AR}$ attack is facilitated by the neighboring electron withdrawing nitro group. The formation of **IR 154** also suggests that either the electrophilicity of the isothiocyanate is relatively low or sterical hindrance of an attack because of the isopropyl group. Both factors explain the failure to incorporate the isothiocyanate moiety at the malonester carbanion of **IR 81** and instead pioneer the intramolecular nucleophilic attack of the carbanion at the C-2 carbon. Unfortunately, the intended thiochromenone **IR 126** was synthetically not accessible via the procedures investigated in this thesis. Further trials were not undertaken in the course of this thesis.

How may the envisaged thiochromenones ultimately be accessed? Optimized reaction conditions in order to isolate the thiochromenone **IR 126** should include less basic reaction conditions at step c (e.g. LiOH, NaOH). Besides, the likelihood of reaction of the isothiocyanate carbon with the malonester carbanion has to be enhanced, either by using less sterically hindered isothiocyanates and/or by utilizing isothiocyanates with decreased +I effect of the alkyl substituent compared to isopropyl isothiocyanate. Considering the latter issue, cyclopropyl isothiocyanate or allyl isothiocyanate should be tried. Comparison of the basicity of cyclopropyl amine (pK_{A} 9.12)¹³², allyl amine (pK_{A} 9.49)⁷⁹ and isopropyl amine (pK_{A} 10.63)⁷⁹ indicates a stronger +I effect of the isopropyl moiety than of the cyclopropyl and allyl moiety. Consequently, the electron density at the nitrogen (and presumably carbon) atom of cyclopropyl and allyl isothiocyanate should be lower than in isopropyl isothiocyanate. Isothiocyanates with electron withdrawing substituents at the alkyl chain, e.g. fluorine, could also be investigated as electron-deficient isothiocyanates.

The limited possibilities of variations of the C-2 substituent of thiochromenones synthesized via isothiocyanates will most likely negatively influence the antimycobacterial activity of these compounds. For BTZs, it has been shown that piperazinyl and branched piperidinyl substituents at position 2 strongly increase antimycobacterial activity (see chapter 3.2). This indicates that cyclic tertiary amines are the substituents of choice. A synthetic pathway to thiochromenones which leaves space for easy chemical variations at position 2 should be developed. Further trials to synthesize thiochromenones as well as dihydroquinolones as possible dual action substrates are the subject of future work in our group.⁷⁰

Chapter Three

3 BIOLOGICAL EVALUATION

In vitro and in vivo experiments to evaluate the antimycobacterial activity of BTZ and BOZ compounds of this thesis were performed in cooperation with our partners, Hans-Knöll-Institut (HKI) Jena (Germany), GlaxoSmithKline (GSK) Tres Cantos, Madrid (Spain), and the School of Biosciences, University of Birmingham (UK).

3.1 AGAR DIFFUSION TEST

In vitro antimicrobial activity of all synthesized BTZ and BOZ derivatives was investigated in an agar diffusion test. DMSO stock solutions of all compounds were diluted with methanol to the test concentration of 100 µg/ml and were then incubated with different test bacilli. Subsequently, the size of inhibition zones was determined visually (Table 4).

Test bacilli for the agar diffusion experiments were *Bacillus subtilis* as Gram-positive rod-shaped control, *Escherichia coli* as Gram-negative rod-shaped control, *Sporobolomyces salmonicolor*, an ubiquitous yeast as eukaryotic microorganism, *Mycobacterium vaccae* as BTZ-sensitive mycobacterium species, and *Mycobacterium aurum* as naturally BTZ-resistant species. *M. vaccae* was selected as a surrogate for *Mtb*. It is a non-pathogenic fast-growing soil mycobacterium, genomically closely related to the slow growing pathogens *Mtb*¹³³ and *M. leprae*¹³⁴ and especially sensitive to the BTZ compound class (U. Möllmann, personal communication). The natural resistance of *M. aurum* to BTZs is due to an amino acid exchange (serine instead of cysteine) at the site of BTZ binding.¹³⁵ Including this species in the first in vitro experiments provides a first idea of the mode of action of the novel BTZ and BOZ derivatives of this thesis, since these compounds should show activity against *M. vaccae*, but not against *M. aurum* if their mode of action is the same as described for BTZ043.

Table 4: Results of agar diffusion experiments for BTZ and BOZ derivatives, n=1

Compound no.	Diameter of inhibition zone (mm)				
	<i>M. vaccae</i> 10670	<i>M. aurum</i> SB 66	<i>B. subtilis</i> 6633	<i>E. coli</i> SG458	<i>Sp. salmoni-</i> <i>color</i> 549
unsubstituted arene moiety, shifted nitro group					
IR 16	0	0	0	0	0
IR 86	0	0	0	0	0
IR 67	0	0	0	0	0
halides at position 7					
IR 53	0	0	0	0	19
IR 56	0	0	0	0	23
IR 62	32	15	12	0	17
IR 69	31	11	12	0	19
IR 74	36	0	0	0	0

Compound no.	Diameter of inhibition zone (mm)				
	<i>M. vaccae</i> 10670	<i>M. aurum</i> SB 66	<i>B. subtilis</i> 6633	<i>E. coli</i> SG458	<i>Sp. salmoni-</i> <i>color</i> 549
IR 76	47	12	0	0	14
IR 102	18	0	0	0	16
IR 108	36	0	0	0	18
amino substituents at position 7					
IR 57	0	0	0	0	0
IR 64	0	0	0	0	0
IR 75	14	0	0	0	0
IR 77	0	0	0	0	0
IR 96	13	0	0	0	12
IR 97	12	11	10	0	12
IR 100	14	13	13	0	0
IR 101	0	0	0	0	0
IR 103	0	0	0	0	0
IR 104	0	0	0	0	0
IR 106	0	0	0	0	0
IR 107	0	0	0	0	0
aryl and heteroaryl substituents at position 2					
IR 51	12	0	0	0	0
IR 52	0	11	12	0	15
IR 61	22	0	19	0	14
IR 82	11	0	0	0	12
IR 87	10	0	0	0	0
IR 88	10	0	0	0	0
branched amino and other amino substituents at position 2					
IR 20	51	12	14	0	0
IR 58	48	0	12	0	0
IR 85	57	12	12	0	0
IR 115	43	11	11	0	12
IR 127 cis	36	0	0	0	0
IR 127 trans	52	0	14	0	0
IR 128	42	0	0	0	0
IR 140	48	12	10	0	0
IR 141	44	0	14	0	0
imidazobenzothiazinones					
IR 47	16	13	0	0	16
IR 59	0	0	0	0	0
IR 78	32	21	12	0	15
IR 79	11	11	0	0	0
IR 80	23	0	13	0	0
IR 98	0	0	0	0	0
IR 105	0	0	0	0	18

Compound no.	Diameter of inhibition zone (mm)				
	<i>M. vaccae</i> 10670	<i>M. aurum</i> SB 66	<i>B. subtilis</i> 6633	<i>E. coli</i> SG458	<i>Sp. salmoni-</i> <i>color</i> 549
benzoxazinones					
IR 95	42	0	0	0	0
IR 112	37	0	0	0	0
IR 113	30	0	0	0	0
IR 114	35	0	0	0	0
IR 125	44	0	0	0	0
other					
IR 154	34	0	10	0	0
reference compounds					
BTZ043 ^{a,b}	34	0	14	0	14
ciprofloxacin ^b	23	35	30	33	nd
amphotericin B ^b	nd	nd	nd	nd	19
solvent control ^b	0	0	0	0	0

^a BTZ043: concentration 0.1 µg/ml for *M. vaccae* 10670, 100 µg/ml for the other test microorganisms

^b maximum diameter of inhibition zone within 5 sets of agar plates

nd: not determined

Considering that the holes for test compound insertion into the agar plates possessed a diameter of 9 mm, only diameters of inhibition zones of more than 20 mm can be regarded as substantial activity.

As expected, unsubstituted BTZs (**IR 16** and **IR 86**) were completely inactive due to the missing nitro group. However, shifting the nitro group to the meta position of the sulfur atom (**IR 67**) also lead to complete loss of activity.

Mixed results were observed for the 7-halide substituted BTZs. Whereas 6,7-difluoro derivatives **IR 53** and **IR 56** were inactive, the 7-chloro-6-fluoro derivatives **IR 62** and **IR 69** as well as their 7-chloro-6-(trifluoromethyl) congeners **IR 74** and **IR 76** showed good activity against *M. vaccae* (inhibition zones > 30 mm). 7-fluoro-6-(trifluoromethyl) compounds **IR 102** and **IR 108** also possessed some activity against *M. vaccae*. All 7-halide compounds showed minor activity against the yeast *Sp. salmonicolor*, indicating some kind of unspecific activity as well. Within this compound set, a substantial beneficial effect of the 6-trifluoromethyl group was seen, since **IR 74** and **IR 76** were more active than the 6-fluoro-analogs (**IR 62** and **IR 69**).

BTZ compounds bearing amino substituents at position 7, ortho to the nitro group, as well as aryl or heteroaryl substituents at position 2 were found to be inactive. Imidazobenzothiazinones showed no or minor activity in the agar diffusion assay, except for the 7-(trifluoromethyl)-derivatives **IR 78** and **IR 80** that displayed activity against *M. vaccae* and minor activity against *M. aurum*, *B. subtilis* and *Sp. salmonicolor*. Again, the increased activity of **IR 78** and **IR 80** compared to **IR 47** presumably results from the trifluoromethyl substituent.

The most active compounds in the agar diffusion assay were found within the subclass of the 2-amino-substituted 8-nitro-6-(trifluoromethyl)-BTZs and BOZs which bear a proton at position 7.

The compounds **IR 20**, **IR 58**, **IR 85**, **IR 115** as well as their BOZ analogs **IR 112**, **IR 113**, **IR 95**, and **IR 114** exhibited considerable inhibition zones selectively against *M. vaccae*. The BOZ analog of PBTZ169, **IR 125**, was the most active BOZ in the test set.

Apparently, branched amino substituents at position 2 of the BTZ scaffold enhance activity. Largest inhibition zones were detected for the dimethyl- and tetramethylpiperidinyl substituted BTZs **IR 85**, **IR 115**, **IR 127 cis**, **IR 127 trans**, and for **IR 128**, which bears the diazabicyclononane moiety of moxifloxacin at position 2.

Surprisingly, the sulfur-free bicycle **IR 154** also exhibited considerable activity against *M. vaccae*, indicating that the existence of the nitro group and its meta trifluoromethyl substituent have the largest impact on antimycobacterial activity regardless of the nature and substituents at the annulated ring.

In general, all active BTZs and BOZs exhibited their antimycobacterial effects against *M. vaccae*, but not *M. aurum*, providing evidence that their molecular mode of action was the same as described for BTZ043.

3.2 MINIMAL INHIBITORY CONCENTRATION

Active compounds from the agar diffusion experiment were transferred to determination of the minimal inhibitory concentration (MIC) against *M. vaccae*, *M. bovis BCG*, and *Mtb H37Rv*. Furthermore, MICs against a DprE1 over-expressor *M. bovis BCG* strain (*M. bovis BCG* pMV261-DprE1) and a DprE1 over-expressor *Mtb* strain was determined for selected compounds in order to confirm the proposed mechanism of action of inhibition of DprE1.

MIC determinations were carried out according to standard test protocols of the cooperation partners (see chapter 7.4). The lowest concentration of test compound, which inhibited growth of the corresponding mycobacteria species was estimated by determination of the number of viable cells present. The indicator dye resazurin was used to measure the metabolic capacity of cells, indicating cell viability. Viable cells of untreated controls retained the ability to reduce resazurin to resorufin which is highly fluorescent and visible by the change from blue to pink color. Non-viable cells rapidly lost metabolic capacity, did not reduce the indicator dye, and thus did not generate a fluorescent signal. The MIC was defined as the lowest concentration of a test compound that did not produce a fluorescent signal and therefore prevented the color change from blue to pink. Results are shown in Table 5.

Table 5: MIC of selected compounds against *M. vaccae*, *Mtb H37Rv*, *M. bovis BCG*, and *M. bovis BCG* over-expressing DprE1

Compound no.	MIC ($\mu\text{mol/l}$)				Ratio (MIC BCG pMV261-DprE1) / (MIC BCG pMV261)
	<i>M. vaccae</i> 10670 (n=1)	<i>Mtb</i> H37Rv (n=3)	<i>M. bovis BCG</i> pMV261 (n=2)	<i>M. bovis BCG</i> pMV261- DprE1 (n=2)	
halides at position 7					
IR 62	9.08	31.3	nd	nd	
IR 69	4.51	62.5	nd	nd	
IR 74	0.51	1.6	0.4	203.1	508
IR 76	< 0.13	1.6	0.4	62.5	156
IR 102	32.96	nd	nd	nd	
IR 108	1.06	6.5	nd	nd	
aryl and heteroaryl substituents at position 2					
IR 51	70.77	nd	nd	nd	
IR 61	82.44	nd	nd	nd	
branched amino and other amino substituents at position 2					
IR 20	1.11	3.3	0.4	62.5	156
IR 58	8.64	5.9	1.1	62.5	57
IR 85	< 0.13	0.8 / 2.0 ^a	0.2	78.1	391
IR 115	< 0.12	1.0 / 2.0 ^a	0.4	> 250.0	> 625
IR 124	nd	< 0.04	nd	nd	
IR 124xHCl	nd	< 0.04	nd	nd	
IR 127 cis	0.26	7.8	nd	nd	
IR 127 trans	< 0.13	0.6	nd	nd	

Compound no.	MIC ($\mu\text{mol/l}$)				Ratio (MIC BCG pMV261-DprE1) / (MIC BCG pMV261)
	<i>M. vaccae</i> 10670 (n=1)	<i>Mtb</i> H37Rv (n=3)	<i>M. bovis</i> BCG pMV261 (n=2)	<i>M. bovis</i> BCG pMV261- DprE1 (n=2)	
IR 128	1.00	nd	nd	nd	
IR 140	1.00	nd	nd	nd	
IR 141	< 0.12	nd	nd	nd	
imidazobenzothiazinones					
IR 47	82.87	nd	nd	nd	
IR 78	4.44	62.5	nd	nd	
IR 80	39.40	nd	nd	nd	
benzoxazinones					
IR 95	0.54	6.5	nd	nd	
IR 112	4.55	15.6	nd	nd	
IR 113	18.10	3.9	nd	nd	
IR 114	0.30	nd	nd	nd	
IR 125	< 0.11	0.31	nd	nd	
other					
IR 154	5.15	nd	nd	nd	
reference compounds					
BTZ043	$1.9 \cdot 10^{-3}$	$2.32 \cdot 10^{-3}$ ⁽⁵⁴⁾	nd	nd	
PBTZ169	nd	< $4.2 \cdot 10^{-4}$ ⁽⁶⁹⁾	nd	nd	
PBTZ A	$6.14 \cdot 10^{-3}$ ⁽⁶⁸⁾	0.06 (MDR <i>Mtb</i>) ⁽⁶⁸⁾	nd	nd	
INH	nd	1.2 ⁽¹²⁰⁾	0.13	0.13	

^a two independent determinations of MIC against *Mtb* H37Rv, differences are within one dilution, which is considered the standard error of the assay

nd: not determined

The data from MIC determinations against *M. vaccae* confirmed the observations from the agar diffusion assay. 2-Aryl/Heteroaryl substituted BTZs (**IR 51**, **IR 61**) and imidazobenzothiazinones (**IR 47**, **IR 80**) failed to show considerable MICs against *M. vaccae*. Imidazobenzothiazinone **IR 78** inhibited the growth of *M. vaccae* with an MIC of 4.44 $\mu\text{mol/l}$, but failed to inhibit growth of *Mtb*.

From the subclass of 7-halide BTZs, the 7-chloro-6-fluoro derivatives **IR 62** and **IR 69** showed MICs against *M. vaccae* in the low μM range but failed to exhibit significant MICs against *Mtb* and were not regarded further. Only the 6-(trifluoromethyl) derivatives **IR 74**, **IR 76**, and **IR 108** were able to inhibit the growth of *M. vaccae* in the nM range (**IR 108** 1.06 μM) and confirmed this substantial antimycobacterial activity with MICs in the low μM range against *Mtb*. This indicates a significant role of the 6-(trifluoromethyl) group in enhancing the inhibitor's activity, possibly via formation of stable H-bonds, which contribute to the inhibitor's positioning in the active site (see chapter 5.1).

Lowest MICs against *M. vaccae* were observed for the 8-nitro-6-(trifluoromethyl) BTZs with branched amino substituents at position 2 (**IR 85**, **IR 115**, and **IR 127**, MIC < 0.13 μM). BTZs

with the simpler amino substituents piperidine (**IR 20**) and morpholine (**IR 58**) as well as diazanonane-substituted **IR 128** exhibited MICs against *M. vaccae* in the low μM range. This trend was also confirmed in the MIC assay against *Mtb*. **IR 20** and **IR 58** showed MICs of 3.3 μM and 5.9 μM , but branched amino substituents **IR 85** and **IR 115** inhibited the growth of *Mtb* at a concentration as low as 1 μM . Both diastereomers of **IR 127** were equipotent against *M. vaccae* (MICs 0.13 - 0.26 μM). Surprisingly, the MICs against *Mtb* of the cis and trans diastereomers of **IR 127** differed (7.8 μM and 0.6 μM), indicating that tight binding of BTZs into the binding pocket may depend on small structural differences of the compound. Benzoxazinones **IR 95**, **IR 112**, **IR 113**, and **IR 114** did not entirely meet the low MICs against *M. vaccae* and *Mtb* of their BTZ analogs, but still displayed MICs against both mycobacteria species in low the μM range. **IR 125**, the BOZ analog of the highly active PBTZ169 (= **IR 124**), inhibited the growth of *M. vaccae* and *Mtb* at a remarkable low concentration of < 0.13 μM and 0.31 μM , respectively. Deplorably, this is still 10 fold higher than the MIC of the corresponding BTZ (**IR 124**, < 0.04 μM). These numbers underline the high efficacy of the novel PBTZ derivatives, e.g. PBTZ169, but also establish the BOZs as new antimycobacterial compounds.

The promising result of the agar diffusion experiment was not entirely confirmed in the MIC assay against *M. vaccae* for sulfur free compound **IR 154**. Its MIC was 5.15 μM which is about 40 fold higher than the MIC of the most active compounds **IR 85**, **IR 115**, and **IR 127 trans**.

In order to confirm the proposed mechanism of action of the novel BTZ compounds via inhibiting the cell wall enzyme DprE1, MICs against a DprE1 over-expressor strain (*M. bovis* BCG pMV261-DprE1) were determined for a subset of compounds. All compounds tested showed a large increase in MIC against the over-expressor strain (\approx 60 – 600 fold) compared to the standard *M. bovis* BCG pMV261 strain. This clearly indicates that BTZ compounds **IR 20**, **IR 58**, **IR 74**, **IR 76**, **IR 85**, and **IR 115** act through inhibiting DprE1.

IR 85 and **IR 115** were also investigated in the *Mtb* H37Rv DprE1 over-expressor strain, where both compounds exhibited MICs above 64 μM . Compared to their MIC against the *Mtb* H37Rv wildtype (1-2 μM), this is a factor 32 increase in MIC and therefore confirms the data from the BCG over-expressor assay and DprE1 as the possible target of the BTZ compounds **IR 85** and **IR 115**.

3.3 IN VIVO ACTIVITY: ULTRA-FAST MURINE MODEL

The most active novel compound **IR 85** was selected for the in vivo evaluation in an ultra-fast murine model of acute TB. The PBTZs **IR 124** and its hydrochloride salt **IR 124xHCl** were also investigated in the ultra-fast-murine model in order to compare the different mouse models in which BTZs have been reported to show activity.

The GSK in-house ultra-fast murine model¹³⁶ is a model of acute TB. Mice were infected with 10^5 CFUs *Mtb* H37Rv by intratracheal infection. Treatment was started at day 5 after infection and continued for 4 days with a single dose oral administration per day of test compound (200 mg/kg). Mice were sacrificed at day 9 and CFUs in the lungs were counted. Moxifloxacin (100 mg/kg, given for 4 days at day 5 after infection (C) and 30 mg/kg given for 8 days at day 1 after infection (D)) was used as control (Figure 49 and Table 6).

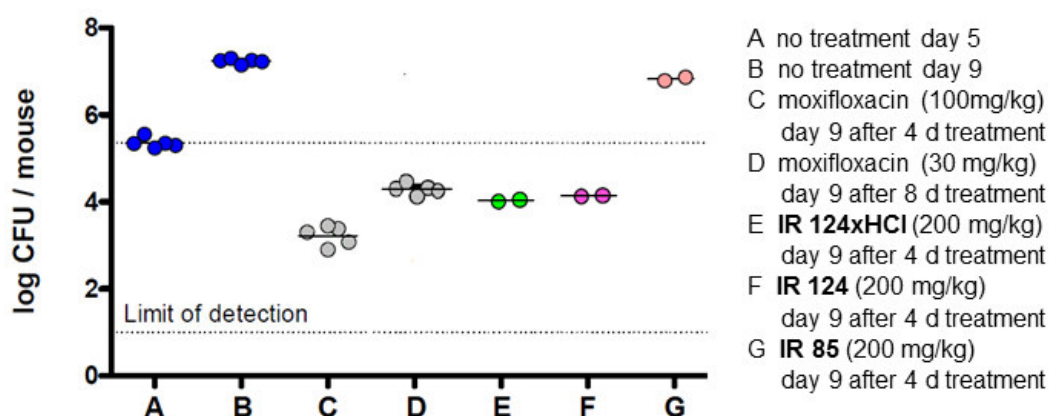


Figure 49: \log_{10} CFU reduction in the ultra-fast murine model of acute TB for **IR 85**, **IR 124**, **IR 124xHCl**, and moxifloxacin (one dot accounts for one test animal)

Table 6: \log_{10} CFU reduction in the ultra-fast murine model

	\log_{10} CFU (lungs)	decrease in \log_{10} CFU (lungs)	p^a	MIC <i>Mtb</i> H37Rv ($\mu\text{mol/l}$)
day 5 untreated	5.4			
day 9 untreated	7.1			
moxifloxacin 100 mg/kg day 9	3.2	4.0	< 0.05	
moxifloxacin 30 mg/kg day 9	4.2	2.8	< 0.05	
IR 85 (200 mg/kg) day 9	> 6.8 ^b	< 0.4		0.8
IR 124xHCl (200 mg/kg) day 9	4.0	3.1	< 0.05	< 0.04
IR 124 (200 mg/kg) day 9	4.1	3.0	< 0.05	< 0.04 < $0.42 * 10^{-3}$ (69)
BTZ043	nd	nd	nd	$2.32 * 10^{-3}$ (54)

^a $p < 0.05$ was considered statistically significant

^b minimum value since CFU were uncountable at the highest plated dilution

Compared to untreated control (B), BTZ **IR 85** (G) was not able to control the mycobacterial infection. However, **IR 124** (F) and its hydrochloride **IR 124xHCl** (E) significantly decreased the number of CFUs in the lungs. The \log_{10} CFU reduction was determined at 3.0 and 3.1 (Figure 49 and Table 6) indicating that the salt formation did not influence in vivo activity. Both compounds seem to display comparable pharmacokinetics and pharmacodynamics, considering their equal in vivo CFU reduction. The reference compound moxifloxacin was used in two different dosing schemes (100 mg/kg BW and 30 mg/kg BW) and significantly decreased the CFU in lungs by 4.0 and 2.8 logs.

The inactivity of **IR 85** was a bit surprising after the in vitro test results. However, the MIC against *Mtb* of **IR 85** was approx. 300 times higher than the MIC of BTZ043 and 1900 times higher than PBTZ169. This MIC increase appears to account for the observed loss of activity in vivo of **IR 85**. Apart from direct target-related activity differences, poor solubility and bioavailability, enhanced metabolism or insufficient uptake into the bacteria cells are other reasons that may be behind the differences observed in vivo.

In vivo data for PBTZ169 (= **IR 124**) had been reported before,⁶⁹ although the murine model differed from the ultra-fast GSK model. Therefore, PBTZ **IR 124** (= PBTZ169) was tested in the ultra-fast GSK murine model to investigate the choice of the in vivo model (e.g. influence of the administration duration, mouse strain used) on the outcome of the in vivo assay and to verify the applicability of the GSK ultra-fast murine model for BTZ and PBTZ in vivo testing. The inventors of PBTZ169, Makarov and Cole, found a CFU reduction of 4.91 logs at a dose of 50 mg/kg in another mouse model of acute TB.⁶⁹ The GSK ultra-fast murine model revealed a CFU reduction of 3.0 for PBTZ169/**IR 124** at a dose of 200 mg/kg. Despite the fourfold higher single dose in the GSK model, the CFU reduction is still approx. 2 logs less compared to Makarov's and Cole's data⁶⁹ (CFU reduction 3.1 logs versus 4.9 logs, compare Table 7). Therefore, the outstanding activity of PBTZ169/**IR 124** found in the Makarov/Cole model was not entirely reproduced in the GSK model and shows that both mouse models provide different in vivo efficacy data for the same compound. Different in vivo potencies were described before for pyrazinamide and rifampicin, which were less active in the GSK model compared to other murine models with Balb/c mice and a longer duration of treatment.^{39,136} Nevertheless, PBTZ169 can be considered as a very effective compound with substantial in vivo activity in both mouse models, underlining its promising antitubercular activity.

The major difference of the ultra-fast GSK model and other mouse models of acute TB is the length of treatment with the test compounds. Cooper et al.⁶⁸ and Makarov et al.^{53,69} investigated their BTZ compounds in mouse models of acute TB with BALB/c mice. The mice were treated BTZs once a day for 4 weeks after intravenous infection with *Mtb* H37Rv. In contrast to this model, the ultra-fast murine model of GSK utilized *Mtb* H37Rv intratracheally infected C57BL/6J mice which were treated with the test compound for 4 days only (see Table 7). Furthermore, the application route of the test compound also influences the log CFU reduction. Orally administered BTZ038 (the racemate of BTZ043, both stereoisomers are equipotent in vitro⁵⁴) decreased CFU in lungs by 0.3-0.5 logs at doses of 12-25 mg/kg,⁵³ whereas BTZ043 given intragastrally (50 mg/kg) in later studies decreased CFU in lungs by

4.4 logs.⁶⁹ However, the different in vivo activities of the racemate, BTZ038, and its S-enantiomer, BTZ043, may have resulted from the higher dose of BTZ043 or from the predominant metabolism of one stereoisomer in mice in the BTZ038 in vivo study.

Table 7: Comparison of the different mouse models of acute TB

	GSK ultra-fast murine model ¹³⁶	Cooper et al. (2012) ⁶⁸	Makarov et al. (2012) ⁶⁹	Makarov, et al. (2007) ⁵³
No. mice/group	2	10	10	10
mice	C57BL/6J	BALB/c	male BALBc/cit	male BALB/c
infection with <i>Mtb</i> H37Rv	10 ⁵ CFU intratracheal	5*10 ⁶ CFU i.v. (eye venous sinus)	5*10 ⁶ CFU i.v. (lateral vein)	5*10 ⁶ CFU i.v. (lateral tail vein)
duration of study	9 d	5 weeks	4.5 weeks	4 weeks
application of test compound	oral	gavage	intragastral	oral
vehicle	1 % methyl cellulose	0.25 % carboxy methyl cellulose	H ₂ O plus 0.5 % acetic acid	carboxy methyl cellulose/water plus PEG400
administration scheme	200 mg/kg, 1x daily, starting day 5 after infection for 4 days	37.5 and 300 mg/kg, 1x daily, 5 d/week, starting day 8 after infection for 28 days	50 mg/kg, 1x daily, 5 d/week, starting day 2 after infection for 28 days	12 and 25 mg/kg, 1x daily, 6 d/week, starting day 1 after infection for 27 days
Result (log ₁₀ reduction of CFU in lungs)				
BTZ038				> 0.30 (12 mg/kg), > 0.54 (25 mg/kg) ⁵³
BTZ043			4.43 ⁶⁹	
isoniazid			4.87 (25 mg/kg) ⁶⁹	> 0.48 (25 mg/kg) ⁵³
PBTZ169 = IR 124	3.0		4.91 ⁶⁹	
IR 124xHCl	3.1			
IR 85	< 0.4			

Despite the lower in vitro activity of **IR 85** compared to BTZ043 and PBTZ169, it was included in the in vivo assay as to investigate if the different in vitro data correlate with different in vivo performance. Since BTZs interfere with an essential enzyme in the cell wall biosynthesis of mycobacteria, they are only active against actively growing bacilli. Considering the slow cell division rate of *Mtb*, it is assumed that the efficacy of BTZs not only depends on target affinity, but also on the time they are administered. For BTZ043 it is known that the activity depends on time more than on dose (U. Möllmann, personal communication and Makarov et al.⁵⁴).

However, in the case of **IR 85**, its lower in vitro activity (compared to BTZ043 and PBTZ169) correlated with poor in vivo performance, indicating that BTZs should display in vitro MICs at

or below 0.1 $\mu\text{mol/l}$. Therefore, **IR 85** needs to undergo medicinal chemistry optimizations to increase activity. In contrast, the different in vivo result for PBTZ169/**IR 124** presumably resulted from the different mouse models viz. the time of drug administration, underlining the time dependency of BTZ/PBTZ activity.

In general, the different murine models for TB in vivo studies are controversially discussed among leading scientists, who also note that not only the mouse strain used, but also the incubation period and duration of drug treatment can affect the efficacy of new drug compounds and mislead the evaluation of their potency (E. Nuermberger and Clif Barry, Gordon Research Conference Barga (Italy) 2013, also compare Koul et al.,²⁹ Franzblau et al.,¹³⁷ and Young¹³⁸).

3.4 CYTOTOXIC AND ANTIPROLIFERATIVE EFFECTS

Active compounds from the agar diffusion experiment were further investigated regarding their cytotoxic and antiproliferative activity. Results are shown in Table 8. Antiproliferative effects were investigated against human umbilical vein endothelial cells (HUVEC) and human myelogenous leukemia cells (K-562). Cytotoxic activity was analyzed in cervical cancer cells (HeLa) and hepatocellular carcinoma cells (HepG2). All assays were conducted according to standard assay protocols of the cooperation partners (see chapter 3.4).

For the HUVEC, K-562 and HeLa assays, compounds were dissolved in DMSO (1 mg/ml) and diluted with DMEM. DMSO as solvent limited the application to concentrations lower than or equal to 5 µg/ml (corresponding to a test compound concentration of approx. 11-15 µM) since DMSO has cytotoxic effects as well, but the addition of DMSO to the test compound solutions was necessary due to their poor aq. solubility (see chapter 4.2.3). Compounds **IR 112** and **IR 115** were measured separately with a maximum concentration of 50 µg/ml (corresponds to approx. 120 µM). Cytotoxic activity against HepG2 was determined with a maximum compound concentration of 50 µM.

The value of antiproliferative activity is given as concentration of test compound where inhibition of proliferation is 50 % compared to untreated control (GI_{50}).

The cytotoxic activity is given as concentration of test compound required for destruction of 50 % of cells compared to untreated control (CC_{50}).

The in vitro therapeutic index (or selectivity index, SI) for selected compounds was calculated (CC_{50} HepG2 / MIC *Mtb* H37Rv and CC_{50} HeLa / MIC *Mtb* H37Rv). This index provides an indication of the selective toxicity against the microbe compared to human cells and is an important parameter for assessing the safety profile of a drug candidate. The larger the index, the safer is the drug for human use. In TB research, compounds with indices above 50 display considerable selectivity towards mycobacteria and provide starting points for further lead optimization.¹³⁹ However, it is not possible to state a universal number considered as sufficient for a drug candidate.¹⁴⁰ Generally, the values for therapeutic indices can vary largely for different antimycobacterial drugs and different cell types tested (e.g. RIF SI_{Mtb/Vero cells} 10,350;¹⁴¹ INH SI_{Mtb/Vero cells} >142;¹⁴¹ INH SI_{Mtb/HepG2} 33,000-65,000^{142,143}).

Table 8: Cytotoxic and antiproliferative effects of selected BTZ and BOZ compounds

Compound no.	antiproliferative activity (µmol/l)		cytotoxic effects (µmol/l)		in vitro therapeutic index	
	HUVEC GI_{50} (n=4)	K-562 GI_{50} (n=4)	HeLa CC_{50} (n=4)	HepG2 CC_{50} (n=2)	CC_{50} HepG2/ MIC (<i>Mtb</i>)	CC_{50} HeLa/ MIC (<i>Mtb</i>)
halides at position 7						
IR 62	1.2	2.0	10.8	nd		0.3
IR 69	1.2	1.4	10.1	nd		0.2
IR 74	0.8	1.5	9.7	26.5	16.6	6.0
IR 76	1.0	1.5	8.6	8.9	5.6	5.4
IR 102	> 13.2	> 13.2	10.8	nd		

Compound no.	antiproliferative activity ($\mu\text{mol/l}$)		cytotoxic effects ($\mu\text{mol/l}$)		in vitro therapeutic index	
	HUVEC G_{i50} (n=4)	K-562 G_{i50} (n=4)	HeLa CC_{50} (n=4)	HepG2 CC_{50} (n=2)	CC_{50} HepG2/ MIC (<i>Mtb</i>)	CC_{50} HeLa/ MIC (<i>Mtb</i>)
IR 108	8.0	11.7	11.1	25.9	4.0	1.7
amino substituents at position 7						
IR 75	> 11.3	> 11.3	> 11.35	nd		
IR 100	> 11.7	> 11.7	> 11.7	nd		
aryl and heteroaryl substituents at position 2						
IR 51	> 14.2	> 14.2	> 14.2	nd		
IR 61	> 16.5	> 16.5	> 16.5	nd		
branched amino and other amino substituents at position 2						
IR 20	> 13.9	> 13.9	> 13.9	> 50.0	> 15.2	> 4.2
IR 58	> 13.8	> 13.8	> 13.8	> 50.0	> 8.5	> 2.4
IR 85	> 12.9	> 12.9	> 12.9	> 50.0	> 62.5	> 16.1
IR 115	> 120.4	> 120.4	> 120.4	> 50.0	> 50.0	> 120.4
IR 127 cis	> 12.9	> 12.9	> 12.9	nd		> 1.7
IR 127 trans	> 12.9	> 12.9	> 12.9	nd		> 21.5
IR 128	11.5	> 12.5	> 12.5	nd		
IR 140	> 12.5	> 12.5	> 12.5	nd		
IR 141	> 11.6	> 11.6	> 11.6	nd		
imidazobenzothiazinones						
IR 47	1.7	2.3	16.0	nd		
IR 78	1.1	1.1	9.4	nd		0.2
IR 80	> 15.8	> 15.8	> 15.8	nd		
benzoxazinones						
IR 95	> 13.5	10.5	> 13.5	21.3	3.3	> 2.1
IR 112	15.4	7.0	26.2	nd		1.7
IR 113	> 14.5	12.5	> 14.5	nd		> 3.7
IR 114	4.5	1.8	9.5	nd		
IR 125	> 11.4	> 11.4	> 11.4	nd		> 36.6
other						
IR 154	> 16.49	> 16.49	> 16.49	nd		
reference compounds						
BTZ043	nd	nd	nd	14.6 ⁽⁶⁹⁾	$\approx 3,100$ ⁽⁶⁹⁾	
PBTZ169	nd	nd	nd	146.0 ⁽⁶⁹⁾	$\approx 66,000$ ⁽⁶⁹⁾	
doxorubicin	nd	nd	nd	0.075		

nd: not determined

Most compounds tested showed a favorable toxicity profile, connoting no cytotoxicity or antiproliferative effects at the highest concentrations tested.

Considerable antiproliferative activity and cytotoxicity was detected for halogen substituted BTZs, both 7-halo-BTZs **IR 62**, **IR 69**, **IR 74**, **IR 76** and **IR 108** as well as the 8-chloro-imidazobenzothiazinones **IR 47** and **IR 78**. The cytotoxic concentration of **IR 62**, **IR 69**, and

IR 78 was lower than their MIC, resulting in therapeutic indices < 1 . These compounds were excluded from further development. The general cytotoxicity of the 7-halo substituted BTZs could also contribute to some extent to the unspecific efficacy of these compounds against the other test organisms in the agar diffusion assays (compare chapter 3.1). BTZs without the 7-chloro substituent (**IR 20**, **IR 58**, **IR 85**, **IR 115**, **IR 127 cis**, **IR 127 trans**, **IR 128**, **IR 140**, and **IR 141**) or possessing a 7-amino substituent (**IR 75**, **IR 100**) as well as 2-aryl/heteroaryl substituted BTZs (**IR 51**, **IR 61**) did not show antiproliferative or cytotoxic effects.

The most active compounds of this thesis, **IR 85** and **IR 115**, did not exhibit any antiproliferative or cytotoxic effects at all concentrations tested. Their therapeutic indices are > 62 and > 50 (HepG2), which underlines their high selectivity against *Mtb* and renders these compounds valuable starting points for hit-to-lead optimization programs.

Comparing the sulfur-containing BTZs with their BOZ counterparts, a slight increase in cytotoxicity and antiproliferative activity within the BOZ compounds was observed. Whereas BTZs **IR 20**, **IR 58**, **IR 85**, and **IR 115** did not show any cytotoxic effects at the highest concentrations tested, their BOZ counterparts **IR 112**, **IR 113**, **IR 95**, and **IR 114** did. This is also reflected by the low therapeutic indices of BOZs, which are in low single-digit range. However, the BOZ analog of PBTZ169, **IR 125**, was not cytotoxic or antiproliferative at all concentrations tested and displayed a therapeutic index (HeLa) of above 36. This indicates that there is no general cytotoxicity of the BOZ compound class and BOZs with piperazinyl substituents at position 2 are the scaffold of choice for further development of BOZs.

The therapeutic indices for BTZ and BOZ compounds of this thesis were considerably lower than those reported for BTZ043 and PBTZ169 (3,100 and 66,000). This mainly results from the decreased antimycobacterial activity (higher MICs than BTZ043 and PBTZ169) rather than from increased cytotoxic effects (exception: 7-chloro substituted BTZs and BOZs).

However, further toxicity studies have to be undertaken to prove finally the therapeutic eligibility of the BTZs and BOZs of this thesis. Since maximum test concentrations for antiproliferative and cytotoxicity assay were limited due to residual DMSO as solvent, these results only give a first idea of which compound subset to choose for future optimizations. 7-Halo substituted BTZs and imidazobenzothiazinones are less promising due to toxicity issues. BTZs with branched amino substituents at position 2 and BOZs with piperazinyl substituents at position 2 exhibit promising in vitro activity and no toxicity was detected in this preliminary assay.

Chapter Four

4 PHARMACOKINETIC EVALUATION

Pharmacokinetic profiling is an important factor in drug research. Pharmacokinetic describes how the body affects a specific drug after administration through the mechanisms of absorption, distribution, metabolism, and finally excretion (ADME). Early in vitro studies on metabolic stability, permeability, and solubility are mainly devised for predicting in vivo pharmacokinetic behavior of a drug candidate or the risk of drug-drug interactions and possible side effects. They allow an understanding of the in vivo fate of a drug candidate with the aim to select a lead candidate.¹⁴⁴

This chapter will address the evaluation of lipophilicity/hydrophobicity, which highly correlates with aq. solubility and bioavailability, of solubility and of metabolic stability.

4.1 CALCULATED LIPINSKI RULE-OF-FIVE PARAMETERS

In vitro results of new drug compounds do not necessarily reflect their in vivo potency. Several factors such as bioavailability, protein binding, metabolism, and clearance influence a drug's in vivo effects and may even lead to total inefficacy despite promising in vitro results. The discrepancy of the correlation of in vitro and in vivo test results has led to the development of the "Lipinski rule-of-five" – setting limits to physicochemical properties of new compounds, which are associated with a great chance of the compound to exhibit favorable drug-like properties especially oral bioavailability.¹⁴⁵ The implementation of the "rule-of-five" is now a basic element in the drug development process although it is no longer obeyed as absolutely as it was in the 1990 to 2000s. Especially in the field of antibacterials, successful drugs have higher hydrophilicity and molecular mass than Lipinski's rules would allow.³¹ For antimycobacterials, the lipophilic mycolate and hydrophilic polyarabinane cell wall layers require them to be amphiphilic including a substantial amount of lipophilicity.

The original "rule-of-five", described by Lipinski et al. in 1996, states that a compound possesses acceptable absorption and permeation properties if it comprises:

- molecular weight below 500 g/mol,
- logP below 5,
- no more than 10 hydrogen bond acceptors (sum of Os and Ns),
- no more than 5 hydrogen bond donors (sum of OHs and NHs).¹⁴⁵

Molecules that fulfill the "rule-of-five" could most likely become oral bioavailable drugs.

Lipinski rule-of-five values were calculated for all test compounds of this thesis in order to get an estimate of their theoretical physicochemical properties and compare them with BTZ043, PBTZ169 and PBTZ A. Values were calculated using Molecular Operating Environment Software (MOE 2012.10, calculation of logP was performed according to Wildman et al.¹⁴⁶) and are given in Table 9.

Table 9: Calculated Lipinski rule-of-five values

Compound no.	M (g/mol)	H-bond donors	H-bond acceptors	calc. logP (octanol/water)	violations of rule of 5
unsubstituted arene moiety, shifted nitro group					
IR 16	246.33	0	3	2.8	0
IR 86	248.30	0	4	1.6	0
IR 67	293.30	0	7	1.5	0
halides at position 7					
IR 53	329.28	0	7	1.8	0
IR 56	327.31	0	6	3.0	0
IR 62	343.77	0	6	3.5	0
IR 69	345.74	0	7	2.3	0
IR 74	393.77	0	6	4.7	0
IR 76	395.75	0	7	3.5	0
IR 102	379.29	0	7	3.0	0
IR 108	377.32	0	6	4.2	0
amino substituents at position 7					
IR 57	396.40	0	9	1.5	0
IR 64	394.43	0	8	2.7	0
IR 75	444.43	0	8	3.8	0
IR 77	446.41	0	9	2.7	0
IR 96	380.40	0	8	2.3	0
IR 97	378.43	0	7	3.4	0
IR 100	428.44	0	7	4.6	0
IR 101	430.41	0	8	3.5	0
IR 103	404.37	0	8	2.9	0
IR 104	402.40	0	7	4.1	0
IR 106	352.39	0	7	2.9	0
IR 107	354.36	0	8	1.7	0
aryl and heteroaryl substituents at position 2					
IR 51	353.28	0	6	4.0	0
IR 52	321.26	0	6	3.0	0
IR 61	303.27	0	6	2.8	0
IR 82	352.29	0	5	4.6	0
IR 87	382.32	0	6	4.6	0
IR 88	386.74	0	5	5.3	1
branched amino and other amino substituents at position 2					
IR 20	359.33	0	6	4.0	0
IR 58	361.30	0	7	2.9	0
IR 85	387.38	0	6	4.8	0
IR 115	415.44	0	6	5.6	1
IR 124	456.49	0	7	4.7	0
IR 124xHCl	492.94	1	7	3.3	0
IR 127	387.38	0	6	4.5	0

Compound no.	M (g/mol)	H-bond donors	H-bond acceptors	calc. logP (octanol/water)	violations of rule of 5
IR 128	400.38	1	7	3.2	0
IR 140	401.36	0	7	4.0	0
IR 141	429.41	0	7	4.7	0
imidazobenzothiazinones					
IR 47	301.69	0	6	2.3	0
IR 59	352.35	0	8	1.5	0
IR 78	351.69	0	6	3.5	0
IR 79	402.35	0	8	2.7	0
IR 80	317.25	0	6	2.8	0
IR 98	386.35	0	7	3.4	0
IR 105	360.32	0	7	2.9	0
benzoxazinones					
IR 95	371.32	0	7	4.1	0
IR 112	343.26	0	7	3.3	0
IR 113	345.23	0	8	2.1	0
IR 114	399.37	0	7	4.9	0
IR 125	415.44	0	6	4.0	0
reference compounds					
BTZ043	431.39	0	8	3.8	0
PBTZ169	456.49	0	7	4.7	0
PBTZ A	507.49	1	9	3.8	1

Most of the BTZ and BOZ compounds of this thesis fulfill the requirements of the Lipinski rule-of-five. Violations are seen in calculated logP values for 2-(4-methoxy)phenyl-BTZ **IR 88** and 2-tetramethylpiperidinyl substituted BTZ **IR 115**.

Comparing BTZs with their corresponding BOZ analog, the calc. logP values of the BOZs are approx. 0.7 log units lower than those of their BTZ counterparts, indicating that BOZs might exhibit less lipophilicity and therefore improved solubility in aq. media.

Characteristic for all BTZ and BOZ compounds is their general lipophilicity, with logP values between 1.5 and 5.6. The imidazobenzothiazinones seem to be less lipophilic (logP 1.5-3.5), followed by the 7-amino and 7-halo substituted BTZs (logP 1.5-4.7). The most lipophilic compounds are BTZs and BOZs with branched and more complex amino substituents at position 2, with the arene moiety bearing NO₂ and CF₃ as fixed substituents (logP 2.1-5.6). These are the compounds with highest in vitro activity against *M. vaccae* and *Mtb*, corroborating that a certain lipophilicity is necessary for antimycobacterial activity.

Compared to the data of reference compounds BTZ043, PBTZ169 and PBTZ A, the calculated rule-of-five values of BTZs and BOZs of this thesis are in the same range. Since poor aq. solubility was already described for BTZ043 and accounting the similar calc. physicochemical data for the novel BTZs and BOZs, low aq. solubility rather than too high lipophilicity is assumed to be an obstacle for our compounds as well.

4.2 SOLUBILITY

Poor solubility in aq. media is a characteristic problem described for antimycobacterial BTZ compounds.⁶⁰ Different groups have addressed this issue and developed the second generation piperazinyl-BTZs, in which the second basic nitrogen atom of the piperazine enables the formation of water-soluble salts, such as hydrochlorides.⁶⁷⁻⁶⁹ Published solubility data is rare for BTZs. Solubility data for some of the most active BTZ and BOZ compounds of this thesis were determined in order to compare them to the previously described BTZs and contribute more data to this particularly pressing issue in BTZ chemistry, which could help to improve pharmacokinetic properties of this promising antitubercular compound class.

4.2.1 Methods of solubility determination

The solubility of a compound in a specific solvent at a specific temperature and pressure is the maximum amount of solid compound homogeneously mixed (= dissolved) with the solvent (= saturated solution). Solubility (S) is expressed in terms of maximum volume or mass of the solute that dissolve in a given volume or mass of a solvent at a given temperature and pressure. The solute is in equilibrium with its most stable crystalline solid form, therefore S describes saturated solutions.¹⁴⁷⁻¹⁴⁹

Lipinski et al. describe two different ways of the general solubilization process of compounds – a thermodynamic solubility and a kinetic solubility. Thermodynamic solubility describes the original physicochemical process of a solid mixed with a solvent, in which an equilibrium exists between solid and solute and is also referred to as intrinsic solubility. The latter describes a process in which supersaturated solutions are formed and the timepoint of first precipitation is determined.¹⁴⁵

Only a few methods to determine the solubility of compounds are routinely in use: the shake-flask method, turbidimetry, and potentiometric titration. Glomme et al.^{148,150} discuss advantages and disadvantages of all three methods. The shake-flask method seems to be the method of choice, since it determines the thermodynamic solubility in contrast to the turbidimetry which measures the kinetic solubility if supersaturated solutions are formed. Potentiometric titration is only applicable for ionizable compounds (acids and bases) and affords a pH-dependent solubility profile.¹⁴⁸ Based on the work of Glomme et al., we decided to employ the shake-flask method. It is suitable for compounds with proposed poor solubility, measures thermodynamic solubility with very accurate results and does not require specific lab equipment besides a HPLC apparatus.^{148,150}

4.2.2 Calculated solubility of selected BTZs and BOZs

Besides experimental solubility determination, which is time and cost consuming, solubilities of new drug substances are calculated to select a set of compounds for further physicochemical assays and medicinal chemistry optimization.

The Yalkowsky equation, developed for non-electrolytes, combines the partition coefficient logP value as a measure of solvation energy and the melting point (m.p.) as a measure of lattice energy in order to predict a compound's solubility logS.¹⁵¹

$$\text{[Yalkowsky equation]} \quad \log S = 0.8 - \log P - 0.01 \times (\text{m.p.} - 25)$$

Solubility was calculated for eight compounds of this thesis, utilizing the Yalkowsky equation, calculated logP values from chapter 4.1, and experimentally determined melting points (Table 10).

Table 10: Calculated solubility of selected BTZ and BOZ compounds

compound no.	m.p. (°C)	calc. logP	calc. logS
IR 20	144	4.0	-4.39
IR 74	218	4.7	-5.83
IR 76	265	3.5	-5.10
IR 80	173	2.8	-3.48
IR 85	135	4.8	-5.10
IR 95	123	4.1	-4.28
IR 124	185	4.7	-5.50
IR 124xHCl	245	3.3	[-4.70] ^b
reference compounds			
BTZ043	193 ^a	3.8	-4.68, -4.73 ⁽⁶⁷⁾
PBTZ A	no data given	3.8	-5.85 ⁽⁶⁷⁾

^a melting point of racemate BTZ038, since no data for BTZ043 is publically available³³

^b hypothetical value, since Yalkowsky equation is only applicable for non-electrolytes

Calculated logS values for the selected BTZ and BOZ compounds (logS -4.4 - -6.1) are within the range of the calculated values for BTZ043 and PBTZ A. The PBTZ scaffold itself does not account for increased solubility when compared to BTZ043, calc. logS values are lower (**IR 124**/PBTZ169: -5.5, PBTZ A: -5.85). The formation of appropriate salts such as the hydrochloride **IR 124xHCl** entails a hypothetical calc. logS of -4.7^b, which is about the same value as BTZ043 and would not suggest this compound to be better soluble.

Consistent with the calc. logP values, the imidazobenzothiazinone **IR 80** is expected to show better solubility since its calc. logS value is about one order of magnitude higher than the one for BTZ043 (logS -3.48 versus -4.68).

4.2.3 Solubility determination via the shake-flask method

The shake-flask method used for solubility determination of seven BTZ und BOZ compounds (**IR 20**, **IR 74**, **IR 76**, **IR 85**, **IR 95**, **IR 124**, **IR 124xHCl**) was slightly adapted from the method described by Glomme.¹⁴⁸ **IR 80** was excluded from solubility determination, since the compound decomposed in the HPLC eluent.

Two stock solutions of each compound were prepared (10 mg compound in 50 ml HPLC eluent ACN:H₂O 1:1 (V/V) + 1 % TFA) and five dilutions from each stock solution were prepared to calculate the calibration curve. Each HPLC sample was determined in duplicate and the mean AUC of both runs used for calculations.

For solubility determination, the compounds were mixed with two different aq. solvents (PBS buffer pH 7.4 and acetate buffer pH 4.5) for 48 h on a rotary shaker at ambient temperature. The presence of a remaining precipitate was confirmed visually after 8 h, 24 h, and 48 h. Subsequently, samples were filtered and the amount of solute determined by HPLC. Solubility determinations as well as HPLC analyses were performed in duplicate. Solubility was calculated utilizing the calibration curve from the standard solutions and is shown in Table 11.

Appreciable solubility was only measured for **IR 20**, **IR 95**, and **IR 124**. For all other compounds, no experimental solubility was determinable. Calculating the corresponding compound concentrations from the AUC of HPLC peaks revealed solubility with negative algebraic signs for **IR 74**, **IR 76**, **IR 85**, and **IR 124xHCl**. Therefore, a hypothetical solubility of 0.001 µg/ml was assigned to these compounds. The negative algebraic signs are presumably a result of the fact that calibration equations were developed from two sets of standard solutions only and therefore are an approximation.

Table 11: Experimental solubility of selected BTZ and BOZ compounds

compound no.	calc. logS	solubility PBS buffer, pH 7.4 (n=2)			solubility HAC/NaAc buffer, pH 4.5 (n=2)		
		µg/ml	µM	logS	µg/ml	µM	logS
IR 20	-4.39	6.9±0.41	19.3±1.14	-4.7	7.3±0.36	20.4±1.00	-4.7
IR 74	-5.83	0.001	0.0025	-8.6 [#]	0.001	0.0025	-8.6 [#]
IR 76	-5.10	0.001	0.0025	-8.6 [#]	0.001	0.0025	-8.6 [#]
IR 85	-5.10	0.001	0.0026	-8.6 [#]	0.001	0.0026	-8.6 [#]
IR 95	-4.28	1.08±0.28	2.9±0.75	-5.5	1.40±0.29	3.78±0.78	-5.4
IR 124	-5.50	0.63±0.01	1.39±0.03	-5.9	1.07±0.06	2.35±0.13	-5.6
IR 124xHCl	-4.70	0.001	0.002	-8.7 [#]	0.001	0.002	-8.7 [#]
reference compounds							
BTZ038			7.8 ^{a(54)}				
BTZ043 ^b	-4.73 ⁽⁶⁷⁾		6.8 ⁽⁶⁷⁾	-5.16 ⁽⁶⁷⁾			
PBTZ A ^b	-5.85 ⁽⁶⁷⁾		11.9 ⁽⁶⁷⁾	-4.93 ⁽⁶⁷⁾			

[#] logS calculated from a hypothetical solubility of 0.001 µg/ml, since measured solubility was found to be between -0.8 and -0.1 µg/ml.

^a no solvent or method of solubility determination given

^b kinetic solubility, method described in supporting information of Karoli et al.⁶⁷

2-Piperidinyl BTZ **IR 20** displayed a logS of -4.7 in both solvents tested, which fit well with the predicted logS of -4.39 and was slightly better than those determined for PBTZ A (-4.93)⁶⁷ and BTZ043 (-5.16).⁶⁷ Therefore, the lower molecular weight of **IR 20** and its less bulky piperidinyl substituent at position 2 (in contrast to the spiro moiety of BTZ043 or piperazinyl moiety in of PBTZ A) contributed to enhanced aq. solubility. Experimentally determined logS of PBTZ **IR 124** also fit well with its predicted value (-5.9 in pH 7.4, -5.6 in pH 4.5, and -5.5 predicted) which was slightly inferior to BTZ043 but within one log unit. However, a solubility between 1.3-2.3 μM for **IR 124** underlines the poor solubility of the piperazinyl substituted BTZs. As expected, solubility of **IR 124** in acidic media is slightly better than at pH 7.4 (2.35 μM versus 1.39 μM), since the second basic nitrogen of the piperazinyl moiety is capable of protonation and salt formation. For BOZ **IR 95**, a logS of -5.5/-5.4 was determined (pH 7.4/4.5), indicating a high hydrophobicity for this compound. As indicated by the calculated physicochemical properties for BTZs and BOZs, the BOZ **IR 95** is less lipophilic and exhibited better aq. solubility than its BTZ analog **IR 85**, for which no solubility could be determined. However, the poor solubility of **IR 95** may have resulted from degradation during the 48 h shaking process in both solvents. HPLC chromatograms of **IR 95** showed a variety of new peaks (Figure 51).

Despite measurable values for the solubility in both solvents tested for **IR 20**, **IR 95**, and **IR 124**, all determined compound concentrations are below 0.1 mg/ml, indicating an “insoluble” compound when referred to the solubility classification system of the European Pharmacopoeia (Table 12).¹⁵²

Table 12: Solubility classification of the European Pharmacopoeia

solubility classification	compound concentration	parts of solvent required for 1 part of solute
very soluble	$\geq 1,000$ mg/ml	≤ 1
freely soluble	100-1,000 mg/ml	1-10
soluble	33-100 mg/ml	10-30
sparingly soluble	10-33 mg/ml	30-100
slightly soluble	1-10 mg/ml	100-1,000
very slightly soluble	0.1-1 mg/ml	1,000-10,000
insoluble	≤ 0.1 mg/ml	$\geq 10,000$

Importantly, the hydrochloride PBTZ **IR 124xHCl**, which was assumed to possess better solubility than **IR 124** due to the ionic character of the compound and increased hydration in aq. media, as well as higher calculated values for logP and logS (compare chapter 4.2.2), failed in the solubility assay. It did not show improved solubility in aq. media at both pH values investigated compared to the free base **IR 124**. This was particularly surprising for pH 4.5, since the basic nitrogen of **IR 124** should be protonated ($\text{pK}_{\text{B}1}$ piperazine 4.19)¹⁵³ and therefore no difference in solubility was expected compared to the hydrochloride salt **IR 124xHCl**. However, the presumable formation of an **IR 124** acetate salt at pH 4.5 indicates that the acetate leads to better solubility than the chloride (**IR 124xHCl**). Hydrochlorides of poorly soluble drug compounds are the most frequent salts due to their simple availability

and physiology, but they do not necessarily entail enhanced solubility.¹⁵⁴ Especially in gastric fluid, with high abundance of chloride ions, hydrochlorides may exhibit poor solubility due to the common-ion effect. In some cases, mesylates of drug compounds or even the free bases were better soluble in chloride-rich media than the corresponding hydrochlorides.¹⁵⁴⁻¹⁵⁶ However, the solubility experiment of this thesis did not include chloride-rich gastric fluid as media. Other effects that account for poor solubility rather than the common-ion effect, such as increased lattice energy of the hydrochloride, might contribute to the poor solubility. Although the formation of salts is the most common and effective method of increasing solubility of acidic and basic drugs in pharmaceutical research,¹⁵⁷ the formation of a hydrochloride was no benefit for the compound's pharmacokinetic properties in this particular case, which is in contrast to the suggestions of Makarov et al.⁶⁹ As expected for the salt **IR 124xHCl**, its poor solubility in organic solvents such as chloroform, methanol, DMSO, and acetone was also observed during the synthesis and structural analysis of the compound. Whether different organic counterions, such as citrates, fumarates or mesylates, or inorganic salts, such as phosphates positively influence the compound's properties is currently investigated in our group.⁷⁰

Besides the poor aq. solubility, some BTZs were shown to partly decompose during the solubility assay. BTZs with the same arene scaffold (**IR 20**, **IR 85**, **IR 124** and **IR 124xHCl**) showed a new peak in the HPLC chromatogram with a retention time of approx. 4.2 min after the 48 h shaking experiment (red arrow, Figure 50). The new peak was observed independently in both media tested (pH 7.4 and pH 4.5). The same retention time for the new peak throughout the BTZs with the same arene substitution pattern implied a common degradation product, e.g. hydrolysis of the benzothiazinone system to yield a 3-nitro-5-(trifluoromethyl)-substituted benzoic acid derivative. This hypothesis also applied for BTZs **IR 74** and **IR 76**, which share the same chloride substituent at the arene moiety and also showed a new peak after the shaking experiment at approx. 4.5 min. Chloride slightly increases lipophilicity of the arene compared to a hydrogen substituent and therefore explains the slight increase in retention time (Figure 50). The possible degradation products could not be characterized by MS because the corresponding samples gave non-interpretable spectra.

The degradation may result from the large amount of buffer/water in which the test compounds were suspended (e.g. enhanced hydrolysis) rather than the influence of the HPLC eluent since the samples for the calibration curve calculations were dissolved in the HPLC eluent and delivered clean HPLC chromatograms with only one peak. Therefore, further experiments to investigate the stability of BTZs and BOZs in aq. media should be undertaken.

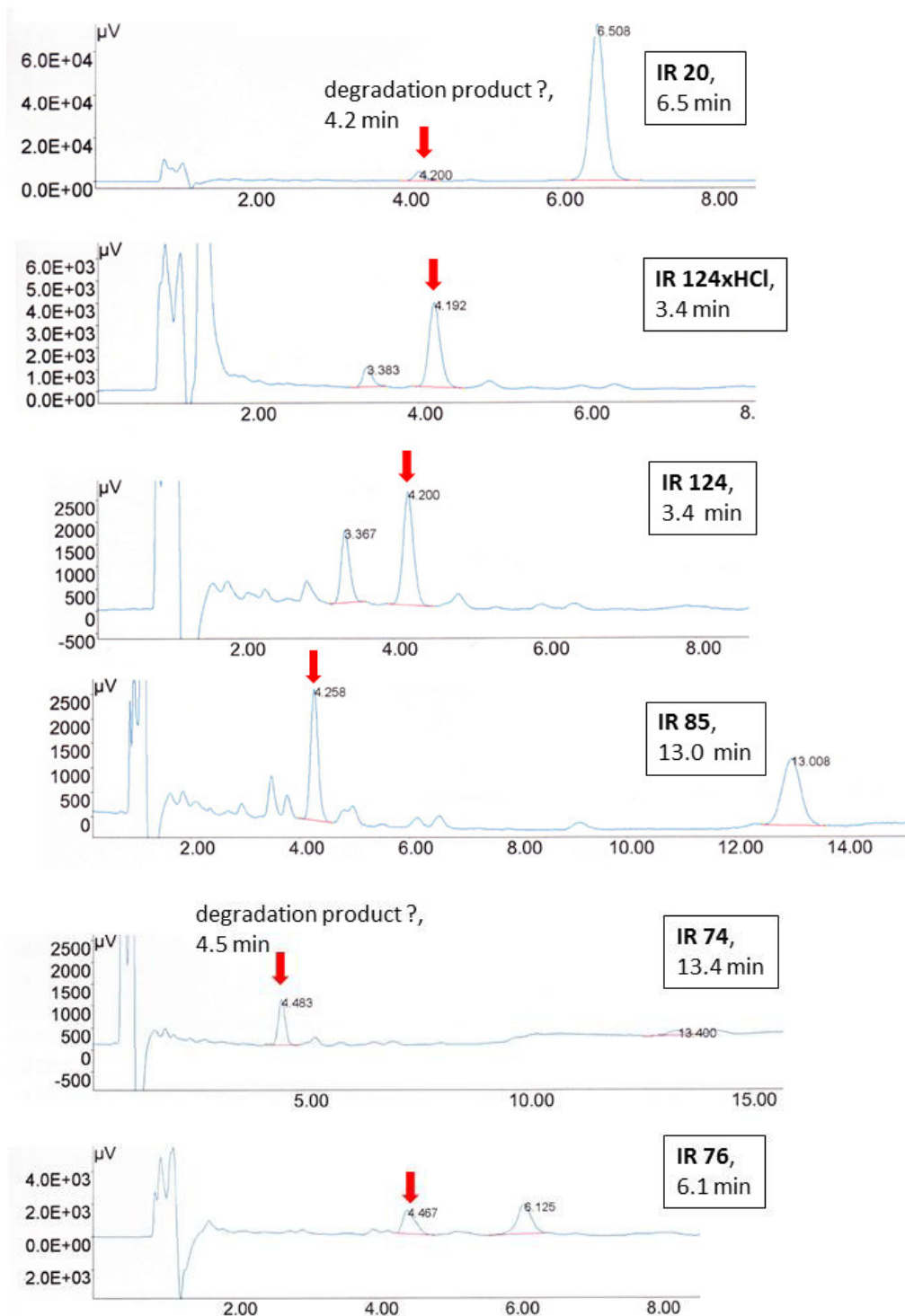


Figure 50: HPLC chromatograms of BTZs IR 20, IR 124xHCl, IR 124, IR 85, IR 74, and IR 76 after 48 h, PBS buffer 7.4. Red arrows indicate the common degradation peak at 4.2 min or 4.5 min.

Degradation of BTZ IR 85 and BOZ IR 95, both comprising the 2,6-dimethylpiperidinyl substituent, was distinctly increased compared to the other compounds in this test set. Besides the common degradation peak for BTZs at 4.2 min, IR 85 showed a variety of new peaks (retention time 3.4 min, 4.2 min, 4.9 min, 6.5 min, and 8.9 min). Therefore, the “insolubility” of IR 85 could either result from profound degradation and/or from actual poor aq. solubility. No considerable difference of degradation pattern was observed in both media

tested. **IR 95** showed new peaks at 3.5 min, 4.5 min, 5.2 min, 6.5 min, 6.8 min and 8.8 min, independent from the pH values of the solubility test media (Figure 51). Therefore, the poor experimentally determined solubility of **IR 95** could either result from the high degradation of the compound and/or an actual poor aq. solubility, as well.

However, the poor stability of **IR 85** and **IR 95** in aq. media did not account for a general instability of these compounds, since both were considerably stable towards microsomal enzymes in vitro (see chapter 4.3).

Chemical and enzymatic stability (as addressed by microsomal stability assays, see chapter 4.3) of BTZ and BOZ compounds need to be evaluated independently since our experiments showed that they do not correlate.

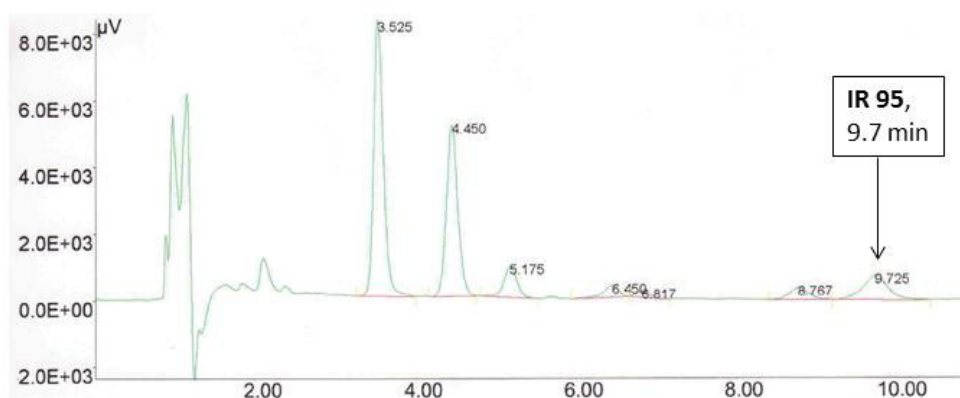


Figure 51: HPLC chromatogram of BOZ **IR 95** after 48 h shaking in PBS buffer pH 7.4

4.3 MICROSOMAL STABILITY

Measuring metabolic stability is an important indicator of a drug's possible metabolic pathway and should ideally include the identification and quantification of major metabolites of a compound. However, the latter issue involves more comprehensive studies.¹⁴⁴ Therefore, first experiments generally aim at the determination of a compound's general stability towards metabolizing enzymes (percentage of remaining compound after a given incubation time), elimination rate (half life), and elimination efficiency of an organ/in vitro system towards a compound (intrinsic clearance, CL_{int}).^{144,158} The intrinsic clearance CL_{int} of a test compound describes the volume which is cleared from the test compound in a specific time by a specific amount of microsomal proteins.

In vitro microsomal stability was determined using human and mouse liver microsomes, which were pooled subcellular fractions that contain membrane bound drug metabolizing enzymes from liver cells. Microsomes were incubated with the test compound and cofactor NADPH and the disappearance of test compound determined at certain time points via LC-MS/MS. From the plot of \ln [peak area ratio] (compound peak area/internal standard peak area) against time, the gradient of the line was determined. Subsequently, half life and intrinsic clearance were calculated using the equations given in chapter 7.3.3.

A subset of the most active BTZ and BOZ compounds of this thesis was selected for stability assays in human and murine liver microsomes; the benzodiazepine midazolam was chosen as control. Stability values are given as intrinsic clearance CL_{int} (ml/(min*g)) and half life ($t_{1/2}$, Table 13).

Table 13: Microsomal stability in human and mouse liver microsomes for selected BTZ and BOZ compounds (n=2)

Compound no.	human liver microsomes		mouse liver microsomes		microsomal stability (remaining %)	
	CL_{int} (ml/(min*g))	$t_{1/2}$ (min)	CL_{int} (ml/(min*g))	$t_{1/2}$ (min)	human	mouse
halides and protons at position 7						
IR 74	10.2 ± 0.1	7.8	3.9	19.3		
IR 76	5.6	12.6	3.0	24		
IR 108	1.8	> 30	0.6	> 30		
branched amino and other amino substituents at position 2						
IR 20	16.5 ± 0.1	5.2	3.5	20.4		
IR 58	0.9	> 30	1.1	> 30		
IR 85	10.9 ± 0.1	6.5	1.9	> 30		
IR 115	> 30	< 5	> 30	< 5		
benzoxazinones						
IR 95	1.3	> 30	< 0.5	> 30		
IR 112	3.6	21.6	1.2	> 30		
IR 113	0.5	> 30	< 0.5	> 30		

Compound no.	human liver microsomes		mouse liver microsomes		microsomal stability (remaining %)	
	CL _{int} (ml/(min*g))	t _{1/2} (min)	CL _{int} (ml/(min*g))	t _{1/2} (min)	human	mouse
reference compounds						
BTZ043	16.2 ⁽⁶⁹⁾		10.3 ⁽⁶⁹⁾		98 ⁽⁶⁷⁾	45 ⁽⁶⁷⁾
BTZ038					77 ⁽¹⁵⁹⁾	
PBTZ169	23.9 ⁽⁶⁹⁾		20.9 ⁽⁶⁹⁾			
PBTZ A					13 ⁽⁶⁷⁾	2 ⁽⁶⁷⁾
midazolam	7.7	9.7	31.9 ± 0.4	< 5		

Clearance categories according to GSK assay protocol: low (CL_{int} < 5 ml/(min*g)), moderate (CL_{int} = 5-15 ml/(min*g)), high (CL_{int} > 15 ml/(min*g))

Accounting data from the human liver microsome assay, compounds **IR 20** and **IR 115**, as well as BTZ043 and PBTZ169, are categorized as high clearance compounds, according to the GSK assay protocol. Compounds **IR 74**, **IR 76**, and **IR 85** rank within the moderate clearance category. Compounds **IR 58** and **IR 108** as well as all BOZ compounds (**IR 95**, **IR 112**, **IR 113**) belong to the low clearance category. In contrast to reference compounds BTZ043 and PBTZ169, for which only small differences in the microsomal stability between human and mouse liver microsomes are reported in the literature,⁶⁹ all tested compounds (except **IR 115**) of this thesis are more stable in mouse than human liver microsomes (mouse liver microsomes: all compounds are ranked within in the low clearance category).

The 2-tetramethylpiperindyl substituted BTZ **IR 115** was found to be unstable with a half life of less than 5 min and CL_{int} above 30 ml/(min*g) in human and mouse liver microsomes. Compared to BTZ043 and PBTZ169, all tested BTZs and BOZs, except **IR 115**, showed improved stability in human and mouse liver microsomes.

BOZ compounds seem to be more stable than their direct BTZ analogs with lower clearance values and increased half life:

BOZ IR 95	CL _{int} 1.3	BTZ IR 85	CL _{int} 10.9
BOZ IR 112	CL _{int} 3.6	BTZ IR 20	CL _{int} 16.5
BOZ IR 113	CL _{int} 0.5	BTZ IR 58	CL _{int} 0.9

Compared to the results from the solubility assay (compare chapter 4.2.3) in which BOZ **IR 95** was found to degrade during the shaking process in aq. media, this increased stability of BOZs towards microsomal enzymes was notable. The decreased stability of BTZs presumably results from oxidation of the bivalent sulfur, although sulfoxide and sulfone metabolites have not been reported for BTZ043 so far. Further studies are needed to support the theory that the replacement of sulfur by oxygen effectively contributes to the compound's stability towards microsomal enzymes and if the degradation seen for **IR 95** in aq. media is a phenomenon of this particular compound or of BOZs in general.

Comparing the amino substituent at position 2, morpholine seems to add some stability to the compounds when compared to their piperidine analogs:

morpholine BTZ IR 58	CL _{int} 0.9	piperidine BTZ IR 20	CL _{int} 16.5
morpholine BTZ IR 76	CL _{int} 5.6	piperidine BTZ IR 74	CL _{int} 10.2
morpholine BOZ IR 113	CL _{int} 0.5	piperidine BOZ IR 112	CL _{int} 3.6

In conclusion, the microsomal stability of the test compounds is better or in the same range (except **IR 115**) as for the lead BTZ compounds BTZ043 and PBTZ169.

However, no detailed data on possible metabolites of BTZ043 and PBTZ169 is available. A possible metabolic pathway of nitroarenes is the reduction of the nitro group to an amino group during phase I metabolism.¹⁶⁰ In fact, the amino metabolite of BTZ043 was found in blood and urine of mice.⁶⁰

Whether BTZs and BOZs of this thesis are converted to their amino metabolites or if other metabolites with pharmacological activity of their own are formed needs to be investigated in future studies.

Chapter Five

5 CO-CRYSTALLIZATION WITH DPRE1

In 2012, two groups published crystal structures of the BTZ target DprE1 with covalently bound inhibitors.^{57,63} Batt et al.⁶³ revealed the crystal structure of *Mtb* DprE1 with a nitroso compound, however not a nitroso BTZ, but with CT325, which is derivative of dinitrobenzamide DNB1 (Figure 52). Dinitrobenzamides (DNBs) were identified as DprE1 inhibitors in a HTS and display high antimycobacterial activity (compare chapter 1.5).¹²⁰

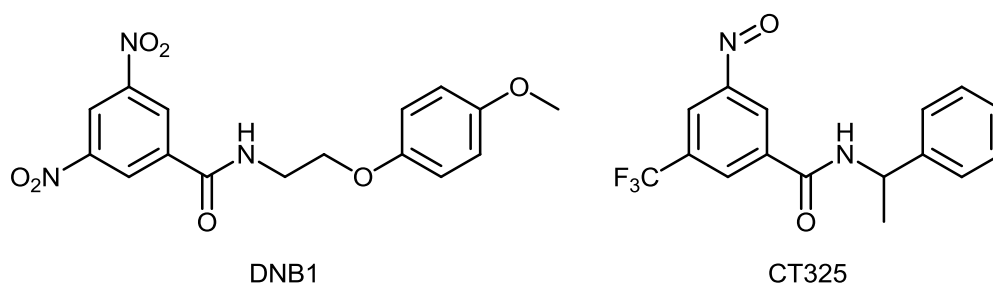


Figure 52: Chemical structures of DNB1 and CT325

The covalent bond of the nitroso group of CT325 to the amino acid cysteine Cys387 was clearly to be seen (Figure 53). The CF₃ group of CT325 formed van der Waals interactions with Gly133 and Lys134 and the side chains of His132, Ser228, and Lys367 (thick hashed lines, Figure 53). The nitroso group was involved in a second strong interaction, viz. a hydrogen bond with the amide group of Asn385 (dashed line).⁶³

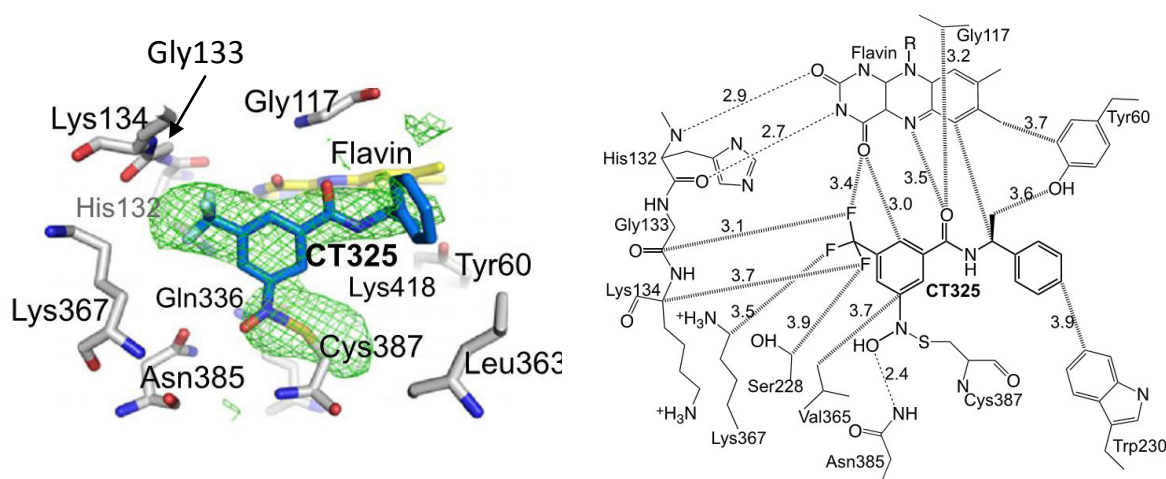


Figure 53: CT325 and its mode of binding at *Mtb* DprE1⁶³

Simultaneously, Neres et al.⁵⁷ performed co-crystallization experiments with BTZ043 and purified DprE1, however not from *Mtb*, but from the non-pathogenic *M. smegmatis* (sequence identity 83 % between *Mtb* and *M. smegmatis* DprE1). On incubation, obviously the nitro group of BTZ043 was reduced to the nitroso group because the X-ray data showed a covalent bond between what was the nitro N atom and Cys394, the homologous amino acid to Cys387 in the *M. smegmatis* enzyme (Figure 54). The CF₃ group of BTZ043 was well placed in a small pocket lined by His139, Gly140, Lys141, and Phe376 and interacted with the amide group of Asn392. No other major interactions were detected for BTZ043, except for a hydrophobic interaction between the side chain of Leu370 and the piperidine ring of BTZ043 as well as a hydrogen bond of the OH of the 'semimercaptal' to a water molecule bridging this hydrogen bond to Tyr67.⁵⁷

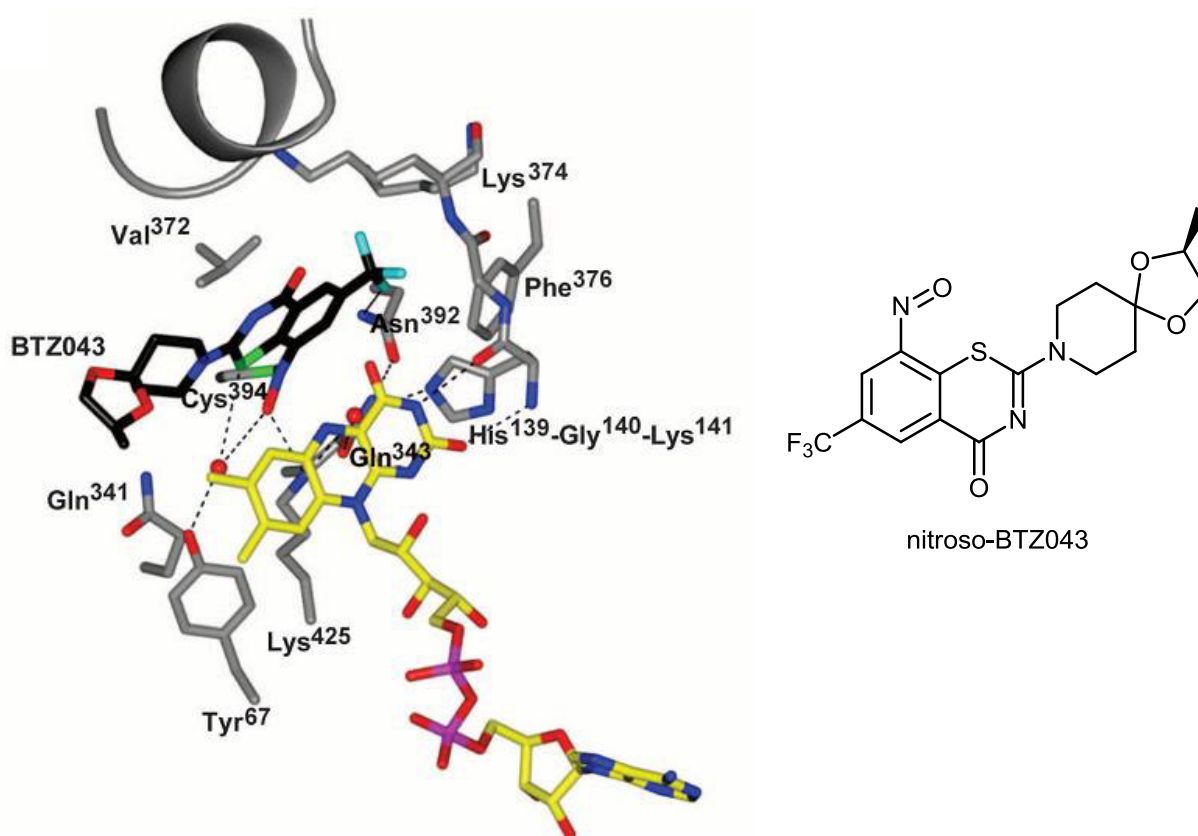


Figure 54: Mode of binding of nitroso-BTZ043 at DprE1 from *M. smegmatis*⁵⁷

Both crystal structures show that the inhibitors are situated parallel to the isoalloxazine of FAD, nicely fitting into the space between the FAD binding site of DprE1 and the cysteine Cys387 (*Mtb*; Cys394 in *M. smegmatis*).

5.1 CRYSTAL STRUCTURE OF BOZ IR 95 WITH DPRE1

The BOZ **IR 95** was chosen for crystallization experiments with the proposed target enzyme DprE1 of *Mtb* in order to confirm the molecular mode of action of the novel BOZs being the same as described for BTZs. Crystallization experiments were conducted by Sarah Batt and Klaus Fütterer in the group of Prof. Besra, University of Birmingham.

After incubation of the test compound with FPR, FAD and DprE1, crystals were grown and X-ray diffraction data generated. FPR is farnesylphosphoryl- β -D-ribofuranose, a surrogate substrate for DprE1, replacing the natural substrate, DPR. It is essential for the formation of FADH₂ from FAD. The cofactor FADH₂ is proposed to be responsible for the formation of the nitroso group; compare Neres et al.⁵⁷ and Trefzer et al.⁵⁸

Figure 55 shows the surface diagram of nitroso-**IR 95** with *Mtb* DprE1, Figure 56 shows the mode of binding of nitroso-**IR 95** in the active site of *Mtb* DprE1. The unbiased difference density clearly indicates covalent attachment of nitroso-**IR 95** to DprE1. There is, however, a slight technical flaw with the geometry of the 'semimercaptal' between nitroso-**IR 95** and Cys387, as the nitrogen of the nitroso group is not exactly planar with the sulfur from Cys387. This flaw is due to geometric restraints used in the structure refinements, but does not alter the overall picture of the mode of binding. The geometry of the covalent bond of nitroso-**IR 95** with Cys387 matches with the one reported for nitroso-BTZ043 in *M. smegmatis* DprE1⁵⁷ (K. Fütterer, personal communication).

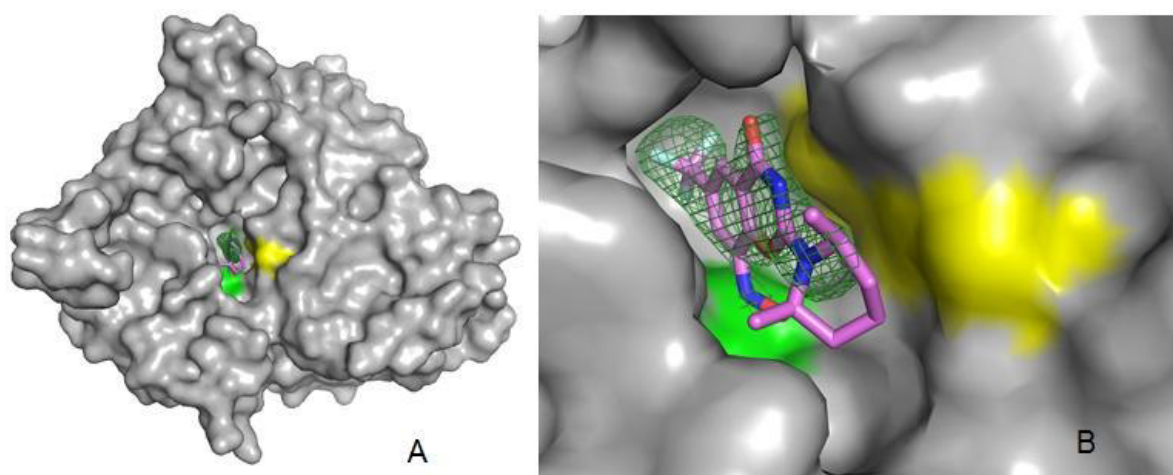


Figure 55: Surface diagram (A) and close-up view (B) of *Mtb* DprE1 with inhibitor **IR 95** bound in the active site

Surface areas belonging to FAD and Cys387 are colored in yellow and green, respectively. Unbiased difference density, contoured at 3σ above background and indicating the presence of the inhibitor, is shown in dark green.

The OH of the semimercaptal covalent bond of nitroso-**IR 95** forms a hydrogen bond to a water molecule and this hydrogen bond is extended by the water molecule to Lys418. This is similar to the structure of nitroso-BTZ043 in *M. smegmatis* DprE1, where a water molecule forms a hydrogen bond to the OH of the semimercaptal and bridges this hydrogen bond to Tyr67.⁵⁷

Figure 56 also shows that besides the covalent bond, the trifluoromethyl group is the key determinant for the orientation of nitroso-**IR 95** in the active site. It forms van der Waals interactions with Gly133, Lys367, Phe369, and Asn385. Furthermore, the carboxyl group of the nitroso-**IR 95** heterocycle interacts with Lys134 and Gly117. The non-covalent interaction of the carboxyl group with Gly117 was also described by Batt et al. for the BTZ-related compound CT325.⁶³

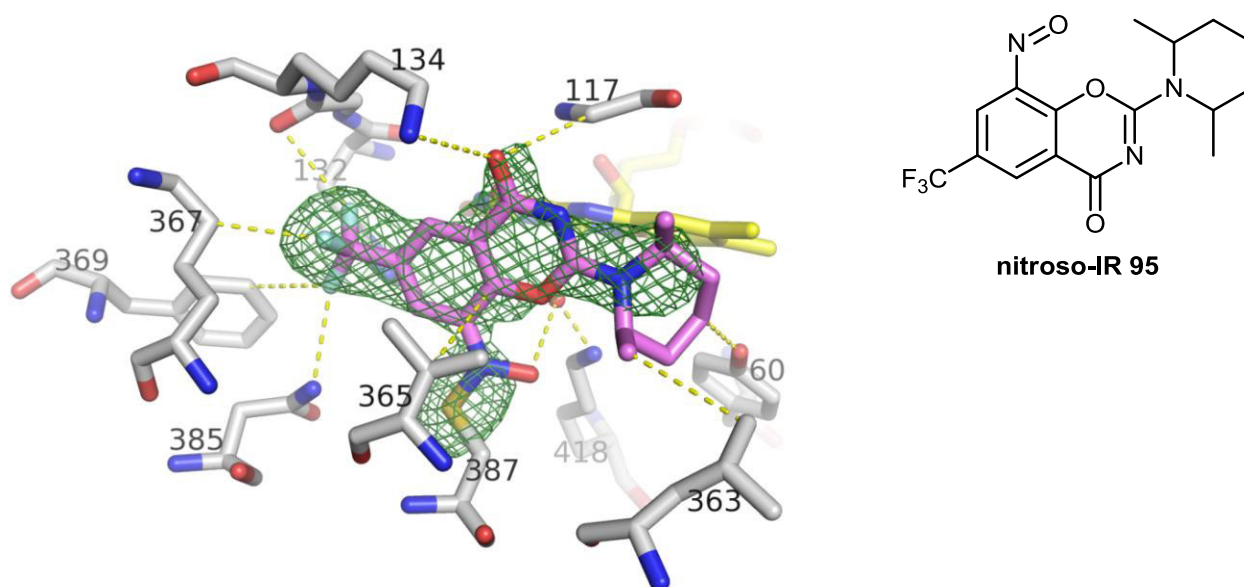


Figure 56: Mode of binding of nitroso-**IR 95** in the active site of *Mtb DprE1*

IR 95 is shown in purple sticks, FAD in yellow and protein residues in grey sticks. Amino acid side chains located within a 4 Å radius around the inhibitor are included in the view and labeled by their sequence number. Yellow dashed lines indicate the shortest contact between a residue and the inhibitor. Oxygen and nitrogen are colored red and blue. Unbiased difference density, contoured at 3 σ above the mean, was calculated using coordinates of protein plus flavin, prior to incorporation of **IR 95** in the structure model.

In conclusion, the mode of binding of **IR 95** to *Mtb DprE1* is the same as the one reported for BTZ043⁵⁷ and CT325,⁶³ which not only proves that BOZ compounds such as **IR 95** exhibit their activity through inhibition of the same target as the BTZ compounds, but also establishes the BOZs as new class of antimycobacterial compounds on the 'magic' drug target DprE1.

Chapter Six

6 CONCLUSION AND SUGGESTIONS FOR FURTHER BTZ DEVELOPMENT*

Novel synthetic pathways to BTZs

The classic synthetic pathway (method A, chapter 2.1.1) for the synthesis of the BTZ scaffold was investigated extensively with various compounds. It was shown to be suitable for a wide range of substituents. However, the competing formation of benzamide derivatives instead of the BTZ scaffold was an undesired side reaction in most of the syntheses. This was partly overcome, with higher yield and less side products, by modifications such as conducting the classic pathway at lower temperatures than reported. This modification, simple as it was, proved to be a major optimization of probably all BTZ syntheses via the classic pathway.

The dithiocarbamate pathway (method B, chapter 2.1.2) and the alkylxanthogenate pathway (method C, chapter 2.1.3) were proved to be viable in two cases.

A new straightforward three step synthesis via thioureas and corresponding benzoylchlorides (method E, chapter 2.1.5) was successfully developed for the synthesis of the BTZ scaffold, allowing wide variation of substituents at the crucial and variable position 2. The advantage of this novel method is the avoidance of toxic and problematic reagents and side products, e.g. H_2S , CS_2 and CH_3I . Toluene - the solvent of choice for this novel pathway - belongs to the class 2 solvents according to ICH guideline Q3C.¹⁶¹ *The use of class 1 solvents for the synthesis of BTZ043, PBTZ169 and novel BTZs is suggested and currently under investigation in the context of another thesis.*⁷⁰ To conclude, the novel thiourea pathway clears the way for an urgently needed GMP compliant synthesis of preclinical BTZ candidates.

An important aspect of this synthetic method is the accessibility of the corresponding thiourea derivatives. Some can easily be synthesized according to known procedures^{80,81} for simple amines such as piperidine, morpholine and piperazines. However, branched amines with methyl groups next to the amino group do not or only marginally yield thiourea derivatives. *Optimized syntheses to such and other asymmetrically substituted thiourea reagents, building on work from this thesis, have already been developed in our group in the context of another thesis,*⁷⁰ *further improving the versatility of the thiourea approach to BTZs.*

* Suggestions for further BTZ drug development in this chapter are indicated by italics.

BOZs: A novel antimycobacterial class

The novel pathway (method E) was successfully transferred to the synthesis of 1,3-benzoxazinones (BOZs). For five BTZs, the corresponding BOZ counterparts were synthesized. The corresponding urea derivatives were easily accessible via aminolysis of the amines with urea according to known procedures.⁸³ In contrast, branched amines with methyl groups next to the amino group did not afford urea derivatives. In these cases, a modification of the classic method A for BTZs led to the corresponding BOZs in acceptable yields.

Generally, yields in the BOZ syntheses are lower than those of their corresponding BTZ counterparts. Due to the lower nucleophilicity of oxygen compared to sulfur, the ring closure to BOZs occurs slower and in all cases necessitated the addition of auxiliary bases such as DIPEA to scavenge the evolving HCl and to shift the equilibrium towards the side of reaction products. *Future work should focus on optimizing synthetic procedures to the 1,3-BOZ scaffold.*

Crystal structure of BOZ IR 95 with DprE1

The BOZ **IR 95** was co-crystallized with *Mtb* DprE1 to reveal the crystal structure of the active enzyme-compound adduct. The data clearly prove covalent bonding of the active nitroso derivative with the cysteine 387 of DprE1. Hence, BOZs share the same mechanism of action with BTZ043.

Imidazo-BTZs

Besides 38 BTZs with various substituents at positions 2, 6, and 7, seven imidazobenzothiazinones were synthesized. Normally, base catalysis was employed in this reaction. We found that acid catalysis improved the yield of imidazobenzothiazinones in most cases. Presumably, the activation of the benzoylchloride moiety with POCl₃ accelerated the nucleophilic attack of imidazolidine-2-thione.

Thiochromenones

The synthesis of thiochromenone derivatives was not finalized due to the cumbersome implementation of the Grohe-Heitzer reaction conditions for 2-chloro-3-nitro-5-(trifluoromethyl)benzoic acid starting materials and the unexpected ring closure to ethyl 5-nitro-8-oxo-3-(trifluoromethyl)bicyclo[4.2.0]octa-1,3,5-triene-7-carboxylate (**IR 154**) during the attempted thiochromenone synthesis. *Apart from this preliminary study, several alternative pathways are discussed (chapter 2.4.2) for future optimized approaches to thiochromenones as possible dual action (DprE1 and gyrase inhibition) compounds.*

Patent application

Various intermediate compounds and especially the test compounds had not been described before. Novel BTZs and BOZs as well as the synthetic thiourea pathway (method E) were included in a patent application at the German Patent Office (AZ DE102012012117.2; 20.06.2012). Intermediates, which were synthesized for the first time, include some thiourea reagents as well as substituted arenes. *Presently, Hans-Knöll-Institut Jena as the inventor and leader of BTZ research and our research group are preparing to join our patents and patent applications for taking one or two BTZs into and beyond preclinical development.*

Biological evaluation

All test compounds were evaluated in an agar diffusion assay against two mycobacteria species (*M. vaccae*, *M. aurum*), plus one Gram-positive (*B. subtilis*) and Gram-negative (*E. coli*) strain and a eukaryotic yeast (*Sp. salmonicolor*). Of the 51 test compounds, 21 showed considerable activity against *M. vaccae*. None of the active compounds showed substantial activity against *M. aurum*, which is naturally resistant to BTZs due to an amino acid exchange in DprE1, indicating the mechanism of action could be the same as the one reported for BTZ043. 26 compounds were transferred to MIC determination against *M. vaccae* and 18 compounds to the MIC determination against *Mtb*. 20 compounds showed MICs against *M. vaccae* in the single-digit μM range of which ten compounds displayed MICs below 1 μM . Of the 18 compounds in the *Mtb* assay, only six displayed MICs below 1 μM . In all cases where comparable MICs against *M. vaccae* and *Mtb* were available, MICs against *Mtb* were about 10 fold higher than those observed against *M. vaccae* and ranged between 0.3-1.0 μM for the most active compounds. Reference compound **IR 124**, identical to PBTZ169,⁶⁹ showed an MIC against *Mtb* of < 0.04 μM .

The most active compounds of this thesis belong to BTZs with branched amino substituents at position 2 and an arene moiety bearing the 8-nitro and 6-trifluoromethyl group (**IR 85**, **IR 115**, **IR 127 trans**) as well as 2-morpholinyl/piperidinyl-7-chloro-8-nitro-6-trifluoromethyl BTZs **IR 76** and **IR 74**. The most active BOZ was the analog of **IR 124**, viz. the 2-[4-(cyclohexylmethyl)piperazin-1-yl] substituted scaffold (**IR 125**). However, its MIC against *Mtb* was about 10 fold higher than for the analogous BTZ derivative **IR 124**.

In general, MICs observed for *M. vaccae* were lower than those observed for *Mtb*, underlining *M. vaccae*'s excellent susceptibility to the BTZ compound class and confirming this mycobacteria species as a suitable and easy-to-handle *Mtb* surrogate for the biological evaluation of DprE1 targeting antimycobacterials.

For selected compounds, MICs against DprE1 over-expressor strains were determined. All compounds showed a significant increase of MIC in these over-expressor strains, which was further proof that they were inhibitors of the epimerase DprE1.

All compounds with activity in the agar diffusion assay were tested for their antiproliferative and cytotoxic effects. In general, 7-chloro-substituted BTZs showed considerable cytotoxic effects, whereas most BTZs and BOZs with branched amines at position 2 showed no relevant toxicity.

Three compounds were evaluated *in vivo* in an ultra-fast murine model of acute TB. The PBTZ **IR 124** and its hydrochloride **IR 124xHCl** were confirmed to have excellent *in vitro* and *in vivo* activity. Data had been reported for PBTZ169 (= **IR 124**) only,⁶⁹ thus, our results show that the free base PBTZ169/**IR 124** and its hydrochloride salt **IR 124xHCl** are equipotent *in vivo*. The 2-(2,6-dimethylpiperidin-1-yl) substituted BTZ **IR 85** was inactive in this particular *in vivo* model. Reasons for this are discussed in chapter 3.3.

Pharmacokinetic evaluation

Lipinski rule-of-five parameters were calculated for all compounds, and except for **IR 88** and **IR 115**, no violations of the rule-of-five were observed. In general, all BTZs and BOZs are rather lipophilic compounds. *This will need to be addressed either through medicinal chemistry variations or special formulations to ascertain sufficient solubility and bioavailability.* However, the most lipophilic compounds (highest calc. logP) were the most active compounds in the MIC assays, indicating that BTZs and BOZs must exhibit a certain level of lipophilicity for antimycobacterial activity. This presumably results from the essential passage through the lipid-rich mycobacterial cell envelope, which is less or not permeable for hydrophilic compounds.

The aqueous solubility at two different pH values (7.4 and 4.5) was determined for selected compounds. All compounds showed very poor solubility in the experiment, with logS values ranging from -4.7 to -8.1. Referring to the Ph.Eur. classification of solubility, all compounds were “practically insoluble or insoluble”, which is the same category as for BTZ043. Therefore, no BTZ or BOZ analog of this thesis showed better solubility than BTZ043. The poor aqueous solubility seems to be a general obstacle of the BTZ chemical scaffold. *Further chemical optimization approaches should focus on the incorporation of larger hydrophilic substituents, such as carboxylic or sulfonic acids into the BTZ scaffold.* We showed in one case that the formation of the hydrochloride of a BTZ with a tertiary amino group did not enhance aqueous solubility.

Concomitantly, the microsomal stability of selected BTZ and BOZ compounds was investigated. Except for **IR 115**, all compounds showed increased stability towards human and mouse liver microsomes compared to BTZ043 and PBTZ169 (lower CL_{int} values, longer half life). BOZs were slightly more stable than their BTZ counterparts, presumably resulting from the lack of a bivalent oxidizable sulfur atom.

Structure activity relationships

The analysis of our MIC data with *M. vaccae* and *Mtb* allowed for preliminary structure activity relationships, also taking into account data that is in the public domain presently. This thesis provides the first SAR analysis of the antimycobacterial activity of a wide range of BTZs.

The following conclusions were drawn from the antimycobacterial assays and are summarized in Figure 57:

- BTZ derivatives without a nitro group or with a nitro group shifted to position 7 are completely inactive, underlining the essentiality of the nitro group at the correct position (C-8) for BTZ activity.
- Replacing trifluoromethyl at position 6 with fluorine leads to a decrease of activity. Therefore, the trifluoromethyl group substantially influences the antimycobacterial activity, presumably due to its contribution to the correct binding into the binding pocket of the target enzyme DprE1, which was confirmed by the crystal structure of **IR 95** with DprE1.
- Halide substituents at position 7 influence antimycobacterial activity differently. Whereas 7-chloro derivatives show acceptable MICs, 7-fluoro derivatives are less efficient. However, 7-chloro substituted BTZs also display noticeable cytotoxicity.
- Amino substituents at position 7 render the compounds completely inactive.
- Aryl or heteroaryl substituents at position 2 abolish antimycobacterial activity.
- Imidazobenzothiazinones are less active than their BTZ analogs.
- The highest influence on activity is implemented through variations of the amino substituent at position 2. Branched amines such as methyl substituted piperidines and 4-alkyl-substituted piperazines enhance activity pronouncedly.
- Replacement of sulfur by its bioisoster oxygen leads to minor decrease of activity, but these compounds still comprise antimycobacterial activity, establishing the BOZ compounds as a novel antimycobacterial scaffold.
- BOZs are more stable in human and mouse liver microsomes than their BTZ counterparts, but less stable in aqueous media.

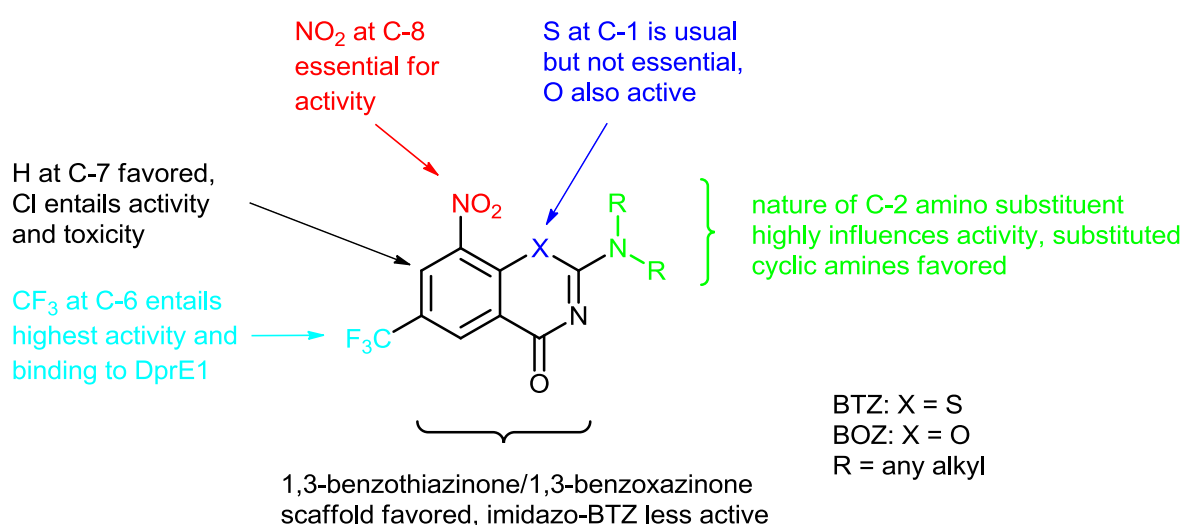


Figure 57: Structure activity relationships of BTZs and BOZs

In summary, regarding substituents at the arene moiety of BTZs and BOZs, derivatives with the 8-nitro- and 6-trifluoromethyl-BTZ/BOZ pharmacophore are most active in vitro. Other substituents such as halides and amines were poorly tolerated on the BTZ/BOZ system. Space for chemical variation was seen at the side-chain in position 2 of the BTZ and BOZ scaffold. A variety of cyclic amines was tolerated, whereas branched and more complex amines substantially enhanced activity compared to simple amines such as piperidine and morpholine. However, aryl and heteroaryl substituents at position 2 were not tolerated and completely inactive. These findings are in agreement with findings by other researchers who developed novel BTZ derivatives. Although no comprehensive structure activity relationships for antimycobacterial BTZs are available, it seems to be common knowledge among BTZ researchers that the most active derivatives must carry the 8-nitro and 6-trifluoromethyl group and the substituent at position 2 leaves space for pharmacological and pharmacokinetic tuning.^{67,69} Our findings provide some systematic basis for this hypothesis.

General optimization goals for BTZs/BOZs of this thesis must meet two major issues – activity and solubility. Activity relies on the 8-nitro group to a great extent, although other factors, such as the side chain at position 2 presumably highly influence the compound's binding and orientation at the binding pocket of DprE1. More complex amino substituents at position 2 enhance activity. Furthermore, the nature of the position 2 substituent will also contribute to lipophilicity and solubility of the compound, since this seems to be the only truly variable position of the BTZ/BOZ scaffold. Possible amino side chains should bear a second basic nitrogen (e.g. piperazine derivatives) for salt formation to enhance solubility. Additionally, the introduction of larger hydrophilic groups such as acetyl-, sulfonyl-, or hydroxyl-substituted amines could contribute to higher hydrophilicity as well as the utilization of more space of the binding pocket at the target enzyme. A second major variation is the replacement of the 8-nitro group with other electrophilic groups, capable of the reaction with the cysteine of DprE1 without bioactivation (e.g. maleimide). The prospects of success of the replacement of the nitro group may be small, since highly reactive electrophiles might entail fast metabolic inactivation or/and higher toxicity of the compounds.

Outlook

BTZs and BOZs are very promising antimycobacterial compound classes. Further studies will have to optimize the compounds' physicochemical properties, especially regarding aq. solubility and stability of the compounds both in vitro and metabolically (in vivo). The sparse information on the stability of BTZs clearly illustrates the need for more specific and comparable data on stability, e.g. in culture media, in gastric fluid, in human plasma, and the identification and characterization of possible in vivo metabolites.

The BOZs of this thesis are the first antimycobacterial representatives of this chemical scaffold. They promise to be more stable in vivo than their BTZ counterparts. Further medicinal chemistry variations will have to focus on improving their synthesis and enhancing their antimycobacterial activity in order to meet the in vitro and in vivo activity of the best current BTZs.

Regarding the novel synthetic thiourea pathway, further studies will have to optimize the synthesis and widen the accessibility of the thiourea reagents and implement the use of GMP compliant solvents of class 1 throughout the whole synthetic procedure.

A replacement of the nitro group with other pharmacophors capable of forming a covalent bond with the cysteine 387 in DprE1 should be developed in order to avoid possible inactivation (and possibly toxification) via reduction of the nitro group by host enzymes.

The synthesis of thiochromenones and dihydroquinolones should be pursued in order to develop perhaps highly antimycobacterial compounds with a dual mode of action – inhibition of DprE1 and DNA gyrase.

The outstanding antimycobacterial activity of BTZ043 and PBTZ169 suggests that DprE1 may only be one target of these compounds. Upon reduction to the corresponding nitroso derivatives, it is possible that these nitroso-BTZs bind to other enzymes in the mycobacterial cell and contribute to the low MICs. Therefore, the incubation of nitroso derivatives with mycobacterial cell lysates and subsequent analysis of all covalent compound-enzyme adducts could reveal secondary targets of BTZs.

Furthermore, nitroso-BTZs will be a valuable tool to reveal the complete mechanism of action of BTZs and elucidate the pathway of bioactivation (e.g. confirmation or refutation of the theory of Tiwari et al.⁶² in enzymatic studies).

Chapter Seven

7 EXPERIMENTAL SECTION

7.1 CHEMICALS AND MATERIALS

All chemicals were purchased from Sigma Aldrich, Alfa Aesar, VWR, Carl Roth, Fisher Scientific or Acros Organics and were used without further purification. MFSDA was stored with molsieve 3 Å under argon atmosphere. All organic solvents, piperidine, 2,6-dimethylpiperidine, 2,2,6,6-tetramethylpiperidine, POCl₃, TEA, and DIPEA were distilled prior to use and stored with molsieve 3 Å. All solids were dried in a glass oven (Büchi TO-51, Büchi Labortechnik, Flawil, Switzerland) at 60 °C, 20 mbar for 60-120 min prior to use. The notation 'hexane' in the description of the syntheses refers to *n*-hexane. Freeze-dried KF was prepared as following: dissolving KF in H₂O, lyophilization for 48 h, storage under argon atmosphere. Malonic acid monoethyl ester was synthesized as following: 200 mg potassium monoethylmalonate were dissolved in 1 ml H₂O and cooled to 0 °C. 100 µl 12 M HCl were added slowly, keeping the temperature below 5 °C. After 10 min of stirring, the mixture was extracted with EE (3x), the combined organic layers dried over MgSO₄ and the solvent evaporated.

Glassware for reactions under argon atmosphere were oven-dried at 100 °C for 2 h prior to use, evacuated and flushed with argon immediately. The process of evacuation and argon flushing was repeated for 3-5 times.

7.2 INSTRUMENTAL SETTINGS AND ANALYSES

Chromatography

Analytical thin layer chromatography (TLC) was performed on Merck silica gel 60 F₂₅₄ precoated plates, Merck KGaA, Darmstadt, Germany. Visualizations were accomplished with an UV lamp (254 nm) or I₂ stain. Given *R_f* values are uncorrected.

Flash chromatography was performed as follows: Merck silica gel 60 (40-63 µm) was suspended in appropriate eluent, poured into glass columns of appropriate size and the so packed flash columns were equilibrated with approx. two column volumes of eluent. The compound mixture was either dissolved in approx. 2 ml eluent and applied to the column or mixed with Celite 545 and acetone, the solvent evaporated and the residual celite-compound mixture applied as solid onto the flash column. Eluents for flash chromatography were chosen according to TLC eluents and separation problem and elution was performed either isocratically or with a gradient according to the separation problem.

Purification of compounds via MPLC was either performed on a PuriFlash 430 apparatus of Interchim, Montluçon, France or a Büchi MPLC, Flawil, Switzerland, consisting of the

following modules: pump modul C601, UV detector C-630, fraction collector C-660, Büchi Sepacore Record software and cartridge C-670. For the Büchi system, cartridges were packed manually using the cartridge C-670 and Merck silica gel 60 (40-63 μm). For the PuriFlash system, prepacked columns with silica gel of different pore sizes (15-50 μm) and different packing quantities (12-30 g silica gel) were used, according to the separation problem. The maximum compound load per column was 5 % (m/m) of the silica gel quantity. Eluents for MPLC were chosen according to TLC eluents and separation problem and elution was performed either isocratically or with a gradient according to the separation problem.

Melting point

Melting points were determined on a Boetius melting point apparatus and are uncorrected.

NMR spectrometry

NMR spectra were recorded on a Varian (now Agilent Technologies, Böblingen, Germany) Inova 500 MHz or Agilent Technologies VNMRS 400 MHz. Chemical shifts (δ) are reported in parts per million (ppm) relative to the residual non-deuterated solvent peak in the corresponding spectra (chloroform δ 7.26, methanol δ 3.31, acetone δ 2.04, DMSO δ 2.49). Signals with defined multiplicities are characterized as follows: s – singlet, bs – broad singlet, d – doublet, dd – double doublet, ddd – double doublet of doublet, dt – doublet of triplet, t – triplet, q – quartet, m – multiplet and coupling constants (J) are given in Hertz (Hz). NMR spectra were analyzed using mestrec23 software.

Mass spectrometry

Electrospray ionization (ESI) mass spectra were recorded on a LCQ Classic of Thermo Finnigan, San Jose, California, USA. The sample was dissolved in an appropriate solvent and applied to the ESI interface via a syringe pump (injection volume 20 μl). Parameters: capillary temperature 220 $^{\circ}\text{C}$, voltage 4.5 kV, scanning range 50-2000 m/z.

Electron impact (EI) mass spectra were recorded on an AMD 402 of AMD Intectra GmbH, Harpstedt, Germany, with a medium ionization voltage of 70 eV.

Gas chromatography was performed on a Hewlett Packard 5890 Series II *Plus* gas chromatograph combined with a Hewlett Packard 5972 Series mass selective detector. 10 μl of the sample were injected, which was run in the purge value split mode. The temperature of the injector was 250 $^{\circ}\text{C}$. The oven temperature was 70 $^{\circ}\text{C}$ until 1 min after solvent delay, then raised to 250 $^{\circ}\text{C}$ at 10 $^{\circ}\text{C}$ per min. The solvent delay for recording was 2.5 min for acetone and 9.5 min for 1,2-dichlorobenzene. The temperature of the interface between gas chromatograph and mass detector was 280 $^{\circ}\text{C}$. The column was a Merck capillary column CP-SIL 8 MS with a length of 30 m, a layer thickness of 0.25 μm and an inner diameter of 0.25 mm (ID). Analysis of data was accomplished with Hewlett Packard HP G1034C MS ChemStation Software.

The positive ion high resolution ESI mass spectra were obtained from a Bruker Apex III Fourier transform ion cyclotron resonance (FT-ICR) mass spectrometer (Bruker Daltonics, Billerica, USA) equipped with an Infinity cell, a 7.0 Tesla superconducting magnet (Bruker), an RF-only hexapole ion guide and an external electron spray ion source (Agilent, off axis spray, voltages: endplate, -3.700 V; capillary, -4.200 V; capillary exit, $+100$ V; skimmer 1, $+15.0$ V; skimmer 2, $+6.0$ V). Nitrogen was used as drying gas at 150°C . The sample solutions (in methanol) were introduced continuously via a syringe pump with a flow rate of $120\ \mu\text{l/h}$. The data were evaluated by the Bruker XMASS 7.0.8 software.

Combustion analysis

Elemental analyses were performed on a CHNS-932 apparatus of Leco-Corporation, St. Joseph, Michigan, USA or an Elementar vario EL apparatus of Elementar Analysensysteme GmbH, Hanau, Germany.

IR spectra

IR spectra were recorded on a IFS 28 FTIR spectrometer of Bruker (Billerica, USA) with a Thermo Spectra-Tech ATR unit (Thermo Scientific). Compounds were dissolved in an appropriate solvent (acetone, methanol or chloroform) and placed on a 20 mm ZnSe-Fresnel crystal. The angle of incidence was 45° .

7.3 PHARMACOKINETIC EVALUATION METHODS

7.3.1 Solubility determination

Solubilities of compounds were determined using the shake flask method.

Primarily, standard solutions of test compounds were prepared and analyzed via HPLC to determine calibration equations. Two independent standard solution sets were prepared for each compound, dissolving approx. 10 mg test compound in a mixture of ACN:H₂O 1:1 (V/V) + 0.1 % TFA. This standard solution no. 1 equals approx. 200 $\mu\text{g/ml}$. It was diluted with ACN:H₂O 1:1 (V/V) + 0.1 % TFA to give standard solution no. 2 with a concentration of approx. 100 $\mu\text{g/ml}$. Four other standard solutions were prepared in the same manner, with the lowest concentration of standard solution no. 6 being approx. 6.25 $\mu\text{g/ml}$. The standard solutions 2-6 were analyzed via HPLC in duplicate and the mean AUC of compound peaks was used for calculation of the calibration equation, using Origin 6.OG(2)[®] software. Following this procedure, two independent calibration equations were calculated from the two standard solutions sets.

The HPLC analysis was performed on a Jasco HPLC apparatus, Germany, with following modules: autosampler Jasco 851-AS Intelligent Sampler, pump: Jasco PU-980 Intelligent HPLC Pump, detector: UV-975 Intelligent UV/VIS Detector and control module Jasco LC-NetII/ADC. The flow rate was 1 ml/min, eluent ACN:H₂O 1:1 (V/V) + 0.1 % TFA, detection at wave length of $\lambda = 250$ nm and an injection volume of 20 μl . The column was a LiChroCART[®] 125-4, RP-18e (5 μm), with 12.5 cm length and 4 mm diameter from Merck KGaA, Darmstadt, Germany. Data analysis of HPLC spectra was performed using Borwin software.

In duplicate, approx. 2-5 mg of test compound were mixed with 2 ml of solvent and shaken at \approx 230 rpm at rt for 48 h utilizing a GFL 3015 rotary shaker from Rettberg Laborgeräte Glasapparatebau, Göttingen, Germany. Two different solvents were tested in the solubility assay, PBS buffer pH 7.4 (8.18 g NaCl, 0.20 g KCl, 1.78 g Na₂HPO₄*2H₂O, 0.24 g KH₂PO₄ in 1000 ml water, equal to 140 mM NaCl, 2.7 mM KCl, 10 mM Na₂HPO₄*2H₂O, 1.8 mM KH₂PO₄) and acetic acid/sodium acetate buffer pH 4.5 (100 μ l acetic acid 99.5 %, 0.12 g NaAc in 100 ml water, equal to 17.4 mM acetic acid, 14.6 mM NaAc). The pH values of buffers were controlled with Schott Geräte pH-Meter CG 822.

After 8 h, 24 h and 48 h, the existence of solid in the test vials was checked visually.

After 48 h, the sample solutions were drawn into a syringe and filtered through hydrophilic nylon syringe filters (Roth Rotilabo®-Spritzenfilter, 0.2 μ m, 30 mm diameter) into HPLC vials. Concentrations of the sample solutions from the shake flask method were determined via HPLC in duplicate and the mean AUC of the two runs was used for calculation of concentration. The solubility in each assayed solvent was calculated independently with the two calibration equations. Following this calculating procedure, four values of solubility for each test compound in one solvent were calculated. The solubility given is the mean value of these four values.

7.3.2 Calculated Lipinski rule-of-five

Lipinski rule-of-five data as well as Mulliken charges were calculated with Molecular Operating Environment software (MOE 2012.10) in the group of Prof. Wolfgang Sippl, Institute of Pharmacy, Martin Luther University Halle-Wittenberg, Germany.

7.3.3 Microsomal stability

Pooled mouse and human liver microsomes were purchased from Xenotech. Microsomes (final protein concentration 0.5 mg/ml), MgCl₂ (final concentration 5 mM) and test compound (final substrate concentration 0.5 μ M; final DMSO concentration 0.5 %) in 0.1 M phosphate buffer pH 7.4 were pre-incubated at 37 °C prior to the addition of NADPH (final concentration 1 mM) to initiate the reaction. The final incubation volume was 600 μ l. A control incubation was included for each compound tested where 0.1 M phosphate buffer pH 7.4 is added instead of NADPH (minus NADPH). One control compound was included with each species. All incubations were performed singularly for each test compound. Each compound was incubated for 30 min and samples (90 μ l) of incubate were taken at 0, 5, 15, 20, and 30 min. The control (minus NADPH) was sampled at 30 min only. The reactions were stopped by the addition of sample to 200 μ l ACN:methanol 3:1 (V/V) containing internal standard. The terminated samples were centrifuged at 2.500 rpm for 20 min at 4 °C to precipitate the protein. Following protein precipitation, the samples were analyzed using LC-MS/MS conditions. The ln of the peak area ratio (compound peak area/internal standard peak area) was plotted against the time.

The elimination of the compound from the system is a kinetic process of first order, mathematically described by the *e*-function:^{158,162}

$$c(t) = c_0 * e^{-kt} = c_0 * 10^{-kt/2.3}$$

Plotting the same process as semilogarithmic graph, the slope of the resulting straight line correlates with the elimination rate constant k:

$$k = - \text{slope} / 2.303$$

The half life can be calculated from the e-function:

$$c_0/2 = c_0 * e^{-kt_{1/2}} \quad \rightarrow \ln 2 = kt_{1/2} \quad \rightarrow t_{1/2} [\text{min}] = 0.693/k$$

The intrinsic clearance CL_{int} was determined utilizing the following equation (V is the incubation volume of microsomal protein in ml/g):

$$CL_{\text{int}} [\text{ml}/(\text{min} * \text{g})] = V * 0.693 / t_{1/2} = V * k$$

V (ml/g) = volume of incubation / protein in the incubation

Clearance categories for this protocol are: low: $CL_{\text{int}} < 5 \text{ ml}/(\text{min} * \text{g})$, moderate: $CL_{\text{int}} 5\text{--}15 \text{ ml}/(\text{min} * \text{g})$, high: $CL_{\text{int}} > 15 \text{ ml}/(\text{min} * \text{g})$.

7.4 BIOLOGICAL EVALUATION METHODS

7.4.1 Agar diffusion assay

The inocula of *E. coli* SG 458, *Sp. salmonicolor* SBUG 549, *B. subtilis* ATCC 6633, *M. aurum* SB 66, and *M. vaccae* IMET 10670 were prepared by incubating a few well-isolated colonies from an angular agar culture with 3 ml of nutrient solution for 16 h at 37 °C. The solution was diluted with aq. NaCl (0.9 %) to a bacterial density (turbidity of solution) compared to McFarland standard 0.5 (Biomérieux).

The test compound (1 mg) was dissolved in 1 ml DMSO and this stock solution diluted with methanol to a test concentration of 100 µg/ml. Reference compounds were BTZ043 (0.1 µg/ml for *M. vaccae*, 100 µg/ml for the other test organisms), ciprofloxacin (5 µg/ml), and amphotericin B (10 µg/ml).

Culture plates for antibacterial activity were filled with 34 ml standard culture broth (Merck NA1 for *E. coli* SG 458, *B. subtilis* ATCC 6633, *M. aurum* SB 66, and *M. vaccae* IMET 10670; malted agar (composition: Difco malt extract 40 g/l, yeast extract OHLY 4 g/l, Difco agar 15 g/l, aqua dest. 1 l, pH 5.7-6.0, autoclaved 20 min at 121 °C) for *Sp. salmonicolor* SBUG 549) and inoculated with the corresponding microorganism inoculum so that the cell count is approx. 10^7 . Plates were set aside on a flat surface for drying. Subsequently, holes of 9 mm diameter were punched into the culture medium in which 50 µl of the test compound solution was injected. Inoculated plates were incubated at 30 °C (*Sp. salmonicolor*) or 37 °C (*B. subtilis*, *E. coli*, *M. aurum*, *M. vaccae*) for 24 h.

Determination of antibacterial and antifungal activity was performed optically by measuring diameters of inhibition zones.

7.4.2 MIC determination

M. vaccae (HKI Jena)

MIC against *M. vaccae* was determined by the micro broth dilution method in Mueller-Hinton broth according to NCCLS guidelines.¹⁶³

Preparation of inoculum: 20 ml culture medium for mycobacteria (glycerol 1 %, meat extract 0.5 %, peptone (pancreatic from casein) 0.5 %, NaCl 0.3 %, aqua dest., pH 7.0) were inoculated with 0.5 ml preparatory culture and incubated at 32 °C for 48 h. The inoculum was adjusted to McFarland standard 0.5 (Biomérieux) and diluted to 10⁶ CFU/ml.

Stock solutions of the test compounds (1 mg in 1 ml DMSO) were diluted with methanol to a starting concentration of 400 µg/ml. 50 µl of these drug solutions were added to row 1, column A-E of 96-well microtiter plates, prepared with 50 µl Mueller-Hinton broth. 50 µl reference compound (ciprofloxacin or BTZ043) was added to column F, row 1 (final concentration of reference compound in row 1 = 100 µg/ml). Columns G and H were reserved for solvent control and growth control. Twelve twofold dilutions of test compound solutions were performed from row 1 to row 12 in order to achieve final test concentrations of 100 µg/ml in row 1 and 0.05 µg/ml in row 12 on microtiter plates.

50 µl of inoculum were added to each vial of the 96-well microtiter plate. The final concentration of inoculum was 5*10⁵ CFU/ml. Plates were incubated at 37 °C for 48 h. 30 µl of a resazurin solution (0.01 % in aqua dest.) were added to each well and plates incubated for another 24 h at 37 °C. The influence of test compounds on *M. vaccae* was measured by determination of the lowest compound concentration where no viable cells of *M. vaccae* are detectable (color change of indicator dye resazurin from pink to blue). Fluorescence was detected after 72 h with a Nephelocan Ascent 1.4 automatic plate reader (Labsystems, Vantaa, Finland) at λ = 630 nm.

M. tuberculosis H37Rv (GSK Tres Cantos)

MIC determinations for each test compound were performed in triplicate in 96-well flat-bottomed polystyrene microtiter plates. Ten twofold drug dilutions in neat DMSO starting at 200 µM were performed. These drug solutions (5 µl each) were added to 95 µl Middlebrook 7H9 medium (Difco cat. no. 271310; columns A-H, rows 1-10 of the plate layout). Isoniazid was used as a positive control; eight twofold dilutions of isoniazid starting at 160 mg/ml were prepared, and 5 µl of this control curve were added to 95 µl Middlebrook 7H9 medium (row 11, columns A-H). Neat DMSO (5 µl) was added to row 12 (growth and blank controls). The inoculum was standardized to approx. 1*10⁷ CFU/ml and diluted 1:100 (V/V) in Middlebrook 7H9 broth (Middlebrook ADC enrichment, a dehydrated culture medium that supports the growth of mycobacterial species; Becton-Dickinson cat. no. 211887) to produce the final inoculum of H37Rv strain (ATCC 25618). This inoculum (100 µl) was added to the entire plate except wells G-12 and H-12 (blank controls). All plates were placed in a sealed

box to prevent drying of the peripheral wells, and were incubated at 37 °C without shaking for 6 d.

A resazurin solution was prepared by dissolving one tablet of resazurin (Resazurin Tablets for Milk Testing; VWR International Ltd. cat. no. 330884Y) in 30 ml sterile phosphate-buffered saline (PBS); this solution was added to each well (25 µl per well). Fluorescence was measured (Spectramax M5, Molecular Devices, $\lambda_{\text{ex}} = 530 \text{ nm}$, $\lambda_{\text{em}} = 590 \text{ nm}$) after 48 h to determine the MIC value.

DprE1 over-expressor strains (GSK Tres Cantos)

The measurement of the minimum inhibitory concentration (MIC) for each tested compound was performed in 96 wells flat-bottom, polystyrene microtiter plates. Eleven twofold drug dilutions in neat DMSO starting at the appropriate concentration were performed from column 1 to 12. 5 µl of these drug solutions were added to 95 µl of Middlebrook 7H9 medium. Six duplicates of the plate were prepared, two for BCG over-expressing DprE1, two for BCG carrying the empty plasmid and two for BCG wild type.

The inoculum (BCG over-expressing DprE1, BCG transformed with the empty plasmid and BCG wild type) was standardized to approx. $1 \cdot 10^5$ CFU/ml in Middlebrook 7H9 broth. This inoculum (100 µl) was added to the entire plate but H7 to H12 wells (blank controls). All plates were placed in a sealed box to prevent drying out of the peripheral wells and they were incubated at 37 °C for 6 d.

A resazurin solution was prepared by dissolving one tablet of resazurin (Resazurin Tablets for Milk Testing; VWR International Ltd. cat. no. 330884Y) in 30 ml sterile phosphate-buffered saline (PBS); this solution was added to each well (25 µl per well). Fluorescence was measured (Spectramax M5, Molecular Devices, $\lambda_{\text{ex}} = 530 \text{ nm}$, $\lambda_{\text{em}} = 590 \text{ nm}$) after 48 h to determine the MIC value.

7.4.3 Antiproliferative and cytotoxicity assays

Antiproliferative assay against HUVEC and K-562 as well as cytotoxicity assay in HeLa were performed by Dr. Hans-Martin Dahse, Hans-Knöll-Institut, Jena according to previously described procedures.¹⁶⁴

Cells of HUVEC (ATCC CRL-1730), K-562 (DSM ACC 10), and HeLa (DSM ACC 57) were cultured in DMEM (CAMBREX 12-614F), RPMI 1640 (CAMBREX 12-167F), and RPMI 1640 (CAMBREX 12-167F), respectively. All cells were grown in the appropriate cell culture medium supplemented with 10 ml/l ultraglutamine 1 (CAMBREX 17-605E/U1), 500 µl/l gentamicin sulfate (CAMBREX 17-518Z), and 10 % heat inactivated fetal bovine serum (PAA A15-144) at 37 °C in high density polyethylene flasks (NUNC 156340).

Antiproliferative assay: The test compounds were dissolved in DMSO before being diluted in DMEM. The adherent cells were harvested at the logarithmic growth phase after soft trypsinization, using 0.25 % trypsin in PBS containing 0.02 % EDTA (Biochrom KG L2163; Biochrom, Berlin, Germany). For each experiment approx. 10,000 cells were seeded with 0.1 ml culture medium per well of the 96-well microplates (NUNC 167008).

Cytotoxic assay: HeLa cells were pre-incubated 48 h without the test substances. The dilutions of the compounds were carried out carefully on the subconfluent monolayers of HeLa cells after the pre-incubation time.

After preparing the HUVEC, K-562, and HeLa test plates as described above, the cells were incubated with dilutions of the test substances for 72 h at 37 °C in a humidified atmosphere and 5 % CO₂.

To estimate the influence of chemical compounds on cell proliferation of K-562, the number of viable cells present in multi-well plates via CellTiter-Blue1 assay with resazurin was determined. Under these experimental conditions, the signal from the CellTiter-Blue1 reagent is proportional to the number of viable cells. The adherent HUVEC and HeLa cells were fixed by glutaraldehyde and stained with a 0.05 % solution of methylene blue for 15 min. After gently washing, the stain was eluted with 0.2 ml of 0.33 N HCl. The optical densities were measured at 660 nm in SUNRISE microplate reader (TECAN, Switzerland). The GI₅₀ and CC₅₀ values were defined as the value at the intersection of the dose response curve with the 50 % line, compared to untreated control. These comparisons of the different values were performed with the software Magellan (TECAN).

Cytotoxicity assay in HepG2 (GSK Tres Cantos)

Actively growing HepG2 cells were removed from a T-175 TC flask using 5 ml of Eagle's MEM (containing 10 % FBS / 1 % NEAA / 1 % penicillin + streptomycin) and were dispersed in the medium by repeated pipetting. Seeding density was checked to ensure that new monolayers are not more than 50 % confluent at the time of harvesting. Cell suspension was added to 500 ml of the same medium at a final density of 1.2×10^8 cells per ml. 25 µl of this cell suspension (typically 3,000 cells per well) were dispensed into the wells of 384-well clear bottom Greiner plates (catalogue number, 781091) using a Multidrop. Prior to addition of the cell suspension, these plates were dispensed with 250 nl of the screening compounds using an Echo 555. Plates were allowed to incubate at 37 °C and a relative humidity of 80 % for 48 h in the presence of 5 % CO₂. After the incubation period, the plates were allowed to equilibrate at rt for 30 min before proceeding to develop the luminescent signal. The signal developer, CellTiter-GloT (Promega) was equilibrated at rt for 30 min and added to the plates (25 µl per well) using a Multidrop. The plates were left for 10 min at rt for stabilization and were subsequently read using a ViewLux (Perkin Elmer).

7.4.4 Co-Crystallization experimental methods

Crystallization experiments were carried out by Sarah Batt and Klaus Fütterer, School of Biosciences, University of Birmingham, UK.

Mtb DprE1 was expressed in *E. coli* BL21 and purified as described.⁶³ Prior to setting up crystallization experiments, approx. 600 µl of 50 µM DprE1 was incubated at 37 °C for 2 h with 25 µM FAD, 50 µM **IR 95**, 100 µM farnesylphosphoryl-β-D-ribose (FPR) and 1 mM MgCl₂ in order to facilitate conversion to active nitroso form and covalently bind to DprE1. After this incubation, the protein was dialysed into 20 mM Tris pH 8.5, 10 mM NaCl and 10 % glycerol and then concentrated to 400 µM before setting up crystal trays.

Crystals were grown by sitting drop vapour diffusion, aided by a Mosquito (TTP Labtech) liquid handling robot, over a reservoir containing 30-35 % (V/V) polypropylene glycol 400, 0.1 M imidazole pH 7.5. Crystals were mounted in nylon loops without further treatment and frozen in liquid nitrogen.

X-ray diffraction data to 2.4 Å resolution were recorded from monoclinic crystals on beamline I03 at the Diamond Light Source (Didcot, Oxfordshire, UK), and processed using XDS.¹⁶⁵ Initial phases were obtained by molecular replacement, using the structure of *apo* DprE1 as a search model (pdb entry: 4FEH). The model was built and refined using Coot, Refmac and Phenix.Refine.¹⁶⁶⁻¹⁶⁸ The model of the covalently bound **IR 95** inhibitor was included in the later stages of the refinement, and the final model converged at R-factors of 24.1 % (R_{free} , 5 % of reflections) and 21.2 % (R_{cryst} , Table 14).

Table 14: Statistics of X-ray diffraction data and of model refinement

X-ray diffraction data	<i>DprE1:IR 95</i>
Crystal	SB343
	DprE1:IR 95
Beamline	Diamond I03
Wavelength	0.97631
Space group	<i>P</i> 21
Cell parameters a,b,c (Å)	78.6, 85.4, 80.4, $\beta = 103.2^\circ$
Molecules per asymmetric unit	2
Resolution (Å)	78.3 - 2.38
High resolution shell (Å)	2.45 - 2.38
R _{merge} (%)	4.8 (51.3)
Total observations	212,901
Unique reflections	40,283
I/ σ (I)	16.3 (2.1)
Completeness (%)	97.1 (80.7)
Multiplicity	5.3 (3.6)
Refinement	
Resolution range	78.3 - 2.38
Unique reflections	40,251
R _{cryst} (%)	21.2
R _{free} (%)	24.1
No of non-hydrogen atoms	6,511
Protein + FAD	6,396
Ligand	42
Solvent	73
RMSD bonds (Å)	0.008
RMSD angles (°)	1.18
B-factors	
Wilson (Å ²)	53.0
Average (Å ²)	67.8
Protein + FAD (Å ²)	67.9
IR 95 (Å ²)	75.1
Solvent (Å ²)	57.2
RMSD B-factors	4.1
Ramachandran plot	
Favored region	97.6
Allowed regions	2.4
Disallowed (number)	0

7.5 SYNTHESSES

All compounds marked with ⁿ are novel compounds and do not possess a CAS registry number (SciFinder database search, 19.07.2013).

All compounds marked with ^p were included in the patent application (German Patent Office, AZ DE102012012117.2; 20.06.2012).

All final products of the synthetic trials were dried in vacuum.

General procedure I: Formation of acid chlorides

The corresponding benzoic acid was dissolved in toluene, 2 equivalents of SOCl₂ were added, the mixture was refluxed for 2 h and subsequently the solvent was evaporated under reduced pressure. The obtained benzoylchloride was dried in vacuum for several min and used immediately for the next reaction step without further purification.

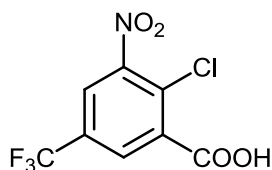
General procedure II: Formation of thiourea reagents

Dry NaSCN was suspended in acetone and cooled to 5 °C. An equimolar amount of benzoylchloride was dissolved in acetone and added dropwise. Subsequently, the mixture was stirred for 2 h at 5 °C. Equimolar amounts of the corresponding amine were dissolved in acetone, added dropwise at approx. 10 °C and the mixture stirred for 2 h at rt. After evaporation of the solvent, the residue was suspended in a small amount (approx. 4-8 mol equivalents) of conc. HCl and heated to 90 °C for 1 h. After carefully neutralizing the mixture with conc. NH₃, the product was collected after precipitation via setting aside the mixture for 48 h at 8 °C or extracting the mixture with chloroform and subsequent flash chromatography of the combined organic layers.

General procedure III: Adapted classic BTZ pathway (method A) with adjusted temperature

Under argon atmosphere, dry KSCN was suspended in acetone and cooled to 5 °C. An equimolar amount of the corresponding benzoylchloride (synthesis via general procedure I) was dissolved in acetone and added dropwise, subsequently the mixture was stirred for 2 h at 5 °C. Equimolar amounts of the corresponding amine were dissolved in acetone, added dropwise at approx. 10 °C and the mixture stirred for 2 h at rt. After evaporation of the solvent, the crude product was purified by flash chromatography.

7.5.1 2-chloro-3-nitro-5-(trifluoromethyl)benzoic acid (IR 05)



66 ml (1.25 mol) sulfuric acid 95-97 % were cooled to 10 °C in an ice bath. 5.139 g (25 mmol) of pestled 2-chloro-5-(trifluoromethyl)benzonitrile was added. Keeping the temperature between 10-15 °C, 26 ml (0.625 mol) of fuming nitric acid was added dropwise. After complete addition of the nitric acid, the mixture was carefully heated to 120-130 °C and stirred for 45 min. After cooling to rt, the mixture was poured onto 100 ml of crushed ice. The resulting suspension was stirred for 30 min to release remaining nitrous gases. The precipitate was filtered off, washed with cold water and dried.

White needles

Yield 6.343 g (94.0 %)

m.p. 175-178 °C (water) (lit. 175-177 °C)⁷⁸

¹H NMR (400 MHz, DMSO-*d*₆) δ 14.34 (bs, 1H, COOH), 8.65 (s, 1H, Ar-H), 8.35 (s, 1H, Ar-H)

¹³C NMR (100 MHz, DMSO-*d*₆) δ 164.2, 149.6, 135.6, 129.6 (q, ³J_{C,F} = 3.6 Hz), 128.7 (q,

²J_{C,F} = 34.2 Hz), 127.1, 123.9 (q, ³J_{C,F} = 3.6 Hz), 122.2 (q, ¹J_{C,F} = 273.3 Hz)

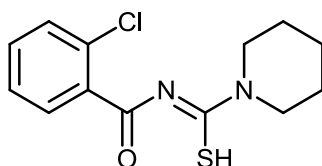
MS (ESI) 268.2 [M-H]⁻

R_f 0.28 (toluene:ethanol 1:1 (V/V))

M 269.56 g/mol

C₈H₃ClF₃NO₄

7.5.2 N-[(2-chlorophenyl)carbonyl]piperidine-1-carboimidothioic acid (IR 12)



Synthesis of 2-chlorobenzoylchloride from 15.65 g (0.1 mol) 2-chlorobenzoic acid according to general procedure I.

Under argon atmosphere, 7.60 g (0.1 mol) NH₄SCN were dissolved in 50 ml acetone. 2-chlorobenzoylchloride was dissolved in 50 ml acetone and added dropwise. A white precipitate formed. The mixture was heated to 40 °C for 5 min, the precipitate filtered off and the filtrate used for the next reaction step.

Under argon atmosphere, 9.88 ml (0.1 mol) piperidine in 50 ml acetone were added dropwise to the solution of 2-chlorobenzoylisothiocyanate. The mixture was stirred at rt for 30 min and heated to reflux for 2 min. After cooling, the solvent was evaporated under reduced pressure and the brown residue recrystallized from a mixture of EA and PE (1:4 (V/V)).

White needles

Yield 4.98 g (17.6 %)

m.p. 125-127 °C (EA:PE 1:4 (V/V))

^1H NMR (400 MHz, CDCl_3) δ 7.62 (m, 1H, Ar-H), 7.41 (m, 2H, Ar-H), 7.33 (m, 1H, Ar-H), 4.11 (bs, 2H, N-CH₂), 3.66 (bs, 2H, N-CH₂), 1.71 (m, 6H, CH₂-CH₂-CH₂)

^{13}C NMR (100 MHz, $\text{DMSO}-d_6$, 60°C) δ 177.6, 162.9, 135.0, 131.0, 129.8, 129.3, 128.7, 126.6, 50.9 (bs, 2 CH₂), 25.1 (bs, 2 CH₂), 23.0

MS (EI) 282 (M)

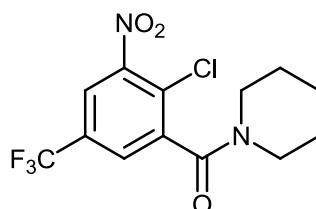
Elemental analysis	calc.	C 55.21	H 5.35	N 9.91	S 11.34
	found	C 54.75	H 5.22	N 10.06	S 11.43

R_f 0.14 (EA:PE 1:4 (V/V)), R_f 0.62 (toluene:ethanol 9:1 (V/V))

M 282.79 g/mol

$\text{C}_{13}\text{H}_{15}\text{ClN}_2\text{OS}$

7.5.3 1-([2-chloro-3-nitro-5-(trifluoromethyl)phenyl]carbonyl)piperidine (IR 13)



Synthesis of 2-chloro-3-nitro-5-(trifluoromethyl)benzoylchloride (**IR 06**) from 1.62 g (6.0 mmol) 2-chloro-3-nitro-5-(trifluoromethyl)benzoic acid (**IR 05**) according to general procedure I.

Under argon atmosphere, 456 mg (6.0 mmol) NH_4SCN were dissolved in 10 ml acetone. **IR 06** was dissolved in 10 ml acetone and added dropwise. A white precipitate formed. The mixture was heated to 40 °C for 5 min, the precipitate filtered off and the filtrate used for the next step.

Under argon atmosphere, 660 μl (6.0 mmol) piperidine, dissolved in 10 ml acetone, were added dropwise to the solution of 2-chloro-3-nitro-5-(trifluoromethyl)benzoylisothiocyanate. The mixture was stirred at rt for 30 min and heated to reflux for 2 min. After cooling, the solvent was evaporated under reduced pressure and the crude product pre-purified by flash chromatography (eluent toluene:ethanol 9:1 (V/V)). The corresponding fractions were

combined, treated with charcoal, filtered and concentrated under reduced pressure. The yellow solid was recrystallized from a mixture of EA and PE (1:4 (V/V)).

Pale yellow platelets

Yield 76 mg (3.7 %)

m.p. 104-106 °C (EA:PE 1:4 (V/V))

^1H NMR (CDCl_3) δ 8.06 (s, 1H, Ar-H), 7.71 (s, 1H, Ar-H), 3.74 (bs, 2H, N-CH₂), 3.16 (m, 2H, N-CH₂), 1.69 (bs, 4H, CH₂-CH₂-CH₂), 1.51 (bs, 2H, CH₂-CH₂-CH₂)

^{13}C NMR (100 MHz, CDCl_3) δ 163.1, 148.6, 140.7, 130.7 (q, $^2J_{\text{C,F}} = 35.3$ Hz), 127.5 (q, $^3J_{\text{C,F}} = 3.8$ Hz), 127.2, 122.4 (q, $^3J_{\text{C,F}} = 3.1$ Hz), 122.1 (q, $^1J_{\text{C,F}} = 272.1$ Hz), 48.1, 43.1, 26.5, 25.5, 24.4

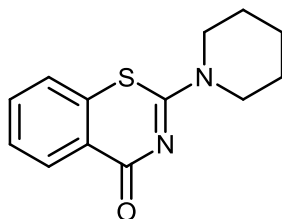
MS (EI) 336 (M)

R_f 0.60 (toluene:ethanol 9:1)

M 336.69 g/mol

$\text{C}_{13}\text{H}_{12}\text{ClF}_3\text{N}_2\text{O}_3$

7.5.4 2-(piperidin-1-yl)-4H-1,3-benzothiazin-4-one (IR 16)



The complete reaction was conducted under argon atmosphere.

96 mg NaH (60 % w/w dispersion on mineral oil, equivalent to 58 mg NaH, 2.40 mmol) were suspended in 10 ml DMF at 0 °C. 339 mg (1.2 mmol) N-[(2-chlorophenyl)carbonyl]piperidine-1-carboimidothioic acid (**IR 12**) were dissolved in 10 ml DMF and added dropwise. The reaction mixture was stirred at 70 °C for 14 d, after 3 d first traces of product were detectable via TLC. After 14 d, another 90 mg NaH (60 % w/w dispersion on mineral oil, equivalent to 54 mg NaH, 2.20 mmol) were added and the mixture stirred for another 5 d at 70 °C. After cooling, the solvent was evaporated and the residue dissolved in chloroform. The organic phase was washed with water and concentrated under reduced pressure. The crude product was purified by flash chromatography twice (eluent chloroform).

Pale yellow solid

Yield 66 mg (22.6 %)

m.p. 158-159 °C (chloroform) (lit. 179-181 °C, ACN)¹⁶⁹

^1H NMR (500 MHz, CDCl_3) δ 8.43 (dd, 1H, Ar-H, $^3J = 7.8$ Hz, $^4J = 1.6$ Hz), 7.48 (dt, 1H, Ar-H, $^3J = 7.8$ Hz, $^3J = 7.3$ Hz, $^4J = 1.6$ Hz), 7.41 (dt, 1H, Ar-H, $^3J = 7.8$ Hz, $^3J = 7.3$ Hz, $^4J = 1.2$ Hz), 7.30 (dd, 1H, Ar-H, $^3J = 7.8$ Hz, $^4J = 1.2$ Hz), 3.84 (m, 4H, CH₂-N-CH₂), 1.70 (m, 6H, CH₂-CH₂-CH₂)

^{13}C NMR (100 MHz, CDCl_3) δ 169.3, 161.9, 132.6, 132.0, 130.4, 128.0, 125.4, 122.6, 47.6 (bs, 2 CH_2), 25.8 (bs, 2 CH_2), 24.5

MS (EI) 246 (M)

MS (ESI) 269.3 $[\text{M}+\text{Na}]^+$

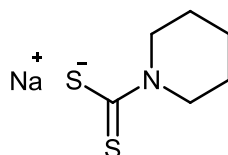
Elemental analysis	calc.	C 63.39	H 5.73	N 11.37	S 13.02
	found	C 63.09	H 5.71	N 10.96	S 12.45

R_f 0.25 (toluene:ethanol 9:1 (V/V))

M 246.33 g/mol

$\text{C}_{13}\text{H}_{14}\text{N}_2\text{OS}$

7.5.5 sodium (piperidin-1-yl)carbothioylsulfanide (IR 17)



A solution of 8.0 g (0.2 mol) NaOH in 20 ml cold water was added to 12 ml (0.2 mol) carbon disulfide at 0-5 °C. 19.8 ml (0.2 mol) piperidine were dissolved in 38 ml cold water and added dropwise over a period of 30 min. The mixture was then stirred for another 2 h. The crude product precipitated and was filtered off and dried.

Pale beige solid

Yield 20.86 g (57.0 %)

^1H NMR (400 MHz, CD_3OD) δ 4.35 (m, 4H, $\text{CH}_2\text{-N-CH}_2$), 1.63 (m, 6H, $\text{CH}_2\text{-CH}_2\text{-CH}_2$)

^{13}C NMR (100 MHz, CD_3OD) δ 211.0, 53.2 (2 CH_2), 27.0 (2 CH_2), 25.5

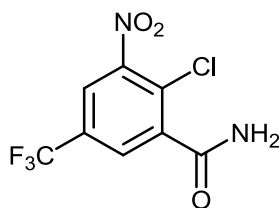
MS (ESI) 160.19 $[\text{M}-\text{Na}]^-$

R_f 0.79 (chloroform:methanol 9:1 (V/V))

M 183.27 g/mol

$\text{C}_6\text{H}_{10}\text{NNaS}_2$

7.5.6 2-chloro-3-nitro-5-(trifluoromethyl)benzamide (IR 18)



Synthesis of 2-chloro-3-nitro-5-(trifluoromethyl)benzoylchloride (**IR 06**) from 684 mg (2.5 mmol) 2-chloro-3-nitro-5-(trifluoromethyl)benzoic acid (**IR 05**) according to general procedure I.

IR 06 was dissolved in 2 ml ACN and added slowly to 10 ml aq. NH₃ (25 %) at -20 °C. After 10 min, 10 ml EA were added. The organic layer was separated, washed with water until neutral pH reaction of the water phase, dried over MgSO₄ and the solvent removed under reduced pressure to yield the final product.

Yellow solid

Yield 662 mg (97.1 %)

m.p. 194-196 °C (EA) (lit. 195-197 °C)⁵³

¹H NMR (400 MHz, mixture CDCl₃ & CD₃OD) δ 8.08 (d, 1H, Ar-H, ⁴J = 1.6 Hz), 7.93 (d, 1H, Ar-H, ⁴J = 1.6 Hz)

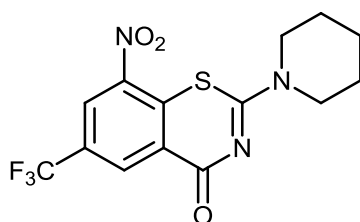
MS (EI) 268 (M)

R_f 0.65 (toluene:ethanol 9:1 (V/V))

M 268.58 g/mol

C₈H₄ClF₃N₂O₃

7.5.7 8-nitro-2-(piperidin-1-yl)-6-(trifluoromethyl)-4H-1,3-benzothiazin-4-one (IR 20)^{np}



method B (dithiocarbamate pathway)

3.738 g (14 mmol) 2-chloro-3-nitro-5-(trifluoromethyl)benzamide (**IR 18**) were dissolved in 250 ml ethanol. 3.843 g (21 mmol) sodium (piperidin-1-yl)carbothioylsulfanide (**IR 17**) were added and the mixture stirred at rt for 20 h. The solvent was evaporated and the residue pre-purified via flash chromatography (eluent toluene:ethanol 98:2 (V/V)). The intermediate 3-nitro-2-[(piperidin-1-yl)carbothioylsulfanyl]-5-(trifluoromethyl)benzamide (**IR 19**) as well as

the final product **IR 20** were obtained as mixture from the flash chromatography. The corresponding fractions were combined and the eluent removed under reduced pressure. The residue (3.612 g, approx. 9 mmol) was dissolved in 100 ml ethanol. 3.58 g (10 mmol) Na_2HPO_4 were added and the mixture refluxed for 6 h. The inorganic salt was filtered off and the filtrate concentrated under reduced pressure. The crude product was purified by flash chromatography twice (eluent toluene and chloroform). Yield 1.854 g (36.9 %).

method E (thiourea pathway)

Synthesis of 2-chloro-3-nitro-5-(trifluoromethyl)benzoylchloride (**IR 06**) from 50 mg (0.19 mmol) 2-chloro-3-nitro-5-(trifluoromethyl)benzoic acid (**IR 05**) according to general procedure I.

33 mg (0.23 mmol) piperidine-1-carbothioamide (**IR 50**) were dissolved in 10 ml toluene and heated to 70 °C. **IR 06** was dissolved in 2 ml toluene and added dropwise. Upon complete addition, the mixture was stirred at 90 °C for 2 h, the solvent evaporated under reduced pressure and the crude product purified by flash chromatography (eluent TBME). Yield 57.8 mg (86.9 %).

adapted method A (classic pathway, adjusted temperature)

According to general procedure III, starting from 100 mg (0.37 mmol) 2-chloro-3-nitro-5-(trifluoromethyl)benzoic acid (**IR 05**). Purification via flash chromatography (eluent TBME). Yield 16 mg (12.0 %).

Yellow solid

m.p. 138-144 °C (toluene:ethanol 9:1 (V/V))

^1H NMR (500 MHz, CDCl_3) δ 9.06 (d, 1H, Ar-H, $^4J = 2.1$ Hz), 8.71 (d, 1H, Ar-H, $^4J = 2.1$ Hz), 3.94 (m, 4H, $\text{CH}_2\text{-N-CH}_2$), 1.75 (m, 6H, $\text{CH}_2\text{-CH}_2\text{-CH}_2$)

^{13}C NMR (125 MHz, CDCl_3) δ 166.5, 161.5, 144.0, 134.3, 133.3 (q, $^3J_{\text{C,F}} = 3.2$ Hz), 129.5 (q, $^2J_{\text{C,F}} = 35.4$ Hz), 126.8, 125.9 (q, $^3J_{\text{C,F}} = 3.7$ Hz), 122.4 (q, $^1J_{\text{C,F}} = 273.0$ Hz), 47.9 (bs, 2 CH_2), 25.9 (bs, 2 CH_2), 24.3

MS (EI) 359 (M)

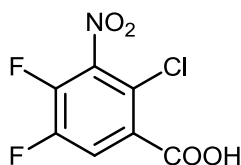
Elemental analysis	calc.	C 46.80	H 3.37	N 11.69	S 8.92
	found	C 46.91	H 3.38	N 11.55	S 9.54

R_f 0.53 (chloroform), R_f 0.44 (TBME:ethanol 97.5:2.5 (V/V))

M 359.32 g/mol

$\text{C}_{14}\text{H}_{12}\text{F}_3\text{N}_3\text{O}_3\text{S}$

7.5.8 2-chloro-4,5-difluoro-3-nitrobenzoic acid (IR 29)



500 mg (2.6 mmol) 2-chloro-4,5-difluorobenzoic acid were added to 7 ml (0.13 mol) sulfuric acid (100 %) at 10 °C. 2.8 ml (65 mmol) fuming nitric acid (100 %) were added slowly keeping the temperature below 10 °C. After complete addition of the nitric acid, the mixture was stirred at rt for 2 h, then cooled to 10 °C and poured onto 15 ml crushed ice. The resulting suspension was stirred at rt for 60 min to release remaining nitrous gases. The precipitate was filtered off, washed with a small amount of cold water and dried in vacuum. The crude product was purified by flash chromatography (eluent EA).

White needles

Yield 177 mg (28.0 %)

m.p. 174-178 °C (EA) (lit. 176-178 °C)⁸⁹

¹H NMR (400 MHz, CD₃OD) δ 8.11 (dd, 1H, Ar-H, ²J_{H,F} = 10.3 Hz, ³J_{H,F} = 8.2 Hz)

¹³C NMR (100 MHz, CD₃OD) δ 162.7, 147.7 (dd, ¹J_{C,F} = 254.1 Hz, ²J_{C,F} = 11.1 Hz), 143.7 (dd,

¹J_{C,F} = 265.1 Hz, ²J_{C,F} = 17.2 Hz), 142.0, 127.9 (dd, ³J_{C,F} = 5.3 Hz, ⁴J_{C,F} = 4.2 Hz), 120.6 (dd,

²J_{C,F} = 20.2 Hz, ³J_{C,F} = 1.2 Hz), 120.2 (d, ³J_{C,F} = 4.6 Hz)

MS (EI) 237 (M)

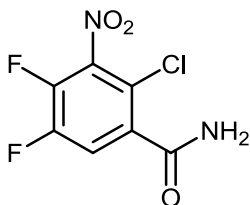
Elemental analysis	calc.	C 35.39	H 0.85	N 5.90
	found	C 35.08	H 0.98	N 5.90

R_f 0.03 (chloroform)

M 237.55 g/mol

C₇H₂ClF₂NO₄

7.5.9 2-chloro-4,5-difluoro-3-nitrobenzamide (IR 32)ⁿ



Synthesis of 2-chloro-4,5-difluoro-3-nitrobenzoylchloride according to general procedure I from 75 mg (0.32 mmol) 2-chloro-4,5-difluoro-3-nitrobenzoic acid (IR 29). The resulting 2-chloro-4,5-difluoro-3-nitrobenzoylchloride was dissolved in 5 ml ACN and slowly added to 10 ml aq. NH₃ (10 %) at -20 °C. After 10 min 10 ml EA were added, the organic phase was

separated and washed with brine until neutral pH reaction of the water phase. The organic layer was dried over MgSO_4 and evaporated to yield the crude product.

Yellow solid

Yield 49 mg (64.7 %)

m.p. 167-169 °C (EA)

^1H NMR (400 MHz, CDCl_3) δ 7.82 (dd, 1H, Ar-H, $^3J_{\text{H,F}}=9.6$ Hz, $^4J_{\text{H,F}}=7.9$ Hz), 6.20 (bs, 1H, NH_2), 5.97 (bs, 1H, NH_2)

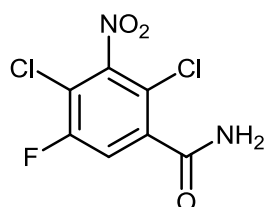
MS (EI) 236 (M)

R_f 0.49 (EA)

M 236.56 g/mol

$\text{C}_7\text{H}_3\text{ClF}_2\text{N}_2\text{O}_3$

7.5.10 2,4-dichloro-5-fluoro-3-nitrobenzamide (IR 39)ⁿ



Synthesis of 2,4-dichloro-5-fluoro-3-nitrobenzoylchloride according to general procedure I from 500 mg (1.96 mmol) 2,4-dichloro-5-fluoro-3-nitrobenzoic acid.

The 2,4-dichloro-5-fluoro-3-nitrobenzoylchloride was dissolved in 5 ml ACN and added slowly to 10 ml aq. NH_3 (10 %) at -40 °C. After 10 min, 20 ml EA were added. The organic layer was separated, washed with water until neutral pH reaction of the water phase, dried over MgSO_4 and the solvent removed under reduced pressure.

White needles

Yield 462 mg (93.2 %)

m.p. 180-181 °C (EA)

^1H NMR (400 MHz, $\text{DMSO-}d_6$) δ 8.13 (bs, 1H, NH_2), 7.98 (d, 1H, Ar-H, $^3J_{\text{H,F}}=8.7$ Hz), 7.97 (bs, 1H, NH_2)

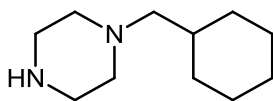
HR MS m/z 250.9430 $[\text{M-H}]^-$, calc. for $[\text{C}_7\text{H}_2\text{Cl}_2\text{FN}_2\text{O}_3]^-$ 250.9432

R_f 0.59 (toluene:ethanol 1:1 (V/V))

M 253.02 g/mol

$\text{C}_7\text{H}_3\text{Cl}_2\text{FN}_2\text{O}_3$

7.5.11 1-(cyclohexylmethyl)piperazine (IR 40)



1.970 ml (14.1 mmol) (bromomethyl)cyclohexane, 1.320 ml (12.8 mmol) 1-formylpiperazine, 2.123 g (15.4 mmol) pestled K_2CO_3 and 30 mg (0.18 mmol) KI were suspended in 15 ml ACN under argon atmosphere and refluxed for 23 h. After evaporation of the solvent, 5 ml 5 M NaOH and 10 ml ethanol were added to the residue and refluxed for 4 h. The organic solvent was removed under reduced pressure, the gelatinous residue diluted with water and extracted with DCM. The combined organic layers were dried over $MgSO_4$ and concentrated under reduced pressure to yield the crude product which was purified by flash chromatography (eluent chloroform:methanol 9:1 (V/V) plus few drops NH_3).

Pale yellow oil

Yield 1.39 g (60.0 %)

1H NMR (400 MHz, $CDCl_3$) δ 2.82 (m, 4H, CH_2-N-CH_2), 2.29 (m, 4H, CH_2-N-CH_2), 2.03 (d, 2H, $N-CH_2-CH$, $^3J = 7.1$ Hz), 1.81 (bs, 1H, NH), 1.66 (m, 5H, cyclohexyl), 1.43 (m, 1H, $N-CH_2-CH$), 1.23 (m, 3H, cyclohexyl), 0.80 (m, 2H, cyclohexyl)

^{13}C NMR (100 MHz, $CDCl_3$) δ 66.3, 55.0 (2 CH_2), 46.1 (2 CH_2), 34.8, 31.9 (2 CH_2), 26.8, 26.1 (2 CH_2)

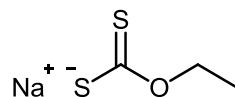
MS (ESI) 183.3 $[M+H]^+$

R_f 0.23 (chloroform:methanol 9:1 (V/V) plus few drops NH_3)

M 182.31 g/mol

$C_{11}H_{22}N_2$

7.5.12 sodium (ethoxymethanethioyl)sulfanide (IR 42)



2.10 g (53 mmol) NaOH were suspended in 100 ml abs. ethanol. 3.14 ml (52 mmol) CS_2 were added and the mixture stirred at rt for 12 h. The solvent was evaporated and the white residue dried in vacuum. The solid was dissolved in water, extracted with chloroform (3x) and hexane (1x) to remove side products. The water was evaporated under reduced pressure to yield the crude product.

Pale yellow solid

Yield 5.07 g (67.1 %)

m.p. 220 °C (water)

^1H NMR (500 MHz, D_2O) δ 4.39 (q, 2H, CH_2 , $^3J = 7.1$ Hz), 1.27 (t, 3H, CH_3 , $^3J = 7.1$ Hz)

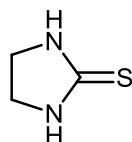
MS (ESI) 121.2 [$\text{M}-\text{Na}$] $^-$

R_f 0.30 (chloroform:methanol 9:1 (V/V))

M 144.19 g/mol (sodium salt), M 122.21 g/mol

$\text{C}_3\text{H}_5\text{NaOS}_2$

7.5.13 imidazolidine-2-thione (IR 45)



1.20 g (0.02 mol) of ethylene diamine were dissolved in 20 ml pyridine. 7.60 g (0.1 mol) CS_2 were added and the mixture refluxed for 5 h. After cooling, the mixture was poured onto 200 ml of TBME. The resulting precipitate was filtered off, washed with a small amount of TBME and dried in vacuum.

Beige solid

Yield 1.102 g (53.9 %)

m.p. 196-199 °C (TBME) (lit. 198-200 °C)¹¹⁸

^1H NMR (400 MHz, D_2O) δ 3.757 (s, 4H, $\text{CH}_2\text{-CH}_2$)

^{13}C NMR (100 MHz, D_2O) δ 181.2, 44.5 (2 CH_2)

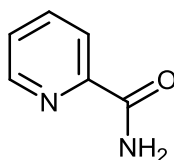
MS (EI) 102 (M)

R_f 0.35 (chloroform:methanol 9:1 (V/V))

M 102.16 g/mol

$\text{C}_3\text{H}_6\text{N}_2\text{S}$

7.5.14 pyridine-2-carboxamide (IR 46)



Synthesis of picolinic acid chloride from 1.23 g (10 mmol) picolinic acid according to general procedure I.

The picolinic acid chloride was suspended in 30 ml ACN and added dropwise to 20 ml aq. NH_3 (25 %) at 0 °C. The color of the reaction mixture turned purple. After 10 min, 10 ml of EA were added to the reaction mixture. The organic layer was separated, washed with brine,

dried over MgSO_4 and evaporated under reduced pressure. The crude product was purified by flash chromatography (eluent chloroform:methanol 95:5 (V/V)).

Yield 565 mg (46.3 %)

m.p. 95-99 °C (chloroform:methanol 95:5 (V/V)) (lit. 105-106 °C)^{SciFinder}

^1H NMR (400 MHz, CDCl_3) δ 8.55 (dd, 1H, Ar-H, $^3J = 4.8$ Hz, $^4J = 0.8$ Hz), 8.19 (d, 1H, Ar-H, $^3J = 7.9$ Hz), 7.84 (ddd, 1H, Ar-H, $^3J = 7.7$ Hz, $^4J = 1.2$ Hz), 7.84 (bs, 1H, NH_2), 7.43 (ddd, 1H, Ar-H, $^3J = 7.7$ Hz, $^3J = 4.8$ Hz, $^4J = 1.2$ Hz), 5.82 (bs, 1H, NH_2)

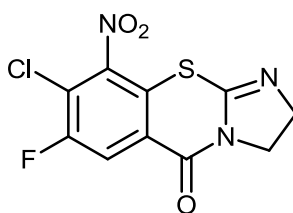
MS (EI) 122 (M)

R_f 0.53 (chloroform:methanol 9:1 (V/V))

M 122.13 g/mol

$\text{C}_6\text{H}_6\text{N}_2\text{O}$

7.5.15 8-chloro-7-fluoro-9-nitro-2,3-dihydro-5H-imidazo[2,1-*b*][1,3]benzothiazin-5-one (IR 47)^{np}



Synthesis of 2,4-dichloro-5-fluoro-3-nitrobenzoylchloride from 750 mg (3.00 mmol) 2,4-dichloro-5-fluoro-3-nitrobenzoic acid according to general procedure I.

In a three-neck flask, flushed with argon, 204 mg (2.00 mmol) imidazolidine-2-thione (**IR 45**) were dissolved in 14 ml dry pyridine at 0-5 °C. 2,4-dichloro-5-fluoro-3-nitrobenzoylchloride was dissolved in 2 ml toluene and added dropwise, keeping the temperature at 0-10 °C. Subsequently, the mixture was heated to 50 °C for 40 min. After cooling, the reaction mixture was poured onto 200 ml of crushed ice. A brownish oil, which contained the crude product, was separated. 100 ml of chloroform were added to the crude product and washed with water to remove remaining pyridine. The organic layer was evaporated under reduced pressure. The crude product was purified by flash chromatography (eluent chloroform). Fractions containing the product were combined, the solvent evaporated and the solid residue washed with 1 ml chloroform to yield the purified product.

Pale yellow solid

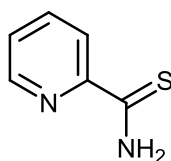
Yield 47.3 mg (7.8 %)

m.p. 135-137 °C (chloroform)

^1H NMR (500 MHz, acetone- d_6) δ 7.71 (d, 1H, Ar-H, $^3J_{H,F} = 8.7$ Hz), 4.34 (m, 2H, CH_2), 3.82 (m, 2H, CH_2)

^{13}C NMR (125 MHz, DMSO- d_6) δ 178.0, 162.9, 156.0 (d, $^1J_{\text{C,F}} = 252.2$ Hz), 147.7, 138.4 (d, $^3J_{\text{C,F}} = 7.8$ Hz), 118.4 (d, $^2J_{\text{C,F}} = 24.9$), 118.2 (d, $^3J_{\text{C,F}} = 4.1$ Hz), 113.8 (d, $^2J_{\text{C,F}} = 23.9$ Hz), 46.2, 41.3
MS (EI) 301 (M)
HR MS m/z 301.9800 $[\text{M}+\text{H}]^+$, calc. for $[\text{C}_{10}\text{H}_6\text{FN}_3\text{O}_3\text{S}]^+$ 301.9797
 R_f 0.39 (chloroform:methanol 9:1)
 M 301.68 g/mol
 $\text{C}_{10}\text{H}_5\text{ClFN}_3\text{O}_3\text{S}$

7.5.16 pyridine-2-carbothioamide (IR 48)



809 mg (2.00 mmol) Lawessons reagent (2,4-bis(4-methoxyphenyl)-1,3,2,4-dithiadiphosphetane-2,4-disulfide) were added to a suspension of 488 mg (4.00 mmol) pyridine-2-carboxamide (**IR 46**) in 20 ml toluene and stirred at 80-85 °C for 17 h. After cooling, 10 ml water were added and the mixture extracted with EA. The combined organic layers were dried over MgSO_4 and evaporated to give a brown solid. The crude product was purified by flash chromatography (eluent chloroform).

Yellow solid

Yield 523 mg (94.6 %)

m.p. 136-139 °C (chloroform) (lit. 138-140)^{SciFinder}

^1H NMR (400 MHz, CDCl_3) δ 9.48 (bs, 1H, NH_2), 8.68 (d, 1H, Ar-H, $^3J = 8.1$ Hz), 8.50 (m, 1H, Ar-H), 7.81 (dt, 1H, Ar-H, $^3J = 8.1$ Hz, $^3J = 7.5$, $^4J = 1.9$ Hz), 7.68 (bs, 1H, NH_2), 7.43 (m, 1H, Ar-H)

^{13}C NMR (100 MHz, CDCl_3) δ 195.8, 150.5, 147.1, 137.1, 126.3, 125.1

MS (EI) 138 (M)

R_f 0.61 (chloroform:methanol 9:1 (V/V))

M 138.19 g/mol

$\text{C}_6\text{H}_6\text{N}_2\text{S}$

7.5.17 morpholine-4-carbothioamide (IR 49)



Synthesis according to general procedure II, starting from 4.35 ml (50 mmol) morpholine. Work-up after neutralization: the mixture was kept at 8 °C for 48 h, the precipitate filtered off, washed with a small amount of chloroform and dried.

White solid

Yield 1.09 g (14.9 %)

m.p. 173-177 °C (water) (lit. 177 °C)⁸⁰

¹H NMR (400 MHz, CD₃OD) δ 3.78 (m, 4H, CH₂-O-CH₂), 3.65 (m, 4H, CH₂-N-CH₂)

¹³C NMR (100 MHz, DMSO-*d*₆) δ 181.3, 65.6 (2 CH₂), 47.4 (2 CH₂)

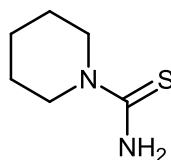
MS (EI) 146 (M)

R_f 0.42 (chloroform:methanol 9:1 (V/V))

M 146.21 g/mol

C₅H₁₀N₂OS

7.5.18 piperidine-1-carbothioamide (IR 50)



Synthesis according to general procedure II, starting from 4.95 ml (50 mmol) piperidine.

Work-up after neutralization: the mixture was kept at 8 °C for 48 h, the brown oil which settled on the bottom of the flask was separated and purified by flash chromatography twice (eluent chloroform). The fractions containing the product were combined, the solvent evaporated and the remaining crude product treated with a few ml of toluene. A white precipitate formed, which was filtered off and dried.

White solid

Yield 611 mg (8.5 %)

m.p. 123-126 °C (toluene) (lit. 128 °C)⁸⁰

¹H NMR (400 MHz, CDCl₃) δ 3.73 (m, 4H, CH₂-N-CH₂), 1.67 (m, 6H, CH₂-CH₂-CH₂)

¹³C NMR (100 MHz, CDCl₃) δ 180.3, 49.4 (2 CH₂), 25.5 (2 CH₂), 23.8

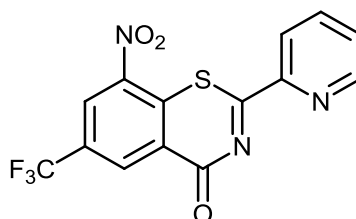
MS (ESI) *m/z* 145.0 [M+H]⁺

R_f 0.59 (chloroform:methanol 9:1 (V/V))

M 144.24 g/mol

$C_6H_{12}N_2S$

7.5.19 8-nitro-2-(pyridin-2-yl)-6-(trifluoromethyl)-4H-1,3-benzothiazin-4-one (IR 51)^{np}



Synthesis of 2-chloro-3-nitro-5-(trifluoromethyl)benzoylchloride (**IR 06**) according to general procedure I from 538 mg (2.00 mmol) 2-chloro-3-nitro-5-(trifluoromethyl)benzoic acid (**IR 05**).

IR 06 was dissolved in 2 ml toluene and added to a solution of 138 mg (1.00 mmol) pyridine-2-carbothioamide (**IR 48**) in 50 ml toluene. The mixture was heated to reflux for 3 h, let cool to rt and the solvent evaporated under reduced pressure. The crude product was purified by flash chromatography (eluent chloroform).

Yellow solid

Yield 179 mg (50.7 %)

m.p. 202-206 °C (chloroform)

1H NMR (400 MHz, $CDCl_3$) δ 9.14 (d, 1H, Ar-H, $^4J = 2.1$ Hz), 8.87 (d, 1H, Ar-H, $^4J = 2.1$ Hz), 8.80 (d, 1H, Het-Ar-H, $^3J = 4.8$ Hz), 8.52 (d, 1H, Het-Ar-H, $^3J = 7.9$ Hz), 7.94 (dt, 1H, Het-Ar-H, $^3J = 7.9$ Hz, $^3J = 7.7$ Hz, $^4J = 1.7$ Hz), 7.60 (ddd, 1H, Het-Ar-H, $^3J = 7.7$ Hz, $^3J = 4.8$ Hz, $^4J = 1.2$ Hz)

MS (EI) 353 (M)

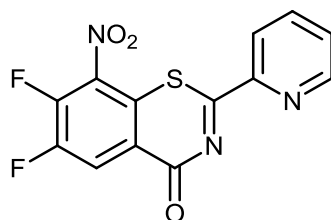
Elemental analysis	calc.	C 47.60	H 1.71	N 11.89	S 9.08
	found	C 47.52	H 1.47	N 11.51	S 9.23

R_f 0.28 (chloroform)

M 353.28 g/mol

$C_{14}H_6F_3N_3O_3S$

7.5.20 6,7-difluoro-8-nitro-2-(pyridin-2-yl)-4H-1,3-benzothiazin-4-one (IR 52)^{np}



Synthesis of 2-chloro-4,5-difluoro-3-nitrobenzoylchloride from 50 mg (0.21 mmol) 2-chloro-4,5-difluoro-3-nitrobenzoic acid (**IR 29**) according to general procedure I.

The 2-chloro-4,5-difluoro-3-nitrobenzoylchloride was dissolved in 2 ml toluene and added to a solution of 22 mg (0.16 mmol) pyridine-2-carbothioamide (**IR 48**) in 15 ml toluene. After heating to reflux for 4 h, the solvent was evaporated under reduced pressure and the crude product purified by flash chromatography twice (eluent chloroform).

Yellow solid

Yield 7.2 mg (14.2 %)

m.p. 190-194 °C (chloroform)

¹H NMR (400 MHz, CDCl₃) δ 8.77 (ddd, 1H, Het-Ar-H, ³J = 4.8 Hz, ⁴J = 1.7 Hz, ⁴J = 0.9 Hz), 8.63 (dd, 1H, Ar-H, ³J_{H,F} = 9.6 Hz, ⁴J_{H,F} = 7.6 Hz), 8.50 (td, 1H, Het-Ar-H, ³J = 7.9 Hz, ⁴J = 1.0 Hz), 7.95 (dt, 1H, Het-Ar-H, ³J = 7.8 Hz, ³J = 7.7 Hz, ⁴J = 1.7 Hz), 7.61 (ddd, 1H, Het-Ar-H, ³J = 7.6 Hz, ³J = 4.8 Hz, ⁴J = 1.2 Hz)

¹³C NMR (100 MHz, CDCl₃) δ 175.1, 166.8, 151.7, 150.6 (dd, ¹J_{C,F} = 259.0 Hz, ²J_{C,F} = 11.8 Hz), 149.4, 148.2 (dd, ¹J_{C,F} = 275.8 Hz, ²J_{C,F} = 16.8 Hz), 144.8, 137.7, 129.3, 128.6, 122.2 (dd, ²J_{C,F} = 18.7 Hz, ³J_{C,F} = 2.7 Hz), 121.9, 119.6

MS (EI) 321 (M)

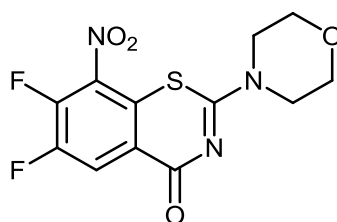
Elemental analysis	calc.	C 48.60	H 1.57	N 13.08	S 9.98
	found	C 48.28	H 1.58	N 12.39	S 9.37

R_f 0.30 (chloroform)

M 321.26 g/mol

C₁₃H₅F₂N₃O₃S

7.5.21 6,7-difluoro-2-(morpholin-4-yl)-8-nitro-4*H*-1,3-benzothiazin-4-one (IR 53)^{np}



Synthesis of 2-chloro-4,5-difluoro-3-nitrobenzoylchloride from 50 mg (0.21 mmol) 2-chloro-4,5-difluoro-3-nitrobenzoic acid (**IR 29**) according to general procedure I.

38.5 mg (0.26 mmol) morpholine-4-carbothioamide (**IR 49**) were dissolved in 15 ml toluene and heated to 80 °C. The 2-chloro-4,5-difluoro-3-nitrobenzoylchloride was dissolved in 5 ml toluene and added dropwise. The mixture was stirred at 80 °C for another hour, then heated to reflux for 2 h. After cooling, the solvent was evaporated under reduced pressure and the crude product purified by flash chromatography (eluent TBME).

Yellow solid

Yield 32.4 mg (46.9 %)

m.p. 208-210 °C (TBME)

¹H NMR (500 MHz, CDCl₃) δ 8.56 (dd, 1H, Ar-H, ³J_{H,F} = 9.7 Hz, ⁴J_{H,F} = 7.7 Hz), 3.94 (m, 4H, CH₂-N-CH₂), 3.79 (m, 4H, CH₂-O-CH₂)

MS (EI) 329 (M)

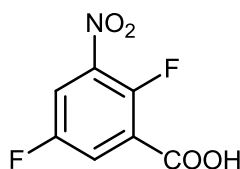
Elemental analysis	calc.	C 43.77	H 2.75	N 12.76	S 9.74
	found	C 43.71	H 2.61	N 12.39	S 9.27

R_f 0.08 (chloroform), R_f 0.27 (TBME:ethanol 97.5:2.5 (V/V))

M 329.28 g/mol

C₁₂H₉F₂N₃O₄S

7.5.22 2,5-difluoro-3-nitrobenzoic acid (IR 54)



316 mg (2.00 mmol) 2,5-difluorobenzoic acid were added to 4 ml sulfuric acid (100 %) at 0 °C. A mixture of 2.5 ml nitric acid (100 %) and 2.5 ml sulfuric acid (100 %) was added dropwise keeping the temperature at 0 °C. The mixture was stirred for another 2 h at 0 °C, poured onto 75 ml of crushed ice and the resulting suspension stirred for 30 min. The

mixture was extracted with EA (17x), the combined organic layers dried over MgSO_4 and evaporated to yield a yellow oil. The crude product was purified by MPLC twice (Büchi MPLC, eluent heptane:EA 1:1 (V/V) with 1 % formic acid, flow rate 30 ml/min).

Pale yellow solid

Yield 127 mg (31.2 %)

m.p. 102-110 °C (heptane:EA 1:1)

^1H NMR (400 MHz, CD_3OD) δ 8.12 (ddd, 1H, Ar-H, $^3J_{\text{H,F}} = 7.4$ Hz, $^4J_{\text{H,F}} = 5.1$ Hz, $^4J_{\text{H,H}} = 3.5$ Hz), 8.00 (ddd, 1H, Ar-H, $^3J_{\text{H,F}} = 8.2$ Hz, $^4J_{\text{H,F}} = 5.7$ Hz, $^4J_{\text{H,H}} = 3.5$ Hz)

^{13}C NMR (125 Hz, CD_3OD) δ 162.8, 156.5 (dd, $^1J_{\text{C,F}} = 247.6$ Hz, $^4J_{\text{C,F}} = 3.7$ Hz), 151.0 (dd, $^1J_{\text{C,F}} = 272.0$ Hz, $^4J_{\text{C,F}} = 3.2$ Hz), 139.0 (m), 123.6 (m), 123.3 (dd, $^2J_{\text{C,F}} = 25.3$ Hz, $^3J_{\text{C,F}} = 1.4$ Hz), 116.6 (dd, $^2J_{\text{C,F}} = 29.0$ Hz, $^3J_{\text{C,F}} = 2.3$ Hz)

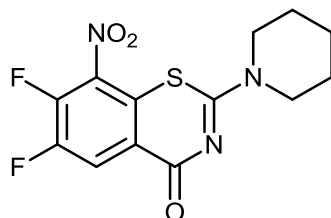
MS (EI) 203 (M)

R_f 0.23 (heptane:EA 1:1 (V/V) with 1 % formic acid)

M 203.10 g/mol

$\text{C}_7\text{H}_3\text{F}_2\text{NO}_4$

7.5.23 6,7-difluoro-8-nitro-2-(piperidin-1-yl)-4H-1,3-benzothiazin-4-one (IR 56)^{np}



Synthesis of 2-chloro-4,5-difluoro-3-nitrobenzoylchloride from 50 mg (0.21 mmol) 2-chloro-4,5-difluoro-3-nitrobenzoic acid (**IR 29**) according to general procedure I.

38 mg (0.26 mmol) piperidine-1-carbothioamide (**IR 50**) were dissolved in 15 ml toluene and heated to 60-70 °C. The 2-chloro-4,5-difluoro-3-nitrobenzoylchloride was dissolved in 5 ml toluene and added dropwise. The mixture was stirred at 70 °C for another hour, then heated to 90 °C for 2 h. After cooling, the solvent was evaporated and the crude product purified by flash chromatography (eluent TBME).

Yellow solid

Yield 17.5 mg (25.5 %)

m.p. 166-171 °C (TBME)

^1H NMR (400 MHz, CDCl_3) δ 8.55 (dd, 1H, Ar-H, $^3J_{\text{H,F}} = 9.8$ Hz, $^4J_{\text{H,F}} = 7.7$ Hz), 3.98 (m, 4H, $\text{CH}_2\text{-N-CH}_2$), 1.74 (m, 6H, $\text{CH}_2\text{-CH}_2\text{-CH}_2$)

^{13}C NMR (100 MHz, CDCl_3) δ 166.0, 160.7, 149.5 (dd, $^1J_{\text{C,F}} = 256.0$ Hz, $^2J_{\text{C,F}} = 11.8$ Hz), 147.6 (dd, $^1J_{\text{C,F}} = 273.5$ Hz, $^2J_{\text{C,F}} = 16.8$ Hz), 144.5, 125.0 (m), 122.8 (dd, $^2J_{\text{C,F}} = 19.1$ Hz, $^3J_{\text{C,F}} = 1.9$ Hz), 120.7 (m), 47.9 (bs, 2 CH_2), 25.9 (bs, 2 CH_2), 24.3

MS (EI) 327 (M)

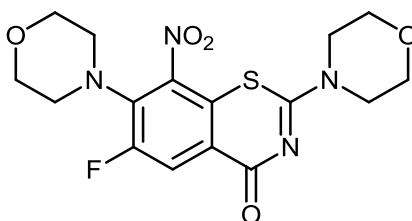
Elemental analysis	calc.	C 47.70	H 3.39	N 12.84	S 9.80
	found	C 47.96	H 3.32	N 12.35	S 9.64

R_f 0.41 (TBME:ethanol 97.5:2.5 (V/V))

M 327.31 g/mol

$\text{C}_{13}\text{H}_{11}\text{F}_2\text{N}_3\text{O}_3\text{S}$

7.5.24 6-fluoro-2,7-bis(morpholin-4-yl)-8-nitro-4H-1,3-benzothiazin-4-one (IR 57)^{np}



The complete reaction was conducted under argon atmosphere.

48 mg (0.14 mmol) 7-chloro-6-fluoro-2-(morpholin-4-yl)-8-nitro-4H-1,3-benzothiazin-4-one (IR 69) and 48 μl (0.28 mmol) DIPEA were dissolved in 15 ml DMF. 14.5 μl (0.17 mmol) morpholine were dissolved in 3 ml DMF and added dropwise. The mixture was stirred at rt for 2 h, after which another 14.5 μl (0.17 mmol) morpholine were added and the mixture stirred for another 20 h. The solvent was evaporated under reduced pressure and the crude product purified by flash chromatography twice (eluent chloroform).

Orange solid

Yield 34.4 mg (62.4 %)

m.p. 245-250 $^{\circ}\text{C}$ (chloroform)

^1H NMR (400 MHz, CDCl_3) δ 8.29 (d, 1H, Ar-H, $J_{\text{H,F}} = 12.2$ Hz), 3.90 (m, 4H, $\text{CH}_2\text{-N-CH}_2$), 3.78 (m, 8H, 2x $\text{CH}_2\text{-O-CH}_2$), 3.18 (m, 4H, $\text{CH}_2\text{-N-CH}_2$)

^{13}C NMR (100 MHz, CDCl_3) δ 167.1, 161.8, 157.2 (d, $^1J_{\text{C,F}} = 253.8$ Hz), 141.6 (d, $^3J_{\text{C,F}} = 3.9$ Hz), 137.7 (d, $^2J_{\text{C,F}} = 14.0$ Hz), 123.0 (d, $^4J_{\text{C,F}} = 3.1$ Hz), 120.1 (d, $^2J_{\text{C,F}} = 23.4$ Hz), 118.3 (d, $^3J_{\text{C,F}} = 7.0$ Hz), 66.9 (2 CH_2), 66.3 (2 CH_2), 50.8, 50.7, 46.7 (2 CH_2)

MS (EI) 396 (M)

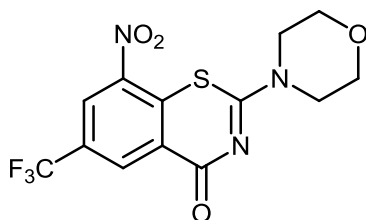
Elemental analysis	calc.	C 48.48	H 4.32	N 14.12	S 8.09
	found	C 48.38	H 4.01	N 16.61	S 7.79

R_f 0.44 (TBME:ethanol 20:1 (V/V))

M 396.39 g/mol

$\text{C}_{16}\text{H}_{17}\text{FN}_4\text{O}_5\text{S}$

7.5.25 2-(morpholin-4-yl)-8-nitro-6-(trifluoromethyl)-4H-1,3-benzothiazin-4-one (IR 58)^{np}



method A (classic pathway)

Synthesis of 2-chloro-3-nitro-5-(trifluoromethyl)benzoylchloride (**IR 06**) according to general procedure I from 809 mg (3.00 mmol) 2-chloro-3-nitro-5-(trifluoromethyl)benzoic acid (**IR 05**).

The next steps were conducted under argon atmosphere.

IR 06 was dissolved in 10 ml acetone and added dropwise to a solution of 291 mg (3.00 mmol) KSCN in 10 ml acetone. Upon complete addition, the mixture was heated to 40 °C for 5 min and then let cool again to rt. 261 μ l (3.00 mmol) morpholine were dissolved in 10 ml acetone and added dropwise. The mixture was stirred for another 30 min at rt, then heated to reflux for 2 min. After cooling, the solvent was evaporated under reduced pressure and the crude product was pre-purified by flash chromatography twice (eluent chloroform). The fractions containing product were combined, the solvent evaporated and the residue recrystallized from TBME. Yield 150 mg (13.8 %).

method E (thiourea pathway)

Synthesis of 2-chloro-3-nitro-5-(trifluoromethyl)benzoylchloride (**IR 06**) according to general procedure I from 50 mg (0.18 mmol) 2-chloro-3-nitro-5-(trifluoromethyl)benzoic acid (**IR 05**). 34 mg (0.23 mmol) morpholine-4-carbothioamide (**IR 49**) were dissolved in 10 ml toluene and heated to 50-60 °C. **IR 06** was dissolved in 2 ml toluene and added dropwise. Upon complete addition, the mixture was stirred at 90 °C for 2 h. TLC showed completion of reaction. The solvent was evaporated and the crude product purified by flash chromatography (eluent TBME). Yield 49 mg (74.8 %).

Yellow solid

m.p. 181-183 °C (TBME)

¹H NMR (500 MHz, CDCl₃) δ 9.08 (d, 1H, Ar-H, ⁴J = 1.5 Hz), 8.75 (d, 1H, Ar-H, ⁴J = 1.5 Hz), 4.01 (m, 4H, CH₂-N-CH₂), 3.82 (m, 4H, CH₂-O-CH₂)

¹³C NMR (125 MHz, CDCl₃) δ 166.3, 162.6, 143.9, 133.7, 133.5 (q, ³J_{C,F} = 3.7 Hz), 129.9 (q, ²J_{C,F} = 35.9 Hz), 126.8, 126.1 (q, ³J_{C,F} = 3.7 Hz), 122.3 (q, ¹J_{C,F} = 272.5 Hz), 66.3 (bs, 2 CH₂), 46.7 (bs, 2 CH₂)

MS (EI) 361 (M)

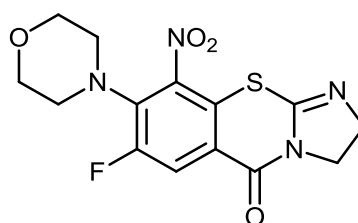
Elemental analysis	calc.	C 43.22	H 2.79	N 11.63	S 8.87
	found	C 43.72	H 2.69	N 11.57	S 8.66

R_f 0.22 (toluene:ethanol 9:1 (V/V)), R_f 0.29 (TBME:ethanol 97.5:2.5 (V/V))

M 361.30 g/mol

$C_{13}H_{10}F_3N_3O_4S$

7.5.26 7-fluoro-8-(morpholin-4-yl)-9-nitro-2,3-dihydro-5H-imidazo[2,1-b][1,3]benzothiazin-5-one (IR 59)^{np}



The complete reaction was conducted under argon atmosphere.

50 mg (0.16 mmol) 8-chloro-7-fluoro-9-nitro-2,3-dihydro-5H-imidazo[2,1-b][1,3]benzothiazin-5-one (**IR 47**) were dissolved in 10 ml DMF. 196 μ l (2.20 mmol) morpholine were added and the mixture stirred for 4.5 h at rt. The mixture was poured onto crushed ice and extracted with chloroform. The combined organic layers were dried over $MgSO_4$, the solvent evaporated and the crude product purified by flash chromatography (eluent chloroform). The fractions containing the product were combined, the solvent was evaporated and the remaining residue treated with few ml of hexane to facilitate precipitation of the final product.

Orange needles

Yield 24 mg (41.1 %)

m.p. 202-203 °C (hexane)

1H NMR (500 MHz, mixture CD_3OD & acetone- d_6) δ 8.06 (d, 1H, Ar-H, $J_{H,F}$ = 12.7 Hz), 4.03 (m, 2H, CH_2), 3.97 (m, 2H, CH_2), 3.71 (m, 4H, CH_2-O-CH_2), 3.16 (m, 4H, CH_2-N-CH_2)

^{13}C NMR (100 MHz, $CDCl_3$) δ 157.2, 155.9 (d, $^1J_{C,F}$ = 251.4 Hz), 151.0, 140.9, 138.6 (d, $^2J_{C,F}$ = 13.7 Hz), 123.6 (d, $^4J_{C,F}$ = 3.4 Hz), 119.9 (d, $^2J_{C,F}$ = 24.4 Hz), 118.6 (d, $^3J_{C,F}$ = 7.2 Hz), 66.8 (2 CH_2), 53.6, 50.7, 50.6, 44.7

MS (EI) 352 (M)

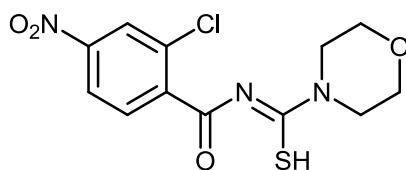
Elemental analysis	calc.	C 47.72	H 3.72	N 15.90	S 9.10
	found	C 47.46	H 3.71	N 15.22	S 9.07

R_f 0.56 (chloroform:methanol 95:5 (V/V))

M 352.34 g/mol

$C_{14}H_{13}FN_4O_4S$

7.5.27 N-[(2-chloro-4-nitrophenyl)carbonyl]morpholine-4-carboimidothioic acid (IR 60)ⁿ



Synthesis of 2-chloro-4-nitrobenzoylchloride according to general procedure I from 403 mg (2.00 mmol) 2-chloro-4-nitrobenzoic acid.

The next 2 steps were conducted under argon atmosphere.

2-chloro-4-nitrobenzoylchloride was dissolved in 10 ml 1,2-dichlorobenzene and added to a solution of 210 mg (2.60 mmol) NaSCN in 10 ml 1,2-dichlorobenzene. 11.7 μ l SnCl₄ were added with a syringe and the mixture heated to 180 °C for 2 h. After cooling to rt, the precipitate of NaCl was filtered off. A solution of 174 μ l (2.00 mmol) morpholine in 5 ml 1,2-dichlorobenzene was added dropwise to the remaining solution of acyl isothiocyanate. After complete addition, the mixture was stirred for another 30 min at rt. The resulting precipitate was filtered off, washed with a small amount of chloroform and dried.

Beige solid

Yield 390 mg (59.1 %)

m.p. 187-190 °C (chloroform)

¹H NMR (400 MHz, DMSO-*d*₆) δ 11.33 (bs, 1H, SH), 8.29 (d, 1H, Ar-H, ⁴*J* = 2.4 Hz), 8.19 (dd, 1H, Ar-H, ³*J* = 8.6 Hz, ⁴*J* = 2.4 Hz), 7.76 (d, 1H, Ar-H, ³*J* = 8.6 Hz), 4.04 (m, 2H, morpholine), 3.67 (m, 6H, morpholine)

MS (EI) 329 (M)

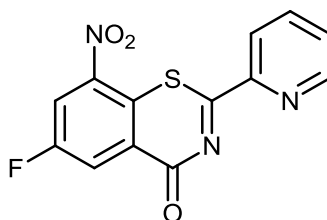
Elemental analysis	calc.	C 43.71	H 3.67	N 12.74	S 9.72
	found	C 44.17	H 3.58	N 12.68	S 10.18

R_f 0.47 (toluene:ethanol 9:1 (V/V))

M 329.76 g/mol

C₁₂H₁₂ClN₃O₄S

7.5.28 6-fluoro-8-nitro-2-(pyridin-2-yl)-4H-1,3-benzothiazin-4-one (IR 61)^{np}



Synthesis of 2,5-difluoro-3-nitrobenzoylchloride according to general procedure I from 97 mg (0.45 mmol) 2,5-difluoro-3-nitrobenzoic acid (**IR 54**).

2,5-difluoro-3-nitrobenzoylchloride was dissolved in 2 ml toluene and added to a solution of 44 mg (0.32 mmol) pyridine-2-carbothioamide (**IR 48**). The mixture was heated to reflux for 3 h, let cool to rt and the solvent evaporated under reduced pressure. The crude product was purified by flash chromatography twice (eluent chloroform).

Yellow solid

Yield 56 mg (58.1 %)

m.p. 201-204 °C (chloroform)

¹H NMR (400 MHz, CDCl₃) δ 8.78 (d, 1H, Het-Ar-H, ³J_{H,H} = 4.4 Hz), 8.64 (dd, 1H, Ar-H,

³J_{H,F} = 7.8 Hz, ⁴J_{H,H} = 3.1 Hz), 8.51 (d, 1H, Het-Ar-H, ³J_{H,H} = 7.8 Hz), 8.43 (d, 1H, Ar-H,

³J_{H,F} = 7.4 Hz, ⁴J_{H,H} = 3.1 Hz), 7.78 (dt, 1H, Het-Ar-H, ³J_{H,H} = 7.8 Hz, ³J_{H,H} = 7.3 Hz, ⁴J_{H,H} = 1.6 Hz),

7.58 (ddd, 1H, Het-Ar-H, ³J_{H,H} = 7.3 Hz, ³J_{H,H} = 4.7 Hz, ⁴J_{H,H} = 0.8 Hz)

¹³C NMR (100 MHz, CDCl₃) δ 176.7, 167.6 (d, ⁴J_{C,F} = 3.1 Hz), 161.1 (d, ¹J_{C,F} = 255.4 Hz), 152.3,

149.4, 145.6 (d, ³J_{C,F} = 6.2 Hz), 137.6, 129.6 (d, ⁴J_{C,F} = 3.1 Hz), 128.4, 126.6 (d, ³J_{C,F} = 7.8 Hz),

123.8 (d, ²J_{C,F} = 21.8 Hz), 121.9, 119.0 (d, ²J_{C,F} = 28.0 Hz)

MS (EI) 303 (M)

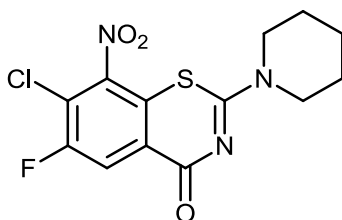
Elemental analysis	calc.	C 51.49	H 1.99	N 13.86	S 10.57
	found	C 51.70	H 2.15	N 12.98	S 9.96

R_f 0.43 (chloroform)

M 303.27 g/mol

C₁₃H₆FN₃O₃S

7.5.29 7-chloro-6-fluoro-8-nitro-2-(piperidin-1-yl)-4H-1,3-benzothiazin-4-one (IR 62)^{np}



Synthesis of 2,4-dichloro-5-fluoro-3-nitrobenzoylchloride according to general procedure I from 276 mg (1.08 mmol) 2,4-dichloro-5-fluoro-3-nitrobenzoic acid.

116 mg (0.80 mmol) piperidine-1-carbothioamide (**IR 50**) were dissolved in 10 ml toluene and heated to 90 °C. 2,4-dichloro-5-fluoro-3-nitrobenzoylchloride was suspended in 5 ml toluene and added dropwise. After complete addition, the mixture was refluxed for 12 h. After cooling, the solvent was evaporated under reduced pressure and the crude product purified by flash chromatography (eluent TBME).

Yellow solid

Yield 67.6 mg (24.6 %)

m.p. 165-175 °C (TBME)

¹H NMR (400 MHz, CDCl₃) δ 8.40 (d, 1H, Ar-H, ³J_{H,F} = 8.6 Hz), 3.86 (m, 4H, CH₂-N-CH₂), 1.73 (m, 6H, CH₂-CH₂-CH₂)

¹³C NMR (100 MHz, CDCl₃) δ 166.1, 159.6, 157.1 (d, ¹J_{C,F} = 255.6 Hz), 145.8, 124.1 (d, ³J_{C,F} = 6.5 Hz), 123.0 (d, ⁴J_{C,F} = 3.8 Hz), 120.2 (d, ²J_{C,F} = 23.3 Hz), 119.6 (d, ²J_{C,F} = 23.7 Hz), 48.1 (bs, 2 CH₂), 25.8 (bs, 2 CH₂), 24.3

MS (EI) 343 (M)

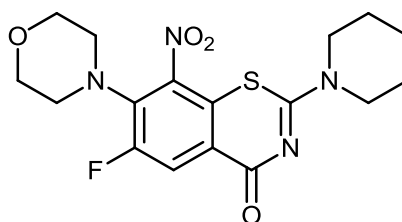
Elemental analysis	calc.	C 45.42	H 3.23	N 12.22	S 9.33
	found	C 45.65	H 2.89	N 12.15	S 8.37

R_f 0.29 (TBME), R_f 0.13 (chloroform)

M 343.76 g/mol

C₁₃H₁₁ClFN₃O₃S

7.5.30 6-fluoro-7-(morpholin-4-yl)-8-nitro-2-(piperidin-1-yl)-4H-1,3-benzothiazin-4-one (IR 64)^{np}



67 μ l (0.77 mmol) morpholine were added to a solution of 82 mg (0.24 mmol) 7-chloro-6-fluoro-8-nitro-2-(piperidin-1-yl)-4H-1,3-benzothiazin-4-one (**IR 62**) in 20 ml DMF and the mixture stirred for 4 h at rt. After evaporation of the solvent under reduced pressure, the crude product was purified by flash chromatography twice (eluent chloroform).

Orange solid

Yield 65.5 mg (69.5 %)

m.p. 83-90 °C (chloroform)

¹H NMR (500 MHz, CDCl₃) δ 8.29 (d, 1H, Ar-H, ³J_{H,F} = 12.3 Hz), 3.83 (m, 8H, CH₂-N-CH₂, CH₂-O-CH₂), 3.17 (m, 4H, CH₂-N-CH₂), 1.71 (m, 6H, CH₂-CH₂-CH₂)

¹³C NMR (100 MHz, CDCl₃) δ 167.2, 160.6, 157.2 (d, ¹J_{C,F} = 253.4 Hz), 142.1 (d, ³J_{C,F} = 4.3 Hz), 137.3 (d, ²J_{C,F} = 14.4 Hz), 123.2 (d, ⁴J_{C,F} = 3.5 Hz), 119.9 (d, ²J_{C,F} = 23.4 Hz), 118.6 (d, ³J_{C,F} = 7.4 Hz), 66.9 (2 CH₂), 50.8, 50.7, 47.9 (bs, 2 CH₂), 25.8 (bs, 2 CH₂), 24.3

MS (EI) 394 (M)

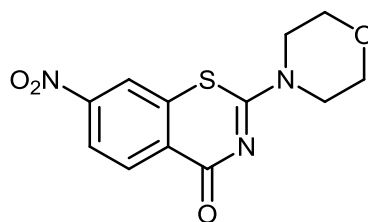
Elemental analysis	calc.	C 51.77	H 4.86	N 14.20	S 8.13
	found	C 51.54	H 4.78	N 13.68	S 7.55

R_f 0.48 (chloroform:methanol 98:2 (V/V)), R_f 0.05 (chloroform)

M 394.42 g/mol

C₁₇H₁₉FN₄O₄S

7.5.31 2-(morpholin-4-yl)-7-nitro-4H-1,3-benzothiazin-4-one (IR 67)^{np}



210 mg (0.64 mmol) N-[(2-chloro-4-nitrophenyl)carbonyl]morpholine-4-carboimidothioic acid (**IR 60**) were dissolved in 60 ml acetone and stirred at rt for 4 weeks. After evaporation of the solvent the crude product was purified via MPLC twice (Puriflash System, column:

Puriflash column 15 silica HP, eluent: gradient TBME:ethanol 100:0 to 0:100 (V/V) in 36 min or 18 min, flow rate 20 ml/min).

Yellow solid

Yield 24 mg (12.8 %)

m.p. 222-228 °C (chloroform)

^1H NMR (500 MHz, CDCl_3) δ 8.60 (d, 1H, Ar-H, $^3J = 9.2$ Hz), 8.22 (m, 2H, Ar-H), 3.93 (bs, 4H, $\text{CH}_2\text{-N-CH}_2$), 3.81 (m, 4H, $\text{CH}_2\text{-O-CH}_2$)

^{13}C NMR (100 MHz, CDCl_3) δ 167.2, 161.8, 149.4, 133.7, 132.1, 127.3, 122.6, 121.1, 66.3 (bs, 2 CH_2), 46.2 (bs, 2 CH_2)

MS (EI) 293 (M)

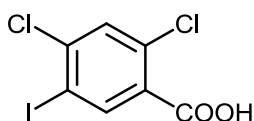
Elemental analysis	calc.	C 49.14	H 3.78
	found	C 49.44	H 3.87

R_f 0.25 (TBME:ethanol 20:1 (V/V)), R_f 0.23 (toluene:ethanol 9:1 (V/V))

M 293.30 g/mol

$\text{C}_{12}\text{H}_{11}\text{N}_3\text{O}_4\text{S}$

7.5.32 2,4-dichloro-5-iodobenzoic acid (IR 68)



414 mg (2.10 mmol) sodium iodate (NaIO_3) and 1.06 g (8.30 mmol) iodine were mixed with 30 ml sulfuric acid (95-97 %) and stirred at rt for 12 h. 2.0 g (10 mmol) 2,4-dichlorobenzoic acid were added and the mixture stirred for another 24 h at rt. The mixture was poured onto crushed ice, the precipitate filtered off and dried in vacuum.

Pale pink solid

Yield 2.912 g (91.9 %)

m.p. 179-188 °C (H_2SO_4)

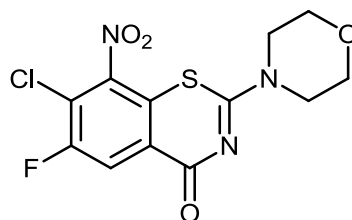
^1H NMR (400 MHz, $\text{DMSO-}d_6$) δ 13.71 (s, 1H, COOH), 8.26 (s, 1H, Ar-H), 7.84 (s, 1H, Ar-H)

MS (EI) 316 (M)

M 316.91 g/mol

$\text{C}_7\text{H}_3\text{Cl}_2\text{IO}_2$

7.5.33 7-chloro-6-fluoro-2-(morpholin-4-yl)-8-nitro-4H-1,3-benzothiazin-4-one (IR 69)^{np}



Synthesis of 2,4-dichloro-5-fluoro-3-nitrobenzoylchloride from 568 mg (2.40 mmol) 2,4-dichloro-5-fluoro-3-nitrobenzoic acid according to general procedure I.

234 mg (1.60 mmol) morpholine-4-carbothioamide (**IR 49**) were dissolved in 10 ml toluene and heated to 80 °C. 2,4-dichloro-5-fluoro-3-nitrobenzoylchloride was suspended in 5 ml toluene and added dropwise. After complete addition, the mixture was refluxed for 18 h. After cooling, the solvent was evaporated under reduced pressure and the crude product purified by flash chromatography (eluent TBME:ethanol 97.5:2.5 (V/V)).

Yellow solid

Yield 115 mg (20.7 %)

m.p. 222-226 °C (TBME:ethanol 95:5 (V/V))

¹H NMR (400 MHz, CDCl₃) δ 8.36 (d, 1H, Ar-H, ³J_{H,F} = 8.4 Hz), 3.82 (m, 4H, CH₂-N-CH₂), 3.73 (m, 4H, CH₂-O-CH₂)

MS (EI) 345 (M)

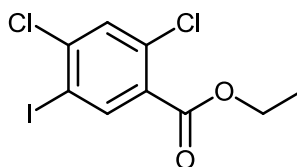
Elemental analysis	calc.	C 41.69	H 2.62	N 12.15	S 9.27
	found	C 41.43	H 2.54	N 11.67	S 8.99

R_f 0.56 (TBME:ethanol 20:1 (V/V)), R_f 0.18 (TBME)

M 345.73 g/mol

C₁₂H₉ClFN₃O₄S

7.5.34 ethyl 2,4-dichloro-5-iodobenzoate (IR 70)ⁿ



1.8 g (5.70 mmol) 2,4-dichloro-5-iodobenzoic acid (**IR 68**), 9 ml ethanol, and 364 μl (6.80 mmol) sulfuric acid (95-97 %) were dissolved in 41 ml toluene. The mixture was refluxed for 16 h in a Dean-Stark apparatus while dropwise adding 18 ml of ethanol. 1 ml of sulfuric acid (95-97 %) was added and the mixture refluxed for another 24 h. After cooling,

the mixture was washed with water, the organic layer separated, dried over MgSO_4 and evaporated under reduced pressure. The crude product was purified by flash chromatography (eluent hexane:EA 20:1 (V/V)).

Colorless oil with fruity smell

Yield 1.073 g (54.6 %)

^1H NMR (500 MHz, CDCl_3) δ 8.27 (s, 1H, Ar-H), 7.52 (s, 1H, Ar-H), 4.38 (q, 2H, O- CH_2 ,

$^3J = 7.2$ Hz), 1.39 (t, 3H, CH_3 , $^3J = 7.2$ Hz)

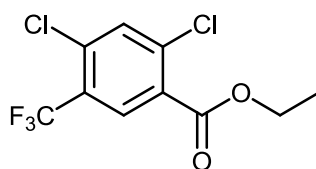
MS (EI) 344 (M)

R_f 0.33 (hexane:EA 20:1 (V/V))

M 344.96 g/mol

$\text{C}_9\text{H}_7\text{Cl}_2\text{IO}_2$

7.5.35 ethyl 2,4-dichloro-5-(trifluoromethyl)benzoate (IR 71)ⁿ



The complete reaction was conducted under argon atmosphere.

100 mg (0.52 mmol) cuprous iodide (CuI) were suspended in 40 ml DMF. 1.1 ml (8.60 mmol) methyl-2,2-difluoro-2-(fluorosulfonyl)acetate (MFSDA) and 1.816 g (5.20 mmol) ethyl 2,4-dichloro-5-iodobenzoate (**IR 70**), dissolved in 2 ml DMF, were added. The mixture was heated to 85 °C for 12 h. After cooling, the reaction mixture was added dropwise to a mixture of 48 ml hexane and 36 ml sat. NaHCO_3 solution (4:3 (V/V)). The hexane layer was separated. The aq. layer was extracted with hexane (3x), the combined hexane layers dried over MgSO_4 and the solvent removed under reduced pressure. The crude product was purified by flash chromatography (eluent hexane:EA 20:1 (V/V)).

Colorless oil with fruity smell which slowly crystallizes

Yield 1.252 g (83.3 %)

^1H NMR (400 MHz, CDCl_3) δ 8.17 (s, 1H, Ar-H), 7.62 (s, 1H, Ar-H), 4.42 (q, 2H, O- CH_2 ,

$^3J = 7.2$ Hz), 1.41 (t, 3H, CH_3 , $^3J = 7.2$ Hz)

^{13}C NMR (125 MHz, CDCl_3) δ 164.5, 139.2, 136.8, 134.5, 131.2 (q, $^3J_{\text{C,F}} = 5.5$ Hz), 129.6, 127.9 (q, $^2J_{\text{C,F}} = 32.7$ Hz), 122.8 (q, $^1J_{\text{C,F}} = 273.6$ Hz), 62.3, 14.2

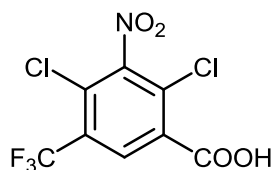
MS (GC-MS, EI) 10.3 min, 286 (M)

R_f 0.12 (heptane)

M 287.06 g/mol

$\text{C}_{10}\text{H}_7\text{Cl}_2\text{F}_3\text{O}_2$

7.5.36 2,4-dichloro-3-nitro-5-(trifluoromethyl)benzoic acid (IR 73)ⁿ



317 mg (1.30 mmol) ethyl 2,4-dichloro-5-(trifluoromethyl)benzoate (**IR 71**) were suspended in 7 ml sulfuric acid (100 %) and cooled to 0 °C. Keeping the temperature between 0-10 °C, 3 ml fuming nitric acid (100 %) were added dropwise. After complete addition, the mixture was carefully heated to 110 °C and stirred for 2 h. After cooling the mixture was poured onto 10 ml crushed ice and stirred for 30 min to release remaining nitrous gases. The resulting precipitate was filtered off, washed with a small amount of cold water and dried in vacuum.

White solid

Yield 322 mg (82.1 %)

m.p. 219-220 °C (water)

¹H NMR (400 MHz, CDCl₃) δ 8.45 (s, 1H, Ar-H)

¹³C NMR (125 MHz, CD₃OD) δ 163.3, 150.6, 131.8, 130.4 (q, ³J_{C,F} = 5.3 Hz), 129.5, 128.0 (q, ²J_{C,F} = 33.6 Hz), 126.8, 121.5 (q, ¹J_{C,F} = 273.5 Hz)

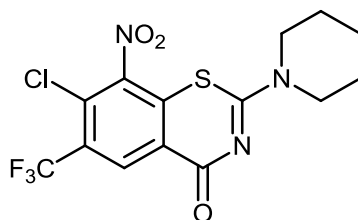
MS (EI) 303 (M)

Elemental analysis	calc.	C 31.61	H 0.66	N 4.61
	found	C 31.68	H 0.74	N 4.44

M 304.01 g/mol

C₈H₂Cl₂F₃NO₄

7.5.37 7-chloro-8-nitro-2-(piperidin-1-yl)-6-(trifluoromethyl)-4H-1,3-benzothiazin-4-one (IR 74)^{np}



Synthesis of 2,4-dichloro-3-nitro-5-(trifluoromethyl)benzoylchloride from 400 mg (1.31 mmol) 2,4-dichloro-3-nitro-5-(trifluoromethyl)benzoic acid (**IR 73**) according to general procedure I.

236 mg (1.64 mmol) piperidine-1-carbothioamide (**IR 50**) were dissolved in 50 ml toluene and heated to 80 °C until completely dissolved. 2,4-dichloro-3-nitro-5-(trifluoromethyl)-

benzoylchloride was dissolved in 10 ml toluene and added dropwise. After complete addition, the mixture was stirred at 80 °C for 1 h and then let cool to rt. The solvent was evaporated under reduced pressure to yield the crude product, which was purified by flash chromatography twice (eluent chloroform).

Yellow solid

Yield 347 mg (67.3 %)

m.p. 215-218 °C (chloroform)

^1H NMR (400 MHz, CDCl_3) δ 8.91 (s, 1H, Ar-H), 4.07 (bs, 2H, N- CH_2), 3.70 (bs, 2H, N- CH_2), 1.77 (m, 6H, $\text{CH}_2\text{-CH}_2\text{-CH}_2$)

^{13}C NMR (100 MHz, CDCl_3) δ 165.7, 158.3, 146.9, 131.4, 130.5 (q, $^3J_{\text{C,F}} = 5.3$ Hz), 128.7 (q, $^2J_{\text{C,F}} = 33.2$ Hz), 128.4, 122.8, 121.6 (q, $^1J_{\text{C,F}} = 274.3$ Hz), 48.2 (bs, 2 CH_2), 26.0 (bs, 2 CH_2), 24.2

MS (EI) 393 (M)

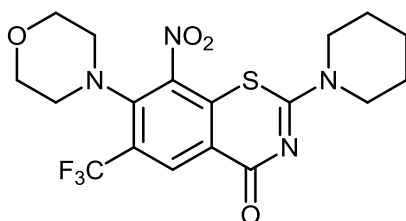
Elemental analysis	calc.	C 42.70	H 2.82	N 10.67	S 8.14
	found	C 43.04	H 2.69	N 10.70	S 7.71

R_f 0.40 (TBME:ethanol 20:1 (V/V))

M 393.77 g/mol

$\text{C}_{14}\text{H}_{11}\text{ClF}_3\text{N}_3\text{O}_3\text{S}$

7.5.38 7-(morpholin-4-yl)-8-nitro-2-(piperidin-1-yl)-6-(trifluoromethyl)-4H-1,3-benzothiazin-4-one (IR 75)^{mp}



The complete reaction was conducted under argon atmosphere.

29 mg ($7.62 \cdot 10^{-5}$ mol) 7-chloro-8-nitro-2-(piperidin-1-yl)-6-(trifluoromethyl)-4H-1,3-benzothiazin-4-one (IR 74) were dissolved in 10 ml DMF. 52 μl ($5.97 \cdot 10^{-4}$ mol) morpholine and 13 μl ($7.62 \cdot 10^{-5}$ mol) DIPEA were added and the mixture refluxed for 2.5 h. The solvent was evaporated under reduced pressure and the crude product purified by flash chromatography twice (eluent chloroform).

Bright yellow solid

Yield 16 mg (47.3 %)

m.p. 189-192 °C (chloroform)

^1H NMR (400 MHz, CDCl_3) δ 8.89 (s, 1H, Ar-H), 3.82 (m, 4H, $\text{CH}_2\text{-N-CH}_2$), 3.77 (m, 4H, $\text{CH}_2\text{-O-CH}_2$), 3.12 (m, 4H, $\text{CH}_2\text{-N-CH}_2$), 1.72 (m, 6H, $\text{CH}_2\text{-CH}_2\text{-CH}_2$)

^{13}C NMR (125 MHz, CDCl_3) δ 166.7, 159.3, 146.9, 145.6, 131.9 (q, $^3J_{\text{C,F}} = 5.8$ Hz), 131.4, 129.1 (q, $^2J_{\text{C,F}} = 30.7$ Hz), 122.7 (q, $^1J_{\text{C,F}} = 274.0$ Hz), 120.5, 66.9 (2 CH_2), 51.5 (2 CH_2), 48.1 (bs, 2 CH_2), 25.9 (bs, 2 CH_2), 24.3

MS (EI) 444 (M)

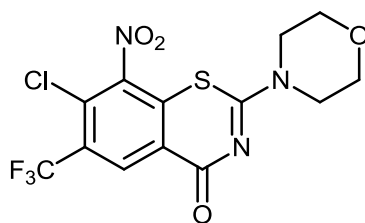
Elemental analysis	calc.	C 48.65	H 4.31	N 12.61	S 7.21
	found	C 48.54	H 2.15	N 12.03	S 6.56

R_f 0.19 (chloroform)

M 444.43 g/mol

$\text{C}_{18}\text{H}_{19}\text{F}_3\text{N}_4\text{O}_4\text{S}$

7.5.39 7-chloro-2-(morpholin-4-yl)-8-nitro-6-(trifluoromethyl)-4H-1,3-benzothiazin-4-one (IR 76)^{np}



Synthesis of 2,4-dichloro-3-nitro-5-(trifluoromethyl)benzoylchloride from 200 mg (0.66 mmol) 2,4-dichloro-3-nitro-5-(trifluoromethyl)benzoic acid (**IR 73**) according to general procedure I.

120 mg (0.82 mmol) morpholine-4-carbothioamide (**IR 49**) were dissolved in 38 ml toluene and heated to 55 °C until completely dissolved. 2,4-dichloro-3-nitro-5-(trifluoromethyl)benzoylchloride was dissolved in 10 ml toluene and added dropwise. After complete addition, the mixture was heated to 75-80 °C for 12 h. After cooling, the solvent was evaporated under reduced pressure to yield the crude product, which was purified by flash chromatography (eluent chloroform).

Yellow solid

Yield 156 mg (60.0 %)

m.p. 263-265 °C (chloroform)

^1H NMR (500 MHz, CDCl_3) δ 8.91 (s, 1H, Ar-H), 3.95 (m, 4H, $\text{CH}_2\text{-N-CH}_2$), 3.82 (m, 4H, $\text{CH}_2\text{-O-CH}_2$)

^{13}C NMR (125 MHz, CDCl_3) δ 165.5, 159.5, 146.8, 130.9, 130.6 (q, $^3J_{\text{C,F}} = 5.3$ Hz), 129.1 (q, $^2J_{\text{C,F}} = 33.6$ Hz), 128.8, 122.7, 121.5 (q, $^1J_{\text{C,F}} = 274.5$ Hz), 66.2 (bs, 2 CH_2), 47.0 (bs, 2 CH_2)

MS (EI) 395 (M)

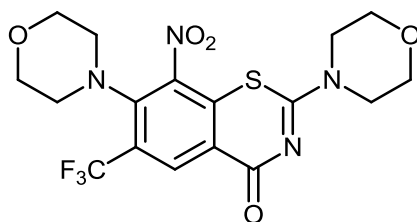
Elemental analysis	calc.	C 39.45	H 2.29	N 10.62	S 8.10
	found	C 39.56	H 2.03	N 10.52	S 7.93

R_f 0.39 (TBME:ethanol 20:1 (V/V))

M 395.74 g/mol

$C_{13}H_9ClF_3N_3O_4S$

7.5.40 2,7-bis(morpholin-4-yl)-8-nitro-6-(trifluoromethyl)-4H-1,3-benzothiazin-4-one (IR 77)^{np}



The complete reaction was conducted under argon atmosphere.

75 mg (0.19 mmol) 7-chloro-2-(morpholin-4-yl)-8-nitro-6-(trifluoromethyl)-4H-1,3-benzothiazin-4-one (IR 76) were dissolved in 30 ml DMF. 132 μ l (1.5 mmol) morpholine and 32 μ l (0.19 mmol) DIPEA were added and the mixture refluxed for 1.5 h. The solvent was evaporated under reduced pressure and the crude product purified by flash chromatograph three times (eluent chloroform).

Bright yellow solid

Yield 41.6 mg (49.2 %)

m.p. 249-251 °C (chloroform)

1H NMR (500 MHz, $CDCl_3$) δ 8.87 (s, 1H, Ar-H), 3.94 (m, 4H, CH_2 -N- CH_2), 3.78 (m, 4H,

CH_2 -O- CH_2), 3.75 (m, 4H, CH_2 -O- CH_2), 3.10 (m, 4H, CH_2 -N- CH_2)

^{13}C NMR (125 MHz, $CDCl_3$) δ 166.5, 160.4, 146.7, 146.0, 132.2 (q, $^3J_{C,F}$ = 5.8 Hz), 131.0, 129.4 (q, $^2J_{C,F}$ = 31.2 Hz), 122.6 (q, $^1J_{C,F}$ = 274.0 Hz), 120.3, 66.9 (2 CH_2), 66.3 (bs, 2 CH_2), 51.5 (2 CH_2), 46.8 (bs, 2 CH_2)

MS (EI) 446 (M)

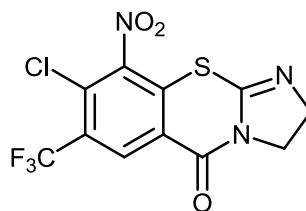
Elemental analysis	calc.	C 45.74	H 3.84	N 12.55	S 7.18
	found	C 45.67	H 3.86	N 11.83	S 7.21

R_f 0.08 (chloroform)

M 446.40 g/mol

$C_{17}H_{17}F_3N_4O_5S$

7.5.41 8-chloro-9-nitro-7-(trifluoromethyl)-2,3-dihydro-5H-imidazo[2,1-b][1,3]benzothiazin-5-one (IR 78)^{np}



Synthesis of 2,4-dichloro-3-nitro-5-(trifluoromethyl)benzoylchloride from 100 mg (0.33 mmol) 2,4-dichloro-3-nitro-5-(trifluoromethyl)benzoic acid (**IR 73**) according to general procedure I.

Under argon atmosphere, 51 mg (0.49 mmol) imidazolidine-2-thione (**IR 45**) were suspended in 15 ml toluene and heated to 40 °C. 2,4-dichloro-3-nitro-5-(trifluoromethyl)benzoylchloride was suspended in 5 ml toluene and 60 μ l (0.65 mmol) POCl₃ were added. This mixture was subsequently added dropwise to the pre-heated solution of imidazolidine-2-thione (**IR 45**). After complete addition, the reaction mixture was heated to 90 °C and stirred for 2 h. After cooling, the mixture was washed with water (2x) and sat. NaHCO₃ solution (1x). The organic layer was separated, dried over MgSO₄ and evaporated under reduced pressure. The crude product was purified by flash chromatography (eluent TBME).

Yellow solid

Yield 34 mg (29.6 %)

m.p. 157-166 °C (TBME)

¹H NMR (400 MHz, CDCl₃) δ 8.71 (s, 1H, Ar-H), 4.12 (m, 4H, CH₂-CH₂)

¹³C NMR (125 MHz, CDCl₃) δ 156.0, 148.9, 146.4, 131.7, 130.7, 130.0 (q, ³J_{C,F} = 5.3 Hz), 128.4 (q, ²J_{C,F} = 33.6 Hz), 124.1, 121.4 (q, ¹J_{C,F} = 274.5 Hz), 53.7, 44.9

MS (EI) 351 (M)

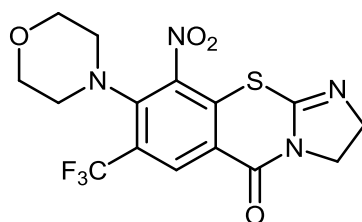
Elemental analysis	calc.	C 37.57	H 1.43	N 11.95	S 9.12
	found	C 37.35	H 1.52	N 11.31	S 8.61

R_f 0.27 (TBME)

M 351.69 g/mol

C₁₁H₅ClF₃N₃O₃S

7.5.42 8-(morpholin-4-yl)-9-nitro-7-(trifluoromethyl)-2,3-dihydro-5H-imidazo[2,1-b][1,3]benzothiazin-5-one (IR 79)^{np}



23 mg ($6.54 \cdot 10^{-5}$ mol) 8-chloro-9-nitro-7-(trifluoromethyl)-2,3-dihydro-5H-imidazo[2,1-b][1,3]benzothiazin-5-one (**IR 78**) were dissolved in 15 ml DMF. 40 μ l (0.46 mmol) morpholine and 11 μ l ($6.54 \cdot 10^{-5}$ mol) DIPEA were added and the mixture stirred at rt for 2.5 h. The solvent was evaporated under reduced pressure and the crude product purified by flash chromatography (eluent TBME).

Orange solid

Yield 14 mg (53.2 %)

m.p. 167-182 °C (TBME)

^1H NMR (400 MHz, acetone- d_6) δ 8.51 (s, 1H, Ar-H), 3.96 (m, 4H, $\text{CH}_2\text{-CH}_2$), 3.63 (m, 4H, $\text{CH}_2\text{-O-CH}_2$), 3.02 (m, 4H, $\text{CH}_2\text{-N-CH}_2$)

MS (EI) 402 (M)

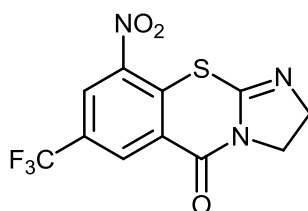
HR MS m/z 403.0679 $[\text{M}+\text{H}]^+$, calc. for $[\text{C}_{15}\text{H}_{14}\text{F}_3\text{N}_4\text{O}_4\text{S}]^+$ 403.0682

R_f 0.33 (TBME)

M 402.35 g/mol

$\text{C}_{15}\text{H}_{13}\text{F}_3\text{N}_4\text{O}_4\text{S}$

7.5.43 9-nitro-7-(trifluoromethyl)-2,3-dihydro-5H-imidazo[2,1-b][1,3]benzo-thiazin-5-one (IR 80)^{np}



Synthesis in dry pyridine

Synthesis of 2-chloro-3-nitro-5-(trifluoromethyl)benzoylchloride (**IR 06**) from 300 mg (1.10 mmol) 2-chloro-3-nitro-5-(trifluoromethyl)benzoic acid (**IR 05**) according to general procedure I.

Under argon atmosphere, 84 mg (0.83 mmol) imidazolidine-2-thione (**IR 45**) were suspended in 10 ml dry pyridine at 0-5 °C. **IR 06**, dissolved in 1 ml toluene, was added dropwise, keeping the temperature between 0-10 °C. Upon complete addition, the mixture was stirred for 4 h at 10-20 °C, subsequently heated to 60 °C for 50 min. After cooling, 50 ml water were added. The mixture was extracted with chloroform, the organic layer washed with water, dried over MgSO₄ and evaporated to yield a brown residue which slowly crystallizes. The residue was washed with 100 ml water and filtered to give a bright yellow solid as crude product, which was purified by flash chromatography (eluent chloroform). Yield 43 mg (12.3 %).

Synthesis with POCl₃

Synthesis of 2-chloro-3-nitro-5-(trifluoromethyl)benzoylchloride (**IR 06**) from 100 mg (0.37 mmol) 2-chloro-3-nitro-5-(trifluoromethyl)benzoic acid (**IR 05**) according to general procedure I.

Under argon atmosphere, 57 mg (0.56 mmol) imidazolidine-2-thione (**IR 45**) were dissolved in 10 ml of toluene and heated to 40 °C. **IR 06** and 68 µl (0.74 mmol) POCl₃ were dissolved in 5 ml toluene and added dropwise. The mixture was stirred at 40 °C for 30 min and then heated to 90 °C for 12 h. After cooling, the mixture was washed with sat. NaHCO₃ solution (2x), the organic layer separated, dried over MgSO₄ and evaporated under reduced pressure. The crude product was purified by flash chromatography (eluent TBME). Yield 54 mg (46.0%).

Yellow needles

m.p. 159-166 °C (chloroform), m.p. 165-173 °C (TBME)

¹H NMR (400 MHz, acetone-*d*₆) δ 8.75 (d, 1H, Ar-H, ⁴*J* = 2.2 Hz), 8.70 (d, 1H, Ar-H, ⁴*J* = 2.2 Hz), 3.96 (m, 4H, CH₂-CH₂)

¹³C NMR (125 MHz, CDCl₃) δ 156.4, 151.3, 143.6, 135.9, 132.8 (q, ³*J*_{C,F} = 3.8 Hz), 129.2 (q, ²*J*_{C,F} = 35.5 Hz), 128.0, 127.5 (q, ³*J*_{C,F} = 3.8 Hz), 122.2 (q, ¹*J*_{C,F} = 272.6 Hz), 53.7, 44.9

MS (EI) 317 (M)

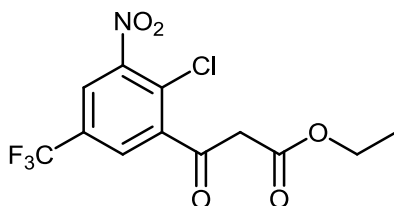
Elemental analysis	calc.	C 41.65	H 1.19	N 13.25	S 10.11
	found	C 42.01	H 1.81	N 13.17	S 10.20

*R*_f 0.43 (chloroform:methanol 98:2 (V/V)), *R*_f 0.27 (TBME)

M 317.24 g/mol

C₁₁H₆F₃N₃O₃S

7.5.44 ethyl 3-[2-chloro-3-nitro-5-(trifluoromethyl)phenyl]-3-oxopropanoate (IR 81)



Synthesis of 2-chloro-3-nitro-5-(trifluoromethyl)benzoylchloride (**IR 06**) from 200 mg (0.74 mmol) 2-chloro-3-nitro-5-(trifluoromethyl)benzoic acid (**IR 05**) according to general procedure I.

Under argon atmosphere, 196 mg (1.48 mmol) malonic acid monoethyl ester and catalytic amounts (tip of a spatula) of biquinoline were dissolved in 3.5 ml THF and cooled to -50 °C. A solution of *n*-BuLi (2.5 M in hexane, approx. 1.5 ml) was added slowly, until a pink/brown color remained at -5 °C. Subsequently, the mixture was cooled to -87 °C and **IR 06**, dissolved in 1.3 ml THF, added dropwise. The color of the mixture changed to brown. After adjusting to rt, 2 ml 1 M HCl were added to the mixture, upon which a phase separation of a bright orange upper phase and colorless bottom phase was visible. After extraction with EE (3x), drying over MgSO₄ and evaporation of the combined organic layers, the crude product was purified by flash chromatography (eluent hexane:toluene, gradient 30-100 % (V/V) toluene).

Yellow oil

Yield 51 mg (20.1 %)

¹H NMR (400 MHz, CDCl₃) δ 12.52 (s, 1H, enol OH), 8.03 (d, 1H, Ar-H, ⁴J = 2.2 Hz), 7.97 (d, 1H, Ar-H, ⁴J = 2.2 Hz), 5.54 (s, 1H, enol CH), 4.30 (q, 2H, O-CH₂, ³J = 7.1 Hz), 1.34 (t, 3H, CH₃, ³J = 7.1 Hz)

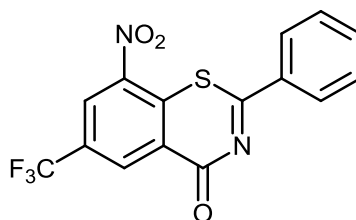
MS (EI) 339 (M)

R_f 0.40 (toluene), R_f 0.18 (hexane:toluene 1:1 (V/V))

M 339.65 g/mol

C₁₂H₉ClF₃NO₅

7.5.45 8-nitro-2-phenyl-6-(trifluoromethyl)-4*H*-1,3-benzothiazin-4-one (IR 82)^{np}



Synthesis of 2-chloro-3-nitro-5-(trifluoromethyl)benzoylchloride (**IR 06**) from 200 mg (0.74 mmol) 2-chloro-3-nitro-5-(trifluoromethyl)benzoic acid (**IR 05**) according to general procedure I.

IR 06 was dissolved in 2 ml toluene and added to a solution of 76 mg (0.56 mmol) thiobenzamide in 20 ml toluene at rt. The mixture was heated to reflux for 5 h. The solvent was evaporated under reduced pressure and the crude product purified by flash chromatography (eluent chloroform).

Yellow solid

Yield 84 mg (32.1 %)

m.p. 180-184 °C (chloroform)

¹H NMR (400 MHz, CDCl₃) δ 9.15 (d, 1H, Ar-H, ⁴J = 2.0 Hz), 8.91 (d, 1H, Ar-H, ⁴J = 2.0 Hz), 8.29 (m, 1H, Ar-H), 7.72 (m, 1H, Ar-H), 7.60 (m, 2H, Ar-H)

¹³C NMR (100 MHz, CDCl₃) δ 175.3, 167.1, 144.0, 136.1, 135.8, 134.8, 134.1 (q, ³J_{C,F} = 3.4 Hz), 131.2 (q, ²J_{C,F} = 35.9 Hz), 129.4 (2 CH), 128.3 (2 CH), 126.8 (q, ³J_{C,F} = 3.4 Hz), 125.8, 122.2 (q, ¹J_{C,F} = 273.5 Hz)

MS (EI) 352 (M)

Elemental analysis	calc.	C 51.14	H 2.00	N 7.95	S 9.10
	found	C 51.19	H 1.89	N 7.88	S 9.91

R_f 0.55 (chloroform)

M 352.29 g/mol

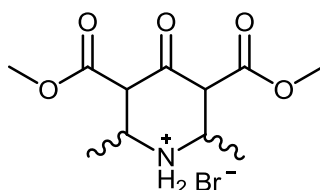
C₁₅H₇F₃N₂O₃S

7.5.46 2,6-dimethylpiperidin-4-one (IR 83)



2.2 ml (15 mmol) acetone-1,3-dicarboxylic acid methyl ester and 1.7 ml (30 mmol) acetaldehyde were mixed in a 50 ml flask at 0 °C. 1.48 g (15 mmol) NH_4Br were dissolved in 10 ml of a mixture of methanol: H_2O 1:1 (V/V) and added dropwise over a period of 30 min. The mixture was stirred at rt for 3 d. Subsequently, the solvent was almost completely removed under reduced pressure to yield a white-yellow suspension, which was covered with 15 ml EA and set aside at rt for 12 h in a small flask (15-20 ml). The resulting precipitate was filtered off, washed with chloroform and EA and dried in vacuum to yield the intermediate 3,5-bis(methoxycarbonyl)-2,6-dimethyl-4-oxopiperidin-1-ium bromide (**IR 130**). The filtrate was again concentrated under reduced pressure, but not until dryness, covered with 15 ml EA and set aside again to yield a second batch of intermediate **IR 130**.

Intermediate: 3,5-bis(methoxycarbonyl)-2,6-dimethyl-4-oxopiperidin-1-ium bromide (IR 130):



White solid

Yield 1.9 g (39.1 %)

m.p. 173-177 °C, decomposition (chloroform) (lit. 175 °C, decomposition)¹⁰⁴

¹H NMR (400 MHz, D_2O) δ 3.75 (m, 2H, $\text{CH}-\text{C}(=\text{O})-\text{CH}$), 3.73 (s, 6H, 2 $\text{O}-\text{CH}_3$), 3.67 (m, 2H, 2x $\text{CH}-\text{CH}_3$), 1.24 (d, 6H, 2x CH_3 , $^3J = 6.6$ Hz)

MS (ESI) m/z 244.0 $[\text{M}+\text{H}]^+$ (free base)

M 243.26 g/mol (free base), M 324.17 g/mol (hydrobromide)

$\text{C}_{11}\text{H}_{17}\text{NO}_5$ (free base), $\text{C}_{11}\text{H}_{18}\text{BrNO}_5$ (hydrobromide)

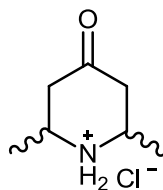
Hydrolysis and decarboxylation

1.9 g **IR 130** was mixed with 3.5 ml conc. HCl and heated to 70 °C for 18 h. Remaining HCl was removed under reduced pressure to yield the hydrochloride salt of 2,6-dimethylpiperidin-4-one (**IR 83xHCl**) as a white solid product.

In some cases, precipitation of the hydrochloride salt of **IR 83** did not occur after removal of the excess HCl. Product purification was then achieved by dissolving the residue in aq. NH_3 and extraction with chloroform. The combined organic layers were concentrated under

reduced pressure and purified via flash chromatography (eluent TBME plus few drops NH_3) to afford the free base **IR 83**.

2,6-dimethyl-4-oxopiperidin-1-ium chloride (IR 83xHCl):



Pale yellow solid

Yield 0.9 g (36.7 %, in relation to starting materials acetaldehyde, NH_4Br and acetone-1,3-dicarboxylic acid methyl ester)

m.p. 220-230 °C (lit. 227-229 °C)¹⁰³

^1H NMR (*only cis isomer*) (400 MHz, CDCl_3) δ 2.93 (m, 2H, 2 $\text{CH}-\text{CH}_3$), 2.26 (dd, 2H, $\text{CH}_2-\text{C}(=\text{O})-\text{CH}_2$, $^2J = 13.5$ Hz, $^3J = 2.2$ Hz), 1.98 (dd, 2H, $\text{CH}_2-\text{C}(=\text{O})-\text{CH}_2$, $^2J = 13.3$ Hz, $^3J = 12.5$ Hz), 1.14 (d, 6H, 2 CH_3 , $^3J = 6.3$ Hz)

^1H NMR (*mixture cis and trans isomer, ratio approx. 4:1, determined by NMR integrals*) (400 MHz, CDCl_3) δ 3.48 (m, 2H, 2 $\text{CH}-\text{CH}_3$, *trans*), 2.93 (m, 2H, 2 $\text{CH}-\text{CH}_3$, *cis*), 2.42 (ddd, 2H, $\text{CH}_2-\text{C}(=\text{O})-\text{CH}_2$, $^2J = 13.7$ Hz, $^3J = 4.9$ Hz, $^3J = 1.5$ Hz, *trans*), 2.26 (dd, 2H, $\text{CH}_2-\text{C}(=\text{O})-\text{CH}_2$, $^2J = 13.5$ Hz, $^3J = 2.2$ Hz, *cis*), 2.08 (ddd, 2H, $\text{CH}_2-\text{C}(=\text{O})-\text{CH}_2$, $^2J = 13.8$ Hz, $^3J = 6.7$ Hz, $^3J = 1.5$ Hz, *trans*), 1.98 (dd, 2H, $\text{CH}_2-\text{C}(=\text{O})-\text{CH}_2$, $^2J = 13.3$ Hz, $^3J = 12.5$ Hz, *cis*), 1.14 (d, 6H, 2 CH_3 , $^3J = 6.3$ Hz, *cis*), 1.12 (d, 6H, 2 CH_3 , $^3J = 6.6$ Hz, *trans*)

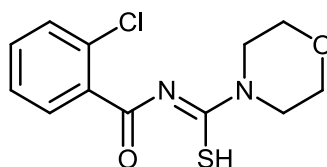
MS (ESI) m/z 128.1 $[\text{M}+\text{H}]^+$ (free base)

R_f 0.29 (TBME plus few drops NH_3)

M 127.18 g/mol (free base), M 163.65 g/mol (hydrochloride)

$\text{C}_7\text{H}_{13}\text{NO}$ (free base), $\text{C}_7\text{H}_{14}\text{ClNO}$ (hydrochloride)

7.5.47 N-[(2-chlorophenyl)carbonyl]morpholine-4-carboimidiothioic acid (IR 84)



Synthesis of 2-chlorobenzoylchloride according to general procedure I from 2.00 g (13 mmol) 2-chlorobenzoic acid.

The next 2 steps were conducted under argon atmosphere.

The 2-chlorobenzoylchloride was dissolved in 10 ml acetone and added dropwise to a solution of 1.26 g (13 mmol) KSCN in acetone at rt. After complete addition, the mixture was

heated to 40 °C for 5 min. After cooling to rt, 1.0 ml (13 mmol) morpholine, dissolved in 10 ml acetone, were added dropwise. The mixture was stirred for another 30 min at rt, heated to reflux for 2 min and subsequently the solvent was evaporated under reduced pressure to yield the crude product, which was purified by MPLC (Büchi MPLC, eluent chloroform, flow rate 30 ml/min) and flash chromatography (eluent toluene:ethanol 98.5:1.5 (V/V)). The fractions containing the product were combined, the solvent evaporated and the crude product recrystallized from toluene.

White solid

Yield 438 mg (11.9 %)

m.p. 176 °C (toluene)

¹H NMR (400 MHz, CDCl₃) δ 7.68 (d, 1H, Ar-H, ³J = 7.4 Hz), 7.41 (m, 3H, Ar-H), 4.24 – 3.78 (m, 8H, morpholine)

MS (EI) 284 (M)

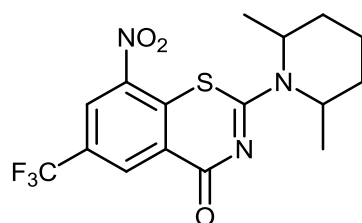
Elemental analysis	calc.	C 50.61	H 4.60	N 9.84	S 11.26
	found	C 50.24	H 4.47	N 9.43	S 11.36

R_f 0.38 (toluene:ethanol 9:1 (V/V))

M 284.76 g/mol

C₁₂H₁₃N₂O₂S

7.5.48 2-(2,6-dimethylpiperidin-1-yl)-8-nitro-6-(trifluoromethyl)-4H-1,3-benzothiazin-4-one (IR 85)^{np}



method A (classic pathway)

Synthesis of 2-chloro-3-nitro-5-(trifluoromethyl)benzoylchloride (**IR 06**) from 250 mg (0.93 mmol) 2-chloro-3-nitro-5-(trifluoromethyl)benzoic acid (**IR 05**) according to general procedure I.

The next 2 steps were conducted under argon atmosphere.

IR 06 was dissolved in 6 ml acetone and added dropwise to a solution of 90 mg (0.93 mmol) KSCN in 6 ml acetone at rt. After complete addition, the mixture was heated to 40 °C for 5 min and then let cool again to rt. 125 μl (0.93 mmol) 2,6-dimethylpiperidine were dissolved in 6 ml acetone and added dropwise. The mixture was stirred for another 30 min, then heated to reflux for 2 min. After cooling the solvent was evaporated under reduced pressure and the crude product was pre-purified by flash chromatography (eluent chloroform). The

fractions containing product were combined, the solvent evaporated and the residue recrystallized from hexane. Yield 52 mg (14.6 %).

adapted method A (classic pathway, adjusted temperature)

Synthesis according to general procedure III, starting from 200 mg (0.74 mmol) 2-chloro-3-nitro-5-(trifluoromethyl)benzoic acid (**IR 05**).

Purification of crude product was achieved by flash chromatography twice (eluent DCM and chloroform:hexane 1:1 (V/V)). The fractions containing product were combined, the organic solvent evaporated and the residue recrystallized from hexane. Yield 98 mg (34.1 %).

method E (thiourea pathway)

Synthesis of 2-chloro-3-nitro-5-(trifluoromethyl)benzoylchloride (**IR 06**) from 50 mg (0.18 mmol) 2-chloro-3-nitro-5-(trifluoromethyl)benzoic acid (**IR 05**) according to general procedure I.

IR 06 was dissolved in 2 ml toluene and added dropwise to a preheated solution of 40 mg (0.23 mmol) 2,6-dimethylpiperidine-1-carbothioamide (**IR 118**) at 70 °C. The mixture was refluxed for 2 h, the solvent evaporated and the crude product purified by flash chromatography (eluent TBME). Yield 17 mg (23.7 %).

Yellow solid

m.p. 133-135 °C (hexane)

¹H NMR (500 MHz, CDCl₃) δ 9.11 (d, 1H, Ar-H, ⁴J = 2.2 Hz), 8.74 (d, 1H, Ar-H, ⁴J = 2.2 Hz), 5.50 (bs, 1H, N-CH-CH₃), 4.61 (bs, 1H, N-CH-CH₃), 1.95 (m, 1H, CH₂-CH₂-CH₂), 1.78 (m, 4H, CH₂-CH₂-CH₂), 1.65 (m, 1H, CH₂-CH₂-CH₂), 1.42 (m, 6H, 2 CH₃)

¹³C NMR (100 MHz, CDCl₃) δ 166.2, 161.9, 144.0, 134.7, 133.2 (q, ³J_{C,F} = 3.5 Hz), 129.4 (q, ²J_{C,F} = 35.4 Hz), 126.9, 125.8 (q, ³J_{C,F} = 3.5 Hz), 122.4 (q, ¹J_{C,F} = 273.3 Hz), 50.0, 49.1, 30.5, 29.8, 20.5, 19.9, 14.1

MS (ESI) *m/z* 388.20 [M+H]⁺

MS (EI) 387 (M)

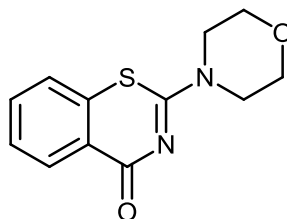
Elemental analysis	calc.	C 49.61	H 4.16	N 10.85	S 8.28
	found	C 49.99	H 3.99	N 10.84	S 7.76

R_f 0.48 (toluene:ethanol 9:1 (V/V)), *R_f* 0.50 (TBME), *R_f* 0.08 (DCM)

M 387.38 g/mol

C₁₆H₁₆F₃N₃O₃S

7.5.49 2-(morpholin-4-yl)-4*H*-1,3-benzothiazin-4-one (IR 86)



The complete reaction was conducted under argon atmosphere.

350 mg (1.23 mmol) N-[(2-chlorophenyl)carbonyl]morpholine-4-carboimidothioic acid (**IR 84**) were suspended in 10 ml DMF and the mixture cooled to 0 °C. 94 mg NaH (60 % w/w dispersion on mineral oil, equivalent to 56 mg NaH, 2.35 mmol) were added and the mixture heated to 70-80 °C for 11 days. The mixture was cooled to rt, carefully poured onto 50 ml crushed ice and extracted with chloroform. The combined organic layers were dried over MgSO₄ and concentrated under reduced pressure. The crude product was purified by flash chromatography twice (eluent chloroform).

Pale yellow solid

Yield 14 mg (4.6 %)

m.p. 160-165 °C (chloroform) (lit. 186-187 °C, ACN)¹⁶⁹

¹H NMR (400 MHz, CDCl₃) δ 8.39 (dd, 1H, Ar-H, ³J = 7.8 Hz, ⁴J = 1.4 Hz), 7.50 (dt, 1H, Ar-H, ³J = 7.4 Hz, ³J = 7.8 Hz, ⁴J = 1.6 Hz, ⁴J = 1.4 Hz), 7.42 (dt, 1H, Ar-H, ³J = 7.4 Hz, ³J = 7.8 Hz, ⁴J = 1.2 Hz, ⁴J = 1.4 Hz), 7.31 (dd, 1H, Ar-H, ³J = 7.8 Hz, ⁴J = 1.2 Hz), 3.88 (m, 4H, CH₂-O-CH₂), 3.74 (m, 4H, CH₂-N-CH₂)

¹³C NMR (100 MHz, CDCl₃) δ 169.2, 162.7, 132.1, 132.0, 130.5, 128.3, 125.5, 122.9, 66.3 (2 CH₂), 46.2 (2 CH₂)

MS (EI) 248 (M)

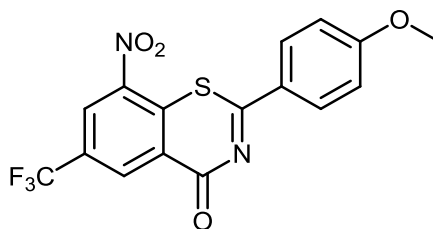
Elemental analysis	calc.	C 58.05	H 4.87	N 11.28	S 12.91
	found	C 57.91	H 5.02	N 10.81	S 11.88

R_f 0.20 (toluene:ethanol 9:1 (V/V))

M 248.30 g/mol

C₁₂H₁₂N₂O₂S

7.5.50 2-(4-methoxyphenyl)-8-nitro-6-(trifluoromethyl)-4H-1,3-benzothiazin-4-one (IR 87)^{np}



Synthesis of 2-chloro-3-nitro-5-(trifluoromethyl)benzoylchloride (**IR 06**) from 200 mg (0.74 mmol) 2-chloro-3-nitro-5-(trifluoromethyl)benzoic acid (**IR 05**) according to general procedure I.

IR 06 was dissolved in 2 ml toluene and added to a solution of 93 mg (0.56 mmol) 4-methoxy-thiobenzamide in 20 ml toluene. The mixture was heated to reflux for 1 h. After cooling and evaporation of the solvent, the crude product was purified by flash chromatography twice (eluent chloroform).

Pale yellow solid

Yield 39 mg (13.6 %)

m.p. 244-245 °C (chloroform)

¹H NMR (400 MHz, CDCl₃) δ 9.05 (d, 1H, Ar-H, ⁴J = 1.6 Hz), 8.81 (d, 1H, Ar-H, ⁴J = 1.6 Hz), 8.24 (d, 2H, Ar-H, ³J = 9.0 Hz), 7.00 (d, 2H, Ar-H, ³J = 9.0 Hz), 3.87 (s, 3H, OCH₃)

MS (EI) 382 (M)

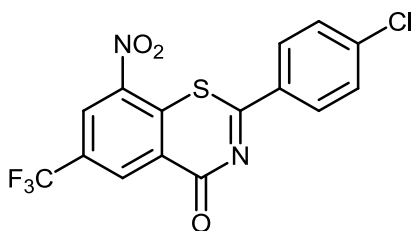
Elemental analysis	calc.	C 50.27	H 2.37	N 7.33	S 8.39
	found	C 50.14	H 2.37	N 6.94	S 7.58

R_f 0.37 (chloroform)

M 382.31 g/mol

C₁₆H₉F₃N₂O₄S

7.5.51 2-(4-chlorophenyl)-8-nitro-6-(trifluoromethyl)-4*H*-1,3-benzothiazin-4-one (IR 88)^{np}



Synthesis of 2-chloro-3-nitro-5-(trifluoromethyl)benzoylchloride (**IR 06**) from 500 mg (1.85 mmol) 2-chloro-3-nitro-5-(trifluoromethyl)benzoic acid (**IR 05**) according to general procedure I.

IR 06 was dissolved in 10 ml toluene and added to a solution of 318 mg (1.85 mmol) 4-chloro-thiobenzamide in 40 ml toluene. The mixture was heated to reflux for 1.5 h and stirred for another 12 h at rt. After evaporation of the solvent, the crude product was purified by flash chromatography three times (eluent chloroform).

Pale yellow needles

Yield 155 mg (21.7 %)

m.p. 220-221 °C (chloroform)

¹H NMR (400 MHz, CDCl₃) δ 9.11 (d, 1H, Ar-H, ⁴J = 2.2 Hz), 8.89 (d, 1H, Ar-H, ⁴J = 2.2 Hz), 8.22 (d, 2H, Ar-H, ³J = 8.9 Hz), 7.55 (d, 2H, Ar-H, ³J = 8.8 Hz)

¹³C NMR (100 MHz, CDCl₃) δ 174.0, 167.0, 144.0, 141.7, 135.7, 134.1, 134.1 (q, ³J_{C,F} = 3.5 Hz), 131.4 (q, ²J_{C,F} = 35.8 Hz), 129.8 (2 CH), 129.5 (2 CH), 126.8 (q, ³J_{C,F} = 3.5 Hz), 125.8, 122.2 (q, ¹J_{C,F} = 273.6 Hz)

MS (EI) 386 (M)

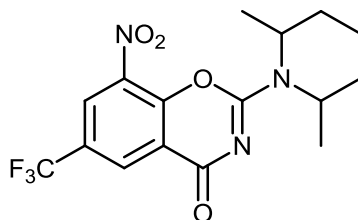
Elemental analysis	calc.	C 46.59	H 1.56	N 7.24	S 8.29
	found	C 47.05	H 1.60	N 7.13	S 8.04

R_f 0.46 (chloroform)

M 386.73 g/mol

C₁₅H₆ClF₃N₂O₃S

7.5.52 2-(2,6-dimethylpiperidin-1-yl)-8-nitro-6-(trifluoromethyl)-4H-1,3-benzoxazin-4-one (IR 95)^{np}



method A (classic pathway)

Synthesis of 2-chloro-3-nitro-5-(trifluoromethyl)benzoylchloride (**IR 06**) according to general procedure I from 500 mg (1.80 mmol) 2-chloro-3-nitro-5-(trifluoromethyl)benzoic acid (**IR 05**).

The next 2 steps were conducted under argon atmosphere.

IR 06 was dissolved in 10 ml acetone and added dropwise to a solution of 150 mg (1.80 mmol) KOCN in 10 ml acetone at rt. After complete addition, the mixture was heated to 40 °C for 5 min and then let cool again to rt. 250 μ l (1.80 mmol) 2,6-dimethylpiperidine were dissolved in 10 ml acetone and added dropwise. The mixture was stirred for another 30 min, then heated to reflux for 2 min. After cooling the solvent was evaporated under reduced pressure and the crude product was purified by flash chromatography five times (eluent 3x chloroform, 1x toluene:ethanol 99:1 (V/V), 1x hexane:EA 3:1 (V/V)). Yield 43.7 mg (6.5 %).

adapted method A (classic pathway, adjusted temperature)

Synthesis of 2-chloro-3-nitro-5-(trifluoromethyl)benzoylchloride (**IR 06**) according to general procedure I from 500 mg (1.80 mmol) 2-chloro-3-nitro-5-(trifluoromethyl)benzoic acid (**IR 05**).

The next 2 steps were conducted under argon atmosphere.

IR 06 was dissolved in 10 ml acetone and added dropwise to a solution of 150 mg (1.80 mmol) KOCN in 10 ml acetone at 5-10 °C. After complete addition, the mixture was stirred for 2 h at 5 °C. 306 μ l (1.80 mmol) DIPEA were added, 250 μ l (1.80 mmol) 2,6-dimethylpiperidine were dissolved in 10 ml acetone and added dropwise keeping the temperature between 5-10 °C. The mixture was stirred for another 2 h at 5-10 °C, subsequently warmed to rt and stirred for another 9 d, until TLC showed no further turnover of starting materials. The solvent was evaporated under reduced pressure and the crude product was purified by flash chromatography twice (eluent chloroform:hexane 2:1 (V/V)). Yield 100 mg (15.0 %).

Pale yellow solid

m.p. 120-123 °C (chloroform)

^1H NMR (400 MHz, CDCl_3) δ 8.72 (d, 1H, Ar-H, $^4J = 2.2$ Hz), 8.55 (d, 1H, Ar-H, $^4J = 2.3$ Hz), 4.97 (bs, 1H, N-CH-CH₃), 4.80 (bs, 1H, N-CH-CH₃), 1.89 (m, 1H, CH₂-CH₂-CH₂), 1.75 (m, 4H, CH₂-CH₂-CH₂), 1.60 (m, 1H, CH₂-CH₂-CH₂), 1.39 (m, 6H, 2 CH₃)

^{13}C NMR (125 MHz, CDCl_3) δ 163.2, 155.5, 148.9, 136.3, 131.0 (q, $^3J_{\text{C,F}} = 3.4$ Hz), 127.3 (q, $^2J_{\text{C,F}} = 35.5$ Hz), 126.8 (q, $^3J_{\text{C,F}} = 3.4$ Hz), 122.3 (q, $^1J_{\text{C,F}} = 273.5$ Hz), 120.5, 48.4, 48.2, 30.0, 29.6, 21.1, 19.9, 13.4

MS (EI) 371 (M)

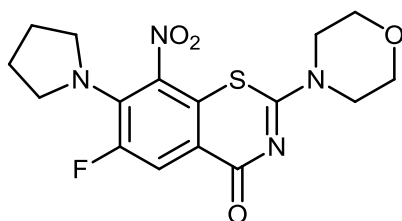
Elemental analysis	calc.	C 51.75	H 4.34	N 11.32
	found	C 51.78	H 4.08	N 11.11

R_f 0.44 (chloroform), R_f 0.13 (chloroform:hexane 2:1 (V/V))

M 371.31 g/mol

$\text{C}_{16}\text{H}_{16}\text{F}_3\text{N}_3\text{O}_4$

7.5.53 6-fluoro-2-(morpholin-4-yl)-8-nitro-7-(pyrrolidin-1-yl)-4H-1,3-benzothiazin-4-one (IR 96)^{np}



37 μl (0.45 mmol) pyrrolidine were added to a solution of 24 mg ($6.94 \cdot 10^{-5}$ mol) 7-chloro-6-fluoro-2-(morpholin-4-yl)-8-nitro-4H-1,3-benzothiazin-4-one (**IR 69**) in 5 ml DMF and stirred at rt for 1 h. After removal of the solvent under reduced pressure, the crude product was purified by flash chromatography (eluent TBME:ethanol 97.5:2.5 (V/V)).

Orange solid

Yield 15.1 mg (57.3 %)

m.p. 231-236 °C (TBME)

^1H NMR (400 MHz, CDCl_3) δ 8.15 (d, 1H, Ar-H, $^3J_{\text{H,F}} = 15.1$ Hz), 3.90 (m, 4H, CH₂-N-CH₂), 3.76 (m, 4H, CH₂-O-CH₂), 3.50 (m, 4H, CH₂-N-CH₂), 1.96 (m, 4H, CH₂-CH₂)

MS (EI) 380 (M)

HR MS m/z 381.1024 $[\text{M}+\text{H}]^+$, calc. for $[\text{C}_{16}\text{H}_{18}\text{FN}_4\text{O}_4\text{S}]^+$ 381.1027

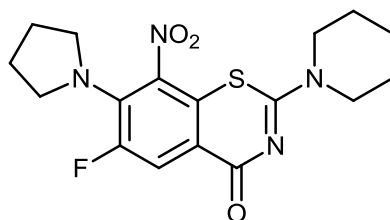
Elemental analysis	calc.	C 50.52	H 4.50	N 14.73	S 8.43
	found	C 49.80	H 4.38	N 13.27	S 7.99

R_f 0.44 (TBME:ethanol 97.5:2.5 (V/V))

M 380.39 g/mol

$\text{C}_{16}\text{H}_{17}\text{FN}_4\text{O}_4\text{S}$

7.5.54 6-fluoro-8-nitro-2-(piperidin-1-yl)-7-(pyrrolidin-1-yl)-4*H*-1,3-benzothiazin-4-one (IR 97)^{np}



38 μ l (0.46 mmol) pyrrolidine were added to a solution of 23 mg ($6.69 \cdot 10^{-5}$ mol) 7-chloro-6-fluoro-2-(piperidin-1-yl)-8-nitro-4*H*-1,3-benzothiazin-4-one (**IR 62**) in 8 ml DMF and stirred at rt for 1 h. After removal of the solvent under reduced pressure, the crude product was purified by flash chromatography (eluent TBME).

Orange needles

Yield 11.3 mg (44.6 %)

m.p. 173-180 °C (TBME)

^1H NMR (400 MHz, CDCl_3) δ 8.17 (d, 1H, Ar-H, $^3J_{\text{H,F}} = 15.2$ Hz), 3.87 (m, 4H, $\text{CH}_2\text{-N-CH}_2$), 3.51 (m, 4H, $\text{CH}_2\text{-N-CH}_2$), 1.98 (m, 4H, $\text{CH}_2\text{-CH}_2$), 1.72 (m, 6H, $\text{CH}_2\text{-CH}_2\text{-CH}_2$)

MS (EI) 378 (M)

HR MS m/z 379.1232 $[\text{M}+\text{H}]^+$, calc. for $[\text{C}_{18}\text{H}_{20}\text{FN}_4\text{O}_3\text{S}]^+$ 379.1235

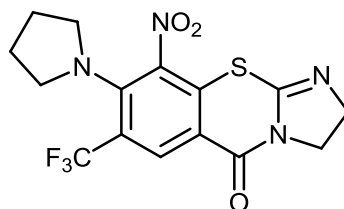
Elemental analysis	calc.	C 53.96	H 5.06	N 14.81	S 8.47
	found	C 54.00	H 4.80	N 14.22	S 8.38

R_f 0.19 (TBME)

M 378.42 g/mol

$\text{C}_{17}\text{H}_{19}\text{FN}_4\text{O}_3\text{S}$

7.5.55 9-nitro-8-(pyrrolidin-1-yl)-7-(trifluoromethyl)-2,3-dihydro-5*H*-imidazo[2,1-*b*][1,3]benzothiazin-5-one (IR 98)^{np}



20 mg ($5.69 \cdot 10^{-5}$ mol) 8-chloro-9-nitro-7-(trifluoromethyl)-2,3-dihydro-5*H*-imidazo[2,1-*b*][1,3]benzothiazin-5-one (**IR 78**), 37 μ l (0.41 mmol) pyrrolidine and 9.7 μ l ($5.69 \cdot 10^{-5}$ mol) DIPEA were dissolved in 10 ml DMF and the mixture stirred at rt for 1 h. The solvent was

evaporated under reduced pressure and the crude product purified by flash chromatography twice (eluent TBME).

Orange solid

Yield 17.1 mg (77.8 %)

m.p. 92-96 °C (TBME)

^1H NMR (400 MHz, CDCl_3) δ 8.58 (s, 1H, Ar-H), 4.04 (m, 4H, $\text{CH}_2\text{-CH}_2$), 3.36 (m, 4H, $\text{CH}_2\text{-N-CH}_2$), 1.96 (m, 4H, $\text{CH}_2\text{-CH}_2$)

MS (EI) 386 (M)

HR MS m/z 387.0733 $[\text{M}+\text{H}]^+$, calc. for $[\text{C}_{15}\text{H}_{14}\text{F}_3\text{N}_4\text{O}_3\text{S}]^+$ 387.0733

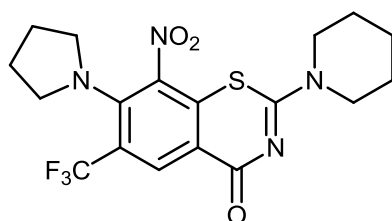
Elemental analysis	calc.	C 46.63	H 3.39	N 14.50	S 8.30
	found	C 47.20	H 3.27	N 13.85	S 7.61

R_f 0.28 (TBME)

M 386.35 g/mol

$\text{C}_{15}\text{H}_{13}\text{F}_3\text{N}_4\text{O}_3\text{S}$

7.5.56 8-nitro-2-(piperidin-1-yl)-7-(pyrrolidin-1-yl)-6-(trifluoromethyl)-4H-1,3-benzothiazin-4-one (IR 100)^{np}



20 mg (5.08×10^{-5} mol) 7-chloro-8-nitro-2-(piperidin-1-yl)-6-(trifluoromethyl)-4H-1,3-benzothiazin-4-one (**IR 74**), 33.5 μl (0.41 mmol) pyrrolidine and 8.65 μl (5.08×10^{-5} mol) DIPEA were dissolved in 10 ml DMF and the mixture stirred at rt for 1.5 h. The solvent was evaporated under reduced pressure and the crude product purified by flash chromatography twice (eluent TBME).

Orange solid

Yield 17.7 mg (81.3 %)

m.p. 175-183 °C (TBME)

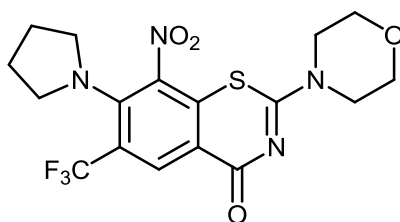
^1H NMR (400 MHz, CDCl_3) δ 8.81 (s, 1H, Ar-H), 3.86 (m, 4H, $\text{CH}_2\text{-N-CH}_2$), 3.31 (m, 4H, $\text{CH}_2\text{-N-CH}_2$), 1.95 (m, 4H, $\text{CH}_2\text{-CH}_2$), 1.69 (m, 6H, $\text{CH}_2\text{-CH}_2\text{-CH}_2$)

MS (EI) 428 (M)

Elemental analysis	calc.	C 50.46	H 4.47	N 13.08	S 7.48
	found	C 51.11	H 4.28	N 12.78	S 7.10

R_f 0.35 (TBME)
 M 428.43 g/mol
 $C_{18}H_{19}F_3N_4O_3S$

7.5.57 2-(morpholin-4-yl)-8-nitro-7-(pyrrolidin-1-yl)-6-(trifluoromethyl)-4*H*-1,3-benzothiazin-4-one (IR 101)^{np}



20 mg ($5.05 \cdot 10^{-5}$ mol) 7-chloro-2-(morpholin-4-yl)-8-nitro-6-(trifluoromethyl)-4*H*-1,3-benzothiazin-4-one (**IR 76**), 33 μ l (0.40 mmol) pyrrolidine and 8.6 μ l ($5.05 \cdot 10^{-5}$ mol) DIPEA were dissolved in 10 ml DMF and the mixture stirred at rt for 1.5 h. The solvent was evaporated under reduced pressure and the crude product purified by flash chromatography (eluent TBME).

Orange solid

Yield 9 mg (41.4 %)

m.p. 235-240 °C (TBME)

1H NMR (400 MHz, $CDCl_3$) δ 8.81 (s, 1H, Ar-H), 3.92 (m, 4H, CH_2 -N- CH_2), 3.78 (m, 4H, CH_2 -O- CH_2), 3.33 (m, 4H, CH_2 -N- CH_2), 1.95 (m, 4H, CH_2 - CH_2)

MS (EI) 430 (M)

HR MS m/z 431.0995 $[M+H]^+$, calc. for $[C_{17}H_{18}F_3N_4O_4S]^+$ 431.0995

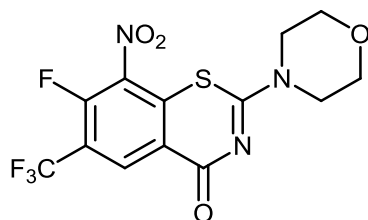
Elemental analysis	calc.	C 47.44	H 3.98	N 13.02	S 7.45
	found	C 47.22	H 3.09	N 12.32	S 8.08

R_f 0.22 (TBME)

M 430.40 g/mol

$C_{17}H_{17}F_3N_4O_4S$

7.5.58 7-fluoro-2-(morpholin-4-yl)-8-nitro-6-(trifluoromethyl)-4H-1,3-benzothiazin-4-one (IR 102)^{np}



The complete reaction was conducted under argon atmosphere.

90 mg (0.23 mmol) 7-chloro-2-(morpholin-4-yl)-8-nitro-6-(trifluoromethyl)-4H-1,3-benzothiazin-4-one (**IR 76**) and 19.8 mg (0.34 mmol) freeze-dried KF were suspended in 6 ml DMF and heated to reflux for 5 h.

After cooling, the solvent was evaporated under reduced pressure and the crude product purified by MPLC twice (Puriflash system, eluent TBME:ethanol 95:5 → 9:1 (V/V)).

Pale yellow solid

Yield 17.9 mg (20.7 %)

m.p. 187-190 °C (hexane:ethanol 95:5 (V/V))

¹H NMR (400 MHz, CDCl₃) δ 8.95 (d, 1H, Ar-H, ⁴J_{H,F} = 6.9 Hz), 3.95 (m, 4H, CH₂-N-CH₂), 3.81 (m, 4H, CH₂-O-CH₂)

MS (EI) 379 (M)

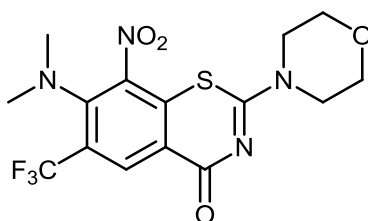
Elemental analysis	calc.	C 41.17	H 2.39	N 11.08	S 8.45
	found	C 41.62	H 2.29	N 10.53	S 8.01

R_f 0.44 (hexane:ethanol 2:1 (V/V))

M 379.29 g/mol

C₁₃H₉F₄N₃O₄S

7.5.59 7-(dimethylamino)-2-(morpholin-4-yl)-8-nitro-6-(trifluoromethyl)-4H-1,3-benzothiazin-4-one (IR 103)^{np}



20 mg (5.05*10⁻⁵ mol) 7-chloro-2-(morpholin-4-yl)-8-nitro-6-(trifluoromethyl)-4H-1,3-benzothiazin-4-one (**IR 76**), 73 μl (0.41 mmol) dimethylamine (25 % dimethylamine in H₂O) and 8.6 μl (5.05*10⁻⁵ mol) DIPEA were dissolved in 10 ml DMF and the mixture stirred at rt for

4 h, then heated to 60 °C for 1 h. After cooling, the solvent was evaporated under reduced pressure and the crude product purified by flash chromatography (eluent TBME).

Orange solid

Yield 16.1 mg (78.8 %)

m.p. 234-236 °C (TBME)

^1H NMR (400 MHz, CDCl_3) δ 8.87 (s, 1H, Ar-H), 3.88 (m, 4H, $\text{CH}_2\text{-N-CH}_2$), 3.80 (m, 4H, $\text{CH}_2\text{-O-CH}_2$), 2.88 (m, 6H, $\text{CH}_3\text{-N-CH}_3$)

MS (EI) 404 (M)

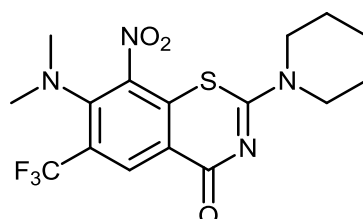
Elemental analysis	calc.	C 44.55	H 3.74	N 13.86	S 7.93
	found	C 44.74	H 3.66	N 13.12	S 7.45

R_f 0.25 (TBME)

M 404.36 g/mol

$\text{C}_{15}\text{H}_{15}\text{F}_3\text{N}_4\text{O}_4\text{S}$

7.5.60 7-(dimethylamino)-8-nitro-2-(piperidin-1-yl)-6-(trifluoromethyl)-4H-1,3-benzothiazin-4-one (IR 104)^{np}



20 mg (5.08×10^{-5} mol) 7-chloro-8-nitro-2-(piperidin-1-yl)-6-(trifluoromethyl)-4H-1,3-benzothiazin-4-one (**IR 74**), 73 μl (0.41 mmol) dimethylamine (25 % dimethylamine in H_2O) and 8.65 μl (5.08×10^{-5} mol) DIPEA were dissolved in 10 ml DMF and the mixture heated to 60 °C for 1 h. After cooling, the solvent was evaporated under reduced pressure and the crude product purified by flash chromatography (eluent TBME).

Orange solid

Yield 16.5 mg (80.7 %)

m.p. 185-188 °C (TBME)

^1H NMR (400 MHz, CDCl_3) δ 8.85 (s, 1H, Ar-H), 3.87 (m, 4H, $\text{CH}_2\text{-N-CH}_2$), 2.85 (m, 6H, $\text{CH}_3\text{-N-CH}_3$), 1.73 (m, 6H, $\text{CH}_2\text{-CH}_2\text{-CH}_2$)

MS (EI) 402 (M)

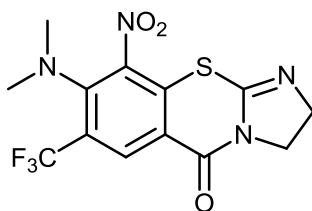
Elemental analysis	calc.	C 47.76	H 4.26	N 13.92	S 7.97
	found	C 47.48	H 4.21	N 13.09	S 7.65

R_f 0.31 (TBME)

M 402.39 g/mol

$\text{C}_{16}\text{H}_{17}\text{F}_3\text{N}_4\text{O}_3\text{S}$

7.5.61 8-(dimethylamino)-9-nitro-7-(trifluoromethyl)-2,3-dihydro-5H-imidazo[2,1-b][1,3]benzothiazin-5-one (IR 105)^{np}



20 mg ($5.69 \cdot 10^{-5}$ mol) 8-chloro-9-nitro-7-(trifluoromethyl)-2,3-dihydro-5H-imidazo[2,1-b][1,3]benzothiazin-5-one (**IR 78**), 82 μ l (0.46 mmol) dimethylamine (25 % dimethylamine in H_2O) and 9.7 μ l ($5.69 \cdot 10^{-5}$ mol) DIPEA were dissolved in 10 ml DMF and the mixture heated to 60 °C for 1 h. After cooling, the solvent was evaporated under reduced pressure and the crude product purified by flash chromatography (eluent TBME).

Yellow solid

Yield 15.4 mg (75.1 %)

m.p. 118-124 °C (TBME)

1H NMR (400 MHz, $CDCl_3$) δ 8.65 (s, 1H, Ar-H), 4.09 (m, 4H, CH_2-CH_2), 2.88 (m, 6H, CH_3-N-CH_3)

^{13}C NMR (125 MHz, $CDCl_3$) δ 157.1, 150.6, 149.3, 143.3, 132.8, 132.4 (q, $^3J_{C,F} = 5.8$ Hz), 125.2 (q, $^2J_{C,F} = 31.2$ Hz), 122.7 (q, $^1J_{C,F} = 273.5$ Hz), 118.2, 53.7, 44.6, 43.2, 43.1

MS (EI) 360 (M)

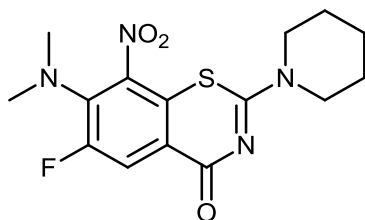
Elemental analysis	calc.	C 43.33	H 3.08	N 15.55	S 8.90
	found	C 43.41	H 2.96	N 14.57	S 8.93

R_f 0.29 (TBME)

M 360.31 g/mol

$C_{13}H_{11}F_3N_4O_3S$

7.5.62 7-(dimethylamino)-6-fluoro-8-nitro-2-(piperidin-1-yl)-4H-1,3-benzothiazin-4-one (IR 106)^{np}



20 mg ($5.82 \cdot 10^{-5}$ mol) 7-chloro-6-fluoro-8-nitro-2-(piperidin-1-yl)-4H-1,3-benzothiazin-4-one (**IR 62**), 84 μ l (0.47 mmol) dimethylamine (25 % dimethylamine in H_2O) and 9.9 μ l

($5.82 \cdot 10^{-5}$ mol) DIPEA were dissolved in 10 ml DMF and the mixture heated to 60 °C for 1 h. After cooling, the solvent was evaporated under reduced pressure and the crude product purified by flash chromatography (eluent TBME).

Orange solid

Yield 14.1 mg (68.8 %)

m.p. 155-158 °C (TBME)

$^1\text{H NMR}$ (400 MHz, CDCl_3) δ 8.24 (d, 1H, Ar-H, $^3J_{\text{H,F}} = 13.1$ Hz), 3.82 (m, 4H, $\text{CH}_2\text{-N-CH}_2$), 2.94 (m, 6H, $\text{CH}_3\text{-N-CH}_3$), 1.72 (m, 6H, $\text{CH}_2\text{-CH}_2\text{-CH}_2$)

MS (EI) 352 (M)

HR MS m/z 353.1076 $[\text{M}+\text{H}]^+$, calc. for $[\text{C}_{15}\text{H}_{18}\text{FN}_4\text{O}_3\text{S}]^+$ 353.1078

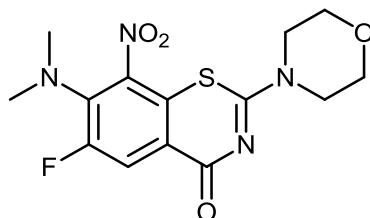
Elemental analysis	calc.	C 51.13	H 4.86	N 15.90	S 9.10
	found	C 50.61	H 4.73	N 15.20	S 8.62

R_f 0.28 (TBME)

M 352.38 g/mol

$\text{C}_{15}\text{H}_{17}\text{FN}_4\text{O}_3\text{S}$

7.5.63 7-(dimethylamino)-6-fluoro-2-(morpholin-4-yl)-8-nitro-4H-1,3-benzothiazin-4-one (IR 107)^{np}



20 mg ($5.78 \cdot 10^{-5}$ mol) 7-chloro-6-fluoro-2-(morpholin-4-yl)-8-nitro-4H-1,3-benzothiazin-4-one (**IR 69**), 83.5 μl ($4.62 \cdot 10^{-4}$ mol) dimethylamine (25 % dimethylamine in H_2O) and 9.8 μl ($5.78 \cdot 10^{-5}$ mol) DIPEA were dissolved in 10 ml DMF and the mixture heated to 60 °C for 3 h. After cooling, the solvent was evaporated under reduced pressure and the crude product purified by flash chromatography (eluent TBME).

Orange solid

Yield 14.5 mg (70.8 %)

m.p. 233-237 °C (TBME)

$^1\text{H NMR}$ (400 MHz, CDCl_3) δ 8.24 (d, 1H, Ar-H, $^3J_{\text{H,F}} = 13.2$ Hz), 3.9 (m, 4H, $\text{CH}_2\text{-N-CH}_2$), 3.78 (m, 4H, $\text{CH}_2\text{-O-CH}_2$), 2.95 (m, 6H, $\text{CH}_3\text{-N-CH}_3$)

MS (EI) 354 (M)

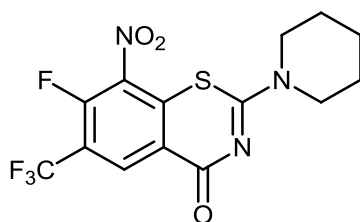
HR MS m/z 355.0873 $[\text{M}+\text{H}]^+$, calc. for $[\text{C}_{14}\text{H}_{16}\text{FN}_4\text{O}_4\text{S}]^+$ 355.0871

R_f 0.16 (TBME)

M 354.36 g/mol

$C_{14}H_{15}FN_4O_4S$

7.5.64 7-fluoro-8-nitro-2-(piperidin-1-yl)-6-(trifluoromethyl)-4H-1,3-benzothiazin-4-one (IR 108)^{np}



The complete reaction was conducted under argon atmosphere.

100 mg (0.25 mmol) 7-chloro-8-nitro-2-(piperidin-1-yl)-6-(trifluoromethyl)-4H-1,3-benzothiazin-4-one (IR 74) and 22 mg (0.38 mmol) freeze-dried KF were suspended in 4 ml DMF and heated to reflux for 5 h.

After cooling, the solvent was evaporated under reduced pressure and the crude product purified by flash chromatography twice (eluent TBME).

Yellow solid

Yield 58 mg (60.7 %)

m.p. 159-163 °C (TBME)

1H NMR (400 MHz, $CDCl_3$) δ 8.94 (d, 1H, Ar-H, $^3J_{H,F} = 6.9$ Hz), 3.86 (m, 4H, CH_2-N-CH_2), 1.74 (m, 6H, $CH_2-CH_2-CH_2$)

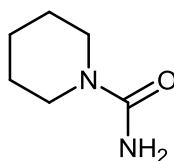
MS (EI) 377 (M)

R_f 0.29 (TBME)

M 377.31 g/mol

$C_{14}H_{11}F_4N_3O_3S$

7.5.65 piperidine-1-carboxamide (IR 110)



1.0 g (16.70 mmol) urea were dissolved in 20 ml piperidine and refluxed for 42 h, until release of ammonia stopped. The amine was removed under reduced pressure and the

resulting oily residue recrystallized from hexane:chloroform (approx. 2:1 (V/V)). Crystals were collected and dried.

Pale yellow platelets

Yield 1.61 g (75.0 %)

m.p. 99-105 °C (hexane:chloroform) (lit. 105-107 °C)⁸³

¹H NMR (500 MHz, CDCl₃) δ 4.45 (bs, 2H, NH₂), 3.32 (m, 4H, CH₂-N-CH₂), 1.57 (m, 6H, CH₂-CH₂)

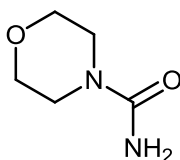
MS (EI) 128 (M)

R_f 0.34 (chloroform:methanol 9:1 (V/V))

M 128.17 g/mol

C₆H₁₂N₂O

7.5.66 morpholine-4-carboxamide (IR 111)



1.0 g (16.70 mmol) urea were dissolved in 20 ml morpholine and refluxed for 40 h, until release of ammonia stopped. The amine was removed under reduced pressure and the resulting oily residue recrystallized from hexane:chloroform (approx. 1:2 (V/V)). Crystals were collected and dried.

Pale yellow platelets

Yield 1.64 g (75.5 %)

m.p. 103-111 °C (hexane:chloroform) (lit. 112-115 °C)⁸³

¹H NMR (500 MHz, CDCl₃) δ 4.53 (bs, 2H, NH₂), 3.69 (m, 4H, CH₂-O-CH₂), 3.38 (m, 4H, CH₂-N-CH₂)

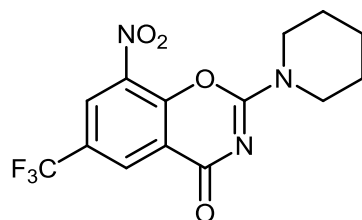
MS (EI) 130 (M)

R_f 0.28 (chloroform:methanol 9:1 (V/V))

M 130.15 g/mol

C₅H₁₀N₂O₂

7.5.67 8-nitro-2-(piperidin-1-yl)-6-(trifluoromethyl)-4H-1,3-benzoxazin-4-one (IR 112)^{np}



Synthesis of 2-chloro-3-nitro-5-(trifluoromethyl)benzoylchloride (**IR 06**) according to general procedure I from 500 mg (1.86 mmol) 2-chloro-3-nitro-5-(trifluoromethyl)benzoic acid (**IR 05**).

297 mg (2.32 mmol) piperidine-1-carboxamide (**IR 110**) and 316 μ l (1.86 mmol) DIPEA were dissolved in 40 ml toluene and heated to 70 °C. **IR 06** was dissolved in 3 ml toluene and added dropwise. Upon complete addition, the mixture was refluxed for 3 h. After cooling, the solvent was removed under reduced pressure and the crude product purified by flash chromatography twice (eluent TBME).

Pale yellow solid

Yield 239 mg (37.5 %)

m.p. 124-126 °C (TBME)

^1H NMR (400 MHz, CDCl_3) δ 8.72 (d, 1H, Ar-H, $^4J = 1.5$ Hz), 8.57 (d, 1H, Ar-H, $^4J = 1.5$ Hz), 3.90 (m, 4H, $\text{CH}_2\text{-N-CH}_2$), 1.75 (m, 6H, $\text{CH}_2\text{-CH}_2\text{-CH}_2$)

^{13}C NMR (125 MHz, CDCl_3) δ 163.2, 155.1, 148.7, 136.2, 131.9, (q, $^3J_{\text{C,F}} = 3.8$ Hz), 127.4 (q, $^2J_{\text{C,F}} = 35.5$ Hz), 126.9 (q, $^3J_{\text{C,F}} = 3.8$ Hz), 122.2 (q, $^1J_{\text{C,F}} = 273.5$ Hz), 120.3, 46.7, 46.0, 25.9, 25.3, 24.0

MS (EI) 343 (M)

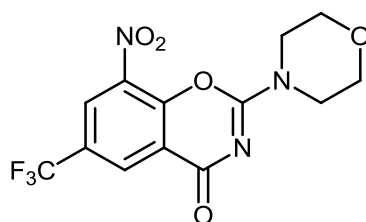
Elemental analysis	calc.	C 48.99	H 3.52	N 12.24
	found	C 49.00	H 3.40	N 12.28

R_f 0.37 (TBME)

M 343.26 g/mol

$\text{C}_{14}\text{H}_{12}\text{F}_3\text{N}_3\text{O}_4$

7.5.68 2-(morpholin-4-yl)-8-nitro-6-(trifluoromethyl)-4*H*-1,3-benzoxazin-4-one (IR 113)^{np}



Synthesis of 2-chloro-3-nitro-5-(trifluoromethyl)benzoylchloride (**IR 06**) according to general procedure I from 250 mg (0.93 mmol) 2-chloro-3-nitro-5-(trifluoromethyl)benzoic acid (**IR 05**).

151 mg (1.16 mmol) morpholine-4-carboxamide (**IR 111**) and 158 μ l (0.93 mmol) DIPEA were dissolved in 30 ml toluene and heated to 70 °C. **IR 06** was dissolved in 4 ml toluene and added dropwise. Upon complete addition, the mixture was refluxed for 2.5 h. After cooling, the solvent was removed under reduced pressure and the crude product purified by flash chromatography (eluent TBME).

Pale yellow solid

Yield 111 mg (34.7 %)

m.p. 204-208 °C (TBME)

^1H NMR (400 MHz, CDCl_3) δ 8.71 (d, 1H, Ar-H, $^4J = 2.3$ Hz), 8.59 (d, 1H, Ar-H, $^4J = 2.3$ Hz), 3.93 (m, 4H, $\text{CH}_2\text{-N-CH}_2$), 3.83 (m, 4H, $\text{CH}_2\text{-O-CH}_2$)

^{13}C NMR (100 MHz, CDCl_3) δ 162.9, 155.4, 148.5, 136.3, 131.1 (q, $^3J_{\text{C,F}} = 3.4$ Hz), 127.8 (q, $^2J_{\text{C,F}} = 35.9$ Hz), 127.1 (q, $^3J_{\text{C,F}} = 3.4$ Hz), 122.1 (q, $^1J_{\text{C,F}} = 273.1$ Hz), 120.3, 66.2, 66.1, 45.4, 45.0

MS (EI) 345 (M)

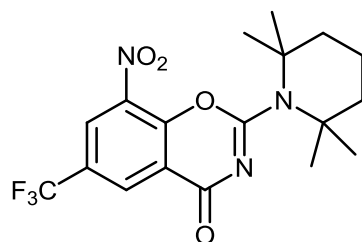
Elemental analysis	calc.	C 45.23	H 2.92	N 12.17
	found	C 44.87	H 2.64	N 11.79

R_f 0.24 (TBME)

M 345.23 g/mol

$\text{C}_{13}\text{H}_{10}\text{F}_3\text{N}_3\text{O}_5$

7.5.69 8-nitro-2-(2,2,6,6-tetramethylpiperidin-1-yl)-6-(trifluoromethyl)-4*H*-1,3-benzoxazin-4-one (IR 114)^{np}



Synthesis of 2-chloro-3-nitro-5-(trifluoromethyl)benzoylchloride (**IR 06**) according to general procedure I from 1.50 g (5.50 mmol) 2-chloro-3-nitro-5-(trifluoromethyl)benzoic acid (**IR 05**). The next reaction steps were conducted under argon atmosphere.

450 mg (5.50 mmol) KOCN were suspended in 30 ml acetone at 5 °C. **IR 06** was dissolved in 15 ml acetone and added dropwise and the mixture stirred for 2 h at 5 °C. A white precipitate of KCl was visible.

918 μ l (5.50 mmol) DIPEA in 2 ml acetone were added. Subsequently, 935 μ l (5.50 mmol) 2,2,6,6-tetramethylpiperidine were dissolved in 15 ml acetone and added dropwise. The mixture was stirred for 2 h at 5-10 °C, then heated to reflux until TLC showed no further intensification of product spot (approx. 12 h). After cooling, the solvent was evaporated, the brown residue purified by MPLC and flash chromatography (7x, eluent hexane:chloroform gradients (0-65 % (V/V) chloroform)). Fractions containing the product were combined and the eluent removed under reduced pressure. The crude product formed a yellow sticky solid, which was treated with 2 ml hexane and 5 min sonic bath. A beige precipitate formed which was filtered off and dried.

Beige solid

Yield 54 mg (2.5 %)

m.p. 146-147 °C (hexane)

¹H NMR (400 MHz, CDCl₃) δ 8.71 (d, 1H, Ar-H, ⁴J = 2.3 Hz), 8.48 (d, 1H, Ar-H, ⁴J = 2.3 Hz), 1.87 (m, 6H, CH₂-CH₂-CH₂), 1.63 (s, 12H, 4x CH₃)

MS (ESI) *m/z* 422.1 [M+Na]⁺

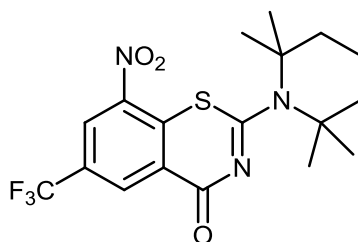
Elemental analysis	calc.	C 54.13	H 5.05	N 10.52
	found	C 54.45	H 4.98	N 10.48

R_f 0.38 (chloroform:hexane 4:1 (V/V))

M 399.36 g/mol

C₁₈H₂₀F₃N₃O₄

7.5.70 8-nitro-2-(2,2,6,6-tetramethylpiperidin-1-yl)-6-(trifluoromethyl)-4H-1,3-benzothiazin-4-one (IR 115)^{np}



Synthesis of 2-chloro-3-nitro-5-(trifluoromethyl)benzoylchloride (**IR 06**) according to general procedure I from 250 mg (0.93 mmol) 2-chloro-3-nitro-5-(trifluoromethyl)benzoic acid (**IR 05**).

The next reaction steps were conducted under argon atmosphere.

IR 06 was dissolved in 10 ml acetone and added dropwise to a solution of 90 mg (0.93 mmol) KSCN in 10 ml acetone at rt. After complete addition, the mixture was heated to 40 °C for 5 min and then let cool again to rt. 158 μ l (0.93 mmol) 2,2,6,6-tetramethylpiperidine were dissolved in 10 ml acetone and added dropwise. The mixture was stirred for another 30 min, then heated to reflux for 2 min. After cooling, the solvent was evaporated under reduced pressure and the crude product was pre-purified by flash chromatography twice (eluent hexane:chloroform 7:3 (V/V)). The fractions containing product were combined, the solvent evaporated and the residue dissolved in a small amount of acetone and hexane. The acetone was carefully evaporated under reduced pressure and the remaining hexane solution kept at 4 °C for 48 h. A precipitate formed which was filtered off and dried.

Yellow needles

Yield 43 mg (11.0 %)

m.p. 145-146 °C (hexane)

¹H NMR (400 MHz, CDCl₃) δ 8.98 (d, 1H, Ar-H, ⁴J = 1.9 Hz), 8.74 (d, 1H, Ar-H, ⁴J = 1.9 Hz), 1.89 (m, 6H, CH₂-CH₂-CH₂), 1.66 (s, 12H, 4x CH₃)

¹³C NMR (125 MHz, CDCl₃) δ 167.6, 167.3, 143.8, 136.3, 133.1 (q, ³J_{C,F} = 3.4 Hz), 129.7 (q, ²J_{C,F} = 35.5 Hz), 127.5, 125.8 (q, ³J_{C,F} = 3.8 Hz), 122.4 (q, ¹J_{C,F} = 273.0 Hz), 60.6 (2 CH), 36.2 (2 CH₂), 30.5 (4 CH₃), 14.3

MS (ESI) *m/z* 416.1 [M+H]⁺, 438.0 [M+Na]⁺

MS (EI) 415 (M)

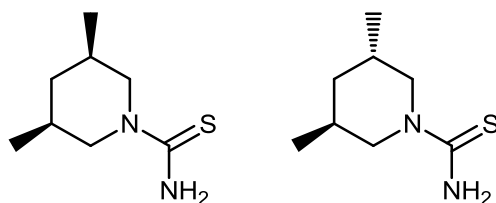
Elemental analysis	calc.	C 52.04	H 4.85	N 10.11	S 7.72
	found	C 52.45	H 4.59	N 10.13	S 8.06

R_f 0.14 (chloroform:hexane 1:1 (V/V))

M 415.43 g/mol

C₁₈H₂₀F₃N₃O₃S

7.5.71 3,5-dimethylpiperidine-1-carbothioamide (IR 116)



Synthesis according to general procedure II, starting from 4.11 g (50 mmol) NaSCN, 5.75 ml (50 mmol) benzoylchloride and 6.63 ml (50 mmol) 3,5-dimethylpiperidine.

Work-up after neutralization: evaporation of the solvent to yield the crude product, which was purified via flash chromatography (eluent chloroform) and MPLC (Puriflash system, eluent chloroform). Diastereomers could not be separated, NMR spectra showed signals for both diastereomers.

Beige solid

Yield 2.95 g (34.3 %)

m.p. 105-109 °C (chloroform)

^1H NMR (400 MHz, CDCl_3) δ 5.67 (bs, 4H, NH_2 , *cis and trans*), 4.46 (m, 2H, $\text{CH}_2\text{-N-CH}_2$, *cis*), 3.88 (m, 2H, $\text{CH}_2\text{-N-CH}_2$, *trans*), 3.30 (m, 2H, $\text{CH}_2\text{-N-CH}_2$, *trans*), 2.46 (m, 2H, $\text{CH}_2\text{-N-CH}_2$, *cis*), 2.01 (m, 2H, $\text{CH-CH}_2\text{-CH}$, *trans*), 1.84 (m, 1H, $\text{CH-CH}_2\text{-CH}$, *cis*), 1.70 (m, 2H, $\text{CH-CH}_2\text{-CH}$, *cis*), 1.45 (t, 2H, $\text{CH-CH}_2\text{-CH}$, $^3J = 6.0$ Hz, *trans*), 0.95 (d, 6H, 2x CH_3 , $^3J = 6.8$ Hz, *trans*), 0.90 (d, 6H, 2x CH_3 , $^3J = 6.7$ Hz, *cis*), 0.77 (q, 1H, $\text{CH-CH}_2\text{-CH}$, $^2J = 13.1$ Hz, $^3J = 11.7$ Hz, *cis*)

MS (EI) 172 (M)

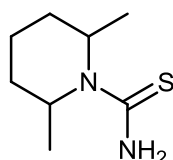
Elemental analysis	calc.	C 55.77	H 9.36	N 16.26	S 18.61
	found	C 56.14	H 9.61	N 15.90	S 18.74

R_f 0.14 (chloroform:methanol 98:2 (V/V))

M 172.29 g/mol

$\text{C}_8\text{H}_{16}\text{N}_2\text{S}$

7.5.72 2,6-dimethylpiperidine-1-carbothioamide (IR 118)



Synthesis according to general procedure II, starting from 811 mg (10 mmol) NaSCN, 1150 μl (10 mmol) benzoylchloride and 1350 μl (10 mmol) 2,6-dimethylpiperidine.

Work-up after neutralization: extraction with chloroform (4x). The combined organic layers were dried over MgSO_4 , the solvent evaporated under reduced pressure and the crude product purified via flash chromatography (eluent chloroform).

White solid

Yield 33 mg (1.9 %)

^1H NMR (400 MHz, CDCl_3) δ 5.73 (bs, 2H, NH_2), 4.85 (m, very broad signal, 2H, CH-N-CH), 1.61 (m, 6H, $\text{CH}_2\text{-CH}_2\text{-CH}_2$), 1.28 (d, 6H, 2x CH_3 , $^3J = 7.1$ Hz)

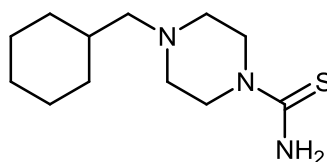
MS (ESI) m/z 173.2 $[\text{M}+\text{H}]^+$

R_f 0.27 (chloroform:methanol 98:2 (V/V))

M_r 172.29 g/mol

$\text{C}_8\text{H}_{16}\text{N}_2\text{S}$

7.5.73 4-(cyclohexylmethyl)piperazine-1-carbothioamide (IR 119)ⁿ



Synthesis according to general procedure II, starting from 356 mg (4.39 mmol) NaSCN , 500 μl (4.39 mmol) benzoylchloride and 853 μl (4.39 mmol) 1-(cyclohexylmethyl)piperazine (**IR 40**). Work-up after neutralization: extraction with chloroform (4x). The combined organic layers were dried over MgSO_4 , the solvent evaporated under reduced pressure and the crude product purified via flash chromatography (eluent chloroform:methanol 0-2 % (V/V)).

White solid

Yield 312 mg (29.4 %)

m.p. 153-157 °C (chloroform:methanol 98:2 (V/V))

^1H NMR (400 MHz, CDCl_3) δ 5.82 (bs, 2H, NH_2), 3.88 (m, 4H, $\text{CH}_2\text{-N-CH}_2$), 2.53 (m, 4H, $\text{CH}_2\text{-N-CH}_2$), 2.22 (m, 2H, $\text{N-CH}_2\text{-CH}$), 1.72 (m, 5H, cyclohexyl), 1.51 (m, 1H, $\text{N-CH}_2\text{-CH}$), 1.19 (m, 3H, cyclohexyl), 0.89 (m, 2H, cyclohexyl)

MS (ESI) m/z 242.1 $[\text{M}+\text{H}]^+$

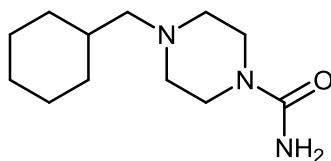
Elemental analysis	calc.	C 59.71	H 9.60	N 17.41	S 13.28
	found	C 59.72	H 9.74	N 16.95	S 12.97

R_f 0.12 (chloroform:methanol 98:2 (V/V))

M 241.40 g/mol

$\text{C}_{12}\text{H}_{23}\text{N}_3\text{S}$

7.5.74 4-(cyclohexylmethyl)piperazine-1-carboxamide (IR 120)ⁿ



275 μ l (1.42 mmol) 4-(cyclohexylmethyl)piperazine (**IR 40**) and 43 mg (0.71 mmol) urea were mixed in a 5 ml flask and heated to 120 °C for 48 h, until release of ammonia stopped. The brown residue was purified by flash chromatography (eluent chloroform:methanol 95:5 (V/V))

Pale brown solid

Yield 121 mg (75.0 %)

m.p. 150-153 °C (chloroform:methanol 95:5 (V/V))

¹H NMR (400 MHz, CDCl₃) δ 4.56 (bs, 2H, NH₂), 3.35 (m, 4H, CH₂-N-CH₂), 2.34 (m, 4H, CH₂-N-CH₂), 2.10 (d, 2H, N-CH₂-CH, ³J = 7.1 Hz), 1.68 (m, 5H, cyclohexyl), 1.45 (m, 1H, N-CH₂-CH), 1.16 (m, 3H, cyclohexyl), 0.83 (m, 2H, cyclohexyl)

MS (ESI) *m/z* 226.2 [M+H]⁺

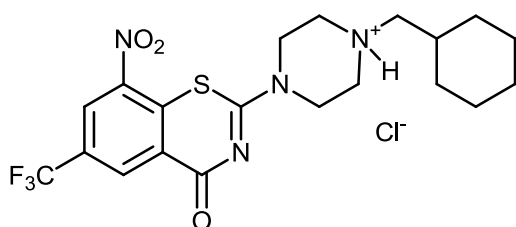
Elemental analysis	calc.	C 63.96	H 10.29	N 18.65
	found	C 63.49	H 10.13	N 18.20

R_f 0.22 (chloroform:methanol 9:1 (V/V)), *R_f* 0.11 (chloroform:methanol 98:2 (V/V))

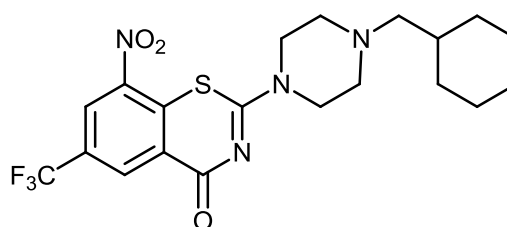
M 225.33 g/mol

C₁₂H₂₃N₃O

7.5.75 2-[4-(cyclohexylmethyl)piperazin-1-yl]-8-nitro-6-(trifluoromethyl)-4*H*-1,3-benzothiazin-4-one (IR 124 = PBTZ169)



hydrochloride salt IR 124xHCl



free base IR 124 (=PBTZ169)

method E (thiourea pathway)

Synthesis of 2-chloro-3-nitro-5-(trifluoromethyl)benzoylchloride (**IR 06**) according to general procedure I from 100 mg (0.37 mmol) 2-chloro-3-nitro-5-(trifluoromethyl)benzoic acid (**IR 05**).

112 mg (0.46 mmol) 4-(cyclohexylmethyl)piperazine-1-carbothioamide (**IR 119**) were dissolved in 20 ml toluene and heated to 70 °C. After dropwise addition of **IR 06**, dissolved in 3 ml toluene, the mixture was heated to reflux for 1 h. A pale yellow precipitate of **IR 124xHCl** formed immediately after addition of **IR 06**, it was filtered off and dried.

2-[4-(cyclohexylmethyl)piperazin-1-yl]-8-nitro-6-(trifluoromethyl)-4H-1,3-benzothiazin-4-one hydrochloride (IR 124xHCl):

Pale yellow needles

Yield 124 mg (68.1 %)

m.p. 241-245 °C (toluene)

¹H NMR (400 MHz, CD₃OD) δ 8.99 (d, 1H, Ar-H, ⁴J = 1.8 Hz), 8.93 (d, 1H, Ar-H, ⁴J = 1.9 Hz), 4.93 (m, 2H, CH₂-N-CH₂), 3.74 (m, 4H, CH₂-N-CH₂), 3.26 (m, 2H, CH₂-N-CH₂), 3.09 (d, 2H, N-CH₂-CH, ³J = 6.5 Hz), 1.83 (m, 5H, cyclohexyl), 1.74 (m, 1H, N-CH₂-CH), 1.34 (m, 3H, cyclohexyl), 1.09 (m, 2H, cyclohexyl)

Elemental analysis

calc.	C 48.73	H 4.91	N 11.37	S 6.50	Cl 7.19
found	C 48.20	H 4.60	N 11.06	S 6.26	Cl 6.90

R_f 0.42 (TBME)

M 492.94 g/mol

C₂₀H₂₄ClF₃N₄O₃S

Extraction of free base IR 124

46 mg **IR 124xHCl** were suspended in 10 ml aq. NaOH (10 %) and stirred at rt for 30 min. The mixture was extracted with chloroform (3x), the combined organic layers were dried over MgSO₄ and the solvent evaporated. Yield 41 mg (96.3 %).

adapted method A (classic pathway, adjusted temperature)

Synthesis of 2-chloro-3-nitro-5-(trifluoromethyl)benzoylchloride (**IR 06**) according to general procedure I from 200 mg (0.74 mmol) 2-chloro-3-nitro-5-(trifluoromethyl)benzoic acid (**IR 05**).

Under argon atmosphere, 72 mg (0.74 mmol) KSCN were suspended in 10 ml acetone at 5 °C. **IR 06** was dissolved in 5 ml acetone and added dropwise, subsequently the mixture was stirred at 5 °C for 1.5 h. 144 μl (0.74 mmol) 1-(cyclohexylmethyl)piperazine (**IR 40**) were dissolved in 5 ml acetone and added dropwise keeping the temperature at 5 °C. The mixture was then stirred at 5-10 °C for 2 h, the solvent evaporated and the crude product purified by flash chromatography twice (eluent TBME). Yield 121 mg (35.4 %).

2-[4-(cyclohexylmethyl)piperazin-1-yl]-8-nitro-6-(trifluoromethyl)-4H-1,3-benzothiazin-4-one
(**IR 124** = PBTZ169):

Yellow solid

m.p. 183-185 °C (TBME) (lit. 184-186 °C)⁶⁹

¹H NMR (400 MHz, CDCl₃) δ 9.10 (d, 1H, Ar-H, ⁴J = 2.1 Hz), 8.75 (d, 1H, Ar-H, ⁴J = 2.1 Hz), 4.01 (m, 4H, CH₂-N-CH₂), 2.54 (m, 4H, CH₂-N-CH₂), 2.18 (d, 2H, N-CH₂-CH, ³J = 7.2 Hz), 1.74 (m, 5H, cyclohexyl), 1.49 (m, 1H, N-CH₂-CH), 1.23 (m, 3H, cyclohexyl), 0.89 (m, 2H, cyclohexyl)

¹³C NMR (100 MHz, CDCl₃) δ 166.4, 162.0, 143.9, 134.1, 133.4 (q, ³J_{C,F} = 3.4 Hz), 129.7 (q, ²J_{C,F} = 35.5 Hz), 126.8, 126.0 (q, ³J_{C,F} = 3.8 Hz), 122.4 (q, ¹J_{C,F} = 273.1 Hz), 65.1, 53.1 (bs, 2 CH₂), 46.6 (bs, 2 CH₂), 35.0, 31.7 (2 CH₂), 26.7, 26.0 (2 CH₂)

MS (EI) 456 (M)

MS (ESI) *m/z* 457.2 [M+H]⁺

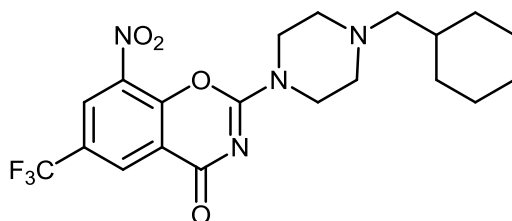
Elemental analysis	calc.	C 52.62	H 5.08	N 12.27	S 7.02
	found	C 52.20	H 4.92	N 11.82	S 6.54

R_f 0.42 (TBME)

M 456.48 g/mol

C₂₀H₂₃F₃N₄O₃S

7.5.76 2-[4-(cyclohexylmethyl)piperazin-1-yl]-8-nitro-6-(trifluoromethyl)-4H-1,3-benzoxazin-4-one (**IR 125**)^{np}



Synthesis of 2-chloro-3-nitro-5-(trifluoromethyl)benzoylchloride (**IR 06**) according to general procedure I from 266 mg (0.98 mmol) 2-chloro-3-nitro-5-(trifluoromethyl)benzoic acid (**IR 05**).

200 mg (0.89 mmol) 4-(cyclohexylmethyl)piperazine-1-carboxamide (**IR 120**) and 500 μl (2.94 mmol) DIPEA were dissolved in 5 ml toluene and heated to 70 °C. **IR 06** was dissolved in 5 ml toluene and added dropwise, the mixture was subsequently refluxed for 1 h and then set aside at rt over night. After removal of the solvent under reduced pressure, the crude product was purified by flash chromatography (eluent chloroform:methanol 98:2 (V/V)).

Yellow solid

Yield 162 mg (41.3 %)

m.p. 199-201 °C (chloroform:methanol 98:2 (V/V))

^1H NMR (400 MHz, CDCl_3) δ 8.72 (d, 1H, Ar-H, $^4J = 2.3$ Hz), 8.58 (d, 1H, Ar-H, $^4J = 2.3$ Hz), 3.93 (m, 4H, $\text{CH}_2\text{-N-CH}_2$), 2.54 (m, 4H, $\text{CH}_2\text{-N-CH}_2$), 2.19 (d, 2H, N- $\text{CH}_2\text{-CH}$, $^3J = 7.1$ Hz), 1.75 (m, 5H, cyclohexyl), 1.47 (m, 1H, N- $\text{CH}_2\text{-CH}$), 1.24 (m, 3H, cyclohexyl), 0.89 (m, 2H, cyclohexyl)

^{13}C NMR (125 MHz, CDCl_3) δ 163.0, 155.2, 148.6, 136.2, 131.0 (q, $^3J_{\text{C,F}} = 3.5$ Hz), 127.6 (q, $^2J_{\text{C,F}} = 35.5$ Hz), 127.0 (q, $^3J_{\text{C,F}} = 3.3$ Hz), 122.2 (q, $^1J_{\text{C,F}} = 273.7$ Hz), 120.3, 65.1, 53.0, 52.5, 45.0 (bs, 2 CH_2), 34.9, 31.7, 31.6, 26.6, 26.0 (2 CH_2)

MS (ESI) m/z 441.22 $[\text{M}+\text{H}]^+$

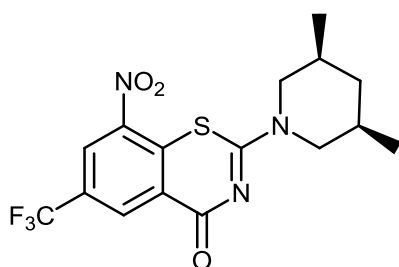
HR MS m/z 441.1741 $[\text{M}+\text{H}]^+$, calc. for $[\text{C}_{20}\text{H}_{24}\text{F}_3\text{N}_4\text{O}_4]^+$ 441.1744

R_f 0.82 (TBME), R_f 0.05 (hexane:TBME 1:1 (V/V))

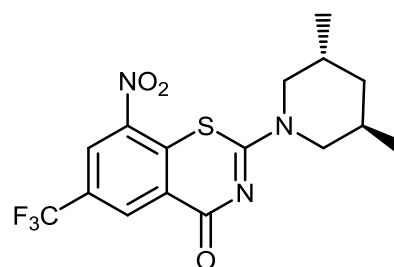
M 440.42 g/mol

$\text{C}_{20}\text{H}_{23}\text{F}_3\text{N}_4\text{O}_4$

7.5.77 2-(3,5-dimethylpiperidin-1-yl)-8-nitro-6-(trifluoromethyl)-4H-1,3-benzothiazin-4-one (IR 127)ⁿ



IR 127 cis



IR 127 trans

Synthesis of 2-chloro-3-nitro-5-(trifluoromethyl)benzoylchloride (**IR 06**) according to general procedure I from 250 mg (0.93 mmol) 2-chloro-3-nitro-5-(trifluoromethyl)benzoic acid (**IR 05**).

200 mg (1.16 mmol) 3,5-dimethylpiperidine-1-carbothioamide (**IR 116**) were dissolved in 25 ml toluene and heated to 70 °C. After dropwise addition of **IR 06**, dissolved in 10 ml toluene, the mixture was heated to reflux for 1 h, then set aside at rt over night. Subsequently, the solvent was evaporated under reduced pressure and the crude product purified by MPLC (3x, Puriflash system, eluent hexane:TBME, gradient 0-100 % (V/V) TBME) and flash chromatography twice (eluent hexane:TBME, gradient 50-100 % (V/V) TBME) to separate both diastereomers:

2-[(3*R*,5*S*)-3,5-dimethylpiperidin-1-yl]-8-nitro-6-(trifluoromethyl)-4*H*-1,3-benzothiazin-4-one (**IR 127 cis**):

Yellow solid

Yield 136 mg (37.9 %)

m.p. 201-202 °C (TBME)

^1H NMR (400 MHz, CDCl_3) δ 9.10 (d, 1H, Ar-H, $^4J = 2.1$ Hz), 8.74 (d, 1H, Ar-H, $^4J = 2.1$ Hz), 5.28 (m, 1H, $\text{CH}_2\text{-N-CH}_2$), 4.25 (m, 1H, $\text{CH}_2\text{-N-CH}_2$), 2.79 (m, 1H, $\text{CH}_2\text{-N-CH}_2$), 2.38 (m, 1H, $\text{CH}_2\text{-N-CH}_2$), 1.95 (m, 1H, $\text{CH-CH}_2\text{-CH}$), 1.77 (m, 2H, $\text{CH-CH}_2\text{-CH}$), 1.02 (m, 6H, 2x CH_3), 0.95 (q, 1H, $\text{CH-CH}_2\text{-CH}$, $J = 12.9$ Hz)

^{13}C NMR (125 MHz, CDCl_3) δ 166.6, 161.3, 144.0, 134.3, 133.3 (q, $^3J_{\text{C,F}} = 3.8$ Hz), 129.5 (q, $^2J_{\text{C,F}} = 35.5$ Hz), 126.8, 125.9 (q, $^3J_{\text{C,F}} = 3.8$ Hz), 122.4 (q, $^1J_{\text{C,F}} = 273.3$ Hz), 53.8 (bs, 2 CH_2), 53.0 (bs, 2 CH_2), 42.1, 32.1 (bs, 2 CH_2), 31.3 (bs, 2 CH_2), 18.8

MS (ESI) m/z 388.3 $[\text{M}+\text{H}]^+$, 410.1 $[\text{M}+\text{Na}]^+$

Elemental analysis	calc.	C 49.61	H 4.16	N 10.85	S 8.28
	found	C 49.20	H 3.86	N 10.72	S 8.22

R_f 0.21 (hexane:TBME 1:1 (V/V))

M 387.38 g/mol

$\text{C}_{16}\text{H}_{16}\text{F}_3\text{N}_3\text{O}_3\text{S}$

2-[(3*S*,5*S*)-3,5-dimethylpiperidin-1-yl]-8-nitro-6-(trifluoromethyl)-4*H*-1,3-benzothiazin-4-one
(**IR 127 trans**):

Yellow solid

Yield 39 mg (10.9 %)

m.p. 97-101 °C (TBME)

^1H NMR (400 MHz, CDCl_3) δ 9.10 (d, 1H, Ar-H, $^4J = 2.1$ Hz), 8.74 (d, 1H, Ar-H, $^4J = 2.1$ Hz), 4.43 (m, 1H, $\text{CH}_2\text{-N-CH}_2$), 3.68 (m, 2H, $\text{CH}_2\text{-N-CH}_2$), 3.46 (m, 1H, $\text{CH}_2\text{-N-CH}_2$), 2.15 (m, 2H, $\text{CH-CH}_2\text{-CH}$), 1.59 (m, 2H, $\text{CH-CH}_2\text{-CH}$), 1.02 (m, 6H, 2x CH_3)

MS (ESI) m/z 388.3 $[\text{M}+\text{H}]^+$, 410.1 $[\text{M}+\text{Na}]^+$

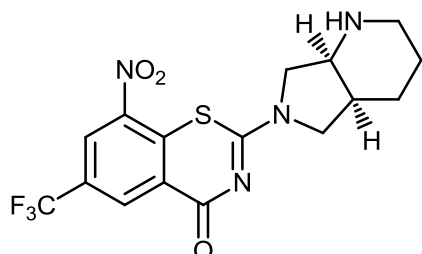
Elemental analysis	calc.	C 49.61	H 4.16	N 10.85	S 8.28
	found	C 49.64	H 3.88	N 10.78	S 8.37

R_f 0.12 (hexane:TBME 1:1 (V/V))

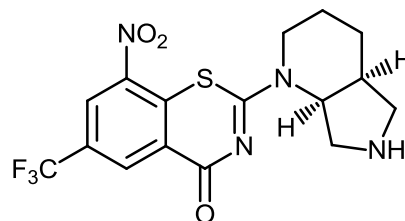
M 387.38 g/mol

$\text{C}_{16}\text{H}_{16}\text{F}_3\text{N}_3\text{O}_3\text{S}$

7.5.78 Mixture: 2-[(4a*S*,7a*S*)-octahydro-1*H*-pyrrolo[3,4-*b*]pyridin-6-yl]-8-nitro-6-(trifluoromethyl)-4*H*-1,3-benzothiazin-4-one and 2-[(4a*S*,7a*S*)-octahydro-1*H*-pyrrolo[3,4-*b*]pyridin-1-yl]-8-nitro-6-(trifluoromethyl)-4*H*-1,3-benzothiazin-4-one (IR 128)ⁿ



2-[(4a*S*,7a*S*)-octahydro-1*H*-pyrrolo[3,4-*b*]pyridin-6-yl]-8-nitro-6-(trifluoromethyl)-4*H*-1,3-benzothiazin-4-one



2-[(4a*S*,7a*S*)-octahydro-1*H*-pyrrolo[3,4-*b*]pyridin-1-yl]-8-nitro-6-(trifluoromethyl)-4*H*-1,3-benzothiazin-4-one

Under argon atmosphere, 23 mg (7.18×10^{-5} mol) 2-ethoxy-8-nitro-6-(trifluoromethyl)-4*H*-1,3-benzothiazin-4-one (**IR 129**) were dissolved in 3 ml toluene, 10 μ l glacial acetic acid were added and the mixture stirred at 40 °C for 1 h. 12 μ l (9.40×10^{-5} mol) (1*S*,6*S*)-2,8-diazabicyclo[4.3.0]nonane were dissolved in 1 ml toluene and added to the reaction mixture. After another 2 h of stirring at 40 °C, the solvent was evaporated under reduced pressure and the crude product purified by flash chromatography twice (eluent chloroform). Fractions containing the product were combined, the solvent evaporated and the oily residue treated with 1 ml hexane, which was finally evaporated to yield the solid product.

Pale yellow solid

Yield 20 mg (69.6 %)

¹H NMR (400 MHz, CDCl₃) δ 9.15 (d, 0.7H, Ar-H, ⁴*J* = 1.6 Hz), 9.13 (d, 1H, Ar-H, ⁴*J* = 1.7 Hz), 8.75 (m, 1.7H, 2 Ar-H), 3.84 (m, 8.5H, 2,8-diazabicyclo[4.3.0]nonane), 3.06 (m, 1.4H, 2,8-diazabicyclo[4.3.0]nonane), 2.70 (m, 1.5H, 2,8-diazabicyclo[4.3.0]nonane), 2.56 (m, 1H, 2,8-diazabicyclo[4.3.0]nonane), 2.39 (m, 0.7H, 2,8-diazabicyclo[4.3.0]nonane), 1.77 (m, 7.5H, 2,8-diazabicyclo[4.3.0]nonane)

MS (ESI) *m/z* 401.25 [M+H]⁺

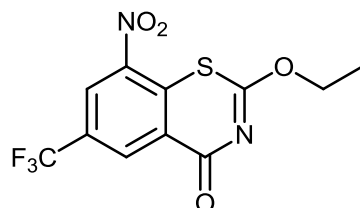
HR MS *m/z* 401.0892 [M+H]⁺, calc. for [C₁₆H₁₆F₃N₄O₃S]⁺ 401.0890

R_f 0.44 (chloroform:methanol 9:1 (V/V))

M 400.38 g/mol

C₁₆H₁₅F₃N₄O₃S

7.5.79 2-ethoxy-8-nitro-6-(trifluoromethyl)-4H-1,3-benzothiazin-4-one (IR 129)



68 mg (0.48 mmol) sodium (ethoxymethanethiyl)sulfanide (**IR 42**) were added to a solution of 100 mg (0.34 mmol) 2-chloro-3-nitro-5-(trifluoromethyl)benzamide (**IR 18**) in ethanol and stirred at rt for 20 h. The solvent was evaporated and the crude product purified by flash chromatography (eluent hexane:EA 3:1 (V/V)).

Yellow needles

Yield 29 mg (24.5 %)

m.p. 63-75 °C (hexane:EA 3:1 (V/V)) (lit. 146-148 °C (ethanol/water))⁷³

¹H NMR (400 MHz, CDCl₃) δ 9.11 (d, 1H, Ar-H, ⁴J = 2.0 Hz), 8.86 (d, 1H, Ar-H, ⁴J = 2.0 Hz), 4.73 (q, 2H, O-CH₂, ³J = 7.1 Hz), 1.49 (t, 3H, CH₃, ³J = 7.1 Hz)

¹³C NMR (100 MHz, CDCl₃) δ 172.8, 167.5, 143.9, 135.8, 134.2 (q, ³J_{C,F} = 3.4 Hz), 130.1 (q, ²J_{C,F} = 35.5 Hz), 126.8 (q, ³J_{C,F} = 3.8 Hz), 126.5, 122.2 (q, ¹J_{C,F} = 273.1 Hz), 67.9, 14.1

MS (EI) 320 (M)

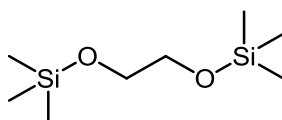
MS (ESI) *m/z* 320.98 [M+H]⁺

R_f 0.33 (hexane:EA 3:1 (V/V))

M 320.24 g/mol

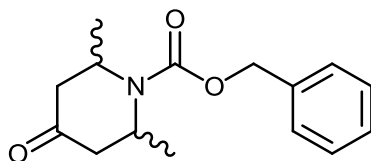
C₁₁H₇F₃N₂O₄S

7.5.80 2,2,7,7-tetramethyl-3,6-dioxa-2,7-disilaoctane (IR 131)



The complete reaction was conducted under argon atmosphere. 500 μl (8.9 mmol) ethylene glycol and 3.7 ml (27.0 mmol) TEA were dissolved in 45 ml DCM and cooled to 0 °C. 2.8 ml (22.0 mmol) chlorotrimethylsilane were added dropwise. Upon complete addition, the ice bath was removed and the mixture stirred until adjusted to rt. A white precipitate formed, which was filtered off and washed with EE. If novel precipitate formed in the filtrate, it was filtered off again and washed with EE until no further precipitation occurred in the organic filtrate. The organic layers were combined and the solvent was removed under reduced

7.5.82 benzyl 2,6-dimethyl-4-oxopiperidine-1-carboxylate (IR 133)



The complete reaction was conducted under argon atmosphere.

110 mg (0.86 mmol) 2,6-dimethylpiperidin-4-one (**IR 83**) and 122 μ l (0.86 mmol) benzyl chloroformate were dissolved in 10 ml DCM at 0 °C. 440 μ l (2.6 mmol) DIPEA were added, subsequently another 10 ml DCM were added and the ice bath removed. The mixture was stirred at rt for 30 min, subsequently washed twice with 1 M HCl. The organic layer was separated, dried over MgSO_4 , and evaporated under reduced pressure. The crude product was purified via flash chromatography (eluent EA:heptane 1:1 (V/V)). NMR showed signals of a mixture of both stereoisomers in approx. 1:1 ratio.

Colorless oil

Yield 22 mg (9.7 %)

^1H NMR (400 MHz, CDCl_3) δ 7.04 (m, 10H, Ar-H, *cis* and *trans*), 4.85 (m, 4H, Ar- CH_2 , *cis* and *trans*), 4.49 (m, 2H, 2x $\text{CH}-\text{CH}_3$, *cis*), 4.13 (m, 2H, 2x $\text{CH}-\text{CH}_3$, *trans*), 2.53 (dd, 2H, $\text{CH}_2-\text{C}(=\text{O})-\text{CH}_2$, $^2J = 17.9$ Hz, $^3J = 6.5$ Hz, *trans*), 2.40 (dd, 2H, $\text{CH}_2-\text{C}(=\text{O})-\text{CH}_2$, $^2J = 15.1$ Hz, $^3J = 7.6$ Hz, *cis*), 2.06 (dd, 2H, $\text{CH}_2-\text{C}(=\text{O})-\text{CH}_2$, $^2J = 17.9$ Hz, $^3J = 1.8$ Hz, *trans*), 1.97 (dd, 2H, $\text{CH}_2-\text{C}(=\text{O})-\text{CH}_2$, $^2J = 14.9$ Hz, $^3J = 2.9$ Hz, *cis*), 0.98 (d, 6H, 2x CH_3 , $^3J = 7.0$ Hz, *cis*), 0.95 (d, 6H, 2x CH_3 , $^3J = 6.6$ Hz, *trans*)

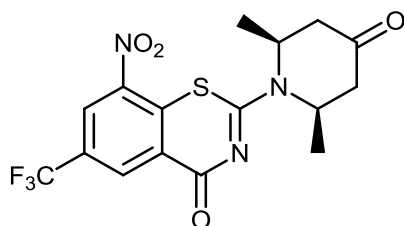
MS (ESI) m/z 261.9 $[\text{M}+\text{H}]^+$

R_f 0.38 (EA:heptane 1:1 (V/V))

M 261.32 g/mol

$\text{C}_{15}\text{H}_{19}\text{NO}_3$

7.5.83 2-[(2*R*,6*S*)-2,6-dimethyl-4-oxopiperidin-1-yl]-8-nitro-6-(trifluoromethyl)-4*H*-1,3-benzothiazin-4-one (IR 140)ⁿ



Synthesis according to general procedure III, starting from 500 mg (1.85 mmol) 2-chloro-3-nitro-5-(trifluoromethyl)benzoic acid (**IR 05**). The hydrochloride salt of 2,6-dimethylpiperidin-

4-one (**IR 83xHCl**) was used as amine during the third step of the synthesis and 2.5 equivalents of DIPEA added to the mixture.

Purification of crude product: Evaporation of acetone yielded a brown oily residue, which was dissolved in chloroform and washed with aq. NH_3 (pH 9) five times. The organic layer was concentrated under reduced pressure and the resulting residue purified by flash chromatography twice (eluent chloroform). The fractions containing product were combined, the solvent evaporated and the oily residue washed with a small amount of hexane to yield a yellow solid.

NMR spectra showed only signals of one stereoisomer (cis). Presumably due to sterical effects, the nucleophilic attack of only one stereoisomer of **IR 83** is favored.

Pale yellow solid

Yield 176 mg (23.7 %)

m.p. 140-145 °C (hexane)

^1H NMR (400 MHz, CDCl_3) δ 9.11 (d, 1H, Ar-H, $^4J = 2.1$ Hz), 8.78 (d, 1H, Ar-H, $^4J = 2.1$ Hz), 5.49 (m, 2H, 2x CH-CH₃), 2.89 (dd, 2H, CH₂-C(=O)-CH₂, $^2J = 15.5$ Hz, $^3J = 7.6$ Hz), 2.53 (dd, 2H, CH₂-C(=O)-CH₂, $^2J = 15.5$ Hz, $^3J = 1.9$ Hz), 1.52 (d, 6H, 2x CH₃, $^3J = 7.0$ Hz)

^{13}C NMR (100 MHz, CDCl_3) δ 204.7, 166.2, 162.1, 144.0, 134.0, 133.4 (q, $^3J_{\text{C,F}} = 3.8$ Hz), 130.0 (q, $^2J_{\text{C,F}} = 35.5$ Hz), 126.5, 126.1 (q, $^3J_{\text{C,F}} = 3.8$ Hz), 122.3 (q, $^1J_{\text{C,F}} = 273.3$ Hz), 51.2 (2 CH₂), 45.0 (2 CH), 22.2 (2 CH₃)

MS (ESI) m/z 402.1 [M+H]⁺

HR MS m/z 402.0732 [M+H]⁺, calc. for [C₁₆H₁₅F₃N₃O₄S]⁺ 402.0730

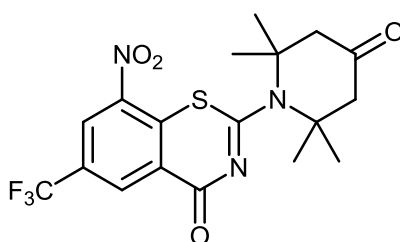
Elemental analysis	calc.	C 47.88	H 3.52	N 10.47	S 7.99
	found	C 47.88	H 3.48	N 10.39	S 8.53

R_f 0.24 (heptane:EA 1:1 (V/V)), R_f 0.13 (chloroform)

M 401.36 g/mol

C₁₆H₁₄F₃N₃O₄S

7.5.84 8-nitro-2-(2,2,6,6-tetramethyl-4-oxopiperidin-1-yl)-6-(trifluoromethyl)-4H-1,3-benzothiazin-4-one (IR 141)ⁿ



Synthesis according to general procedure III, starting from 500 mg (1.85 mmol) 2-chloro-3-nitro-5-(trifluoromethyl)benzoic acid (**IR 05**).

Purification of crude product was achieved by flash chromatography (4x, eluent hexane:chloroform 1:1 (V/V)). The fractions containing product were combined and the organic solvent evaporated. The residue was dissolved in a small amount of chloroform and crystallization was facilitated by slowly adding a small amount of hexane. The precipitate was filtered off and dried.

Yellow needles

Yield 252 mg (31.7 %)

m.p. 159-163 °C (hexane)

^1H NMR (400 MHz, CDCl_3) δ 8.98 (d, 1H, Ar-H, $^4J = 2.1$ Hz), 8.78 (d, 1H, Ar-H, $^4J = 2.1$ Hz), 2.76 (s, 4H, 2x CH_2), 1.77 (s, 12H, 4x CH_3)

^{13}C NMR (100 MHz, CDCl_3) δ 205.8, 167.2, 167.0, 143.9, 135.3, 133.1 (q, $^3J_{\text{C,F}} = 3.8$ Hz) 130.2 (q, $^2J_{\text{C,F}} = 35.5$ Hz), 127.5, 126.1 (q, $^3J_{\text{C,F}} = 3.8$ Hz), 122.3 (q, $^1J_{\text{C,F}} = 273.5$ Hz), 61.5 (2 C), 53.7 (2 CH_2), 31.1 (4 CH_3)

MS (ESI) m/z 429.9 $[\text{M}+\text{H}]^+$, 452.0 $[\text{M}+\text{Na}]^+$

HR MS m/z 430.1047 $[\text{M}+\text{H}]^+$, calc. for $[\text{C}_{18}\text{H}_{19}\text{F}_3\text{N}_3\text{O}_4\text{S}]^+$ 430.1043

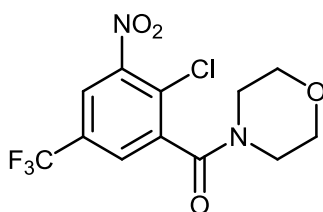
Elemental analysis	calc.	C 50.35	H 4.23	N 9.79	S 7.47
	found	C 50.37	H 4.36	N 9.03	S 7.30

R_f 0.36 (heptane:EA 1:1)

M 429.41 g/mol

$\text{C}_{18}\text{H}_{18}\text{F}_3\text{N}_3\text{O}_4\text{S}$

7.5.85 4-([2-chloro-3-nitro-5-(trifluoromethyl)phenyl]carbonyl)-morpholine (IR 150)



Following the procedure of **IR 58**, method A, **IR 150** was obtained by purification of the corresponding fractions of the flash chromatography via MPLC (Büchi MPLC, eluent toluene, flow rate 30 ml/min).

Yellow solid

Yield 133 mg (13.1 %)

m.p. 104-108 °C (toluene)

^1H NMR (400 MHz, CDCl_3) δ 8.12 (d, 1H, Ar-H, $^4J = 2.7$ Hz), 7.77 (d, 1H, Ar-H, $^4J = 2.7$ Hz), 3.79 (m, 6H, morpholine), 3.26 (m, 2H, morpholine)

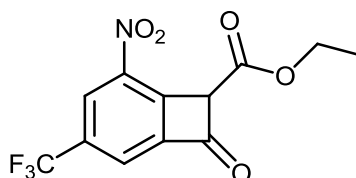
MS (EI) 338 (M)

R_f 0.45 (toluene:ethanol 9:1 (V/V))

M 338.67 g/mol

$C_{12}H_{10}ClF_3N_2O_4$

7.5.86 ethyl 5-nitro-8-oxo-3-(trifluoromethyl)bicyclo[4.2.0]octa-1,3,5-triene-7-carboxylate (IR 154)ⁿ



50 mg (0.15 mmol) ethyl 3-[2-chloro-3-nitro-5-(trifluoromethyl)phenyl]-3-oxopropanoate (**IR 81**), 8 mg (0.15 mmol) KOH (85 %) and 1 mg ($0.29 \cdot 10^{-5}$ mol) *n*-Bu₄NBr were dissolved in 10 ml DMF and stirred at rt for 30 min. After cooling to 0 °C, 23.5 μ l (0.22 mmol) isopropyl isothiocyanate, dissolved in 2 ml DMF, were added dropwise and after adjusting to rt the mixture was stirred for 17 h. 25 ml H₂O and subsequently 10 ml sat. NH₄Cl were added to quench the reaction. The mixture was extracted with EA (4x), the combined organic layers were dried over MgSO₄ and the solvent evaporated under reduced pressure. The crude product was purified by MPLC (Puriflash system, eluent toluene:isopropanol 0-2 % (V/V)).

Yellow solid

Yield 18 mg (40.4 %)

m.p. 92-97 °C (toluene:isopropanol 98:2 (V/V))

¹H NMR (400 MHz, CDCl₃) δ 8.75 (d, 1H, Ar-H, ⁴*J* = 2.3 Hz), 8.53 (d, 1H, Ar-H, ⁴*J* = 2.3 Hz), 5.74 (s, 1H, CH-C=O), 4.43 (q, 2H, CH₂, ³*J* = 7.1 Hz), 1.55 (t, 3H, CH₃, ³*J* = 7.1 Hz)

¹³C NMR (100 MHz, CDCl₃) δ 175.3, 166.6, 147.4, 138.2, 129.0 (q, ³*J*_{C,F} = 3.4 Hz), 127.5 (q, ²*J*_{C,F} = 35.5 Hz), 126.1 (q, ³*J*_{C,F} = 3.8 Hz), 125.7, 122.3 (q, ¹*J*_{C,F} = 273.1 Hz), 89.1, 67.3, 14.2

MS (EI) 303 (M)

R_f 0.06 (toluene)

M 303.19 g/mol

$C_{12}H_8F_3NO_5$

REFERENCES

1. WHO: *Global Tuberculosis Report 2013*. WHO, Geneva, Switzerland, **2013**.
2. WHO: *Fact Sheet No. 104*. WHO, Geneva, Switzerland, **2013**.
3. Lozano, R., Naghavi, M., Foreman, K. et al.: *Global and regional mortality from 235 causes of death for 20 age groups in 1990 and 2010: a systematic analysis for the Global Burden of Disease Study 2010*. *The Lancet* **2012**, 380 (9859), p. 2095-2128.
4. Palomino, J. C., Leao, S. C., Ritacco, V.: *Tuberculosis 2007 - From Basic Science to Patient Care*. 1st ed., www.tuberculosis textbook.com, **2007**.
5. Patel, N. R., Swan, K., Li, X. et al.: *Impaired M. tuberculosis-mediated apoptosis in alveolar macrophages from HIV+ persons: potential role of IL-10 and BCL-3*. *J. Leukocyte. Biol.* **2009**, 86 (1), p. 53-60.
6. Mulu, A., Kassu, A., Huruy, K. et al.: *Tuberculosis - Human Immunodeficiency Virus Coinfection : Bidirectional effect*. *Pharmacologyonline* **2008**, p. 301-318.
7. Bartlett, J. G.: *Tuberculosis and HIV infection: partners in human tragedy*. *J. Infect. Dis.* **2007**, 196 Suppl (Suppl 1), p. S124-125.
8. Nunn, P., Reid, A., De Cock, K. M.: *Tuberculosis and HIV infection: the global setting*. *J. Infect. Dis.* **2007**, 196 Suppl (Suppl 1), p. S5-14.
9. Zhang, Y., Yew, W. W.: *Mechanisms of drug resistance in Mycobacterium tuberculosis*. *Int. J. Tuberc. Lung D.* **2009**, 13 (11), p. 1320-1330.
10. WHO: *Multidrug and extensively drug-resistant TB (M/XDR-TB). 2010 Global Report on Surveillance and response*. WHO, Geneva, Switzerland, **2010**.
11. Brennan, P. J., Nikaido, H.: *The Envelope of Mycobacteria*. *Annu. Rev. Biochem.* **1995**, 64 (1), p. 29-63.
12. Schwalbe, J.: *Gesammelte Werke von Robert Koch, Band 1*. Thieme: Leipzig, **1912**.
13. Koch, O., Selzer, P. M.: *Biologie der Mykobakterien und neue molekulare Targets*. *Pharmazie in unserer Zeit* **2012**, 41 (1), p. 19-26.
14. Székely, R., Wączek, F., Szabadkai, I. et al.: *A novel drug discovery concept for tuberculosis: inhibition of bacterial and host cell signalling*. *Immunol. Lett.* **2008**, 116 (2), p. 225-231.
15. Walburger, A., Koul, A., Ferrari, G. et al.: *Protein kinase G from pathogenic mycobacteria promotes survival within macrophages*. *Science (New York, N.Y.)* **2004**, 304 (5678), p. 1800-1804.
16. Av-Gay, Y., Deretic, V.: *Two-Component Systems, Protein Kinases, and Signal Transduction in Mycobacterium tuberculosis*. In *Tuberculosis and the Tubercle Bacillus*. Cole, S. T., Eisenach, K. D. et al., Eds., ASM Press: Washington, **2005**, p. 359ff.
17. Av-Gay, Y., Davies, J.: *Components of Eukaryotic-like Protein Signaling Pathways in Mycobacterium tuberculosis*. *Microb. Comp. Genom.* **1997**, 2 (1), p. 63-73.
18. Av-Gay, Y., Everett, M.: *The eukaryotic-like Ser/Thr protein kinases of Mycobacterium tuberculosis*. *Trends Microbiol.* **2000**, 8 (5), p. 238-244.
19. Zhang, Y., Yew, W. W., Barer, M. R.: *Targeting persists for tuberculosis control*. *Antimicrob. Agents Chemother.* **2012**, 56 (5), p. 2223-2230.
20. Brennan, P. J.: *Structure, function, and biogenesis of the cell wall of Mycobacterium tuberculosis*. *Tuberculosis (Edinburgh, Scotland)* **2003**, 83 (1-3), p. 91-97.
21. Tahlan, K., Wilson, R., Kastinsky, D. B. et al.: *SQ109 targets MmpL3, a membrane transporter of trehalose monomycolate involved in mycolic acid donation to the cell*

- wall core of Mycobacterium tuberculosis*. Antimicrob. Agents Chemother. **2012**, 56 (4), p. 1797-1809.
22. Grzegorzewicz, A. E., Pham, H., Gundi, V. A. K. B. et al.: *Inhibition of mycolic acid transport across the Mycobacterium tuberculosis plasma membrane*. Nat. Chem. Biol. **2012**, 8 (4), p. 334-341.
 23. Hoffmann, C., Leis, A., Niederweis, M. et al.: *Disclosure of the mycobacterial outer membrane: cryo-electron tomography and vitreous sections reveal the lipid bilayer structure*. Proceedings of the National Academy of Sciences **2008**, 105 (10), p. 3963-3967.
 24. Park, S.-H., Bendelac, A.: *CD1-restricted T-cell responses and microbial infection*. Nature **2000**, 406 (6797), p. 788-792.
 25. Ma, Z., Lienhardt, C., McIlleron, H. et al.: *Global tuberculosis drug development pipeline: the need and the reality*. Lancet **2010**, 375 (9731), p. 2100-2109.
 26. WHO: *Treatment of Tuberculosis Guidelines. Fourth Edition*. WHO, Geneva, Switzerland, **2009**.
 27. WHO: *The Global Plan to Stop TB 2011-2015*. WHO, Geneva, Switzerland, **2011**.
 28. Sacchettini, J. C., Rubin, E. J., Freundlich, J. S.: *Drugs versus bugs: in pursuit of the persistent predator Mycobacterium tuberculosis*. Nat. Rev. Microbiol. **2008**, 6 (1), p. 41-52.
 29. Koul, A., Arnoult, E., Lounis, N. et al.: *The challenge of new drug discovery for tuberculosis*. Nature **2011**, 469 (7331), p. 483-490.
 30. Brown, D.: *Unfinished business: target-based drug discovery*. Drug Discov. Today **2007**, 12 (23-24), p. 1007-1012.
 31. Payne, D. J., Gwynn, M. N., Holmes, D. J. et al.: *Drugs for bad bugs: confronting the challenges of antibacterial discovery*. Nat. Rev. Drug Discov. **2007**, 6 (1), p. 29-40.
 32. Laqua, K., Rudolph, I., Imming, P.: *Die Suche nach neuen Antituberkulotika*. Pharmazie in unserer Zeit **2012**, 41 (1), p. 48-57.
 33. Ginsberg, A. M.: *Drugs in development for tuberculosis*. Drugs **2010**, 70 (17), p. 2201-2214.
 34. Villemagne, B., Crauste, C., Flipo, M. et al.: *Tuberculosis: The drug development pipeline at a glance*. Eur. J. Med. Chem. **2012**, 51 (0), p. 1-16.
 35. *Public summary of opinion on orphan designation. Rifapentine for the treatment of tuberculosis*. EMA, London, Great Britain, **2010**.
 36. *FDA Application No. 204384*. **2012**.
 37. Andries, K., Verhasselt, P., Guillemont, J. et al.: *A diarylquinoline drug active on the ATP synthase of Mycobacterium tuberculosis*. Science (New York, N.Y.) **2005**, 307 (5707), p. 223-227.
 38. Singh, R., Manjunatha, U., Boshoff, H. I. M. et al.: *PA-824 kills nonreplicating Mycobacterium tuberculosis by intracellular NO release*. Science (New York, N.Y.) **2008**, 322 (5906), p. 1392-1395.
 39. Matsumoto, M., Hashizume, H., Tomishige, T. et al.: *OPC-67683, a nitro-dihydroimidazooxazole derivative with promising action against tuberculosis in vitro and in mice*. PLoS Med. **2006**, 3 (11), p. e466.
 40. *Tuberkulose-Zahlen sinken, kein Grund zur Entwarnung*. <http://www.deutsche-apotheker-zeitung.de/spektrum/news/2012/03/23/kein-grund-zur-entwarnung/6838.html>. accessed on 03.05.2013.
 41. *Stop TB Partnership Pipeline*. www.newtbdrugs.org. accessed on 06.08.2013.

42. EMA: *Refusal of the marketing authorisation for Delamanid (delamanid)*. European Medicines Agency, London, UK, **2013**.
43. EMA: *Positive opinion on the marketing authorisation for Deltyba (delamanid)*. European Medicines Agency, London, UK, **2013**.
44. Protopopova, M., Hanrahan, C., Nikonenko, B. et al.: *Identification of a new antitubercular drug candidate, SQ109, from a combinatorial library of 1,2-ethylenediamines*. J. Antimicrob. Chemoth. **2005**, 56 (5), p. 968-974.
45. Ma, Z., Lienhardt, C.: *Toward an optimized therapy for tuberculosis? Drugs in clinical trials and in preclinical development*. Clin. Chest. Med. **2009**, 30 (4), p. 755-768.
46. Williams, K. N., Stover, C. K., Zhu, T. et al.: *Promising antituberculosis activity of the oxazolidinone PNU-100480 relative to that of linezolid in a murine model*. Antimicrob. Agents Ch. **2009**, 53 (4), p. 1314-1319.
47. *TB Alliance Portfolio*. www.tballiance.org. accessed on 06.08.2013.
48. Throm, S.: *TB-Therapie: Beitrag der Industrie, Product-Development Partnerships*. Pressegespräch Tuberkulose 21.03.2013, **2013**.
49. Zumla, A., Nahid, P., Cole, S. T.: *Advances in the development of new tuberculosis drugs and treatment regimens*. Nat. Rev. Drug Discov. **2013**, 12 (5), p. 388-404.
50. Lienhardt, C., Vernon, A., Raviglione, M. C.: *New drugs and new regimens for the treatment of tuberculosis: review of the drug development pipeline and implications for national programmes*. Curr. Opin. Pulm. Med. **2010**, 16 (3), p. 186-193.
51. Rudolph, I., Laqua, K., Imming, P.: *Die Schwindsucht ist nicht verschwunden*. Pharm. Zeitg. **2011**, 156 (8), p. 18-27.
52. Pasca, M. R., Degiacomi, G., Ribeiro, A. L. D. J. L. et al.: *Clinical isolates of Mycobacterium tuberculosis in four European hospitals are uniformly susceptible to benzothiazinones*. Antimicrob. Agents Ch. **2010**, 54 (4), p. 1616-1618.
53. Makarov, V., Cole, S. T., Moellmann, U.: *New Benzothiazinone derivatives and their use as antibacterial agents*. Germany, WO2007134625A1, **2007**.
54. Makarov, V., Manina, G., Mikusova, K. et al.: *Benzothiazinones kill Mycobacterium tuberculosis by blocking arabinan synthesis*. Science (New York, N.Y.) **2009**, 324 (5928), p. 801-804.
55. Trefzer, C., Rengifo-Gonzalez, M., Hinner, M. J. et al.: *Benzothiazinones: prodrugs that covalently modify the decaprenylphosphoryl- β -D-ribose 2'-epimerase DprE1 of Mycobacterium tuberculosis*. J. Am. Chem. Soc. **2010**, 132 (39), p. 13663-13665.
56. Manina, G., Pasca, M. R., Buroni, S. et al.: *Decaprenylphosphoryl- β -D-Ribose 2'-Epimerase from Mycobacterium tuberculosis is a Magic Drug Target*. Curr. Med. Chem. **2010**, 17 (27), p. 3099-3108.
57. Neres, J., Pojer, F., Molteni, E. et al.: *Structural Basis for Benzothiazinone-Mediated Killing of Mycobacterium tuberculosis*. Sci. Transl. Med. **2012**, 4 (150), p. 150ra121.
58. Trefzer, C., Škovierová, H., Buroni, S. et al.: *Benzothiazinones Are Suicide Inhibitors of Mycobacterial Decaprenylphosphoryl- β -d-ribofuranose 2'-Oxidase DprE1*. J. Am. Chem. Soc. **2012**, 134 (2), p. 912-915.
59. Mikusová, K., Huang, H., Yagi, T. et al.: *Decaprenylphosphoryl Arabinofuranose, the Donor of the D-Arabinofuranosyl Residues of Mycobacterial Arabinan, Is Formed via a Two-Step Epimerization of Decaprenylphosphoryl Ribose*. J. Bacteriol. **2005**, 187 (23), p. 8020-8025.
60. Buroni, S., Riccardi, G., Pasca, M. R.: *Fighting against resistant strains: the case of benzothiazinones and dinitrobenzamides*. In *Understanding Tuberculosis - New*

- Approaches to Fighting Against Drug Resistance*. Cardona, P.-J., Ed., InTech: **2012**, p. 273-290.
61. Crellin, P. K., Brammananth, R., Coppel, R. L.: *Decaprenylphosphoryl- β -D-ribose 2'-epimerase, the target of benzothiazinones and dinitrobenzamides, is an essential enzyme in Mycobacterium smegmatis*. PLoS ONE **2011**, 6 (2), p. e16869-e16869.
 62. Tiwari, R., Moraski, G. C., Krchnak, V. et al.: *Thiolates Chemically Induce Redox Activation of BTZ043 and Related Potent Nitroaromatic Anti-Tuberculosis Agents*. J. Am. Chem. Soc. **2013**, 135, p. 3539-3549.
 63. Batt, S. M., Jabeen, T., Bhowruth, V. et al.: *Structural basis of inhibition of Mycobacterium tuberculosis DprE1 by benzothiazinone inhibitors*. Proceedings of the National Academy of Sciences **2012**, 109 (28), p. 11354-11359.
 64. von Richter, V.: *On the action of potassium cyanide on bromonitrobenzene*. Deut. Chem. Ges. Ber. **1871**, 24, p. 220.
 65. Manina, G., Bellinzoni, M., Pasca, M. R. et al.: *Biological and structural characterization of the Mycobacterium smegmatis nitroreductase NfnB, and its role in benzothiazinone resistance*. Mol. Microbiol. **2010**, 77 (5), p. 1172-1185.
 66. Sala, C., Dhar, N., Hartkoorn, R. C. et al.: *Simple model for testing drugs against nonreplicating Mycobacterium tuberculosis*. Antimicrob. Agents Ch. **2010**, 54 (10), p. 4150-4158.
 67. Karoli, T., Becker, B., Zuegg, J. et al.: *Identification of anti-tubercular benzothiazinone compounds by ligand-based design*. J. Med. Chem. **2012**, 55 (17), p. 7940-7944.
 68. Cooper, M., Zuegg, J., Becker, B. et al.: *Benzothiazinone compounds and their use as anti-tuberculosis agents*. Australia, EP2468746A1, **2012**.
 69. Makarov, V., Cole, S.: *2-Piperazin-1-yl-4H-1,3-benzothiazin-4-one derivatives and their use for the treatment of mammalian infections*. Switzerland, WO2012066518A1, **2012**.
 70. Richter, A.: *Synthesis of BTZ derivatives*. Thesis, Martin-Luther-Universität Halle-Wittenberg, Halle (Saale), **in preparation**.
 71. Steinhilber, D., Schubert-Zsilavec, M., Roth, H. J.: *Medizinische Chemie, Targets, Arzneistoffe, Chemische Biologie*. Deutscher Apotheker Verlag: Stuttgart, Germany, **2010**; Vol. 2.
 72. Wang, F., Sambandan, D., Halder, R. et al.: *Identification of a small molecule with activity against drug-resistant and persistent tuberculosis*. Proceedings of the National Academy of Sciences **2013**, p.
 73. Moellmann, U., Makarov, V., Cole, S. T.: *New antimicrobial compounds, their synthesis and their use for treatment of mammalian infection*. Germany, WO2009010163A1, **2009**.
 74. Imrich, J., Kristian, P.: *Synthesis and investigation of enamine-imine tautomerism of 2,6-disubstituted 4H-1,3-thiazin-4-ones*. Collect. Czech. Chem. C. **1982**, 47, p. 3268-3282.
 75. Houben-Weyl: *Houben-Weyl*. p. 878, Band 879.
 76. Koscik, D., Kristian, P., Gonda, J. et al.: *New synthesis of 2-amino-4-oxopyrido[3,2-e]-1,3-thiazines and 1-alkyl(aryl)pyrido[3,2-e]-2-thiouracils*. Collect. Czech. Chem. C. **1983**, 48, p. 3315-3328.
 77. Makarov, V. A.: *Process for the preparation of 2-amino substituted 1,3-benzothiazine-4-ones*. Russia, WO2011132070A1, **2011**.
 78. Welch, D. E., Baron, R. R., Burton, B. A.: *a,a,a-Trifluorotoluamides as Anticoccidial Agents*. J. Med. Chem. **1969**, 12 (2), p. 299-303.

79. Hall, H. K.: *Correlation of the Base Strengths of Amines*. J. Am. Chem. Soc. **1957**, 79 (20), p. 5441-5444.
80. Seybold, G., Dimmler, M., Stange, A.: *Verfahren zur Herstellung von 1,1-disubstituierten Thioharnstoffen*. Germany, DE3314435A1, **1984**.
81. Hartmann, H., Reuther, I.: *Verfahren zur Herstellung von 1,1-disubstituierten Thioharnstoffen*. German Democratic Republic, DD100467A1, **1973**.
82. Lieber, E., Orłowski, R. C.: *Hydrazinolysis of 1-(Alkyldithioate)-piperidine*. J. Org. Chem. **1957**, 22 (1), p. 88-89.
83. Barry, J. E., Finkelstein, M., Hutchins, G. A. et al.: *Hydrogen bonded complexes IV : Urea-phenol complexes*. Tetrahedron **1983**, 39 (13), p. 2151-2156.
84. Forsyth, D. A., Johnson, S. M.: *NMR detection of an unusual eclipsed structure establishes the origin of large specific rotations in chirally deuterated amines*. J. Am. Chem. Soc. **1993**, 115 (8), p. 3364-3365.
85. Nosova, É. V., Liponova, G. N., Kravchenko, M. A. et al.: *Synthesis and tuberculostatic activity of fluorine-containing derivatives of quinolone, quinazolinone, and benzothiazinone*. Pharm. Chem. J. **2008**, 42 (4), p. 169-174.
86. Richter, M., Vogt, A., Pallas, M. et al.: *Verfahren zur Herstellung von Ethylen-bis(N-acyl-isothioharnstoffen)*. Germany, DD299962A5, **1992**.
87. Liu, Y., Bao, W.: *A new method for the synthesis of dithiocarbamates by CuI-catalyzed coupling reaction*. Tetrahedron Lett. **2007**, 48 (27), p. 4785-4788.
88. Deng, M. Z., Caubere, P., Senet, J. P. et al.: *Condensation of Acyl Chloride on Sodium Cyanate: Preparation of Acyl Isocyanates*. Tetrahedron **1988**, 44 (19), p. 6073-6086.
89. Torrens, J., Frigola, C.: *Fluorophenyl-Triazine And Pyrimidine Derivatives As Compounds Acting On The Central Nervous System*. Spain, WO9720827A1, **1997**.
90. Petersen, U., Schriewer, M., Kyselá, E. et al.: *Verfahren zur Herstellung von Benzoessäure-Derivaten*. Germany, DE3631906A1, **1988**.
91. Chupak, L. S., Kaneko, T., Josyula, V. P. V. N. et al.: *Antibacterial Agents*. USA, WO2004069832A2, **2004**.
92. Ahrendt, K. A., Buckmelter, A. J., Grina, J. et al.: *RAF Inhibitor compounds and methods of use thereof*. USA, WO2009111278A2, **2009**.
93. Roy, S., Gregg, B. T., Gribble, G. W. et al.: *Trifluoromethylation of aryl and heteroaryl halides*. Tetrahedron **2011**, 67 (12), p. 2161-2195.
94. Chen, Q.-Y., Wu, S.-W.: *Methyl fluorosulphonyldifluoroacetate; a new trifluoromethylating agent*. J. Chem. Soc. Chem. Comm. **1989**(11), p. 705-705.
95. Shimma, N., Tsukuda, T., Koyano, H. et al.: *Macrocyclic Compound*. Japan, EP2119718A1, **2009**.
96. Tsukuda, T., Kawasaki, K.-i., Komiyama, S. et al.: *HSP90 Inhibitor*. Japan, EP2036895A1, **2009**.
97. Yoneda, Y., Yamamoto, Y., Ataka, K.: *Preparation of 2,3,4-trifluoro-5-trifluoromethylbenzoic acid and its esters*. Japan, JP11080075A, **1999**.
98. Yamamoto, Y., Yoneda, Y., Ataka, K. et al.: *Substituted Trifluorobenzoic Acids, Esters thereof, and Process for Producing the same*. Japan, EP0968994A1, **2000**.
99. Kimura, Y., Suzuki, H.: *Freeze-dried potassium fluoride: Synthetic utility as a fluorinating agent*. Tetrahedron Lett. **1989**, 30 (10), p. 1271-1272.
100. Mukkala, V.-M., Liitti, P., Hemmiläe, I. et al.: *Novel Thiazole-Containing Complexing Agents and Luminescence of Their Europium(III) and Terbium(III) Chelates*. Helv. Chim. Acta **1996**, 79 (1), p. 295-306.

101. Ribeiro da Silva, M. A. V., Cabral, J. I. T. A., Gomes, P. et al.: *Combined Experimental and Computational Study of the Thermochemistry of Methylpiperidines*. The Journal of Organic Chemistry **2006**, 71 (10), p. 3677-3685.
102. Mannich, C.: *Über "offenes" Ekgonin und Tropin*. Arch. Pharm. **1934**, 272 (10-34), p. 323-359.
103. Ulmer, D.: *Piperidinderivate mit biologischer Aktivität*. Thesis, Julius-Maximilians-Universität, Würzburg, **2006**.
104. Goebel, T.: *4-Piperidonderivate als potenzielle DOHH-Inhibitoren: ein neuer Ansatz zur Therapie tropischer Infektionskrankheiten*. Thesis, Julius-Maximilians-Universität, Würzburg, **2011**.
105. Goebel, T., Ulmer, D., Projahn, H. et al.: *In Search of Novel Agents for Therapy of Tropical Diseases and Human Immunodeficiency Virus*. J. Med. Chem. **2007**, 51 (2), p. 238-250.
106. Stach, K., Thiel, M., Bickelhaupt, F.: *Beiträge zur Entwicklung psychotroper Stoffe, 4. Mitt.: Diphenylamin-Derivate mit piperidylsubstituierten Seitenketten*. Monatshefte für Chemie / Chemical Monthly **1962**, 93 (5), p. 1090-1106.
107. Becker, H. G. O., Berger, W., Domschke, G. et al.: *Organikum*. Wiley-Vch Verlag GmbH: Weinheim, **2004**; Vol. 22.
108. Tsunoda, T., Suzuki, M., Noyori, R.: *A facile procedure for acetalization under aprotic conditions*. Tetrahedron Lett. **1980**, 21 (14), p. 1357-1358.
109. Mash, E. A., Hemperly, S. B.: *Mechanistic studies of diastereoselective cyclopropanation via homochiral ketals. 2. Studies with conformationally restricted 2-cyclohexen-1-one ketals*. The Journal of Organic Chemistry **1990**, 55 (7), p. 2055-2060.
110. Wuts, P. G. M., Greene, T. W.: *Greene's Protective Groups in Organic Synthesis*. 4th ed., John Wiley & Sons, Inc.: Hoboken, New Jersey, **2007**.
111. Makings, L. R., Blanco, M. G.-G., Hurley, D. J. et al.: *Modulators of muscarinic receptors*. USA, US2009/0227614A1, **2009**.
112. Ye, X. M., Konradi, A. W., Smith, J. et al.: *Discovery of a novel sulfonamide-pyrazolopiperidine series as potent and efficacious gamma-secretase inhibitors*. Bioorg. Med. Chem. Lett. **2010**, 20 (7), p. 2195-2199.
113. Neipp, C. E., Martin, S. F.: *Synthesis of bridged azabicyclic structures via ring-closing olefin metathesis*. The Journal of Organic Chemistry **2003**, 68 (23), p. 8867-8878.
114. Brown, J. D., Foley, M. A., Comins, D. L.: *A highly stereocontrolled, four-step synthesis of (+/-)-lasubine II*. J. Am. Chem. Soc. **1988**, 110 (22), p. 7445-7447.
115. Abad, J.-L., Gaffney, B. L., Jones, R. A.: *Adenine and Guanine Nucleosides. Syntheses of Guanosine, 2'-Deoxyadenosine, and 2'-Deoxyguanosine*. J. Org. Chem. **1999**, 64 (18), p. 6575-6582.
116. Meanwell, N. A., Dennis, R. D., Roth, H. R. et al.: *Inhibitors of blood platelet cAMP phosphodiesterase. 3. 1,3-Dihydro-2H-imidazo[4,5-b]quinolin-2-one derivatives with enhanced aqueous solubility*. J. Med. Chem. **1992**, 35 (14), p. 2688-2696.
117. Lipunova, G. N., Nosova, E. V., Mokrushina, G. a. et al.: *Fluorocontaining Heterocycles: IX. Derivatives of Imidazo[2,1-b][1,3]benzothiazine*. Russ. J. Org. Chem. **2003**, 39 (2), p. 248-256.
118. Zhivotova, T. S., Gazaliev, A. M., Fazylov, S. D. et al.: *Synthesis and Structure of Some Imidazolidine-2-thiones*. Russ. J. Org. Chem. **2006**, 42 (3), p. 448-450.
119. Dolbier, W. R., Burkholder, C., Abboud, K. A. et al.: *Synthesis of New Tetrafluorobenzo Heteroaromatic Compounds*. The Journal of Organic Chemistry **1994**, 59 (25), p. 7688-7694.

120. Christophe, T., Jackson, M., Jeon, H. K. et al.: *High Content Screening Identifies Decaprenyl- Phosphoribose 2' Epimerase as a Target for Intracellular Antimycobacterial Inhibitors*. PLoS Pathog. **2009**, 5 (10), p. e1000645.
121. Müller, D., Adelsberger, K., Imming, P.: *Organic Preparations with Molar Amounts of Volatile Malodorous Thiols*. Synthetic Commun. **2012**, 43 (11), p. 1447-1454.
122. Boteva, A., Krasnykh, O.: *The methods of synthesis, modification, and biological activity of 4-quinolones (review)*. Chem. Heterocyc. Compd. **2009**, 45 (7), p. 757-785.
123. Mitscher, L. A.: *Bacterial topoisomerase inhibitors: quinolone and pyridone antibacterial agents*. Chem. Rev. **2005**, 105 (2), p. 559-592.
124. Liepa, A. J., Nguyen, O., Saubern, S.: *Synthesis of Some 4-Oxothiochromenes and Related Compounds*. Aust. J. Chem. **2005**, 58 (12), p. 864-869.
125. Kikionis, S., McKee, V., Markopoulos, J. et al.: *A prominent C-acylation–cyclisation synthetic sequence and X-ray structure elucidation of benzothioopyranone derivatives*. Tetrahedron **2008**, 64 (23), p. 5454-5458.
126. Hashimoto, A., Pais, G. C. G., Wang, Q. et al.: *Practical Synthesis and Molecular Structure of a Potent Broad-Spectrum Antibacterial Isothiazoloquinolone*. Org. Process Res. Dev. **2007**, 11 (3), p. 389-398.
127. Engler, M., Rusing, G., Sorgel, F. et al.: *Defluorinated Sparfloxacin as a New Photoproduct Identified by Liquid Chromatography Coupled with UV Detection and Tandem Mass Spectrometry*. Antimicrob. Agents Chemother. **1998**, 42 (5), p. 1151-1159.
128. Schriewer, M.: *1,8-Verbrueckte 4-Chinolon-3-carbonsaeuren und diese enthaltende Arzneimittel*. Germany, DE3600891A1, **1987**.
129. Grohe, K., Heitzer, H.: *Cycloaracylierung von Enaminen, I. Synthese von 4-Chinolon-3-Carbonsaeuren*. Liebigs Ann. Chem. **1987**, p. 29-37.
130. Belliotti, T. R., Kostlan, C. R.: *Novel fenamic acid methyl hydrocamate derivatives having cyclooxygenase and 5-lipoxygenase inhibition*. USA, US5017604, **1991**.
131. Chu, D. T. W., Maleczka, R. E., Nordeen, C. W.: *Synthesis of 4,12-dihydro-4-oxoquino-[1,8a,8-a,b]quinoxaline-5-carboxylic acid derivatives*. J Heterocyclic Chem. **1988**, 25 (3), p. 927-930.
132. Grechin, A. G., Buschmann, H.-J., Schollmeyer, E.: *Complexation of gaseous guests by solid host: I. Quantitative thermodynamic approach for the reactions of β -cyclodextrin with amines using data in aqueous solution*. Thermochim. Acta **2006**, 449 (1–2), p. 67-72.
133. Devulder, G., de Montclos, M. P., Flandrois, J. P.: *A multigene approach to phylogenetic analysis using the genus Mycobacterium as a model*. Int. J. Syst. Evol. Micr. **2005**, 55 (1), p. 293-302.
134. Stanford, J., Rook, G., Convit, J. et al.: *Preliminary taxonomic studies on the leprosy bacillus*. British journal of experimental pathology **1975**, 56 (6), p. 579.
135. de Jesus Lopes Ribeiro, A. L., Degiacomi, G., Ewann, F. et al.: *Analogous Mechanisms of Resistance to Benzothiazinones and Dinitrobenzamides in Mycobacterium smegmatis*. PLoS ONE **2011**, 6 (11), p. e26675.
136. Rullas, J., Garcia, J. I., Beltran, M. et al.: *Fast standardized therapeutic-efficacy assay for drug discovery against tuberculosis*. Antimicrob. Agents Chemother. **2010**, 54, p. 2262-2264.
137. Franzblau, S. G., DeGroot, M. A., Cho, S. H. et al.: *Comprehensive analysis of methods used for the evaluation of compounds against Mycobacterium tuberculosis*. Tuberculosis (Edinburgh, Scotland) **2012**, 92 (6), p. 453-488.

138. Young, D.: *Animal models of tuberculosis*. Eur. J. Immunol. **2009**, 39 (8), p. 2011-2014.
139. Ballell, L., Bates, R. H., Young, R. J. et al.: *Fueling open-source drug discovery: 177 small-molecule leads against tuberculosis*. ChemMedChem **2013**, 8 (2), p. 313-321.
140. Muller, P. Y., Milton, M. N.: *The determination and interpretation of the therapeutic index in drug development*. Nature Reviews Drug Discovery **2012**, p.
141. Poce, G., Bates, R. H., Alfonso, S. et al.: *Improved BM212 MmpL3 Inhibitor Analogue Shows Efficacy in Acute Murine Model of Tuberculosis Infection*. PloS ONE **2013**, 8 (2), p. e56980.
142. Nicod, L., Viollon, C., Regnier, A. et al.: *Rifampicin and isoniazid increase acetaminophen and isoniazid cytotoxicity in human HepG2 hepatoma cells*. Hum. Exp. Toxicol. **1997**, 16 (1), p. 28-34.
143. Tostmann, A., Boeree, M. J., Peters, W. H. M. et al.: *Isoniazid and its toxic metabolite hydrazine induce in vitro pyrazinamide toxicity*. Int. J. Antimicrob. Agents **2008**, 31 (6), p. 577-580.
144. Testa, B., Krämer, S. D., Wunderli-Allenspach, H. et al.: *Pharmacokinetic Profiling in Drug Research - Biological, Physicochemical, and Computational Strategies*. Verlag Helvetica Chimica Acta and WILEY-VCH: Zürich, Switzerland and Weinheim, Germany, **2006**.
145. Lipinski, C. A., Lombardo, F., Dominy, B. W. et al.: *Experimental and computational approaches to estimate solubility and permeability in drug discovery and development settings*. Adv. Drug Deliver. Rev. **1997**, 23 (1-3), p. 3-25.
146. Wildman, S. A., Crippen, G. M.: *Prediction of Physicochemical Parameters by Atomic Contributions*. J. Chem. Inf. Comp. Sci. **1999**, 39 (5), p. 868-873.
147. Larsson, J.: *Methods for measurement of solubility and dissolution rate of sparingly soluble drugs*. Thesis, Lund University, Lund, **2009**.
148. Glomme, A.: *Biorelevante Löslichkeit schwerlöslicher Arzneistoffe*. Thesis, Johann Wolfgang Goethe-Universität, Frankfurt am Main, **2003**.
149. *Thieme Römpf Online Library*. <http://www.roempp.com/>. accessed on 11.12.2013.
150. Glomme, A., Maerz, J., Dressman, J. B.: *Comparison of a miniaturized shake-flask solubility method with automated potentiometric acid/base titrations and calculated solubilities*. J. Pharm. Sci. **2005**, 94 (1), p. 1-16.
151. Yalkowsky, S. H.: *Solubility and solubilization in aqueous media*. American Chemical Society: Washington D.C., **1999**.
152. *5.11 Characters section in monographs*. In *European Pharmacopoeia 6.0*. 6th ed., Council of Europe: Strasbourg, France, **2008**; Vol. 1, p. 659.
153. Budavari, S., O'Neil, M. J., Smith, A. et al.: *The Merck Index*. Merck & Co., Inc.: Whitehouse Station, N.J., USA, **1996**; Vol. 12.
154. Miyazaki, S., Oshiba, M., Nadai, T.: *Precaution on use of hydrochloride salts in pharmaceutical formulation*. J. Pharm. Sci. **1981**, 70 (6), p. 594-596.
155. Bogardus, J. B.: *Common ion equilibria of hydrochloride salts and the Setschenow equation*. J. Pharm. Sci. **1982**, 71 (5), p. 588-590.
156. Kumar, L., Meena, C., Pawar, Y. et al.: *Effect of Counterions on Physicochemical Properties of Prazosin Salts*. AAPS PharmSciTech **2013**, 14 (1), p. 141-150.
157. Sharma, D., Singh, G., Singh, M. et al.: *A review on innovative approaches to enhance solubility and dissolution rate of hydrophobic drugs*. Novel Sci. Int. J. Pharm. Sci. **2012**, 1 (7), p. 486-492.
158. Jaehde, U., Radziwill, R., Kloft, C.: *Klinische Pharmazie*. Wissenschaftliche Verlagsgesellschaft: Stuttgart, Germany, **2010**; Vol. 3.

159. Makarov, V., Manina, G., Mikusova, K. et al.: *Benzothiazinones kill Mycobacterium tuberculosis by blocking arabinan synthesis. Supporting Information*. Science (New York, N.Y.) **2009**, 324 (5928), p. 801-804.
160. Mutschler, E.: *Arzneimittelwirkungen*. Wissenschaftliche Verlagsgesellschaft: Stuttgart, Germany, **1996**; Vol. 7.
161. EMA: *ICH Topic Q3C (R4): Impurities: Guideline for Residual Solvents* European Medicines Agency, London, **2009**.
162. Gugeler, N., Klotz, U.: *Einführung in die Pharmakokinetik*. Govi-Verlag: Eschborn, Germany, **2000**; Vol. 2.
163. Wikler, M. A., Cockerill, F. R., Craig, W. A. et al.: *Methods for Dilution Antimicrobial Susceptibility Tests for Bacteria That Grow Aerobically; Approved Standard - Seventh Edition*. M7-A7, **2006**.
164. Krauth, F., Dahse, H.-M., Rüttinger, H.-H. et al.: *Synthesis and characterization of novel 1,2,4-triazine derivatives with antiproliferative activity*. Bioorg. Med. Chem. **2010**, 18 (5), p. 1816-1821.
165. Kabsch, W.: *XDS*. Acta Crystallogr. D **2010**, 66 (2), p. 125-132.
166. Adams, P. D., Afonine, P. V., Bunkoczi, G. et al.: *PHENIX: a comprehensive Python-based system for macromolecular structure solution*. Acta Crystallogr. D **2010**, 66 (2), p. 213-221.
167. Emsley, P., Lohkamp, B., Scott, W. et al.: *Features and development of Coot*. Acta Crystallogr. D **2010**, 66 (4), p. 486-501.
168. Murshudov, G. N., Skubák, P., Lebedev, A. A. et al.: *REFMAC5 for the refinement of macromolecular crystal structures*. Acta Crystallogr. D **2011**, 67 (4), p. 355-367.
169. Ried, W., Erle, H. E.: *Tautomerism of heterocyclic compounds. IX. Preparation of substituted benzothiazines and benzoxazines via N-aryloxychloroformamidines*. Chem. Ber. **1982**, 115 (4), p. 1662-1664.

ACKNOWLEDGMENTS

I wish to express my sincere gratitude to my supervisor Prof. Dr. Peter Imming, who always trusted me not only as a researcher, delegating this interesting and ambitious topic to me, and always providing encouraging and constructive feedback.

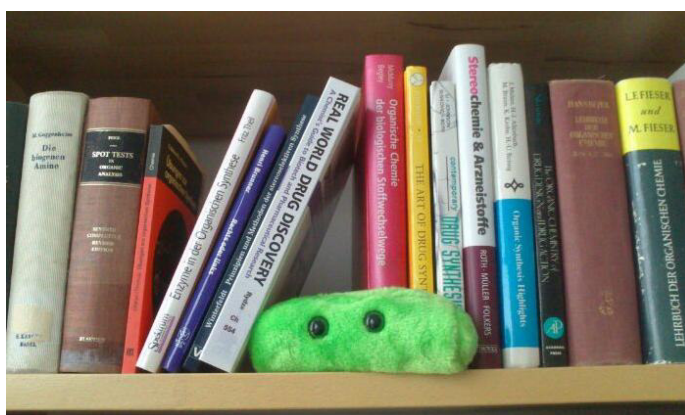
I am deeply indebted to my collaborators for running the assays with my synthetic compounds, promptly providing test results and supporting me in interpreting them. In particular, I thank Dr. Ute Möllmann, Dr. Michael Ramm, Dr. Hans-Martin Dahse, Christiane Weigel, and Kerstin Voigt at Hans-Knöll-Institut Jena, Dr. Lluís Ballell and Dr. Robert Bates at GSK Tres Cantos, Dr. Robert Young, Dr. Onkar Singh, Dr. Chun-wa Chung, and Dr. Argyrides Argyrou at GSK Stevenage, as well as Prof. Gurdyal Besra, Dr. Sarah Batt, and Dr. Klaus Fütterer at the University of Birmingham. A special thanks belongs to Ute Möllmann for the continuous interest in my work and the many helpful discussions.

All members of the Institute of Pharmacy and Institute of Chemistry of the University of Halle also deserve recognition for the analytical characterization of all synthetic compounds and the great work environment. It is, however, not possible to list them all here, but I notably wish to thank the group of Dr. Dieter Ströhl for NMR analyses, Dr. Jürgen Schmidt and Dr. Harry Schmidt for mass spectrometry, Martina Mannd and Elke Neubauer for elemental analyses, Heike Rudolf for IR measurements and Antje Peters for HPLC und UV analyses. Furthermore, I would like to recognize the valuable contributions of all students and diploma students, who worked on synthetic subprojects of this thesis.

I greatly appreciate my fellow lab mates of the group of Prof. Imming for the exceptionally kind environment to work in, the uncountable valuable discussions not only regarding chemistry but also non-work related topics and the memorable time I spent inside and outside lab with Aline, Lily, Katja, Adrian, Marcel, Rico and Tody. Thanks to the 'PI girls', who have all become close friends to me and especially to Tody, who has affectionately welcomed me into the lab, went through all ups and downs of organic and 'interpersonal' chemistry with me and became a friend for lifetime.

I wish to thank Mandy, Anja, Christian, Tody, Simon and Daniel for the critical review of this manuscript. To my friends and the Riege 1, I cherish your unasked support and your time in all circumstances.

I would not have come this far if not for my parents, who wholeheartedly supported me my whole life in all of my plans. To my parents and my whole family, thank you.



CURRICULUM VITAE

Personal Data

Name	Andrea Ines Rudolph
Academic title	Diplom-Pharmazeut
Date of birth	27.01.1983
Place of birth	Karl-Marx-Stadt (now Chemnitz)
Citizenship	German
Sex	female
Residence	Arndtstr. 49, 04275 Leipzig

Professional Experience

since 10/13	Researcher, AMP Therapeutics GmbH, Leipzig
06/09-05/13	PhD Thesis, Martin Luther University Halle-Wittenberg, Department of Pharmaceutical Chemistry, Prof. Imming “Antitubercular Benzothiazinones: Synthesis, Activity, Properties and SAR”
09/08-05/09	Researcher, Galenical Development, Merck Selbstmedikation GmbH, Darmstadt

Education

09/08	Pharmaceutical license (Approbation)
08/08	3 rd phase of pharmaceutical examination
12/07-05/08	Practical year, Paracelsus Apotheke, Leipzig
05/07-11/07	Diploma Thesis, University of Leipzig, Department of Pharmaceutical Chemistry, Prof. Briel “Synthese neuer monozyklischer Diazepine als GABA _A -Modulatoren”
03/07	2 nd phase of pharmaceutical examination
08/04	1 st phase of pharmaceutical examination
10/02-03/07	Pharmacy studies, University of Leipzig
09/98-06/02	Johannes Kepler Gymnasium, Chemnitz, Abitur
09/99-07/00	Folsom High School, Folsom, California, USA
09/95-08/98	Sportgymnasium, Chemnitz

LIST OF PUBLICATIONS

Papers

I. Rudolph, P. Imming.

Antimykobakterielle Imidazopyridine.

Pharmakon **2014**, 2, 4-5.

K. Laqua, I. Rudolph, P. Imming.

Die Suche nach neuen Antituberkulotika.

Pharmazie in unserer Zeit **2012**, 41, 48-57. doi10.1002/pauz.201100452

I. Rudolph, K. Laqua, P. Imming.

Tuberkulose. Schwindsucht ist nicht verschwunden.

Pharmazeutische Zeitung **2011**, 8, 642-651.

D. Briel, I. Rudolph, K. Unverferth, S. Mann.

Synthesis of disubstituted 1,4-diazepines with affinity to GABA_A-receptor subtypes.

Pharmazie **2010**, 65, 641-644. doi10.1691/ph.2010.0559

Patent

I. Rudolph, P. Imming.

Antimykobakteriell wirksame Substanzen, Verfahren zur ihrer Herstellung und deren Verwendung.

Patent Application at the German Patent Office, 20.06.2012, AZ DE102012012117.2

Oral presentation

SAR studies with the novel class of strongly antimycobacterial benzothiazinones.

Gordon Research Seminar: Tuberculosis Drug Development.

20.07.-21.07.2013, Lucca (Barga), Italy.

Posters

I. Rudolph, U. Moellmann, M. Ramm, R. Bates, L. Ballell, P. Imming.

The curious case of antimycobacterial activity and lipophilicity of benzothiazinones.

Gordon Research Conference: Tuberculosis Drug Development.

21.07.-26.07.2013, Lucca (Barga), Italy.

I. Rudolph, M. Ramm, U. Moellmann and P. Imming.

Synthesis and antimycobacterial evaluation of some new benzothiazinone derivatives.

Tuberculosis 2012 - Biology, pathogenesis, intervention strategies.

11.9.-15.9.2012, Paris, France

I. Rudolph, M. Ramm, U. Moellmann, P. Imming.

Synthesis and determination of antimycobacterial activity of tryptanthrin, vasicine, vasicinone and derivatives thereof.

International Congress on Natural Products Research.

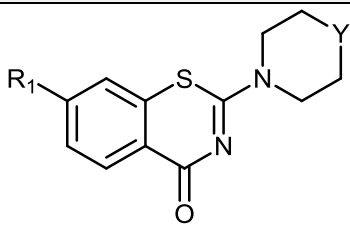
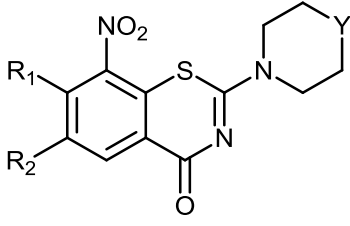
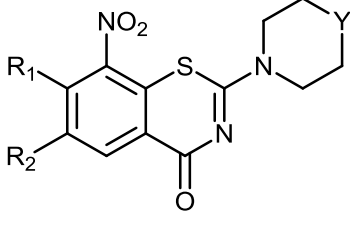
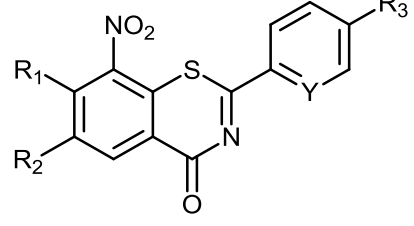
28.07.-01.08.2012, New York City, USA.

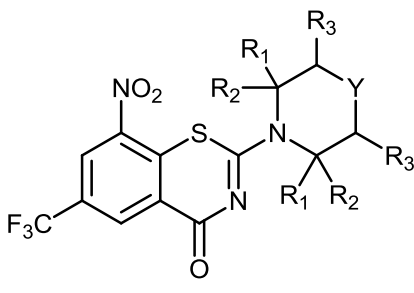
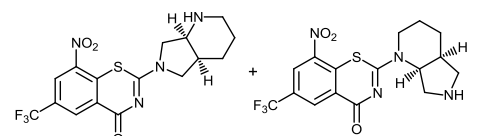
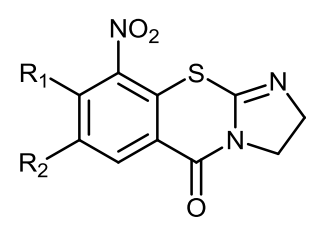
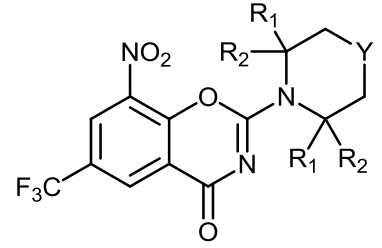
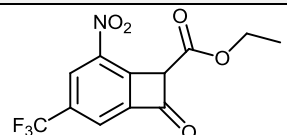
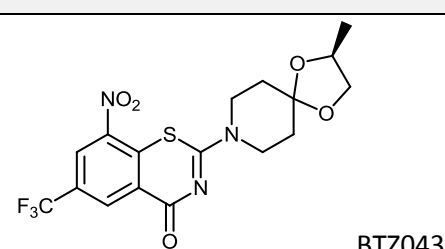
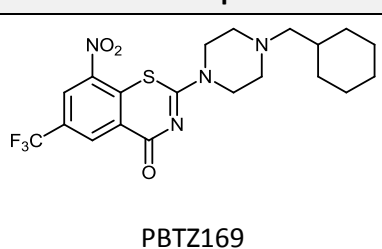
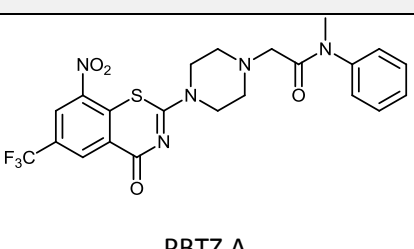
DECLARATION OF ACADEMIC INTEGRITY

With this statement I declare, that I have independently completed the above PhD thesis entitled with "Antitubercular Benzothiazinones: Synthesis, Activity, Properties and SAR". The thoughts taken directly or indirectly from external sources are properly marked as such. This thesis was not previously submitted to another academic institution and has also not yet been published nor have I attempted a former PhD thesis.

Leipzig, 22.01.2014

Andrea Ines Rudolph

Scaffold	compound no.	R ₁	R ₂	R ₃	Y
unsubstituted arene moiety, shifted nitro group					
	IR 16	H	-	-	CH ₂
	IR 86	H	-	-	O
	IR 67	NO ₂	-	-	O
halides at position 7					
	IR 53	F	F	-	O
	IR 56	F	F	-	CH ₂
	IR 62	Cl	F	-	CH ₂
	IR 69	Cl	F	-	O
	IR 74	Cl	CF ₃	-	CH ₂
	IR 76	Cl	CF ₃	-	O
	IR 102	F	CF ₃	-	O
	IR 108	F	CF ₃	-	CH ₂
amino substituents at position 7					
	IR 57	morpholin-4-yl	F	-	O
	IR 64	morpholin-4-yl	F	-	CH ₂
	IR 75	morpholin-4-yl	CF ₃	-	CH ₂
	IR 77	morpholin-4-yl	CF ₃	-	O
	IR 96	pyrrolidin-1-yl	F	-	O
	IR 97	pyrrolidin-1-yl	F	-	CH ₂
	IR 100	pyrrolidin-1-yl	CF ₃	-	CH ₂
	IR 101	pyrrolidin-1-yl	CF ₃	-	O
	IR 103	(CH ₃) ₂ N	CF ₃	-	O
	IR 104	(CH ₃) ₂ N	CF ₃	-	CH ₂
	IR 106	(CH ₃) ₂ N	F	-	CH ₂
IR 107	(CH ₃) ₂ N	F	-	O	
aryl and heteroaryl substituents at position 2					
	IR 51	H	CF ₃	H	N
	IR 52	F	F	H	N
	IR 61	H	F	H	N
	IR 82	H	CF ₃	H	CH
	IR 87	H	CF ₃	OCH ₃	CH
	IR 88	H	CF ₃	Cl	CH

Scaffold	compound no.	R ₁	R ₂	R ₃	Y
branched amino and other amino substituents at position 2					
	IR 20	H	H	H	CH ₂
	IR 58	H	H	H	O
	IR 85	CH ₃	H	H	CH ₂
	IR 115	CH ₃	CH ₃	H	CH ₂
	IR 124 (=PBTZ169)	H	H	H	N-CH ₂ - (cyclohexyl)
	IR 127 cis	H	H	CH ₃	CH ₂
	IR 127 trans	H	H	CH ₃	CH ₂
	IR 140	CH ₃	H	H	C=O
	IR 141	CH ₃	CH ₃	H	C=O
	IR 128	-	-	-	-
imidazobenzothiazinones					
	IR 47	Cl	F	-	-
	IR 59	morpholin-4-yl	F	-	-
	IR 78	Cl	CF ₃	-	-
	IR 79	morpholin-4-yl	CF ₃	-	-
	IR 80	H	CF ₃	-	-
	IR 98	pyrrolidin-1-yl	CF ₃	-	-
IR 105	(CH ₃) ₂ N	CF ₃	-	-	
benzoxazinones					
	IR 95	CH ₃	H	-	CH ₂
	IR 112	H	H	-	CH ₂
	IR 113	H	H	-	O
	IR 114	CH ₃	CH ₃	-	CH ₂
	IR 125	H	H	-	N-CH ₂ - (cyclohexyl)
other					
	IR 154	-	-	-	-
reference compounds					
	BTZ043				
	PBTZ169				
	PBTZ A				